Assessments of patient safety for multidimensional risk management in robotic dentistry

The Safety of Robotic Dentistry

Author
Evie Deaker

Supervisors
Dr Graham Brooker
Prof Hans Zoellner

A thesis submitted in fulfillment of the
requirements of the degree of
Doctor of Philosophy

THE UNIVERSITY OF
SYDNEY
—
Australian Centre for Robotics

Australian Centre for Robotics (ACFR)
School of Aerospace, Mechanical and Mechatronic Engineering
The University of Sydney, Australia

August 2025

Table of Contents

Declaration

I hereby declare that this submission is my own work and that, to the best of my knowledge and belief, it contains no material previously published or written by another person nor material which to a substantial extent has been accepted for the award of any other degree or diploma of the University or other institute of higher learning, except where due acknowledgement has been made in the text.

_____

_____

Evie Deaker 4 August 2025

Authorship Attribution Statement

This thesis contains material previously published in the *Annual International Conference of the IEEE Engineering in Medicine & Biology Society (EMBC)*, under the title, "The Future of Dental Care: The Manipulation of Dental Instruments & Preparation Towards Automated Tooth Cleaning" [214]. For the first manuscript, material comprises Sections 1.2 and 2.1 for background, Section 3.4, Figure 3.7 and Section 3.5, Figure 3.8 for design; and Section 5.3.3, Figure 5.8 and Section A.1 for methods.

This thesis contains material submitted for publication in the *International Journal of Dentistry*, under the title, "Simulated Risk Mapping for Safe Robotic Dental Techniques: Spatial Assessments of Instrument-Patient Interactions" [381]. This comprises of material from Sections 1.3, 1.5 and 5.5 for background, Section 6.3 for methods (Figure 6.3, Figure 6.4, Table 6.2), Section 6.4.1 and Section 6.4.6 for results (Figure 6.13, Figure 6.14, Figure 6.23, Figure 6.24, Figure 6.25, Figure 6.26), and Sections 2.2.4, 2.3, 4.4.3, 6.5 and 7.3 for discussion.

I designed the study, analysed the data and wrote the drafts of the manuscripts and I am listed as lead author in both the publications included in this thesis. In addition to the authorship attribution statements, in cases where I am not the corresponding author of a published item, permission to include the published material has been granted by the corresponding author. No content generated by generative AI tools has been used in the preparation of this thesis.

_____

_____

Evie Deaker 4 August 2025

As supervisor for the candidature upon which this thesis is based, I can confirm that the authorship attribution statements above are correct.

_____

_____

Graham Brooker 4 August 2025

Abstract

Rationale

Dentistry is an essential practice to maintain the health of the oral cavity. Barriers to accessibility, dental fear and the lack of oral health awareness have led to a high prevalence of dental diseases globally. Recent advances in digitisation and technology for oral examinations and procedures have improved the speed and ease of disease diagnosis and dental treatment. Dental robotics has emerged as a new field of dentistry and can provide numerous benefits to dental professionals and society from increased accessibility to improved standardisation of dental techniques. The implementation of robotic systems offers the opportunity to re-imagine the workflow and design of current dental practices in order to promote patient safety and comfort. However, the ability to achieve these aspects has proven challenging due to the potential for unmanageable dynamic risks and the patient's safety remaining a full responsibility of the dental practitioner. This is particularly challenging as international standards for collaborative medical robots are limited to assistive operator-controlled systems with minor progress towards autonomous medical robots. For dental robots to become standard practice, efforts towards ensuring patient safety during autonomous robotic explorations must be investigated.

Methods

To ease the manual workload of dental techniques and to improve accessibility of dental services, shortfalls of current practices and developments in dental digitisation are reviewed for the integration of dental robots to dentistry. Potential dental and robot hazards and available technologies, including cranial-related medical robot designs and COVID-19 test robots, are examined to develop a new design for automated robotic dentistry. These robotic setups were compared and assessed for limitations and benefits to patient safety. This led to the design of

an innovative dental robot setup where patients lie face down on a dental operating chair with the oral cavity accessed from below through a small opening by a dental instrument controlled by a robot encased in a chamber. The revised patient orientation has the potential to significantly reduce the likelihood of choking and quasi-static collisions during automated procedures, as well as limit the transmission of disease. A new workflow for dental robot systems is proposed that integrates more recently developed dental digitisation systems, including non-contact intraoral scanners and optional patient tracking technologies.

The current defined levels of autonomy for medical robots are evaluated for their lack of focus on patient safety. New levels of autonomy are developed to include robot risk awareness for the reducing operator input to allow reductions in the operator's expertise. This promotes heightened patient safety where the operator already has reduced control, awareness and input, while realising the potential gains of accessibility to dental services from using robots. A staged approach for dental robots is recommended to specifically perform charting and scaling for cleaning procedures, before moving to develop more invasive techniques. To ensure patient safety during techniques, a complementary risk supervision system for any dental robot setup is devised that assesses the presence of hazards in the dental environment. This is incorporated into a framework developed for automated risk management that is structured as a defined network for safety-related decision making. The network is then responsible for preventing harm by altering the robot's allowed mode of interaction with the patient based on the tracked risk of identified hazardous situations.

Important measurements for hazardous situations in autonomous dental robotics are proposed as being integrated into supervision blocks for multi-dimensional risks associated with the instrument, dental environment and patient. Measured spatial data from the instrument, which would be collected by patient position tracking sensors, is investigated to detect likely high-risk locations, unsafe control and collisions. The instrument safety measurements for a

simulated dental procedure were created and evaluated in MATLAB for operative site locations for a scanned head model. These measurements were combined to produce a quantified risk output for each location involving the position of the instrument tip, the entry of the instrument through the oral opening, and the tip's proximity to the hard tissue dental arches, as well as to the relaxed soft oral tissues. Experiments were carried out with different dental instruments on the end of a compact less-confrontational robot arm for simple dental applications. Assessments for the movement of a dental instrument around the oral cavity were performed in a virtual environment using the 3D Unity game engine during the live simulations on model dental arches. Forces acting on the instrument were measured and compared to the designed spatial risk measurements for a set of 3D pre-programmed paths in Python.

Results

Preliminary research into the current dental setup highlighted four major challenges to the introduction of robots. These were the high risk of inhalation and ingestion of particles and liquids due to the supine patient posture, resulting in the need for regular suction, the physical position of the patient between the headrest and the dental instrument, creating higher likelihood of quasi-static constrained impacts and limiting patient control, and finally the need to rotate the patient during an emergency to the recovery position. Analysis of the various developed and developing medical robots related to oral applications highlighted areas of improvement for the dental setup for autonomous procedures. Further considerations to develop a safer dental setup included the need to accommodate different levels of robot autonomy, reduce the risk of disease transmission, and reduce the chance of obstructions for integrated visual guidance systems or the robot, such as from people or objects besides the patient's oral cavity. Important features of developing COVID-19 test robots supported a shift in patient posture to be forward-oriented and without a backrest behind the patient's head.

A proposed dental setup with a prone or seated patient posture is described including its advantages and disadvantages. This setup also included the use of a chamber to house the robot, which helps to limit the uncertainties of the robot's environment to the confines of the tracked dental environment, such that the robot should be able to move with more conviction of its joints to manage the procedure without the risk of unexpected collisions with bystanders that could result in harm. Potential benefits include the isolation of noisy instruments and dampening of instrument vibrations with a properly fitted headrest and a change in head pivot point for rotation towards the front of the mouth. A preliminary study assessed the change in position of the dental arch under a 30° rotation and found that there was a high change in unoccupied regions for the traditional supine posture. The least change occurred for the seated position, particularly for the back regions of the dental arch, shortly followed by the prone posture which was best for the front regions. This suggests that the change in patient posture could reduce the likelihood of collisions from head rotations during procedures on conscious patients for autonomous instrument navigation. Nonetheless, patients should be personally assessed to determine if a forward posture would be comfortable for the expected length of the procedure. Finally, the seated or prone posture setup is suited to all levels of autonomy performed by the robot, except assistive techniques involving shared operator control.

A design focused hazard analysis was performed to compare the risks for introducing a robot in the current dental setup compared to a proposed setup with a patient in a prone posture. Of the sixteen likely forms of dental harm, the highest unacceptable residual risks were adverse reactions, medical emergencies, and the potential for an internal high impact collision with tissue damage. Additionally, two remaining areas of concern were the potential dental technique errors and the risk of sharp component inhalation. As risk reduction through design cannot rule out the possibility of these high risks, methods need to be taken to mitigate these risks further for patient safety. The proposed risk management network was designed to detect

high risk situations in order to develop robot risk awareness for a dental robot. Three supervision system blocks were designed to track risk and aid transition to higher levels of autonomy, beginning with the procedure block to reach high autonomy by tracking the instrument's position relative to specific dental features, the observer block for developing full automation with knowledge of changes to the dental environment, and the patient block for advanced awareness of the patient's state of mind.

Four interpreted data (ID) measurements (ID1.1–1.4) were defined for the procedure block and evaluated using a model patient scenario using MATLAB. The tops of head model intraoral scans were used to create a curve to define the shape of the occlusal curve. Transform axes from orthogonal axes vectors of 25 target points from each mouth quadrant were presented with x-axes for the instrument handle designed to closely align with the occlusal curve of the dental arch so that it would be directed more forwards out of the mouth. To compare changes in ID1.1 and ID1.3–1.4 results, measurements were repeated for a shift in dental arch positions by [4,4,4] mm and [4,4,-4] mm for the maxillary and mandibular arches, respectively, and equivalent to a distance of 6.9 mm. For ID1.1, the risk relative to the nearest occlusal curve point reference frame was acceptable at an average of 6/10 but increased to unacceptable at an average of 10/10. For risks around hard oral tissues, the ID1.3 risks increased from acceptable at 5/10 to high at 8.06/10 for the shifted target locations. The shift in locations with respect to the soft oral tissues reduced the ID1.4 peak maximum risk outputs to -2.56/10 from 1.53/10 as the targets were moved into the arches away from the tongue and most of the lip and cheek oral mucosa. ID1.2 risk measurements were compared by reorienting the target axes to improve the handle entry angle. The outputs were high risk, ranging from 8/10 to 10/10, for no change in entry and improved to acceptable risk at 5/10 after the handle rotations.

From simulation experiments, the position of the Meca500 robot relative to the head model caused joint 5 and the elbow joint singularity to reach 90% and 95% of their limits at the start and end of each motion cycle, respectively. Only joint 3 approached close to its 85% limit of only 70° during the motion cycles. With passive model movements, the high risk ProDENT intraoral camera instrument path reached unacceptable risk for ID1.1–1.2 and the low risk ProDENT path only reached unacceptable for ID1.1. By comparison, risks remained acceptable for the ID1.3–1.4 measurements, except for the high risk ProDENT path for ID1.3. ID1.2 just reached high risk for all test cases in the middle of the motion cycle at the back of the mouth, including the ProDENT test cases during active patient model movement and sonic toothbrush and periodontal instrument test cases under passive movement. The changes in total forces were observed over the progress of the motion cycles and compared to the risk output measurements. Maximum total forces on the ProDENT instrument generally ranged from 2.19 N to 4.77 N, except during active jaw movement that produced a maxillary jaw collision that had a sudden high total force of 31.80 N. The maximum forces for the sonic toothbrush and periodontal probe were 1.87 N and 0.55 N, respectively. For preliminary procedure block verification, sudden increases in force measured were usually associated with the timings and magnitudes of the risk data for high risk ID1.1 and 1.3 outputs, while the timing of high risk along the path was most related with the ID1.1–1.3 outputs.

Discussion

Surgical robotics has become more common in procedures to improve visibility, precision and patient outcomes. This thesis aimed to redefine the future of dentistry with the potential inclusion of autonomous dental robots and supervision systems to maximise patient safety. Correct implementation of robots is critical to develop trust in both patients and clinicians, which in turn helps to create a more stable and safe dental environment for robots to perform high quality dental procedures. The innovative dental setup considers changes to

overcome major hazards in the dental environment with the use of devices such as intraoral scanners for oral analysis and dental technique planning. The proposed supervision models reduce the responsibility of the dental operator and to build redundancy for safety into the proposed robotic dental setup. Research design and analysis were undertaken to develop a supervision system to check that the robot's dental instrument is safely navigating the oral cavity. The assessments developed here can be used to inform future risk analyses for medical robots that operate on conscious patients.

Initial dental robot applications were performed with the small Meca500 robot arm that is relatively non-confrontational and would be well suited to small dental practices. This was used to perform analysis on the validity of the spatial risk measurements for the supervision system and review areas for improvement. The 3D dental models in the game engine, Unity, created a dynamic dental environment for dental robot and supervision system testing. Future dental techniques, including charting and scaling, should be developed with dental clinicians to create a series of dental robots with increasing capabilities and define the relative importance of safety measurements for different dental instruments and techniques.

Conclusion

The dental robot design and risk framework developed in this thesis make progress towards overcoming barriers for robotic applications in dental services, with the aim of improving global oral health and access to dental services. If designed and implemented correctly, dental robots will be able to maintain a safe operative environment for a patient and improve working conditions for dentists. As these operating systems are developed, dental robots may begin to operate at high levels of autonomy for relatively low risk dental procedures, beyond those acceptable for traditional surgical procedures. In this way, robotic dentistry can act as a gateway towards true surgical autonomy for dental procedures.

Statement of Contribution

- I carried out the literature survey on the user needs of dental robotics from the perspective of both clinicians and patients to understand the major challenges and motivations for the chosen research problem.
- I carried out the literature survey on background involving dental anatomy and cost of dental services with feedback from Prof Hans Zoellner and Emerita Elizabeth Martin.
- I carried out the literature survey on background involving medical robotic systems, including dental robotics, and regulatory frameworks for autonomous and collaborative robotic systems.
- I investigated and designed the innovative dental setup and workflow for robotic dentistry, following feedback from Dr Graham Brooker and Prof Hans Zoellner.
- I re-designed the levels of medical robot autonomy to include risk and varying operator supervision, and Prof Hans Zoellner envisioned the sequence of dental robots for investment.
- I analysed the hazards of a dental robot system and contributions to risk and patient safety with feedback from Dr Graham Brooker, Prof Hans Zoellner and Emerita Elizabeth Martin.
- I developed the risk management framework for autonomous dental robots to improve robot situation awareness with feedback from Dr Graham Brooker and early input from Dr Ali Haydar Göktoğan as a risk management network that incorporates a supervision system divided into instrument, environment and patient safety.
- I designed and wrote the code for the supervision system spatial risk assessments of the instrument tip position and handle orientation in MATLAB.
- I performed preliminary verification investigations on hardware, including sensors and the robot arm, and the use of Unity for dental applications on tooth models that lead to the design of the Unity-based experimental setup that I used to carry out simulated dental techniques and assessments of instrument spatial safety.
- Conclusions are my own, and influenced by Dr Graham Brooker, Prof Hans Zoellner, Emerita Elizabeth Martin and Dr Ali Haydar Göktoğan.

The above represents an accurate summary of the student's contribution.

_____

_____

Student: Evie Deaker 4 August 2025

_____

_____

Supervisor: Graham Brooker 4 August 2025

List of Authored Publications and Conferences

EMBC Conference 2023

E. M. Deaker, H. Zoellner, A. Haydar Göktoğan, F. E. Martin and G. Brooker, "The Future of Dental Care: The Manipulation of Dental Instruments & Preparation Towards Automated Tooth Cleaning," *2023 45th Annual International Conference of the IEEE Engineering in Medicine & Biology Society (EMBC)*, Sydney, Australia, 2023, pp. 1-4, doi: 10.1109/EMBC40787.2023.10340087.

E. M. Deaker, H. Zoellner, A. Haydar Göktoğan, F. E. Martin and G. Brooker, "The Future of Dental Care: The Manipulation of Dental Instruments & Preparation Towards Automated Tooth Cleaning," *Poster presented at the 2023 45th Annual International Conference of the IEEE Engineering in Medicine and Biology Society (EMBC)*, Sydney, Australia, July 2023.

IADR Conference 2023

E. Deaker, G. Brooker, F. E. Martin, A. H. Göktoğan and H. Zoellner, 2023, "Patient risk management and roadmap for automation of robotic dentistry," *Oral presentation address, 62nd Annual Scientific Meeting for the International Association for Dental, Oral and Craniofacial Research (IADR)*, Australian/New Zealand Division, Sydney, Australia, September 27, Abstract ID: 80.

Journal 2025

E. M. Deaker, H. Zoellner, F. E. Martin, A. H. Göktoğan and G. Brooker, 2025, "Simulated Risk Mapping for Safe Robotic Dental Techniques: Spatial Assessments of Instrument-Patient Interactions." In "Recent Advances in Digital Dentistry: Era of AI and Immersive Technologies (virtual, augmented and mixed reality)." Special Issue, *International Journal of Dentistry*, (submitted).

Acknowledgements

Initially, I would like to begin by thanking the two people that invited me to begin my thesis in robotic dentistry, my supervisors Dr Graham Brooker and Prof Hans Zoellner. I was lucky to have very active supervisors that wanted to meet on a regular basis to discuss my topic, research and wellbeing. To Graham, thank you for your responsive emails, zoom chats and guidance through my PhD. I greatly enjoyed our brainstorming sessions in meetings for developing areas of my project, as well as the annual lunch outing with your other students. I would like to thank Hans for being very welcoming to including me in meetings with other researchers in dentistry to develop my understanding of the field. Also thank you to Hans for accompanying me to attend the biomedical engineering and dental conferences in Sydney and for our coffee catch ups at Ralphs.

Thank you to Emerita Elizabeth Martin and Dr Ali Haydar Göktoğan for your useful feedback throughout the project and for broadening my understanding of dentistry and robotics, respectively. I would also like to acknowledge my supervision panel, Dr Mitch Bryson and again to Emerita Elizabeth Martin, for their attention during progress meetings and providing valuable guidance for the focus of future work. Along with my supervisors, this group of people have helped me shape the project into a piece of work that I am very proud to be a part of and that I know will influence my path into my future career. Thank you to the dental team participants for discussing their research and knowledge of dentistry with me, most notably Associate Prof Dale Howes, Dr Eduardo Delamare, Dr Michael Hornby, and also to Emerita Elizabeth and Dr Ali Haydar Göktoğan for also attending these meetings to share their expertise. Thanks to Dr Ken Hooi from CREED CE and Associate Prof Dale Howes from Sydney Dental Hospital for advice and assistance with the intraoral scanning and model CT

scans, respectively. The research reported in this thesis was supported by the award of a Research Training Program scholarship which I received as a PhD Candidate.

I would like to express my appreciation to the FABLAB team from Mechanical Engineering at the University of Sydney, most notably to Ben van Magill, Julian Guinane, Zach Benitez and Lauren Punter, for your friendship and support as I carried out my PhD endeavours. It has been a joy to see the workspace be used for exciting engineering projects and I have enjoyed that I could be of help to so many students developing into problem solving engineers. I greatly appreciate the opportunity to also be part of the Postgraduate Research in Engineering Student Society (PRESS) after COVID-19 lockdowns. This opportunity made the transition back to campus allow me to meet a great group of researchers from across different fields of engineering and explore more ideas with interesting discussions and a collaborative and friendly environment. I would also like to thank the technical staff and the other researchers from the Australian Centre for Robotics for their assistance in developing my robot setup.

Most of all, I would like to thank the support of my family and friends. To my sister Dione, thank you for your countless hours proof-reading my thesis and helping to express my ideas. I greatly appreciate your continued support and frequent video call check-ins, especially as you are creating your own adventures over in the US. Thank you to my friends and fellow researchers from engineering and the ACFR, especially to Rebecca Simpson, Athiya Azeem, Tara Bartlett and Jack Naylor, for their support as we carried out our PhD research together. I would particularly like to thank my husband, Edmundo IV, for encouraging me to work hard, for your wonderful cooking, your patience and company while working late at night. Finally, I would like to thank my parents, Michelle Deaker and Graeme Deaker, for being my role models in health technology and engineering, listening to my technical concerns and providing logical advice on how to move forward, and also my extended family, for their unconditional support as I carried out my project.

Abbreviations

AHRS – Attitude Heading Reference System
AI – Artificial intelligence
AR – Augmented reality
CAD/CAM – Computer-aided design/computer-aided manufacturing
CBCT – Cone-beam computed tomography
Cobot – Collaborative robot
CPD – Coherent Point Drift
CT – Computed tomography
D-H – Denavit-Hartenberg parameters
DAQ – Data Acquisition
DOF – Degree of freedom
DTW – Dynamic Time Warping
ETA – Event Tree Analysis
EU – European Union
FDA – Food and Drug Administration
FDI – Fédération Dentaire Internationale
FMEA – Failure Modes and Effects Analysis
FTA – Fault Tree Analysis
GDP – Gross domestic product
GSR – Galvanic skin resistance
HRC – Human-Robot Collaboration
HRI – Human-Robot Interaction
HTM – Hazard Traceability Matrix
ICP – Iterative Closest Point
ID – Interpreted Data
IEC – International Electrotechnical Commission
ISO – International Organisation for Standardisation
LA – Local anaesthetic
MDP – Markovian Decision Process
MDR – Medical Device Regulation
MoI – Mode of Interaction
MSD – Musculoskeletal disease
OECD – Organisation for Economic Co-operation and Development

OCT – Optical coherence tomography
PHA – Preliminary hazard analysis P
PMA – Premarket Approval
RMN – Risk management network
RMSE – Root mean square error
ROI – Region of interest
RPN – Risk priority number
SOP – Standard Operating Procedure
STEP – Sequentially Timed Events Plotting
TCP – Transmission Control Protocol
TORS – Transoral robotic surgery
TR – Technical Report
TRF – Tool Reference Frame
UML – Unified Modelling Language
UK – United Kingdom
US – United States
URDF – Unified Robotics Description Format
URS – User Requirements Specifications
VR – Virtual reality
VAS – Visual Analogue Scale
WHO – World Health Organisation
WRF – World Reference Frame
WSTE – Wrong site tooth extraction

Chapter 1: Introduction

1.1 The Oral Cavity and Dental Diseases

The oral cavity, commonly known as ‘the mouth’, is the primary component of the digestive system that breaks down food [1, 2]. Teeth are fixed into sockets in alveolar bone processes that arise from the maxilla (upper) and mandibular (lower) jaw bones. The periodontal ligament is a fibrous tissue that anchors the roots of teeth to the surrounding alveolar bone. The gums are formally called ‘gingivae’ and are dynamic soft tissues, together with the soft and hard palate, oral mucosal lining of the cheeks, lips and tongue (Figure 1.1). While the lips, cheeks and tongue are highly flexible and mobile, they abut gingival and palatal tissues that are firmly attached to underlying bone. The posterior border of the oral cavity is bounded by the soft palate, the palatopharyngeal and palatoglossal arches which enclose the tonsils, and the posterior dorsal surface of the tongue. The mechanical flexibility and mobility of soft tissues combined with their similarity in colour creates a challenge for technology to track important soft tissue features together with movement of teeth in their dental arches during dental procedures.

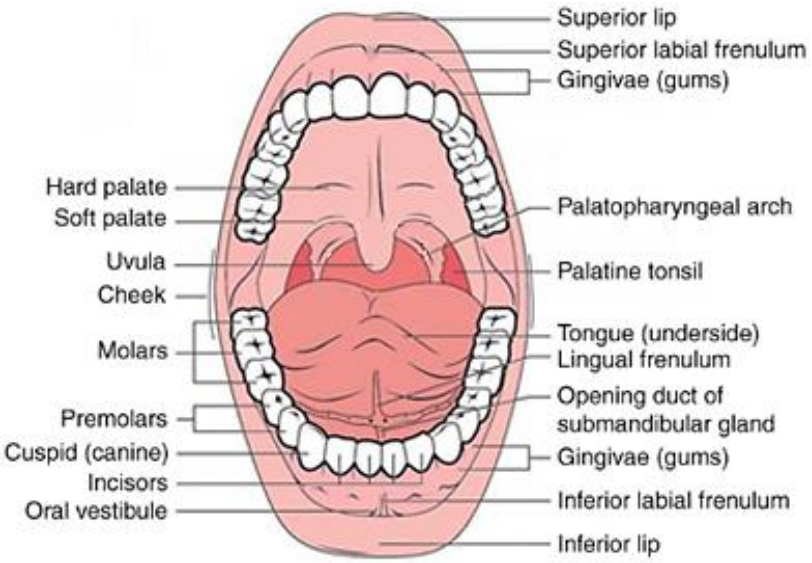

Figure 1.1. Anterior view of the oral cavity with the hard and soft tissues labelled [1].

Humans are heterodonts with four different forms of teeth. From the front to the back of the mouth, these include: incisors adapted for scraping and fine cutting of food; canines that are shaped for grasping meat firmly; premolars formed to aid the shearing of meat; and molars that have cusps for grinding mostly plant foodstuffs [3]. The structural and functional variability of these teeth affects both the diagnosis of dental disease and treatment planning.

Maintaining oral health through preventative teeth cleaning at home and routine cleaning and check-ups by dental professionals is crucial to prevent the onset of dental diseases. Common dental diseases are driven by an adherent bacterial biofilm that evolves via a complex microbial ecology on the surface of teeth. Dental caries occurs when plaque bacteria metabolise fermentable sugars to generate acid waste products, and subsequently demineralise underlying tooth structure [4]. Saliva has antibacterial buffers and high concentrations of calcium and phosphate ions which are capable of slowing and sometimes preventing lesion progression by remineralising early caries lesions [3]. However, as dental caries progresses, bacteria eventually invade the tooth structure itself and can, with time, infect the vascular dental pulp that resides within the tooth and surrounding bone and soft tissues (Figure 1.2) [5].

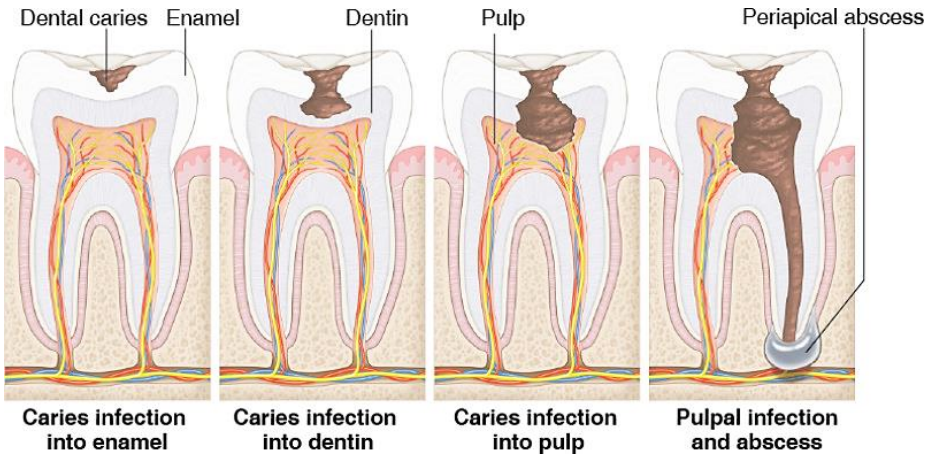

Figure 1.2. A diagram of caries progression to bone infection of a tooth [5].

Bacterial plaque can accumulate at the neck of the tooth and, if left unattended without sufficient teeth cleaning, it can form into hard calcified plaque deposits known as calculus [3]. This can lead to gingivitis as irritation to the gingival soft tissues occurs that causes inflammation and bleeding [3]. The progression of disease can result in periodontitis, a more destructive condition, which impacts the supporting structures of the teeth [6]. In periodontitis, the ligamentous attachment of the tooth to the bone is destroyed and the soft tissue attachment normally at the neck of the tooth moves down along the length of the root. Progressive destruction of the periodontal ligament reduces mechanical support for teeth leading to tooth loosening and eventual loss in severe cases [6-9]. Immediately adjacent gingival soft tissues and bone may be retained so that a 'periodontal pocket' forms and fills with plaque and calculus with the potential to cause a chronic inflammatory response (Figure 1.3). The periodontal pocket is largely inaccessible for regular teeth cleaning at home and requires professional cleaning.

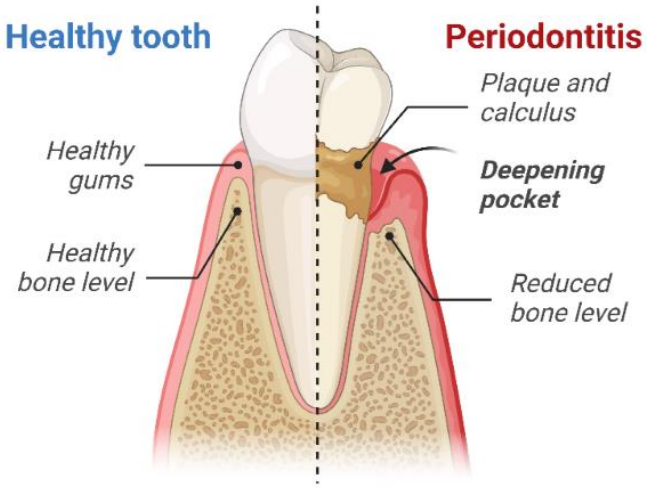

Figure 1.3. A diagram of a tooth where one half shows healthy tissue and the other half is affected by periodontal disease with resorption of the alveolar bone tooth socket, periodontal ligament attachment loss, periodontal pocket formation and receding gingiva [10].

Dental diseases can be categorised as reversible, where there is no permanent damage to the underlying bone structures (Figure 1.4) [3]. With timely diagnosis and early prevention, it is possible to reverse the progression of some common dental diseases and prevent tooth loss. Though, function and aesthetics may be restored following extraction by manufacture of bridges, dentures, or implants anchored in bone. These treatments are typically conducted under local anaesthesia [3].

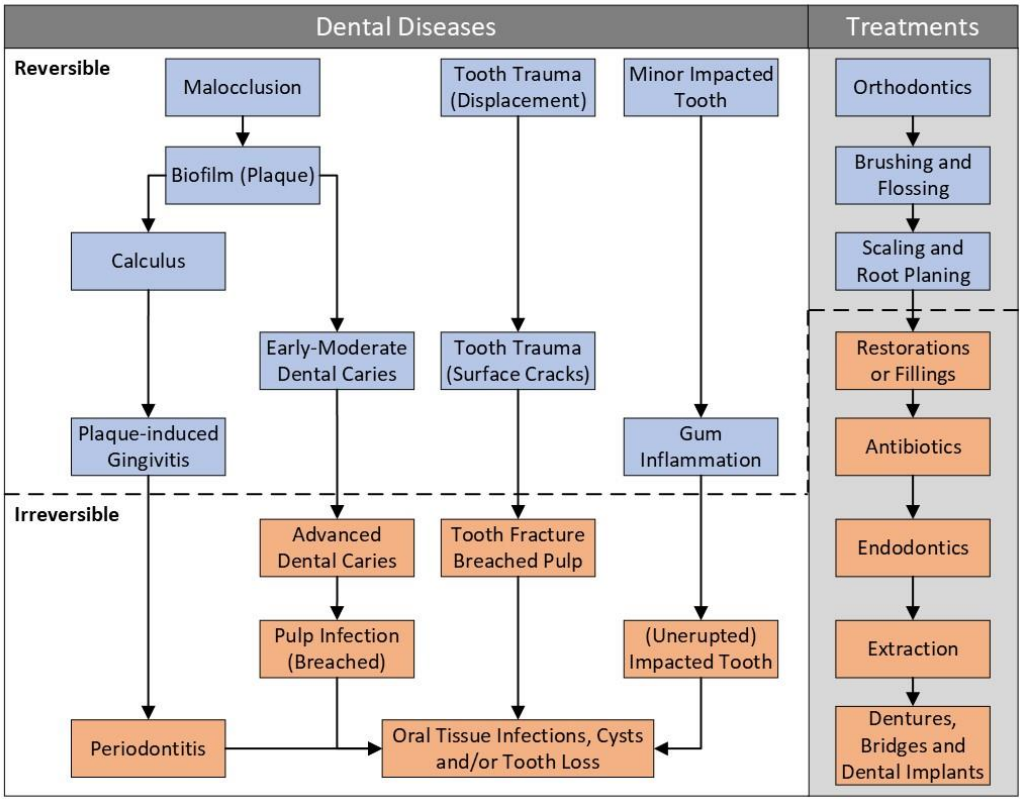

Figure 1.4. The progression from poor oral health to the development of dental diseases, along with dental techniques to manage or treat the diseases. The reversible dental diseases and treatments are in blue, and irreversible dental diseases and treatments are in orange.

Dental health is critical for mental health, perception of appearance, lifestyle, and general wellbeing [11-13]. Oral diseases typically present with a lack of symptoms and pain until disease becomes advanced [7], resulting in a high prevalence of undetected dental disease and complications. Accessibility to dental services is severely limited in many communities, not only due to the inadequate size and maldistribution of the dental workforce, but also the high cost of dental care. This reduces the opportunity for early diagnosis and intervention of dental diseases. This thesis explores the development of autonomous dental robots with a view to overcome accessibility barriers for dental care. If designed and implemented correctly, robotic dentistry has the potential to significantly reduce cost and accessibility barriers, and to improve safety, comfort and effectiveness of dental care.

1.2 Health and Oral Care Costs

Dental disorders, including dental caries, periodontal disease and tooth loss, affect 3.47 billion people globally and are amongst the most common health conditions [14]. Periodontal disease affected 796 million people in 2018, accounting for approximately 23% of oral health conditions [14]. Severe cases were reported to affect 11.2% of the global population between 1990 and 2010 [15]. Untreated dental infections are associated with increased incidence and severity of important systemic conditions including: cardiovascular disease; stroke; low birth weight pregnancies; pulmonary infection; poor diabetic control; and Alzheimer's disease [16-23]. As people over the age of 30 are more susceptible to severe periodontal disease, its prevalence is expected to increase with the aging global population. The World Health Organisation (WHO) estimates that the proportion of the population over 60 years of age with severe periodontal disease will nearly double from 12% in 2015, to 22% by 2050 [24].

The national cost of treating human disease is appreciable, while health expenditure as a proportion of gross domestic product (GDP) has more than doubled over the last 50 years irrespective of nation (Figure 1.5A) [25, 26]. Dental diseases were the third largest direct expenditure for a major disease in Europe (~746 million people), accumulating to €90 billion in 2015, with only diabetes and cardiovascular diseases costing more at €119 billion and €111 billion, respectively [27]. In the United States with a population of approximately 333 million, the estimated direct cost of dental diseases was reported at $119.071 billion USD in 2015 [28], of which approximately 50% was spent on preventive care [29], and national dental expenditure was reported at $165 billion USD in 2020–21 [30]. However, the average dental expenditure among OECD countries remains around 0.4–0.5% of GDP (Figure 1.5B). Without government intervention, widespread improvement of dental education and improved accessibility to quality dental services, the number of people suffering untreated oral diseases is likely to increase as the global population grows and ages.

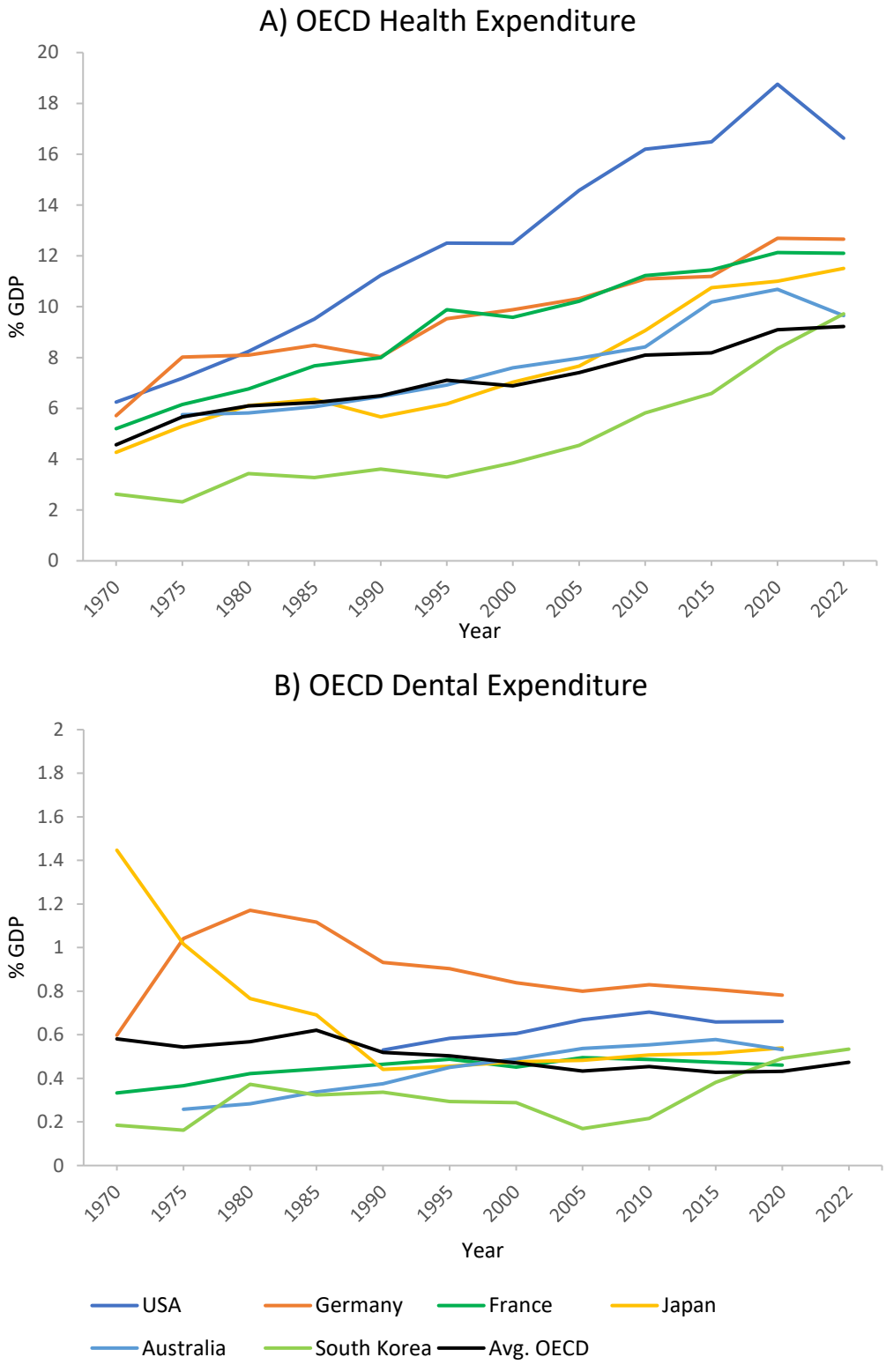

Figure 1.5. Expenditure data as a proportion of GDP for OECD countries over 50 years from 1970 to 2022: A) Health expenditure effectively doubled across all OECD jurisdictions shown over the period 1970 to 2022; B) The proportion of GDP devoted to dental expenditure increased appreciably across most OECD jurisdictions, during the 1970 to 2020 period (data sourced from [31]).

In Australia, there are approximately 72,000 preventable dental hospitalisations that occur per year [32]. Overall, Australia spent $11.077 billion AUD in 2020–2021 providing dental care for a population of about 26 million (Figure 1.6A) [33]. Since a peak of government contribution in 2012, government funding into dental care in Australia has remained at approximately $2.3 billion AUD (~$86.8 AUD per capita), although the costs to other sectors increased from $6.5 billion in 2012 to $8.8 billion AUD in 2021. Of this, individuals and health insurance funds spend $6.489 billion AUD and $2.295 billion AUD, respectively [33]. Despite an ageing population with increasing needs, per capita spending per year has not increased appreciably (Figure 1.6B), suggesting no improvement in access to treatment for dental diseases. Moreover, a survey from 2017–2018 found that 42.5% of the Australian population do not visit a dental professional for a yearly checkup [33].

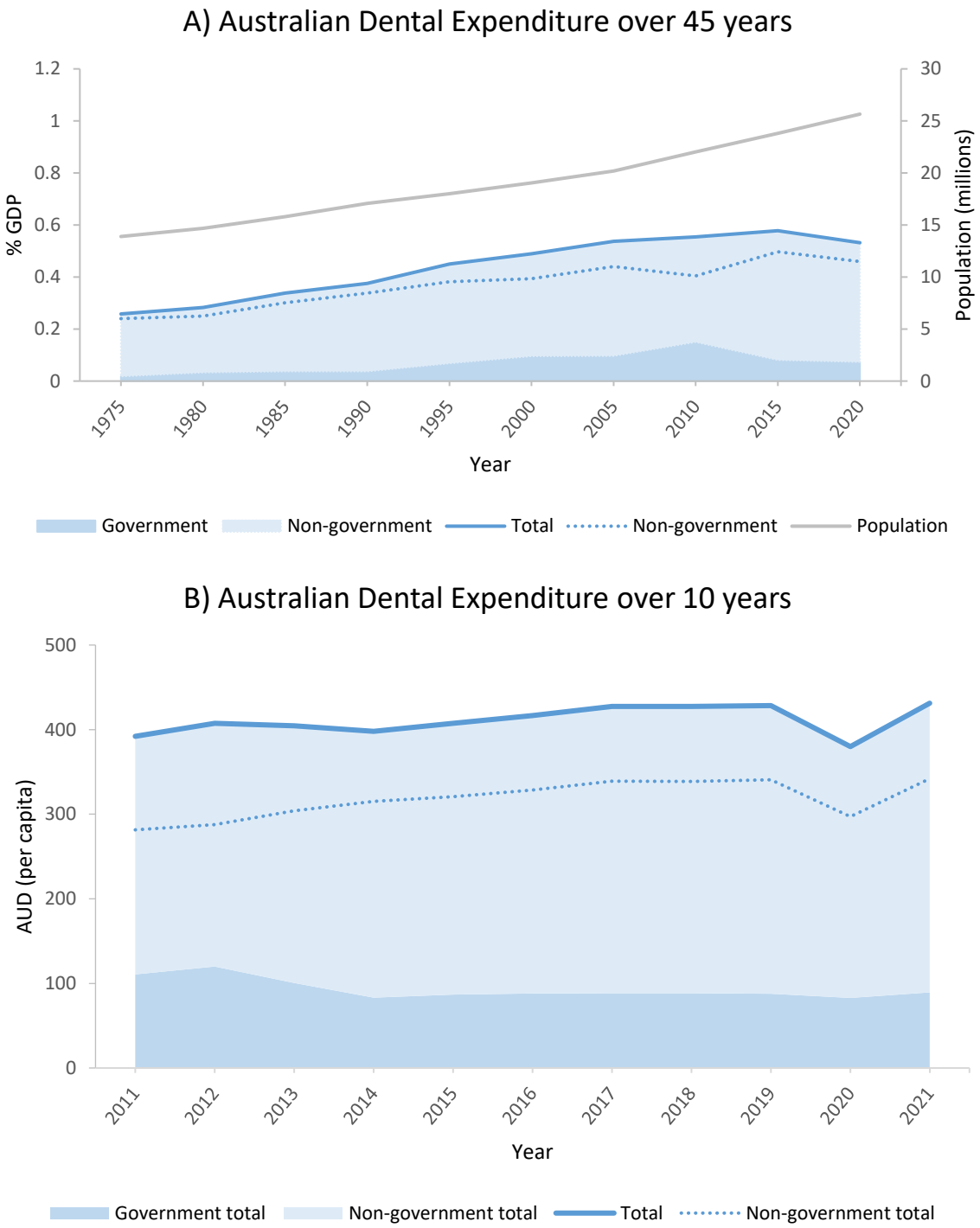

Figure 1.6. Total dental expenditure for government and non-government groups (including individual and health funds) in Australia: A) as a share of GDP from 1975 to 2020 compared to the total Australian population; B) per capita from 2011 to 2021 (data sourced from [31, 33, 34]).

1.3 Barriers to Dental Services and Surgery

Dentistry differs from other surgical specialties, as almost all treatment is delivered to fully conscious patients where local anaesthesia may or may not be required, depending on the procedure performed. Although dental cleaning procedures are considered lower risk than most medical surgical procedures [35], treatment can be uncomfortable or painful. Dental cleaning is considered relatively invasive because the procedure can cause damage to gingival blood vessels with potential for bleeding, and bacteria from plaque enter the circulatory system via damaged gingival microvasculature. Furthermore, the removal of calculus and plaque during cleaning requires administration of appreciable energy to the tooth surface causing discomfort in an emotionally charged part of the body, the face.

While there is a high prevalence of dental disease, cost is a major factor that limits the ability and willingness of individuals to access dental services. High levels of dental anxiety and fear also continue to plague dental services where noisy, sharp and sometimes painful dental instrumentation can be intimidating for patients [36, 37]. In the United Kingdom, a survey of over 7,000 participants reported that 11.6% had high dental anxiety in 2013 [38]. Furthermore, a study of 1,084 Australians in 2010 found that the cost of dental treatment was the greatest contributor to anxiety at 64.5% [39]. From 2016–2017, 2.54 million Australians skipped or delayed necessary dental care at least once, where 1.3 million reported that this was due to the cost of dental care and 435,500 people said they disliked or feared the dentist [40]. The cost could also influence the ability for individuals who have a physical or cognitive disability that affects memory or motor control, such as those with dementia or Alzheimer's Disease, to afford assistance to maintain a healthy mouth [18, 41-44].

With the COVID-19 pandemic in 2020–2021, fear of disease transmission heavily impacted the dental industry [45]. In Australia, this is reflected in a $1.1 billion or $48.47 per capita reduction in dental expenditure in 2019–2020 (Figure 1.6B). During this time,

individuals were forced or opted to skip dental check-ups, and to delay treatments as governments implemented worldwide lockdowns and restricted access to healthcare facilities to emergencies only [46]. A survey in the United States by the Kaiser Family Foundation found that 52% of households had a family member who cancelled or delayed their dental or medical appointment due to the pandemic [47]. Similarly, approximately 73% of participants in a 480-person survey in India chose to not visit the dentist during the pandemic in 2020 and nearly 20% (up 3% from before the pandemic) stated they would not visit the dentist even if they required treatment [48].

Inequity and shortages of dentists are particularly prevalent in countries with large rural populations [49, 50]. In Australia, there are only 26.3 dentists per 100,000 people in remote areas, compared to 63.8 per 100,000 people in major cities in 2020 [32]. This divide is reflected by the incidence of untreated decay with an estimated 37% in remote areas compared to 23% in major cities [51]. This underscores a need to develop technologies that can facilitate robotic tele-dentistry, related to the current thesis. Over 3,000 Australian dentists were reported volunteering an average of 30 days a year in 2011–2012 to overcome the inequality in access to dental services, equating to almost half a million hours [32, 52]. This is now equivalent to around $39.5 million, based on the average dentist income of $76.92 per hour in 2023 [53]. In Taiwan and Thailand, efforts to improve access to dental care through universal health coverage increased overall utilisation of health services, although this was ineffective at reducing inequity and improving accessibility in rural areas [54, 55].

The thesis comprises work towards addressing these barriers using autonomous dental robots. Due to the accessibility of the oral cavity and comparatively low-risk nature of cleaning procedures, developing autonomous robots for dental procedures will act as a launch pad for the more widespread incorporation of robots to address barriers in the medical industry. Similar to difficulties in dentistry, barriers to access remain especially problematic for general surgery.

In 2010, 16.9 million people died for lack of access to general surgery, comprising a staggering 32.9% of all deaths that year [56]. In 2015, 5 billion people could not access surgery and while there are 313 million surgeries per year, only 6% of these are in countries where one third of the global population resides [56]. Furthermore, one-quarter of those who received surgery in 2015, suffered financial catastrophe from the cost [56].

It is clear that there is inequity in access to all aspects of surgery, As one third of the world's population dies each year because of lack of access to surgical services [56], a strong case can be made for the development and deployment of autonomous surgical robots.

1.4 The Potential of Surgical Robotics

Although there has been significant advancement in the mechanical aspects of surgical robots, there has been only limited progress in autonomy. Surgical medical robots still require a surgeon to plan and execute robotic surgical procedures [57]. Autonomy in perioperative decision making remains a critical engineering barrier for surgical robotics.

Advances in surgical robotics and computer-assisted surgery have allowed robots to integrate into medical practices. They have enhanced procedure visibility, precision, quality and miniaturisation, thereby helping to improve patient outcomes and the speed of postoperative recovery [58, 59]. Robot-assisted techniques have been successfully utilised in many procedures, such as cardiac surgery, urology and gynaecology [60]. These systems have been designed to be operated by experienced and trained professionals and offer shorter recovery times and reduced complication rates [61]. Transoral robotic surgery (TORS) uses the da Vinci Surgical System platform by Intuitive and can be controlled by surgeons through remote operation, known as telepresence, acting as an extension of a surgeon’s hands to access tumours of the mouth, throat and skull base by minimally invasive surgery through the oral cavity [62, 63]. This has been found to have lower morbidity, shorter hospitalisation and faster

postoperative recovery, although it is expensive [62, 63]. The upfront cost of a da Vinci platform is more than USD $1 to 2.3 million depending on the system model, with a yearly additional 10% running cost [64, 65].

Traditional robot structures have been built using rigid links for improved position accuracy and precision, however this heightens their potential to harm people during collaborative human-robot applications [66]. Improvements in the safety of robotic technology have allowed for the development of collaborative robots (cobots) that can continue to perform tasks near other humans by actively tracking or reacting to human actions, creating an increasingly shared robot-human workplace [66, 67]. One step further is an autonomous system where the robot functions without an operator. Autonomy has the potential to benefit clinical outcomes, improve procedure consistency, heighten reaction times, optimise procedure duration, reduce the hands-on requirements for operators, and provide economically valuable systems for clinical settings, such as the developing Smart Tissue Autonomous Robot [68]. There is the possibility that robotic surgery can decrease surgical risk, but this can only be achieved with deliberate and proper design.

1.5 The Safety of Collaborative Robots

The most common type of robot has an arm that has six rotational joints with 6-degrees of freedom (DOF), such as the UR5 robot arm by Universal Robots and Meca500 R3 by Mecademic (Figure 1.7A) [69]. Although such robot arms offer the advantage of high precision for surgery, industrial robots produce large torques which place the patient and surgeon at risk of a high force impact. The amount of energy in a collision between a robot and human is affected by: the strength and weight of a robot and its end effector to the instrument or tool; the robot's stopping distance; the relative speed; the response time; the contact area; the design and material compliance; and the effective masses of both the person and the robot [70, 71].

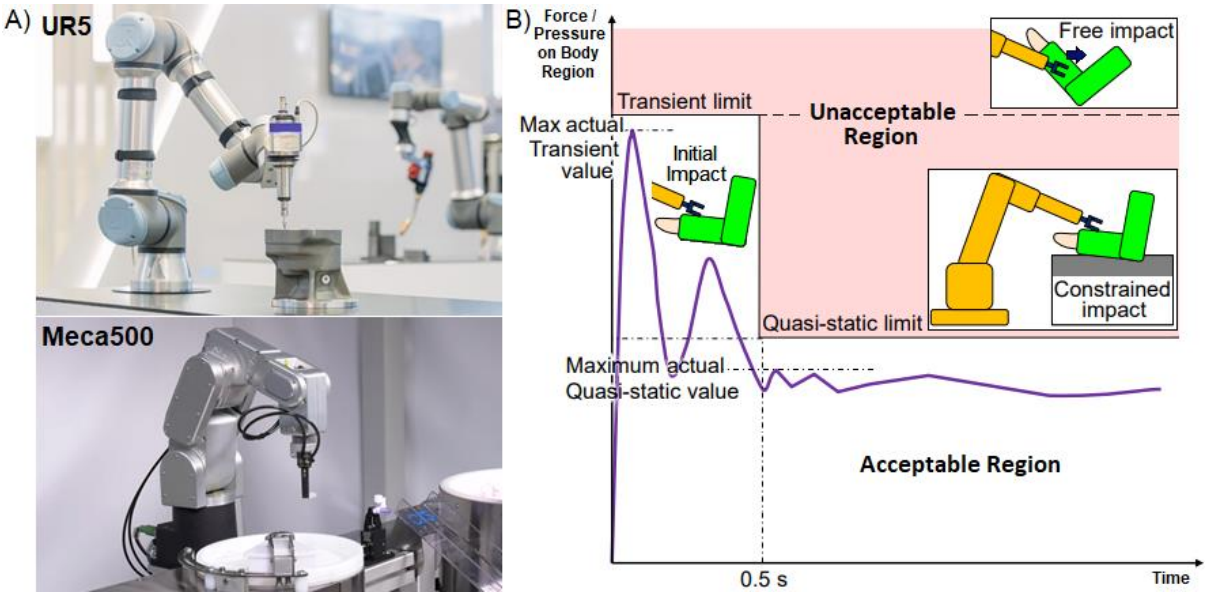

Figure 1.7. A) 6 DOF industrial robot arms (UR5 and Meca500) with revolute joints and B) graphical representation of transient and quasi-static collisions with limits representing the unacceptable regions for harm (red region) [70, 72, 73]. The permissible force regions have a white background. Initial impact that is constrained by another object or the inability to move away produces a constrained impact with a lower accepted force threshold, while free impacts where the human body part can be pushed or moved away.

A controlled human-robot interaction (HRI) can be used to improve robot safety and robot capability, regulating functions for parameters such as speed and torque. Impact with the robot can be described as transient where the person has space to move away on contact, and quasi-static when their movement is restricted against a nearby object in the local space. From the International Organisation for Standardisation (ISO), the standard ISO/TS 15066:2016 "Robots and robotic devices — Safety requirements for Industrial robots" defines that the quasi-static force on contact is measured as the maximum force after 0.5 seconds (Figure 1.7B) [70]. For most regions of the body, the transient limit is double the value of the quasi-static force limit [71].

During a collision with a robot, a patient will experience varying pain and injuries depending on the region of body experiencing the impact. The ISO/TS 15066 defines the biomechanical limit for permissible forces for the head and upper body regions to reduce the

overall risk of serious harm during human-robot collaborative operation (Table 1.1). Robots must not exceed a maximum quasi-static constrained impact of 65 N (squeezing contact) with a human face during any HRI [71, 74]. A slightly higher force of 130 N is allowable to the skull and forehead [71]. The related maximum allowable pressure has also been defined at 110 N/cm^2 for the face and temple region, and 130 N/cm^2 for the middle of the forehead [71]. Nonetheless, the maximum permissible transient forces on critical zones of the head are currently not distinguished from quasi-static force limits (identified as "N/A" for the transient contact multiplier) [71].

Table 1.1. ISO/TS 15066 collaborative maximum allowable forces for quasi-static and transient contact for upper body regions [71, 75].

Body Region	**Specific Body Area**	**Quasi-Static Contact***		**Transient Contact***		**Body Area (front/rear)**
		Pressure (N/cm^2)	Force (N)	Pressure Multiplier	Force Multiplier	
Skull and forehead	Middle of forehead	130	130	N/A	N/A	Front
	Temple	110		N/A		Front
Face	Masticatory muscle	110	65	N/A	N/A	Front
Neck	Neck muscle	140	150	2	2	Rear
	7th neck vertebra	210		2		Rear
Back and shoulders	Shoulder joint	160	210	2	2	Front
	5th lumbar vertebra	210		2	2	Rear
Chest	Sternum	120	140	2	2	Front
	Pectoral muscle	170		2		Front
Key: *Maximum allowable pressure or force						

Safety measures have been developed and standardised for transitioning from an isolated robotic operation to an interactive collaborative environment [76]. The ISO 10218:2011 safety principles related to robotic systems [77, 78] and the collaborative robot technical specification ISO/TS 15066:2016 describes four classes of safety requirements: 1) Safety-rated monitored stop; 2) Hand-guiding; 3) Speed and separation monitoring; and 4) Power and force limiting (Figure 1.8) [66, 79]. These standards were established for a more fail-safe design during HRI.

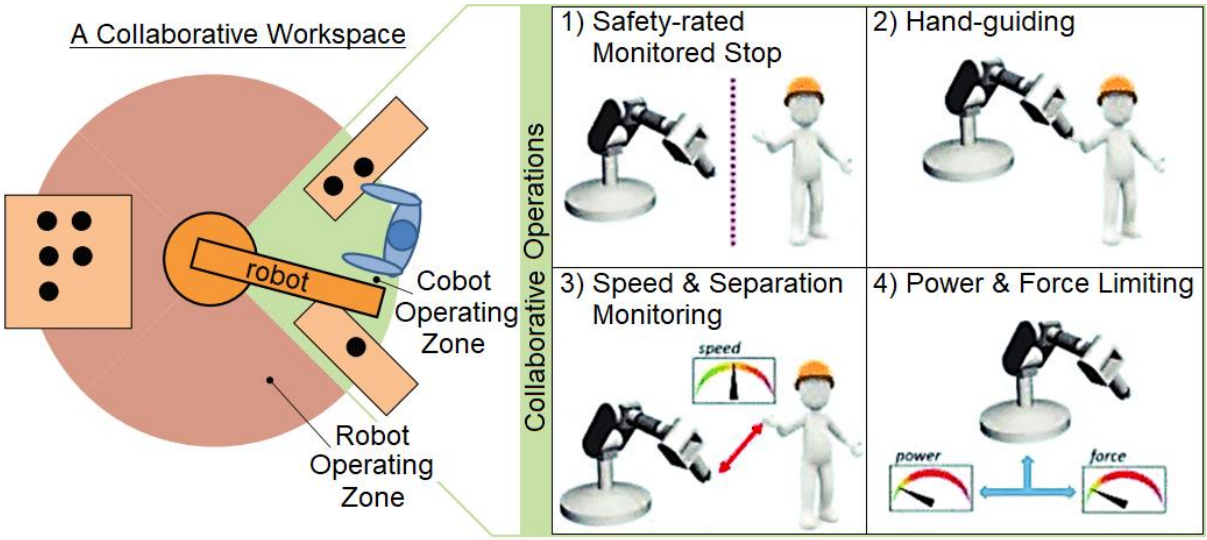

Figure 1.8. ISO/TS 15066 collaborative workspace and operative modes: 1) Safety-rated monitored stop where the robot continues movement until the person is nearby; 2) The robot responds to contact from the operators hand to control or adjust robot movement; 3) The robot's speed is reduced as a function of closeness to nearby persons; and 4) The power and force of the robot is controlled to avoid harmful accidental contact [71, 80].

A safety-rated monitored stop triggers when a person enters a 'static safety zone' near an automated or autonomous robot [66, 81]. In contrast to an emergency stop (e-stop) from ISO 13850:2015, it creates an "invisible fence" to ensure the robot does not move while in close proximity to operators [77, 82]. Speed and separation monitoring was developed so the robot slows or stops when an operator moves too close, and power and force limiting has allowed for increasing human-robot interactions [66, 77, 81]. These are very important for autonomous systems, especially where physical safeguards are impractical or not available, and as such pertain to the work of this thesis [83].

1.6 Research Aims and Thesis Outline

This thesis aims to assess the design of the dental setup and develop methods to manage the dynamic risk environment for transitioning towards greater autonomy for robotic dental systems in a way that maximises patient safety. Developments in this thesis will aim to maximise the benefits to patient comfort, potential improvements in dental care accessibility

and the level of laborious work for dental clinicians. This chapter (Chapter 1) introduced the anatomy of the mouth with background on dental diseases, expenditure and barriers to dental services, and the expected outcomes from the implementation of robots to surgery, while taking note of the constraints and relevant regulatory standards.

Chapter 2 presents an in-depth review of the status of the dental industry and the need for increased adoption of robotics, not just in dentistry but more widely in medicine. This includes issues faced by patients and dentists and current robot and navigation system technology. This assessment is used to develop the user requirement specifications for a dental robot and to propose a roadmap to the adoption of robots with increasing autonomy. A series of autonomous dental robots are identified that reduce the risk and investment barriers to their development and future implementation.

Chapter 3 explores the design setup and planning for robotic dentistry. The design strengths and limitations of robotic technology and their setups used in medical practices are assessed for how these can be improved for automated dental robots. A new design setup is proposed that maximises patient safety during autonomous dental robot procedures, accompanied by a discussion with reference to the Hierarchy of Controls for risk mitigation. A modified dental workflow is proposed for dental robotic procedures that identifies risk tracking as an important component to the development of safe dental robots. Standard levels of robot autonomy are amended to involve the necessary advancements in robot system risk awareness. These developments lead to the recognition that risk management is critical in the development of dental robots. For this reason, the latter of this thesis shifted focus to risk detection methods for real-time risk awareness which were defined within a risk management framework for dental robots.

Chapter 4 describes hazard analysis models and an analysis on patient harm is used to compare the current and proposed dental robot setups. A risk management framework for an autonomous dental robot is devised which comprises a supervision system for risk measurements of instrument, environment and patient safety. These are termed the procedure block, observer block and patient block. The important hazards to detect and track for automated supervision of robotic dental procedures are introduced for each subcomponent. Continuous evaluation of these measures during procedures aim to limit the likelihood of harm in procedures by directing the robot to operate in the acceptable mode of interaction with the patient.

Chapter 5 develops a subcomponent of the safety framework supervision system for spatial risk analysis of instruments operated by an autonomous robot, namely the procedure block. A virtual patient head model is used to analyse locations within the mouth for their instantaneous safety. Instrument safety is divided into four categories: the tip location relative to the nearest tooth; the handle entry location; the closest distance to the localised hard oral tissues; and the estimated closest distance to soft oral tissues. Their method risk outputs are compared for different instrument orientations or target locations around the dental arches.

Chapter 6 investigates the procedure block spatial risk measurements from Chapter 5 in a dynamic 3D environment by simulating diagnostic and cleaning robotic dental procedures. Data was collected to observe the changing forces, head model orientation and robot joint angles from the physical environment. These were compared to the risk measurement outputs calculated for the location of the robot's instrument tip in space for planned instrument paths. These experiments assess the potential for risk tracking to predict patient harm and to minimise the reliance on force-feedback mechanisms as the primary risk management measure for localised instrument control.

Chapter 7 is a discussion of the implications of this body of work for the incorporation of autonomous robots moving forward. Patient and dentist acceptance of autonomous robots is discussed, as well as future directions for research and robot development including the optimisation of dental techniques, the simulation of the dental environment, the use of artificial intelligence and assessments of other potential dental setups.

Chapter 2: A Gateway for Autonomous Surgery

2.1 Introduction

The numerous challenges and shortcomings of current dental practices cannot be overcome without significant changes to the dental environment [29]. Practicing dentists face a suite of challenges due to poor workplace ergonomics and high physical and mental demand that could be mitigated through the use of dental robots (Table 2.1). Specifically, dentists are required to maintain awkward static postures for prolonged periods of time and perform repetitive motions, leading to a significant risk of workplace injury, such as musculoskeletal injuries or pain [84, 85]. Notably, dentists are reported to have a 25% likelihood of becoming disabled [86]. To minimise the risk of developing musculoskeletal diseases (MSDs) and neurological side effects, dental professionals have been recommended to take regular periodic breaks, split time-consuming procedures into multiple appointments and to undertake regular repositioning, stretching, exercise and yoga [85, 87]. Implementation of proper ergonomics in

Bedi *et al.* (2015) was effective in reducing neck and shoulder pain in dentists by half [87], but strategies can force the dentist away from a patient-centric focus during their procedures.

Dentists are also at higher risk of catching a contagious disease from sick patients (Table 2.1). If dentists are cut by instruments contaminated with patient blood, there is potential for an exposure incident via transmission of blood-borne diseases, such as HIV, HBV and HCV [88]. Dentists also have close contact to the mouth of maskless patients and dental procedures using oscillating intraoral handpieces, ultrasonic scalers and air water syringes have high aerosol production [89]. Virus particles, such as the influenza virus, SARS or COVID-19, can be less than 5 microns in size allowing them to remain suspended in the air which makes them highly transmissible in a poorly ventilated environment [89]. During the COVID-19 pandemic, dentists were also affected by personal protective equipment supply shortages [90].

Practitioners are required to recognise when they and their colleagues are experiencing fatigue to help maintain a high standard of care and safety for patients, and to avoid an exposure incident or a patient-care mismatching event [91, 92]. This is crucial to avoid laceration as dentistry involves the use of sharp instruments in a critical region of the body sometimes with poor visibility and limited access [93]. Complications can also include poor root canal treatment, undiagnosed or ignored gum disease and nerve damage from faulty extraction of wisdom teeth or by the dental drill [3, 94]. Moreover, privately owned clinics are less likely to communicate the occurrence of harm that results from dental error, impacting the spread of knowledge and awareness for safety [35, 95, 96].

The lack of visual cues can make identifying the correct tooth a challenge for oral surgeons and dentists, and if there are many carious teeth it can be difficult to identify which teeth are meant to be restored [97-99]. This can cause a wrong site tooth extraction (WSTE) which is a serious incident that is completely preventable and was previously considered a

"never event" [100]. Conventional methods to mark an operative site with a sharpie or a dental burr are not reliable, while a marked radiograph or dental diagram is more accepted [99, 101, 102]. In the Fédération Dentaire Internationale (FDI) numbering system, each tooth is assigned an index defined clockwise from the upper-right region of the mouth (Quadrant 1) to improve accuracy of oral health records and to assist communication between oral health professionals [103]. However, missing or extracted teeth can provide space for the remaining teeth to drift, rendering standard dental charts inaccurate [98, 99].

Table 2.1. Health-related and other challenges affecting dental professionals with case studies.

Issue	Cause	Prevalence: Case studies	References
Musculoskeletal disease (MSD)	Prolonged static postures while performing repetitive tasks using oscillating dental instruments.	85% of dentists (n=71) used handpieces >11 hours/week and 41.2% reported work-related hand-arm vibration syndrome.	[104]
		In Brazil, dentists experienced the highest prevalence of neck pain and female workers had the highest prevalence of lower back pain.	[105]
		In a survey in Australian dentists (n=285), 87.2% had at least one MSD symptom: 57.5% of the neck; 53.7% of the lower back; and 53.3% of the shoulder.	[106]
Hearing Damage	Frequent use of noisy drill turbines and other oscillating instruments.	Obstructed suction (96.5 dBA) and unobstructed suction with an operating dental handpiece (94.8 dBA) exceeded the National Institute for Occupational Safety and Health (NIOSH) eight-hour time-weighted average permissible exposure limit of 85 dBA.	[107]
		USA, Oklahoma: For dentists aged 35–76 years (n = 144 people), the prevalence of tinnitus exceeded estimated national averages.	
Mental health	High stress due to: • Fear of making a mistake, complaints or litigation from malpractice • Dissatisfied or difficult patients • Frequent changes in regulation • Managing time and scheduling to meet targets with high patient turnover	In a UK study (n = 2,053), 54.9% were experiencing high job stress, where 43.8% stated that they could not cope, and 17.6% had seriously considered committing suicide (57.7% in the last 12 months).	[108]
		In a US study (n = 1,988), an average of 52.0% were stressed, 28.7% were emotionally drained, 21.7% reported being burnt out and 19.5% said they were fatigued.	[109]

Disease transmission and workplace injury	Patients may have a contagious disease, and dentists may be injured by sharp contaminated instruments due to non-technical human error.	In March 2020, the New York Times published an article that dentists were the most exposed workers at risk of contracting COVID-19 during the pandemic.	[46]
		Due to time spent sitting and exposure to infectious diseases and radiation, the two unhealthiest jobs in the US were reported as dental hygienists and general dentists.	[110]
		A study in Australia (n = 285) found that over 12 months, 78.5% of dentists had damaged their gloves and 27.7% of dentists had received a sharps injury (often a bur drill tip) or needlestick injury at least once, where 16.1% were contaminated by the patient's body fluids.	[88]
Dental Errors and Malpractice	Problems with situation awareness, fatigue, communication, teamwork, and leadership.	A total of 2,012 dental errors were reported in the UK in 2009, including: • 210 patient injuries where 35% were laceration and 23% involved the lip • 111 medical emergencies • 80 adverse reactions • 72 inhalations or ingestions of foreign objects • 36 wrong site tooth extractions (WSTEs) • 33 infection control incidents.	[93]
	Challenges with wrong site operations from limited number of visual cues, lack of vision, tooth drift (after an extraction), dental record errors and tooth mismatching events.	Wrong site tooth extractions are one of the largest causes for legal claims against oral surgeons and the cost of surgery was a third of all legal claims in the UK in 2006.	[93]
		Confusion between the required quadrant of the mouth has been reported as the cause of 15% of errors.	[97, 99]
		From April 2018 to March 2019, 42 wrong tooth or teeth removal surgeries occurred that accounted for 20% of all wrong site surgeries (previously considered as "never events").	[111]

For many, oral healthcare is impacted by not only the cost but also the lack of access to dental services (Table 2.2). Access to dentists is an ongoing issue in rural communities with fewer practicing dentists causing longer travel time and distance to clinics. Inequity is particularly present in regions such as Africa and Asia with a large rural population [54, 55, 112]. Rural participants of Burkina Faso with their maximum periodontal index scores ranked from 0 to 4, as healthy (0), bleeding (1), calculus (2), shallow pocketing (3) and deep pocketing at ≥6 mm (4), were reported to have more severe periodontal scores than did urban individuals (Table 2.2) [112]. However, the high presence of dental caries in urban areas of Africa is expected to result from the higher rate of sugar consumption [49].

Physical inaccessibility to oral care services can significantly affect the ability of patients to receive timely treatment for oral conditions and increases the occurrence of tooth extraction (Table 2.2) [44]. ICU patients that are dependent on health care providers, usually nurses, to provide their oral care [113, 114]. Elderly or handicapped people can experience upper limb disability or muscle weakness affecting their ability to perform general dental hygiene techniques without assistance [115]. Physical barriers for receiving dental care can include limited transport options, wheelchair-inaccessible practice, and inaccessible dental chairs [116, 117]. Reduced motor skills or dementia increases dependence on dental services or on others for oral care as well as their risk of harm, especially if there are communication difficulties [92, 118-120]. Furthermore, dentists may be unwilling to provide care for patients with cognitive impairment [121].

Table 2.2. Patient-related barriers to quality dental care with case studies.

Issue	Prevalence: Case studies	References
Fewer dentists and long travel time to receive dental care in rural areas	In Australia, there are 25.7 dentists per 100,000 people in remote areas compared to 63.1 per 100,000 people in major cities, contributing to an estimated 37% of people living with untreated decay in remote areas and 23% of those in major cities.	[51, 122]
	In Taiwan and Thailand, efforts to improve access to dental care through universal health coverage were effective in increasing overall utilisation of health services, but ineffective at reducing inequity and improving accessibility from urban to rural areas	[54, 55]
	In Africa, children aged 12–15 years are experiencing high prevalence of caries at 39.4% in urban areas and 27.8% in rural areas.	[49]
	Africa, Burkina Faso: Mean periodontal index score distributions for urban and rural areas, respectively, were 1.44 and 1.58 for 12-year-olds; 1.77 and 1.91 for 18-year-olds; and 2.33 and 2.67 for 35–44-year-olds.	[112]
Patients requiring medical and assistive dental care	Across 59 European ICUs, 67.8% of staff reported difficulties cleaning patient mouths and 39% found it unpleasant. Of these, only 32% had received oral health care training.	[113]
	Nurses (n=77) from 3 ICUs in the US reported the use of a toothbrush 38.9% of the time to provide oral care to intubated patients. Foam swabs (not effective for plaque removal) were reported to be used 91.5% of the time.	[123]
	In surveys, 54.7% of the residents in elderly nursing homes required some support for brushing their teeth, while only 36% of nursing home helpers and rehabilitation hospitals received training on brushing techniques and 64% felt that services were insufficient due to the lack of time.	[115]
	Some health conditions or types of medication can cause xerostomic or “dry mouth”, which heightens their vulnerability to developing oral diseases and dental caries.	[116, 124]
Access for people with physical disabilities or cognitive impairment including elderly or handicapped people	A US survey of spinal cord injury patients (paraplegics and tetraplegics) reported that they are 14.8% less likely to visit the dentist for dental cleaning at 54.6% compared to the general population at 69.4%.	[116]
	Researchers in South Korea found that people with disabilities have significantly higher prevalence of decayed, missing, and fewer filled teeth than people without disabilities. Those with disabilities are more likely to have a tooth extraction, rather than a restoration.	[44]
	Young children, epileptics and those with special needs are advised to be supervised when brushing to manage any injuries.	[125]
	A study in Italy (n = 91) found that 54% of dentists were not willing to treat individuals who could not collaborate during treatment or that had a cognitive impairment.	[121]

Increased robot use in dentistry would be particularly useful for performing repetitive dental procedures, reducing dentist fatigue, and allowing them to stay alert and ready to manage safety hazards or incidents. Robots would also greatly benefit patients and the public as the automation of simple repetitive procedures could promote accessibility to high quality dental services. The use of robots to perform dental procedures could additionally facilitate remote monitoring by expert dentists to rural areas, ease the workload for nurses and others for oral care, and improve access to dental services for patients or people with disability that need frequent professional assistance (Table 2.2). Notably, a number of dental practices transitioned to provide more tele-dental services in Australia as a result of the pandemic, greatly benefiting individuals who are immunocompromised or live in rural areas, but the potential for this was limited to visual inspections with a camera and patient feedback on oral pain [126].

The potential benefits for dental practitioners, patients, and managing the high prevalence of dental diseases globally highlight the extent to be gained from the safe implementation of dental robots. Over the past decade, advancements in medical robotic technologies and guidance navigation systems enable tracking of hard tissues of the oral cavity and dental instruments for precise surgical procedures. In this chapter, the recent developments are considered for their integration into a dental robotic system to facilitate autonomous dental procedures. From this, dental robot user requirements are defined for various dental applications, along with a roadmap for a staged approach to develop a dental robot with increasing capabilities to carry out autonomous dental techniques.

2.2 Current Technologies

Advanced dental implant surgeries with guided or robotic applications have demanded accurate tracking of the mandible. Mandible tracking and measurement methods have been coupled with markers or sensors mounted on mandibular teeth, mechanical linkage systems,

magnetic tracking systems, radiographic tracking, and even more complex video motion analysis [127]. These methods experience trade-offs between cost-efficiency and ease of implementation in clinical settings, accuracy and high processing time, and fixed markers or high radiation exposure [127]. The numerous approaches used highlight the challenges associated with the mandible's high degree of freedom of movement. For dental implant systems, highly accurate methods, such as visual guidance systems and passive arm tracking with marker-based radiographic imaging for the bone structure, have been prioritised to facilitate anatomically appropriate implant placement. An alternative modelling method has been developed called intraoral scanning. These scanners create accurate 3D models of dental arches without the need for radiographic imaging, and they have the additional benefit of generating a model of the gingivae which is required for diagnosis of conditions such as gingivitis during charting.

2.2.1 Visual Guidance Systems

Tracking the movement of both the patient and the dental instrument with a high degree of accuracy in real time is critical for robots to ensure high precision. While distinct objects or features can be used as "landmarks" for tracking [128], structures in the oral cavity have variable size and shape and may have suboptimal contrast in poorly lit environments, and thus complicating identification [128-130]. Fiducial systems incorporate distinct markers that have unique geometric shapes (e.g. barcoded) or high contrast to be quickly identified from visual, optical or laser sensors with a low chance of false positives [128, 129, 131]. Dental visual guidance systems take advantage of the ability to attach fiducial markers to the dental arch, facial regions, and dental instruments in order to track the angle of entry and depth of drilling for accurate implant placement.

Visual guidance systems have been introduced in dentistry for invasive dental procedures to overcome the limitations of human precision [132-134]. These are pre-

programmed “dental assistants” that use a computed tomography (CT) scan to guide oral surgeons to the correct positions for drilling and placing dental implants with real-time visual displays and sometimes with haptics to optimise instrument orientation and positioning [135-137]. A case study using the Navident system with stereoscopic imaging found that an inexperienced operator could accurately and precisely perform endodontic surgery (Figure 2.1A) [133, 134]. Moreover, RoboDent is a high contrast system that uses a stereoscopic infrared camera system and achieves implantations with higher accuracy compared to manual methods (Figure 2.1B) [132, 138].

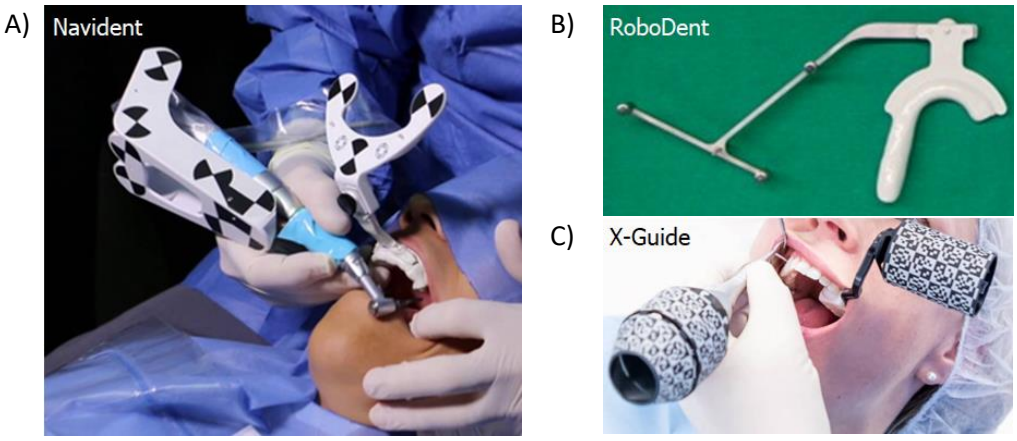

Figure 2.1. Dental visual guidance systems: A) Navident with binary markers; B) RoboDent using reflective spheres; and C) X-Guide with cylindrical coded markers [136, 138, 139].

For marker localisation to be successful, it is important that landmarks are positioned and fixed strategically to aid object tracking and navigation and to ensure a direct line-of-sight if required [128, 140]. A dental arch attachment is necessary as the soft tissues around the mouth do not provide a place to fix the markers, but it does impact the field of view for the dental surgeon. In some cases, while operating on the maxilla, a splint may be attached to the nasal bridge. The markers attached to the patient’s relevant dental arch and the dental instrument do not require power or wires to operate, and can be tracked using triangulation by stereovision [129, 131]. Triangulation is achieved by capturing at least two images of a scene

from slightly different perspectives using a pair of cameras positioned with a fixed and known horizontal displacement [130, 141].

2.2.2 Passive Arm Tracking Systems

Yomi, the assistive dental robot, uses an alternative tracking method. It localises the patient through a dental arch tracking passive multi-link arm, while the instrument is positioned by an active robot arm (Figure 2.2). This removes the risk of line-of-sight obstructions, false positives with coded markers, and errors in triangulation calculations for stereoscopic camera systems during the dynamic procedure. The passive multi-link patient tracker acts as a dentist's finger rest. The connection point for the patient tracker is attached to a patient splint that was registered to the cone-beam computed tomography (CBCT) radiography results from contrasting markers as a fiducial array for localisation [142].

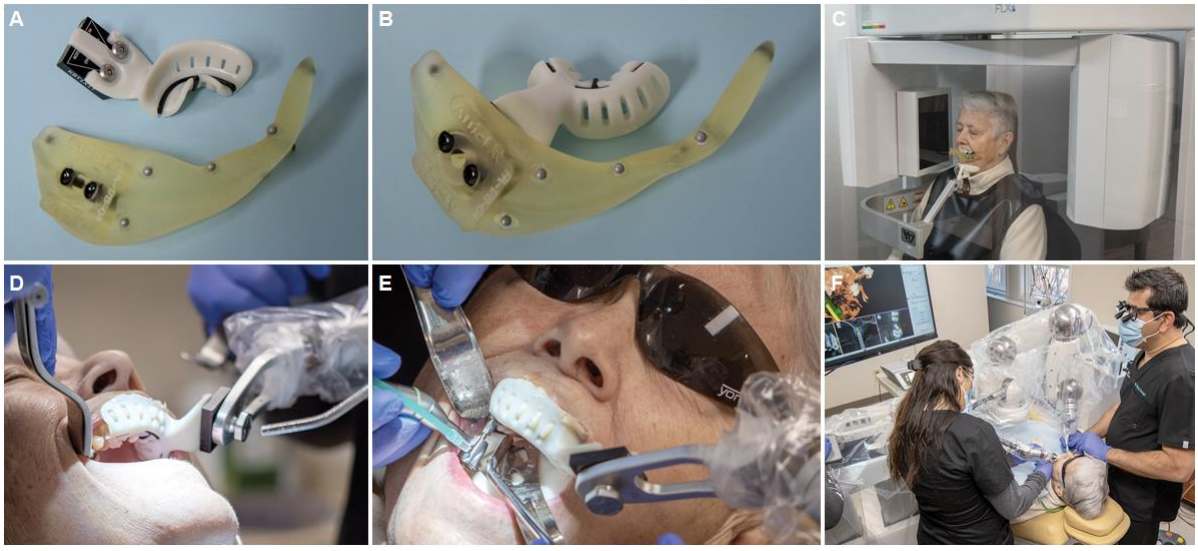

Figure 2.2. Yomi workflow procedure: A) Patient splint and contrasting insert with markers; B) Marker array connected to splint for CBCT; C) Patient undergoing CBCT; D) Yomi patient tracker connected to splint; E) Surgeon's hands controlling the handpiece; F) Operator monitoring with visual confirmation and stabilising haptics [142].

2.2.3 Imaging and Scanning Technologies

Non-contact intraoral scanners were developed to rapidly create real-time 3D digital impressions of the surface of dental arches of the mouth. The use of an intraoral camera was

more effective in detecting dental caries at 42%, compared to a visual examination at 28% [143]. This technique also replaces the conventional material-based impression techniques of mould-casting to improve workflow and patient comfort and also reduces the opportunity for errors from post-processing modifications to the model [144]. Separate intraoral scanners have been developed on the basis of confocal microscopy, optical coherence tomography (OCT), photogrammetry, stereovision, triangulation, interferometry and phase shift principles (Figure 2.3) [145].

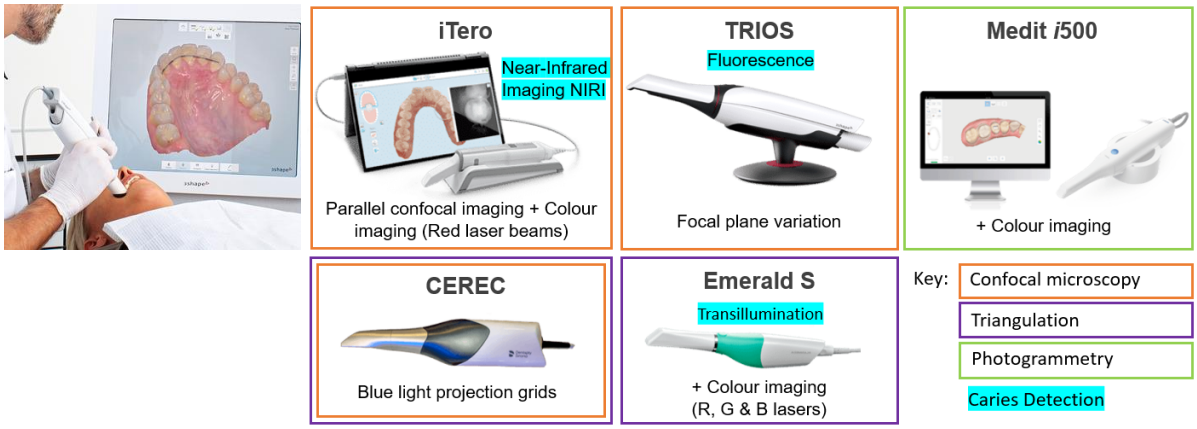

Figure 2.3. Intraoral scanning being performed on a patient and a comparison of different dental scanners [145-149]. Coloured boxes indicate their method(s) of depth imaging, and the highlighted text indicates the technology used to detect dental caries.

The company Invisalign uses intraoral scanners, such as the iTero scanner, to create accurate 3D models of patients' dental arches for orthodontic treatment [150]. Digitisation of impression techniques has increased patient acceptance, reduces the need for physical storage space, and allows 3D models to be sent digitally between clinicians [151]. Their image data can be used to identify surrounding soft tissues based on changes in colour [152]. Kihara *et al.* (2020) reported that intraoral scanners generally have a trueness between 50–250 µm [153]. In one study, the CEREC Primescan scored the highest in accuracy for trueness and precision [154]. Rather than relying on CT scans, automated dental robots would greatly benefit from the use of intraoral scanners.

2.2.4 Collaborative Robot Safety

Medical devices, such as dental robots, must have freedom from unacceptable risk in normal and abnormal operation (e.g. in single fault or failure conditions) [155]. These safety concerns, along with the lack of standards and high upfront cost of robotic systems, have restricted the professional acceptance and use of robots for routine medical applications. Dental robots predating the pandemic, Yomi and the Chinese dental robot, heavily relied on expert planning and supervision for dental robot applications. These were developed to surgically deliver dental implants by acting through the inner surface of the natural orifice, the mouth, and invading into the patient's body [156]. The COVID-19 pandemic accelerated the development of medical robots operating through inner surfaces natural orifices such as the oral cavity with developments in automated and remotely operated COVID-19 testing robots (Figure 2.4) [157, 158].

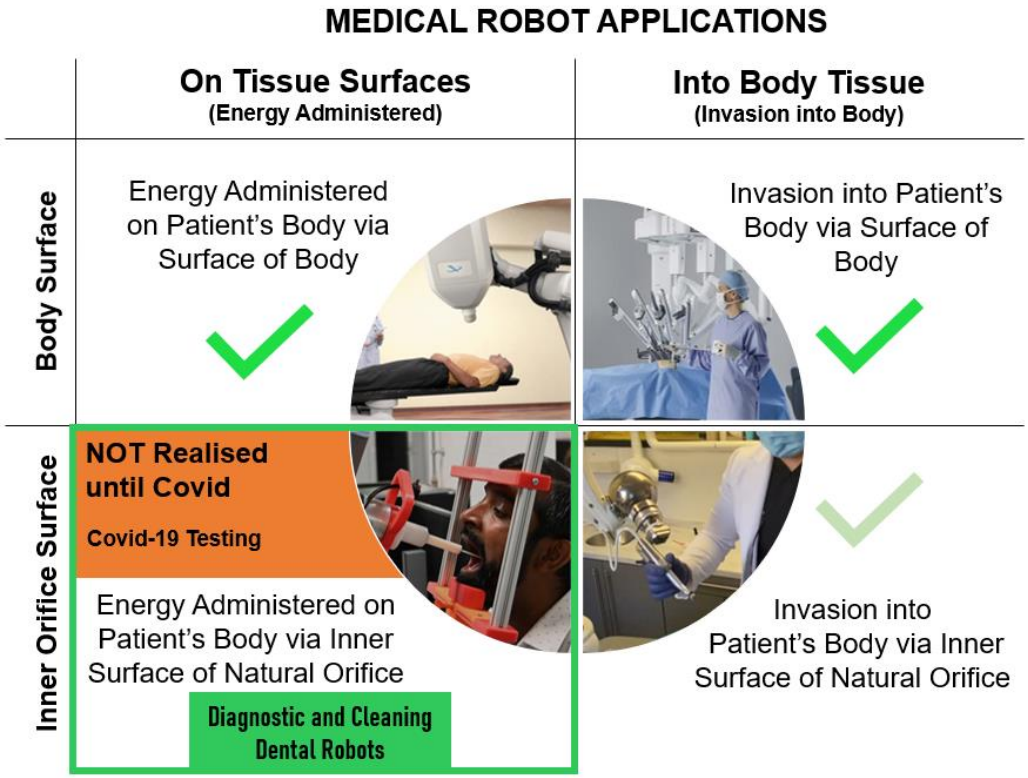

Figure 2.4. Modes of invasiveness for surgical robot systems involved in the scope of the IEC 80601-2-77 international standard for surgical robots (based on [156]).

Focussing on more simple cleaning procedures increases public acceptance for automated robotic procedures, especially where the cost is reduced. A survey from Embry-Riddle Aeronautical University in the United States of 502 people reported a high willingness to dental robotics with 68% respondents accepting the concept of a robot performing less complex dental procedures at full price, like tooth cleaning or whitening [59]. This value increased to 83% if the price could be reduced by 50% [59]. In contrast, 51% of respondents moderately or strongly opposed robotic dentistry, particularly when it involved invasive procedures [59]. Robot system design is important as comfort is critical to build a sense of safety [159]. Frightened patients can experience psychological stress associated with "ethical harm" [160]. The design for an autonomous Korean nasal swab robot, similar to the Chinese dental robot design, was considered terrifying [157]. A robot with a confronting appearance in size is not suitable for dental procedures or simple COVID-19 testing without clear physical protective features, such as a wall or chamber [161-164].

In order for dental robots to perform dental techniques with higher autonomy, they must overcome risk management challenges for safe operation. Current risk management processes are built for human-operated or guided robotic systems where the responsibility and decision making remain with the clinician, restricting the progression towards true automation beyond conditional autonomy (Figure 2.5) [57, 165]. The presence of a conditional autonomy "glass ceiling" is highlighted in a review on surgical robots cleared by the FDA from 2015 to 2023, where 86% of the total 49 surgical robots identified were at Level 1 Robotic Assistance, while 8% had Level 2 Task Autonomy and 6% reached Level 3 Conditional Autonomy [165]. For current medical device risk management systems, hazards are assessed in tables and built into documentation for standard operating procedures (SOPs), but they are not digitally evaluated and tracked throughout a procedure. There is yet to be a systematic method of risk management

for robotic systems that is automated, traceable, and transparent that can communicate risks to users and operators for the highly variable dental environment.

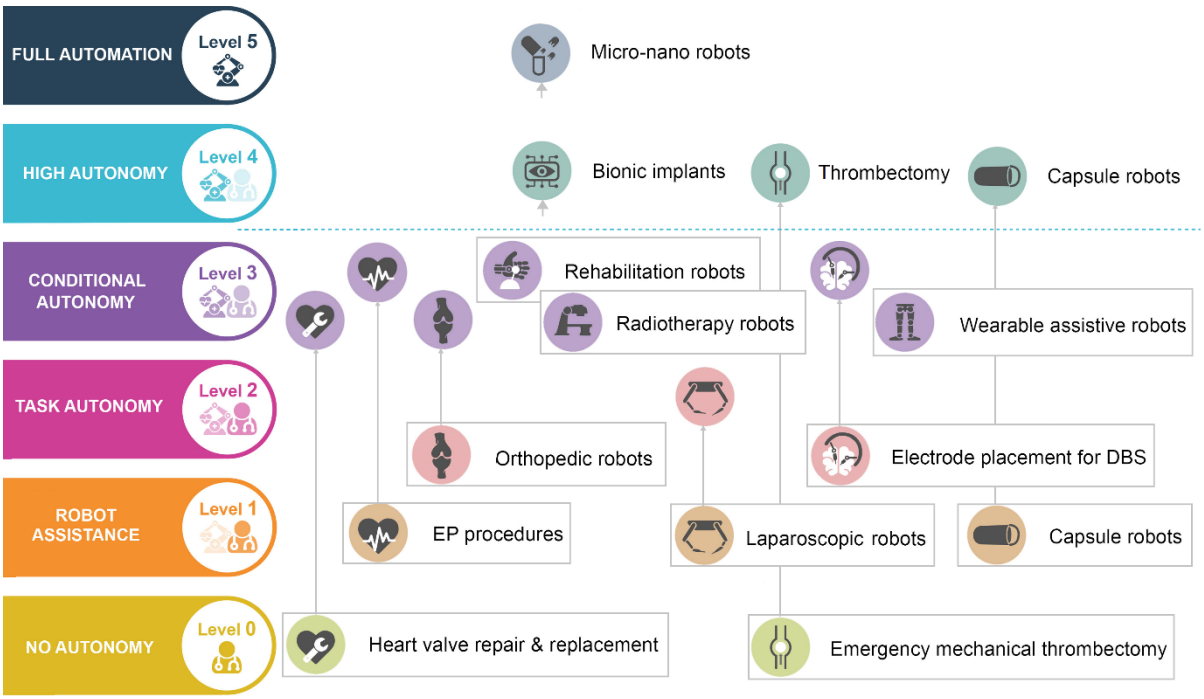

Figure 2.5. Current levels of autonomy for clinical applications with predicted future gains of increased autonomy based on need to improve accessibility (e.g. for emergency mechanical thrombectomy), safety of automation and required functionality. Conditional autonomy "glass ceiling" for most large medical devices indicates barriers due to the safety risks of autonomous systems (modified from [57]).

Robots are limited in the speed of movement for patient safety based on the mass and compliance of the robot, its end effector and the relevant regions of the body of the person, as well as the area of collision. This is particularly important when there is the risk of accidental quasi-static collisions and when using instruments with a small tip size, such as dental instruments, near and around a person's face. For current safety standards, the equations for kinetic energy, E_k, and elastic potential energy, E_p, are equated and assessed with the permissible maximum forces and pressures to define robot limits (Equation 2.1, Equation 2.2) [71, 75]. The kinetic energy takes inputs for mass, m, as the combined values for the robot and human head as elements in series to calculate a total effective mass, as well as the relative velocity, v, of the robot. The mass of the robot is half the mass of the moving robot arm links

and the full mass of the end effector [71, 75]. Assumed masses for parts of the body are used in robot safety assessments (Table 2.3). A collision's potential energy is calculated by the effective spring constant, k, of the deformable body tissue by its displacement, x.

Equation 2.1. $$E_k = \frac{1}{2}mv^2$$

Equation 2.2. $$E_p = \frac{1}{2}kx^2$$

Table 2.3. ISO/TS 15066 effective spring constants and masses for upper body regions based on a total weight of 75 kg [71, 75, 166].

Body Region	**Effective spring constant (k, N/mm)**	**Effective mass (m_H, kg)**
Skull and forehead	150	4.4
Face	75	4.4
Neck	50	1.2
Back and shoulders	35	40
Chest	25	40

2.3 Opportunities for Dental Robotics

Autonomous robotic surgery can offer to address the profound lack of access to surgical procedures globally, that currently accounts for one third of deaths worldwide [56]. There is potential for greater autonomy in robotic surgery to improve standardisation of surgical procedures and outcomes, reduce clinician and patient harm, improve clinician mental health, and reduce the risk of disease transmission. Although the mechanics of general surgical robotics is largely solved, a critical barrier remains in the development of autonomous surgical for decision making which is hampered by the high clinical and investment risks relative to returns for investors, patients and medical practitioners. These risk and investment barriers must be lowered before true general surgical autonomy can be developed.

Compared to other surgical specialties, dental practices have a number of features that significantly reduce the clinical risk and technical difficulty for the early development of

surgical autonomy. General surgical procedures are almost always 'large' in that they require: surgical theatre time; anaesthetic; surgical nursing staff; additional staff and resources for both pre-surgical patient preparation and post-surgical care; and often require incision into the body. This contrasts strongly with dental procedures where the oral cavity is readily accessible without an incision or need for strict surgical sterility. Most dental procedures are performed on teeth which are non-elastic hard tissues, reducing computational challenges relative to surgery that is entirely on soft tissues. Furthermore, dentistry is also mostly procedural with routine techniques for cleaning and diagnosis that are usually completed in short timeframes with one to two operators. Annual or frequent checkups are recommended for everyone in the population that include cleaning, monitoring for the development of disease, and placing or replacing fillings, while individual cases of general surgical procedures are performed in only a small proportion of the population in any given year. These check-ups and procedures, as well as the conditions they treat, are typically not immediately life-threatening [35].

A high degree of autonomy has already been developed for dental implants. A dental assistant, Yomi (FDA approved in 2017 [167]) was created to guide surgeons with physical haptic cues to the correct location for surgery and drilling to match a planned path position, while tracking patient motion, and providing a real-time visual display system (Figure 2.6A) [58, 68, 168]. This device currently costs $150,000 USD with additional fees for implantation [169]. Along with this development, the first fully automated robotic dentistry for implants was developed in China (Figure 2.6B). This system was created to overcome the shortage of dentists in China and the high frequency of human error. It successfully implanted two 3D printed teeth into a patient in an hour with a margin of error of 0.2–0.3 mm [59, 167].

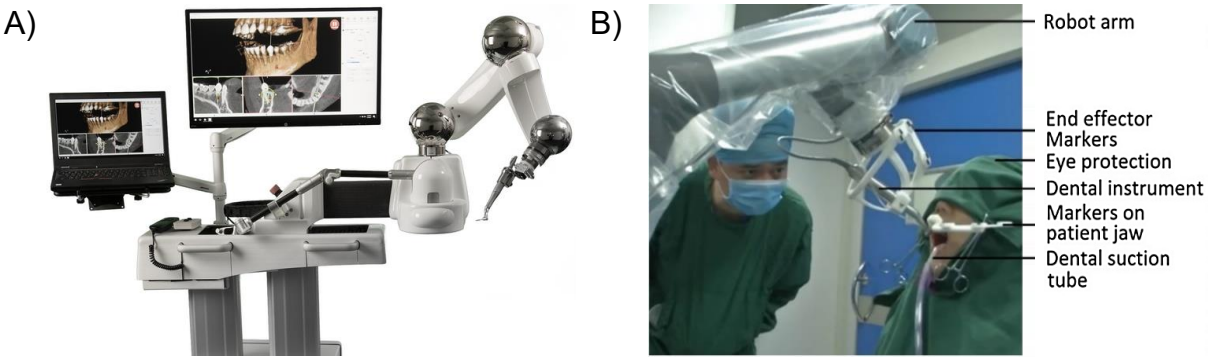

Figure 2.6. A) Yomi system by Neocis with a dental instrument end effector for the surgeon to operate via shared-control; B) Supervised pre-programmed robotic dental implant applications in China with markers on the jaw and instrument (robot end effector) [169, 170].

The digitisation technologies discussed above including navigation systems, passive arm tracker devices with mouth splints and intraoral imaging and scanning devices may be integrated to aid the development of autonomous dental robots by creating sufficiently tracked dental arches for force-regulated cleaning and diagnostic dental techniques. Automation of dental instrument movements in the dynamic dental environment may be best developed using artificial intelligence (AI) machine learning approaches [336]. However, automation involves a large increase in complexity compared to automatic robots due to the potential for interactions occurring outside the robot's planned operation, such that the robot would be able to undertake decision making to perform unassigned tasks in an unconstrained environment [171]. For this to occur, dental robots need to be developed with a sufficiently safe design and be able to consider patient risk, including their individual medical history, in surgical decision-making practices.

While automated clinical decision making is already advancing [172], ethical, clinical, and legal risk barriers limit the removal of the surgeon's guiding hand in life-threatening surgeries. Robotic autonomy in a directly life-threatening procedure is ethically challenging, given the high risk. This, along with the comparatively few individual types of each general surgical procedure performed in any given year, establishes excessively high risk and investment barriers for development of true autonomy in general surgical robotics. Despite

advancements, these systems remain autonomous more in name than nature [173-175]. Current medical device standards are available for robotically assisted systems with the human surgeon remaining responsible for operative sensing and situational awareness, the planning of actions, and direct robotic control [173-175].

The costs of medical robotic systems are expected to reduce over time with improved market competition. A Japanese surgical robot platform, hinotori, launched in 2022 and has been found to have similar patient outcomes, despite the reduced price by 22% compared to the da Vinci robot platform [176-178]. To improve the cost-benefit for dental practices, dentists may be able to provide services to a larger customer market. Reducing the level of operator input with dental robot automation can aid small private dental practices to increase their efficiency with the potential to treat multiple patients at one time, especially when the robots are designed to safely adapt to different procedures. Further, the potential non-monetary long-term benefits to both dentists and patients (Section 2.1) from the implementation of dental robots should be considered in their cost-benefit analyses.

The relatively low risk of dental procedures, along with the extensive market available for any single given procedure, is a further incentive for the high levels of investment that is needed to develop true autonomy. As well as the significant benefits to the dental industry, by solving the problem of autonomy in dental robotics, the foundation will be laid for true general surgical robotic autonomy. With careful design and development, there is hope that the costs of dental robots associated with their safety concerns and barriers to acceptance by dental professionals can be managed and mitigated. Advanced safe medical robots that can effectively reduce the workload of medical operators through automation of time-consuming tasks can reduce healthcare costs and improve access and equity by reducing training and workforce deployment costs.

2.4 Proposed Dental Robot Requirements

An advanced dental robot system should meet or exceed the basic performance of procedures undertaken by human dentists. A proposed set of clinical User Requirements Specifications (URS) for a dental robotic system is shown (Table 2.4). Dental robots should perform procedures autonomously when it is safe and also be able to perform a number of different procedures with relatively high efficiency. The proposed procedures for a dental robot include techniques for diagnosis, such as charting, through to cleaning techniques such as brushing and scaling. The dental robot should have the potential to perform a wider range of procedures in the long-term, including more invasive techniques (i.e. local anaesthetic, extractions and fillings). If this is achieved, dental robots can be developed as a gateway towards automation of medical procedures thanks to its high demand and lower risk in surgery [35].

Table 2.4. Proposed user requirement specifications for the intended use of an autonomous dental robot to operate instruments for diagnostic and cleaning techniques. Developed with reference to Perea-Pérez *et al.* (2020) [95].

Number	Requirement	Descriptions
URS1.1	Ability to use the required dental instrument(s) for dental procedures	Diagnosis: Intraoral camera (imaging); Intraoral scanner (scanning)*; Periodontal probe (charting); Dental explorer (exploring)
URS1.2		Cleaning: Toothbrush or sonic toothbrush (brushing); Scaler or ultrasonic scaler (scaling); Flosser or floss pick (flossing)*; Root planer (root planing)*
URS1.3		Restoration*: Contra-angle drill with bur (drilling); Filling applicator (filling); Contra-angle polishing brush (polishing)
URS1.4		Pain and infection prevention*: Needle (local anaesthetic); File and plugger (root canal); Dental forceps (extraction)
URS2.1	Meet the input requirements for dental procedures	Radiation Usage: Not increase the level of exposure to radiation used in dental practices, i.e. developing a system that is not reliant on radiographic imaging for planning and tracking
URS2.2		Have high precision and accuracy relevant to the dental procedure
URS2.3		Perform procedures on patients with variations in dental anatomy
URS2.4		Access and exit from an operative site in a safe manner on conscious patients (not under anaesthetic)
URS3.1	Reduce or not increase the number of incidents in dental practices	Assess the risk to patients and record the number of incidents and near misses for improved analysis
URS3.2		Design to minimise chance of human error for inhalation or ingestion injuries, wrong site tooth extractions (WSTEs) and infection control incidents
URS3.3		Design to reduce risk of transmission of air-borne and blood-borne diseases, and cross-contamination
URS4.1	Reduce or not increase the procedure length of time	Maintain high efficiency for dental practices
URS4.2		Not increase the level of discomfort to patients by making them sit through longer procedures
URS5.1	Reduce or not increase level of perceived dental pain	Prevent pain in the patient surpassing a level that is beyond uncomfortable
URS5.2		To reduce fear, the robot should be designed to be less visually confrontational

Key: *Potential inclusions for an advanced dental robot system.

Beyond user requirements, there is an abundance of technical requirements for a dental robot that must be met to ensure the safety of dental robotic procedures. This can begin with defining the safe limits for forces and speeds of dental instruments, which should be equivalent to the standardised permissible maximum pressures and effective spring constants for the forehead (or skull) and the masticatory muscle. Therefore, the biomechanical values will be assumed as 130 N/cm^2 and 150 N/mm for the hard dental arches (teeth and gingivae) and 110 N/cm^2 and 75 N/mm for soft oral tissues (oral mucosa) [71, 75] (Table 1.1, Table 2.3).

Human-operated dental procedures rely on years of dental training, traditional human-oriented hazard analyses, and SOPs. For an autonomous robot to collaborate with an untrained patient and perform dental procedures, it must be able to continuously monitor and manage the patient's responses. This ultimately produces a highly variable undefined and complex environment for the robot as shown by a proposed functional connectivity map (Figure 2.7) and the numerous integrated sensing technologies that are needed to reduce the level of uncertainty. Human-robot interaction risks can result from reducible statistical or inherent random variability, a lack of reliable knowledge, and errors [179, 180].

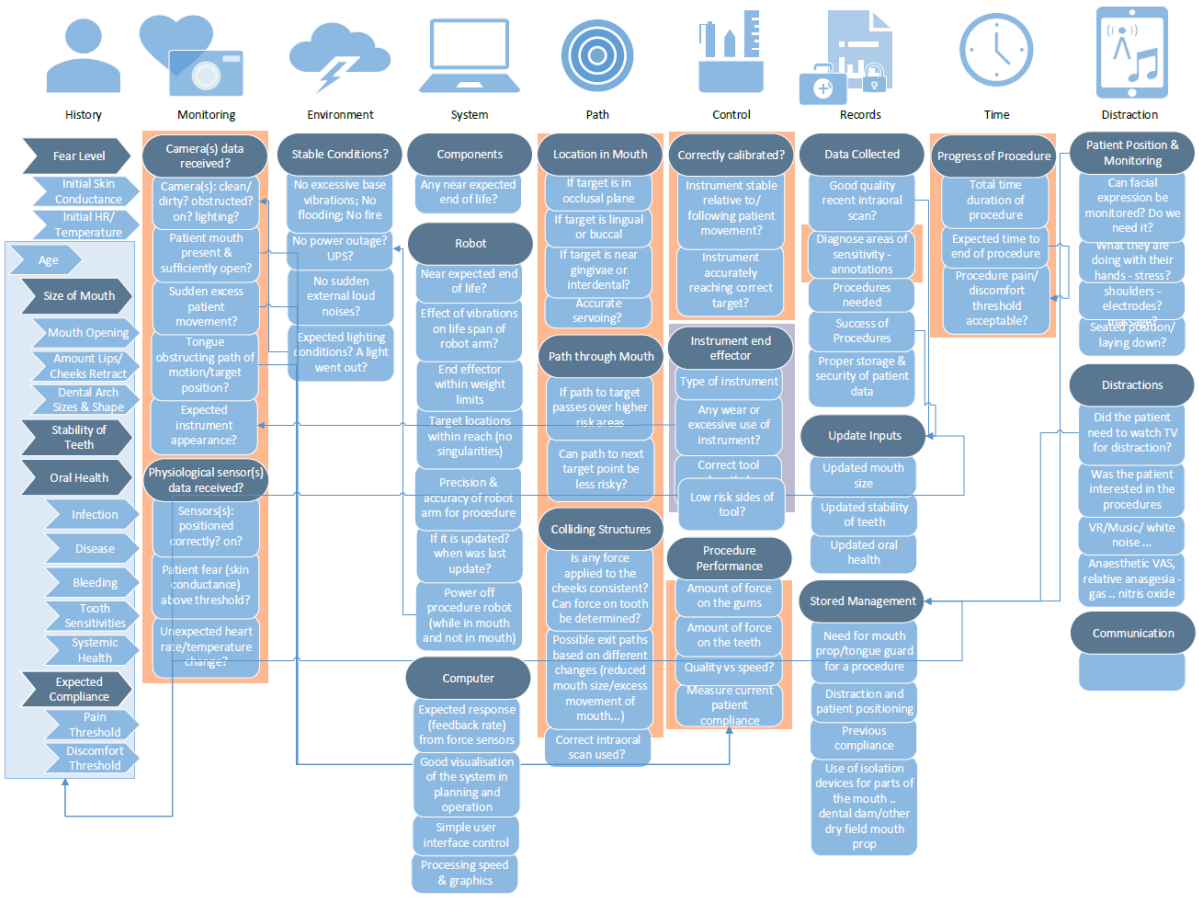

Figure 2.7. Proposed partial functional connectivity map showing categorised risk considerations for robotic dentistry with relevant subcomponents and links for significant dependencies or influences on other factors.

2.5 Proposed Sequence of Dental Robots

To reduce risk and investment barriers for the development of automated dental robotics, a series of dental robots is proposed, each of which has increasing clinical capacity and utility. The robots are intended to satisfy unmet clinical needs in the market, thus establishing a reasonable basis for investment. The development cycle begins with force-control and patient tracking technologies integrated with dental instrument operation to carry out diagnostic and cleaning procedures, herein termed as a ChartBot and a ScaleBot (Figure 2.8). It is anticipated that these early robots would initially rely on intraoral and extraoral 3D scans conducted by clinicians, that would then be integrated into robotic applications for sequential robots of greater sophistication. However, they would entail the solving of a number of key surgical decision-making problems, including: capacity to deal with anatomical variants;

safe instrument manipulation in the oral cavity; analysis of the mechanical forces on teeth and soft tissues; and coping with inconsistent patient movement or orientation. By mastering basic instrumentation, it can lead to developments in robotic tissue handling for more complex dental procedures, such as local anaesthetic delivery (a LABot), tooth extraction (an ExBot) and restorative techniques (a DentBot).

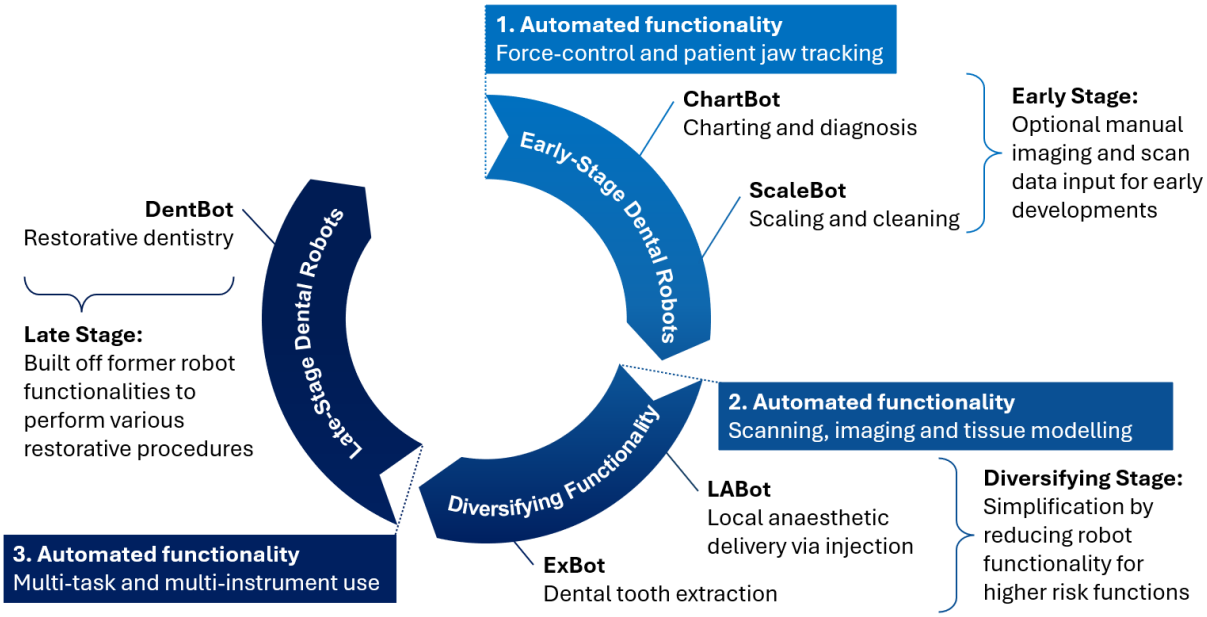

Figure 2.8. Proposed stages for autonomous dental robot systems that could be beneficial to dental practices from anticipated early-stage dental robots to late-stage dental robots, with transitions identified for changing functionality and diversifying technique functionalities.

The functionality roadmap begins with the ChartBot to construct a digital 3D record of the teeth and supporting tissues by integrating optical and radiographic scans with periodontal probing data for diagnosis (Figure 2.9). The ScaleBot would comprise a 'ChartBot' with the additional function of operative scaling and cleaning of teeth, including in periodontal pockets, thereby making it inherently more invasive. Robot capabilities can be investigated to produce the LABot specialised for local anaesthesia delivery via injection, necessitating soft tissue manipulation. ExBot would further expand clinical capacity to remove teeth by extraction with a wider range of instrument selections. This robot would have a capacity for both soft and hard tissue manipulation for safe extraction of teeth. Finally, a robot performing all these tasks, the

DentBot, would build upon the capacities in instrument manipulation and real time autonomous surgical decision making developed in former robots, to deliver the full suite of dental restorative procedures, including fillings, crowns and related treatments.

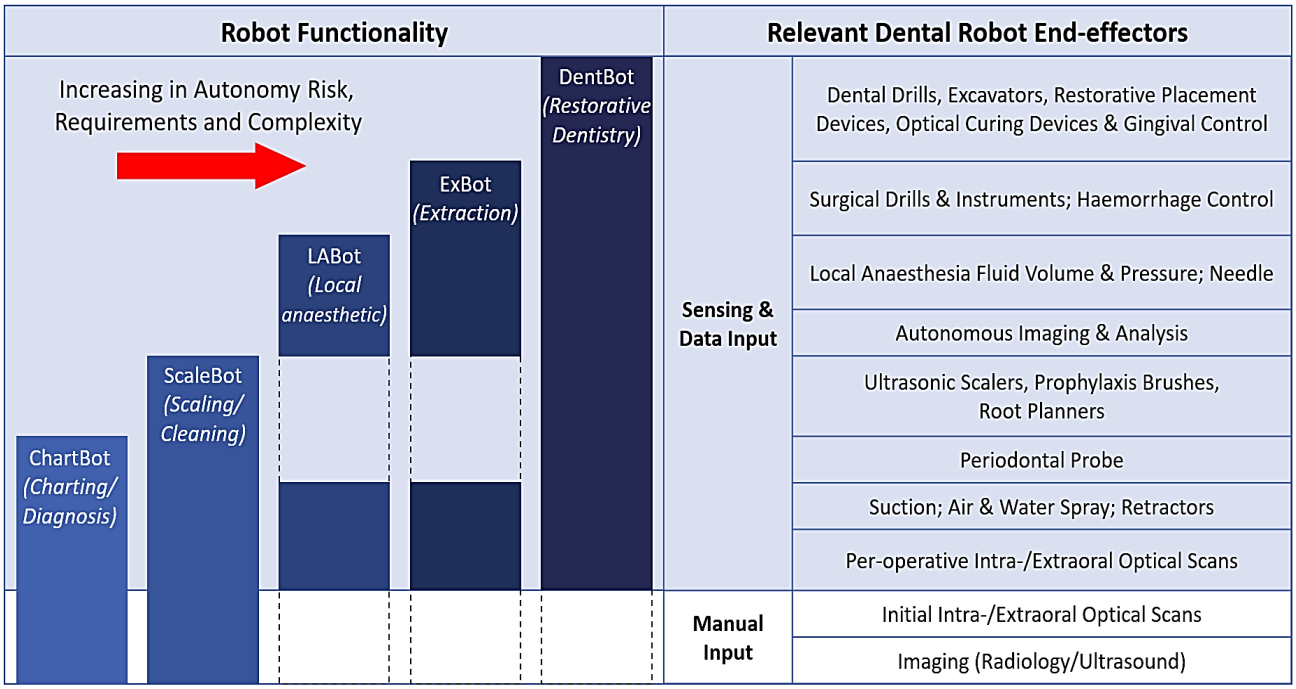

Figure 2.9. Proposed increasing robot functionalities described by the robot dental instrument end effector components for autonomous dental robot systems, highlighting the increasing risk for autonomy, complexity and requirements. Initial manual control of dental instruments as inputs are indicated by a white background and automated control of end effectors have a light blue background.

Necessity to probe periodontal pockets for charting would establish the fundamentals of instrument manipulation with low forces in close association with the hard and soft tissues of teeth in an essentially non-invasive and reversible way for ChartBot. Ideally, its diagnosis capabilities would include identifying fillings and crowns, plaque and calculus deposits, gingivitis and periodontal pockets, and dental decay from intraoral and extraoral data. This dental robot would be of immediate value for dentists, aiding diagnosis, record keeping and treatment planning. The problem of real-time modification of robotic actions and processes in accordance with changing surgical circumstances, such as gingival bleeding, detection of

subgingival calculus, or patient movement, would be solved with successful development of ChartBot.

Progression along the proposed roadmap would permit the development of increasing levels of importance for autonomous surgical decision making. Therefore, the increased risks for robot autonomy and complexities of the dental procedures would need to be managed and accompanied by the necessary safety requirements. To improve dental techniques, dental robots should be informed on the individual medical history of patients, as well as the dental clinical history and complaint, to allow for a nuanced expectation of the patient's response during techniques.

Notably, these initial functionalities for autonomous dental robots were motivated to permit dental clinicians more time to focus on more complex restorative procedures which could create a positive market pressure for robot development. Further, a major expense for dental treatment comprises the cost of supporting dental assistants and dental hygienists for the limited time available to treat patients per day, increasing staff costs while limiting the spread of trained dental personnel to already established dental practices. Therefore, the proposed sequence of dental robots promotes and offers opportunities to enhance dental care accessibility, and their robotic advancements can provide the foundations for robotic control to underpin autonomous robotic dental surgery.

2.6 Discussion

Research into dental robotics and tracking technologies have prioritised the development of enhancing the precision of challenging techniques, such as the drilling angle and depth for a dental implant. The argument to involve robots beyond this, for instance in cleaning techniques, is hindered by the heightened risks of collaborating with a robot, the challenges of safe automation and their main benefit being limited to their precision.

Nevertheless, dental robots can significantly benefit both the patient and the clinician, particularly for cleaning and diagnostic techniques [181, 182]. Dental robots designed with a focus on patient safety could overcome the challenges facing the provision and access to quality dental services to reduce the prevalence of dental disease. In addition, safety management frameworks should be developed in anticipation of the potential expanding autonomous capabilities of a dental robot. Furthermore, the largely surgical aspect of dental procedures provides an opportunity to act as a gateway towards high levels of autonomy for dynamic and more life-threatening surgeries, with a lower barrier to investment.

Since robotic dental procedures need to operate in a dynamic environment with sensors, online or local path planning and navigation may be necessary [183, 184]. Control of the robot needs to be sufficiently accurate, robust and secure while registering the position of recent high resolution intraoral scans without significant delay or excessive computational power. This is important as the robot must hold the dental instruments and dynamically navigate around the dental arches to a target location in order to execute a desired dental technique. The defined user requirements aim to ensure that the robot does not cause unnecessary harm or hinder the quality of automated dental procedures. Future work must be undertaken to evaluate the quality of robotic dental techniques, including assessments of the safety for different dental instruments of varying shape and compliance.

Autonomous surgical robotic technologies are developing faster than the necessary regulatory frameworks. This leaves patients vulnerable to harm in test cases, and also puts the new technology at risk of backlash from the public [185]. Significant progress has been possible in China, where automated dental implant robotic applications and autonomous COVID-19 test robots have been fast-tracked for high demand [59, 161-164, 167, 170, 186], and where the regulatory framework is politically centralised. Similar development of surgical autonomy elsewhere, however, necessitates the development of safety test standards, protocols

and benchmarks [187]. The creation of effective SOPs is critical to meet regulatory compliance requirements for product development. This challenge for medical devices such as dental robots is foreshadowed by the complexity of the functional connectivity map (Section 2.4, Figure 2.7).

To develop thorough regulatory frameworks, it will be necessary to confirm the accuracy of intraoral imaging scan resolutions and registration, as well as the localisation of the dental arches and robotically controlled instruments in pre- and peri-operative robotic planning [188], similar to current visual guidance system technologies. However, for current robotic surgical procedures, this often falls back on quantitative data from patient outcomes from surgery and the number of incidents during test case procedures. These aspects should be taken into account at an early stage of development in dental robotics with ChartBot as the first commercial stepping stone in the proposed development roadmap.

Current navigation guidance systems using stereovision are at risk of line-of-sight obstructions for marker localisation [128, 140]. This is more problematic where dentists are operating in the scene, in cases where they need to change their viewing perspective or the position of their arms. Yomi overcomes this through the use of passive arm tracking [142], while the Chinese robot should not have operators or the patient obstructing the cameras' views during normal operation [170]. Due to the number of preparation steps for the implant procedures, the use of the dental robot systems likely prolongs the total procedure time based on the time taken to setup the navigation markers or fixtures for tracking of the maxilla or mandible [189, 190]. Future designs for a dental robot system should reduce the risk of line-of-sight obstructions in both normal use and unintended use of the robot to avoid harm and limit the amount of preparation needed for low-risk diagnostic and cleaning procedures.

Chapter 3: Setup and Planning for Automation

3.1 Summary

Autonomous operation in the dental environment would ease the manual workload for dentists and can improve accessibility of dental services in rural communities. Advantages and limitations of available robotic technologies, including cranial-related medical robots and COVID-19 test robots, are discussed for their influence on the ease and safety of automation. A novel dental robot system design, along with an updated dental workflow, is proposed where patients lie face down over a small opening where their mouth is accessed from below by a dental instrument controlled by a robot for robotic procedures. This has the potential to reduce the likelihood of choking, high-risk quasi-static collisions, and disease transmission, particularly during a pandemic. New levels of autonomy are designed to include varying robot and operator awareness in order to increase the accessibility of dental services. Finally, the safety of the system design is analysed with respect to the Hierarchy of Controls.

3.2 Introduction

Throughout history, the dental environment has been modified to improve the patient and dentist experience during procedures. Previously, patients were positioned in a seated or upright position while dentists performed procedures standing over them (Figure 3.1A). In modern practice, patients are seated leaning back with their mouth open, while the dentist sits and leans over them (Figure 3.1B). Patients also now wear protective glasses to reduce the chance of eye injury from the use of sharp instruments or chemicals. The change in working position allows dentists to sit during procedures, which assists to reduce the level of fatigue for dentists, and therefore the likelihood of errors and injury. However, dentists still experience a high prevalence of musculoskeletal problems, with issues reported by 87.2% of dentists in Australia [88]. While dentists once worked without gloves or masks with the consequent risk of disease transmission (Figure 3.1A), it is now routine for dentists to be protected with these surgical barriers (Figure 3.1B).

A)  B) 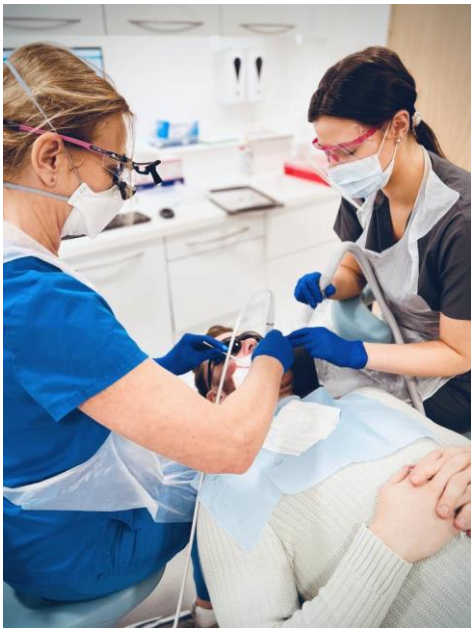

Figure 3.1. Photographs of patients and dentists in typical arrangement during different clinical eras: A) In the early to mid-twentieth century, dentists stood during patient treatment, with patients seated in specialised dental chairs; and B) From the late twentieth to the present time, dentists have treated patients seated, with patients reclined and facing upwards [191, 192].

The modern position presents a number of challenges for the patient with the adoption of robots. Patients are at risk of inhaling or ingesting debris, liquids, dental devices or broken components during procedures [93]. Additionally, there is danger of unexpected collisions (blunt force impact) or lacerations with the patient [93], which could result from dental error, unsafe patient head or jaw movement, and the position of the headrest that prevents the patient from being able to move away when required. To reduce this, dentists operate with a finger rest on teeth of the jaw they are working on to physically track the patient's jaw movement during procedures. This is particularly important as the point of side-to-side rotation which occurs at the headrest can produce large changes in the position of the patient's teeth. Dentists, or more commonly dental assistants, regularly use suction devices to prevent saliva, blood, saline solution or water pooling in the mouth, and to reduce choking hazards. Finally, in an emergency, patients are usually rotated into the recovery position. These postural safety considerations limit the implementation of robotic devices in the current arrangement of dental patients and clinicians.

Over the past decade, robots have had an increasing presence in dentistry. In 2012, a robotic simulator, the dental Robotutor, was created to teach tooth brushing methods using a stepper motor [193]. In 2013-14, the accuracy and repeatability of multi-degree of freedom robot arms was employed for toothbrush design optimisation and efficacy testing [194, 195]. Since then, the concept of Dentronics has been introduced by Grischke *et al.* (2019) for intelligent lightweight assistive robots in dental applications, from cleaning to diagnostic and invasive roles, to support the dentist and dental assistant in routine tasks and enhance reliability and reproducibility in dental care [196]. Assistive guidance systems and robots, namely Yomi by Neocis, have had commercial success in tracking the mandible for dental implants (Figure 3.2) [197].

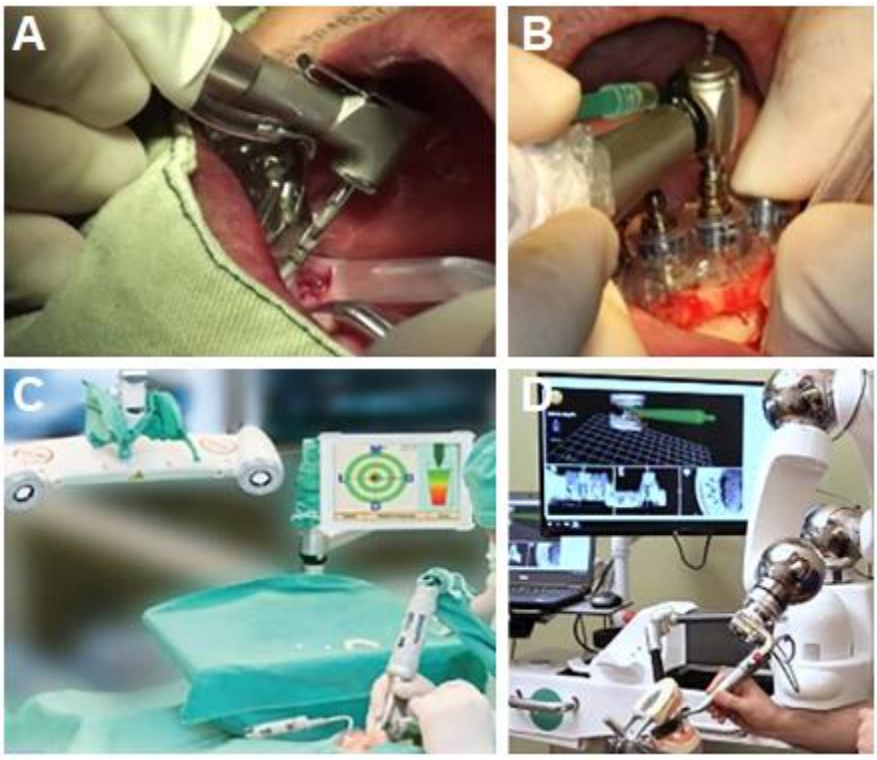

Figure 3.2. Methods for dental implant procedures: A) Freehand by a dentist; B) A dentist using a surgical guide; C) Dynamic navigation with a visual guidance system tracking the patient jaw and dental instrument; and D) Robotically assisted hand-guiding dental implant procedure implanting with Yomi. Images sourced from [197].

The current pathway for surgical robot automation is to progress from manual robots, that largely depend on human input, to robots that require less and less assistance until they become completely autonomous robots and can operate without external assistance (Figure 3.3) [174, 185, 187, 198, 199]. Robots currently used in cranial-related medical surgeries are largely remotely controlled, such as during Transoral Robotic Surgery (TORS) with the da Vinci system, or reliant on customised pre-programmed paths developed from CT scan patient models, such as in the Yomi and assistive guidance systems. Implementation of autonomous robots considering usability, tracking capability, and risk mitigation is crucial to ensure the dental environment remains safe so that dental professionals adopt a more supervisory role.

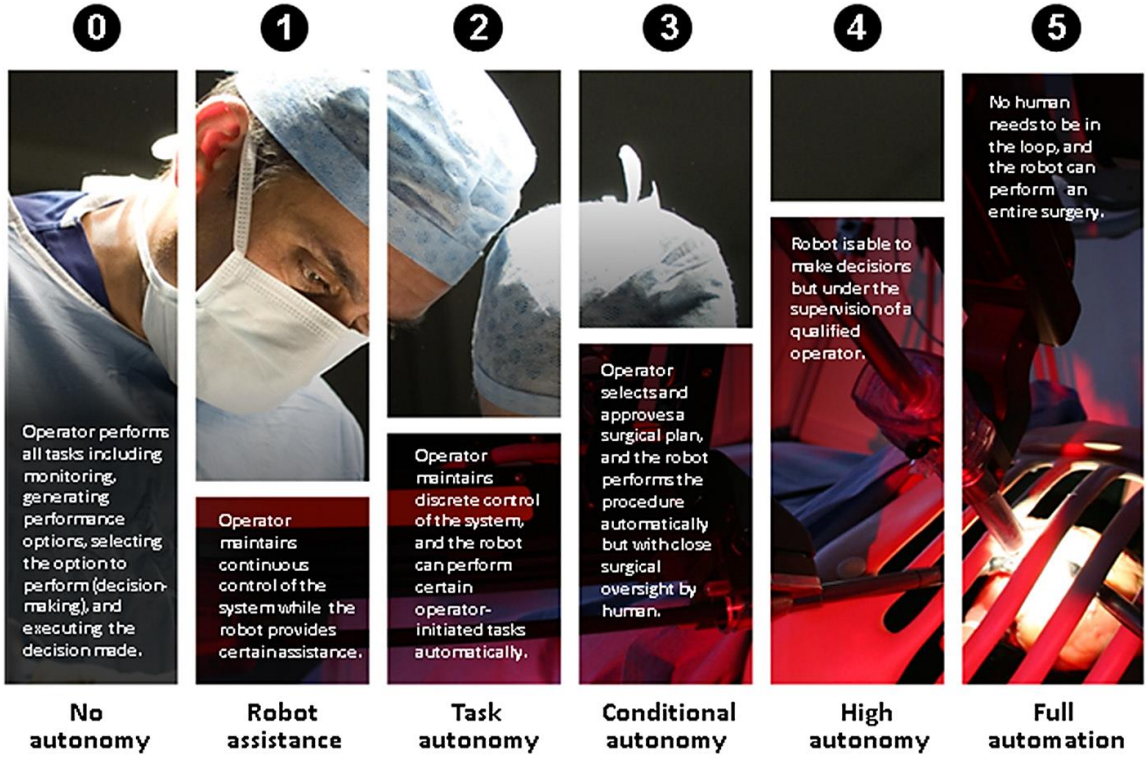

Figure 3.3. Levels of autonomy for robotic surgery as the current pathway to automation [185].

According to the medical electrical equipment technical report, IEC TR 60601-4-1, higher levels of autonomy do not create new hazards but add new sources of hazardous situations [156]. Therefore, it is possible for one design setup for a dental robot system to accommodate multiple levels of autonomy without needing to identify new hazards. Further, the system should be fail-safe, which means that the robotic system does not cause damage to itself or its immediate environment in the event of a failure or error, or during unexpected behaviour or loss of control [200].

In this chapter, a new design for an autonomous dental robot setup is proposed that can be used to treat conscious patients in routine diagnostic and cleaning techniques, as well as more complex procedures such as dental restorations. To formulate this design, current robotic systems for transoral-related operations were analysed and critiqued. The new design proposes the re-orientation of the patient in a face down posture where the robot is isolated in a chamber below or in front of the patient. This is possible due to the separation of the operator from the

operative site. A number of potential benefits from this change in design are discussed, including the reduced likelihood of quasi-static collisions between the patient and the robot.

Following traditional methods of medical device safety, the design choices for controlling risks are assessed with reference to the Hierarchy of Controls [201]. The Hierarchy of Controls ranks methods of actions and safeguards to prioritise the best controls and minimize the likelihood of harm (Figure 3.4). The most effective risk reduction measures are hazard elimination or substitution with a less harmful alternative, thereby producing a more inherently safe design [202-205]. An engineering control in the form of an additional technology or device may remove or isolate a potential hazard to an acceptable level [202-204]. Other hazard control measures include assistive safety features such as alarms or alerts as well as changes in practices and processes through updated operator instruction [205].

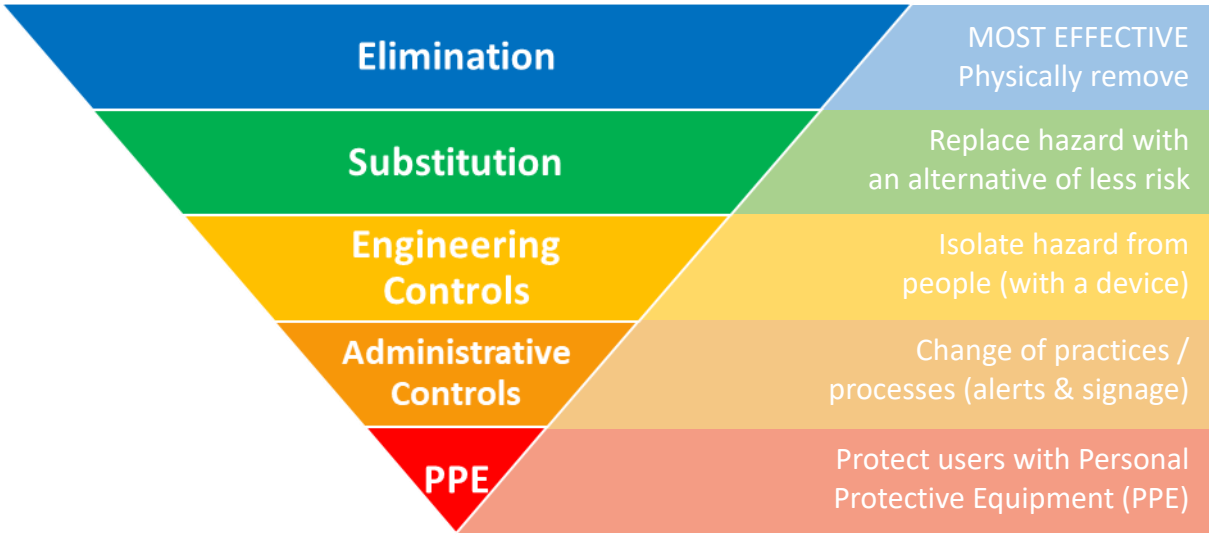

Figure 3.4. The Hierarchy of Controls for risk mitigation methods [206].

3.3 Analysis of Robotic Patient Setups

Current conceptual designs for robotic dental applications have the patient seated and resting back on a headrest with the robot and operator performing the procedure and monitoring from above (Figure 3.5). Applied designs of cranial-related surgical setups include TORS with the da Vinci robotic platform, dental implant applications, and COVID-19 tests that have

advantages and limitations to design a robot system for automation (Table 3.1). A major issue for producing safe, highly accurate medical robotic procedures is the use of strong industrial grade robot arms in a highly collaborative environment. This establishes significant and potentially damaging collision risks for patients and clinicians, especially when operating in an open space. The documented safety measures to manage these risks, mentioned in Chapter 1 (Section 1.5), are currently designed for higher autonomy collaborative industrial robots. To assure patient safety, medical procedures have the surgeon in control throughout the procedure with remotely controlled robots and shared-control robots, like Yomi, that are limited to lower levels of autonomy.

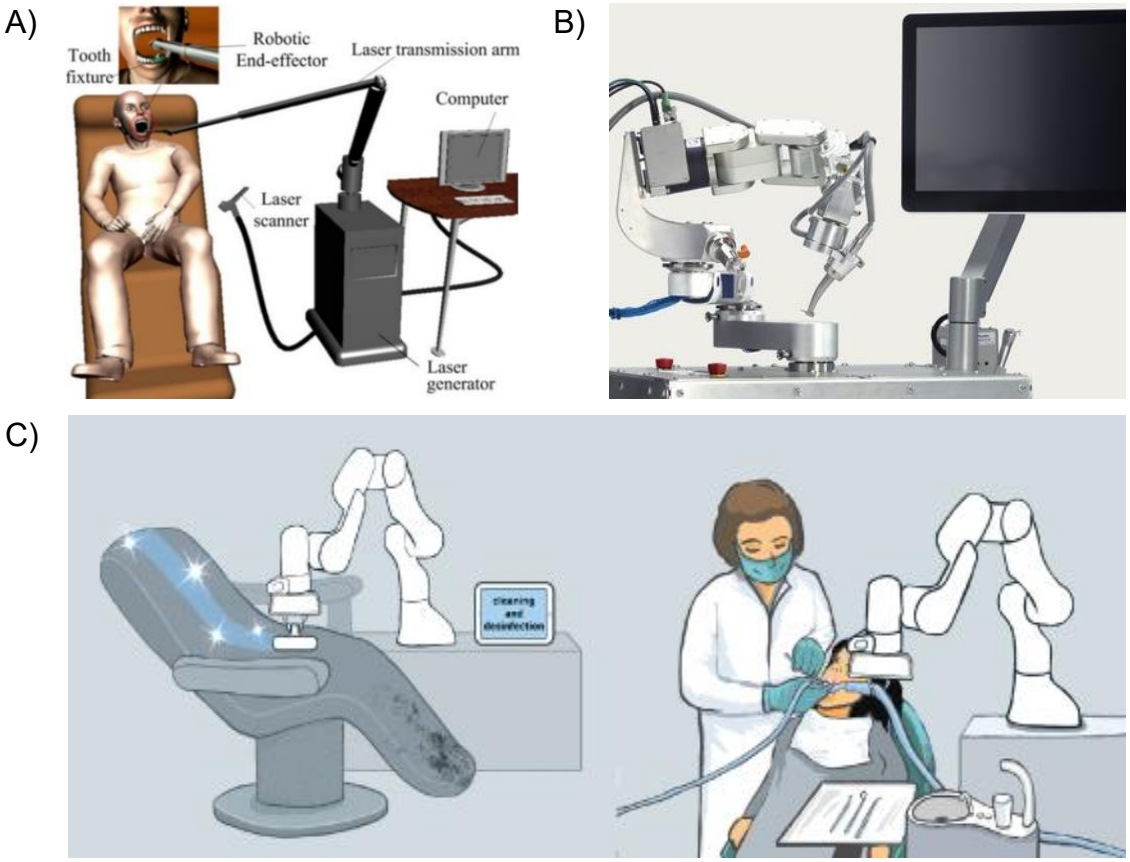

Figure 3.5. A) Conceptual automatic crown preparation to be carried out using robotic laser endodontics with a tooth fixture device [207]. B) Perceptive's dental robot system cart for developing automated crown preparation [208]. C) Conceptual robot assisting cleaning and disinfection procedures, suction and instrument handling [196].

Table 3.1. Operative environment designs with robot use for transoral surgical procedures, dental implantation, and COVID-19 tests: advantages and limitations for an autonomous dental robot system.

Setup	Advantages	Limitations	Image	References
TORS with the da Vinci robotic platform	• Mimics human technique • High-level articulation with high range of motion, dexterity and precision • Dual lens endoscopic camera (real-time 3D visual feedback) • Optional manual removal of robot if required	• Remotely teleoperated with CT scanning • Four robotic arms to manage: three instruments and a 3D stereoscopic endoscope • Patient is put under a general anaesthetic • In emergencies, manual removal of robot from patient in supine (high risk of quasi-static HRI)		[62, 209-213]

Yomi haptic dental implant assistive robot	• Pre-programmed boundaries
	• Awake and conscious patients
	• Only one active robot arm:
	  ○ Accurate active robot arm with instrument (replaces custom guides)
	  ○ Passive chain linkage for jaw motion tracking
		• Direct shared-control guidance
		• Radiographic scan data for jaw localisation pre-programming, and guidance
		• Visual feedback of relative position to jaws (not soft tissues)
		• Supine position for access (high risk of quasi-static HRI)
				[142, 214, 215]

Supervised robotic dental implant applications in China	• Pre-programmed automated implant application • Combined with marker visual guidance systems • Patient seated upright with a fixed suction device • Robot protected by plastic sheeting	• Tracked markers fitted prior to surgery and CT scanned for patient jaw localisation • Patient receives a local anaesthetic • Patient seated against a headrest (high risk of quasi-static HRI) • Lack of eye and face protection • Confrontational large robot		[59, 167, 170, 186, 216]

Automated robotic crown preparation system by Perceptive	• Use of a small compact robot arm • Awake and conscious patient • Bite block (mouth prop) to stabilise mouth and track patient movement • Workflow makes use of intraoral scanner using OCT technology	• Patient positioned in supine-posture the traditional patient posture setup for its robotic procedure • Active dentist-in-the-loop using a foot pedal • Procedure isolated at a single tooth		[208, 217]
Remote COVID-19 test robot study and use in China	• Teleoperated without CT scan • Reduced contact with and visibility of robot (isolated in chamber with a small opening) • Patient free to retract away if they experience pain or discomfort • Limits transmission of disease	• Small opening limits range of motion and instrument types (linear access to the throat) • Only suitable for fast procedures like a throat swab (not a relaxed or comfortable position) • Emergency stop not accessible to patient		[161-164]
COVID-19 test throat or nasal swab robot	• Automated transoral test robot • Patient free to retract away from robot if there is pain or discomfort • User operated which limits transmission of disease	• COVID-19 test system with a swab • No housing chamber around robot large robot or inbuilt protection of facial features • Not suitable for long procedures (patient stretched towards robot or holding up the head rest)		[157, 158, 162]

Despite the high dexterity of the multi-arm da Vinci system, TORS is associated with a 1.4% risk of tooth injury, 1.1% risk of aspiration pneumonia, 0.6% risk of lingual nerve injury and 0.3% risk of death from a postoperative haemorrhage [218]. Other possible injuries from TORS include those to the lip, mucosa, eyes and face due to unwanted collisions between the robot or the surgical instruments and the patient [211]. In particular, the risk of aspiration pneumonia is increased in a supine patient position allowing for easy inhalation of liquid (e.g. saliva) and small foreign objects. The risk of collisions is heightened by the use of multiple robot arms that must operate together. Multi-arm setups are currently only used in remote operation with the da Vinci robotic platform while the patient is under a general anaesthetic.

A safety risk for the da Vinci setup and assistive dental robot systems is the likelihood of a quasi-static collision for the patient who is positioned between the robot and the surgical bed or dental chair. This design hinders the ability to shift from remote and guided systems to increasingly autonomous supervised procedures where there may be more patient movement due to full patient consciousness. These designs may increase the potential risk of otherwise low-risk routine procedures beyond an acceptable level for automation. Unless the robot and patient setup are altered, robots impose an unnecessary heightened risk for low-risk procedures.

In contrast, COVID-19 testing robots' setups have been designed to allow the patient to move away. The remote COVID-19 tests that have been performed on patients have them lean forward towards the robot in a seated position. This style of setup is not possible where clinicians need direct input for instrument control in the operative field. In Singapore, a similar setup was used for COVID-19 nasal swab tests that has an encased user-operated linear actuator named SwabBot [219]. The operator sets up the machine with a disposable nosepiece and protective drapes before the patient positions themselves on the nosepiece and pushes against the chin activator to initiate action [219]. Embracing a similar safety-focused posture arrangement for dental robotics would maximise the potential to shift to higher levels of

autonomy for a dental robot system that has reduced human input from the supervising dental professionals and supports the potential for increasing the level of self-supervision for simple procedures by the patient.

3.4 A Novel Dental Postural Setup

The hazards associated with the traditional dental postural setup limits the introduction of autonomous robots to perform dental procedures. The main hazards include: the risk of collisions to the nearby dentist and patient; high impact quasi-static collisions when pressed against the headrest of the chair; inhalation or ingestion injury from excess water or debris falling down the throat; the patient's inability to move away from the instrument and robot if in pain; and the need to shift the patient into a recovery position in case of an emergency. A flowchart is presented describe the sequence of design choices to the development of a new dental robot setup for undergoing robotic dentistry (Figure 3.6). This new design aims to address multiple hazards present in the traditional dental setup by re-designing the dental setup without the constraint of direct visual and physical access by the dental professional. The proposed design literally "flips" the position of the patient into a more prone posture.

Components of this design include a ventilated chamber to house the robot, a headset to distract the patient or protect their eyes and identity, a "massage table" dental chair, and a console station for the dentist or operator. Cameras within the robot's chamber and on the robot end effector would be used to visually assess the dental environment. Further, the chamber walls should be clear to facilitate visual inspections of the robot's environment. The design is specifically un-defined to highlight that the innovative aspect is the repositioning of the patient in a forward posture and that it could be used with various different dental robots. This was an important consideration to promote market competition to reduce costs for dentists.

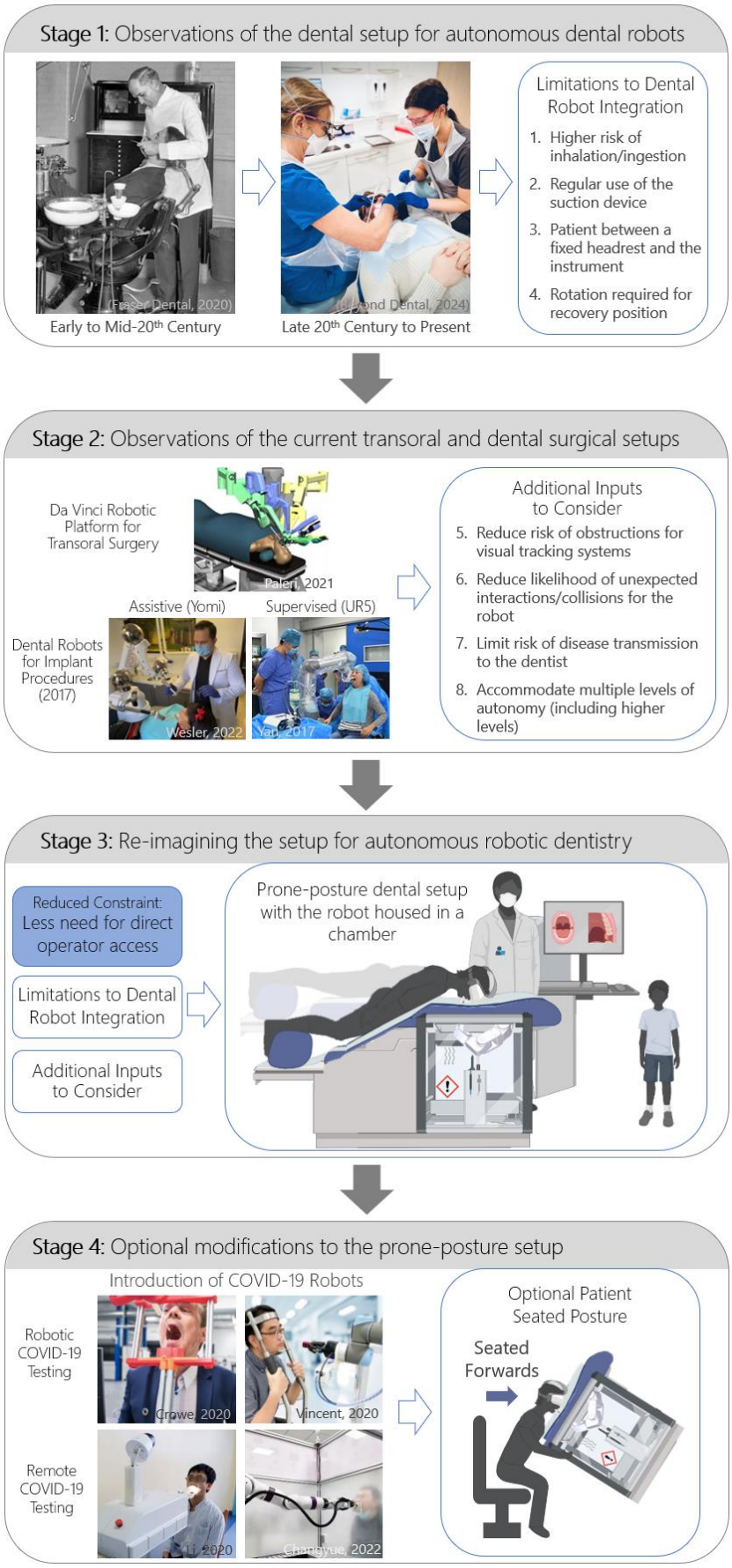

Figure 3.6. Stages to represent the sequence taken to reach the safety-focused design setup for patients undergoing autonomous dental robotic procedures.

The new patient orientation is proposed where the patient is in a prone-like or a forward leaning, face-down position where the robot is isolated in a chamber below the patient (Figure 3.7). In this design, there is no headrest behind the head restricting patient escape. In addition to an emergency stop, patient hand grips on either side of the centrally placed robot are recommended to allow patients to both hold themselves down on the robot in active consent and can be used to push themselves up and away from the robot. Giving patients autonomy in this way can be expected to alleviate an important source of anxiety for dental patients who currently may feel trapped between the dental chair and the dental clinician immediately above them. This also creates more potential for transient collisions with reduced impact, compared to the risk of quasi-static collisions with the traditional dental posture setup.

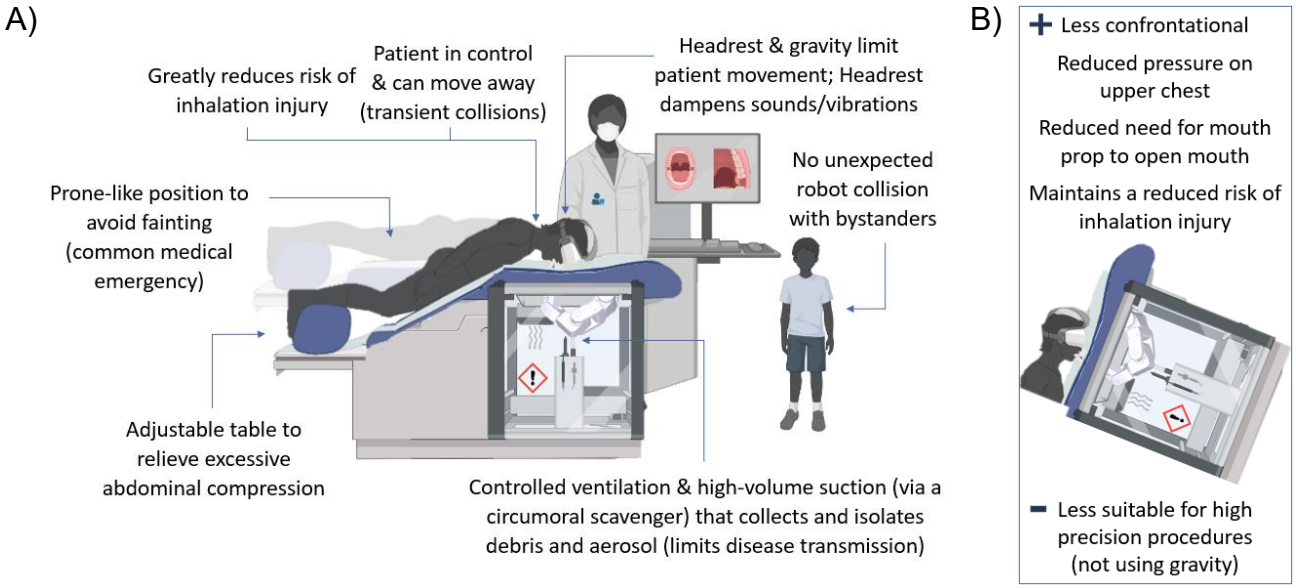

Figure 3.7. Proposed patient posture for dental robot design with the patient in a prone-like position and the robot under the patient in an isolated chamber. A) Benefits are outlined for the patient having a prone-like orientation compared to B) benefits (+) and disadvantages (-) as the system is rotated to a forward-leaning seated position. See Deaker *et al.* (2023) [220].

In this design, the overall safety of dental procedures, the number of infection control procedures, and the productivity of dental practices can be improved. A prone-like position has numerous safety benefits and allows for higher levels of autonomy. Potential advantages of the prone position include: a decreased risk of ingestion or inhalation injury; a reduced need for

suction to remove fluids pooling in the mouth; and the weight of the head against the headrest dampening the instrument's vibrations compared to a supine position. By containing aerosols and bodily fluids such as blood and saliva, as well as by separating the clinical operator from the operative site, the proposed postural setup also aids infection control. The entirety of the chamber contents, including the robot, can be subjected to ultrasonic, chemical or plasma sterilisation, with contamination of complex working parts prevented by removable, disposable elastic sleeves. Additionally, the shift in the point of head rotation from the back of the head to the mouth opening area when face-down maintains a more stable point of entry for the robot.

Saliva ejection may be aided by the development of a suction device, such as a circumoral scavenger that surrounds the outside of the mouth entrance to collect fluid exiting out of the mouth with the help of gravity. Additionally, Vaseline could be used to reduce the sensation of dripping saliva or water on the lips. The variability in the incline of the patient's body provides opportunity to maximise their comfort. The prone position may be considered more uncomfortable for some patients. For instance, patients that may find it difficult to lie on their front with more pressure on their upper chest, abdomen or face for extended periods of time, such as for pregnant patients, older patients or for those with severe obesity or facial trauma. For clinical surgeries where it is optimal to have a patient in prone, gel pads can be used to support the patient to avoid bed sores and nerve damage. This was used in Li *et al.* (2024) which reported that 64.2% of patients underwent vaginal natural orifice transluminal endoscopic surgery (vNOTES) in prone position [221]. This posture reduced the average surgical time by approximately 19 minutes to 1 hour and 38 minutes, while only increasing the procedure preparation time by about 6 minutes [221]. This would have resulted from the surgeons experiencing greater convenience for operation and exhibits a lower rate of surgical conversion [221].

The main risk of prone positioning, lending it to being considered more uncomfortable for some patients, is the occurrence of pressure and nerve injuries [222]. Surprisingly, during the pandemic, the prone position was considered a therapy for COVID-19 patients with acute respiratory distress syndrome (ARDS) for its benefits of uniform lung pressure and improved ventilation of the posterior lung regions [223]. However, unlike short dental treatments, the risk of developing pressure and nerve injuries was high as patients were left in prone for up to and over 24 hours [222]. Nevertheless, the optional seated position is likely to be essential to broaden the range of potential patients for robotic dentistry. Ideally, the robot chamber would not extend beyond the upper chest to allow for various body shapes to sit comfortably during procedures. The seated position can also reduce the amount of handling needed to position frail patients. This is important as dentists should not need to assist patients to get their body into position beyond the positioning of their head and arms. This could risk increasing the risk of musculoskeletal disease among dentists, as recognised as a risk for health care workers treating ARDS patients [224].

Dental robot systems should not be very confronting to patients as many people already experience high levels of anxiety during dental procedures [36-40]. The consideration of using a small and relatively quiet robot arm may help to reduce stress for patients. However, as robotic technology advances, the next generation is more likely to have a more positive experience with the advanced technology [83]. The efforts to mitigate effects of dental phobia are limited in the traditional patient setup as patients are very aware of the procedure performed with direct vision of the instruments used. This challenges the impact of distraction techniques that have been attempted to reduce patient stress. The proposed setup could provide opportunities to desensitise patients from the procedure being performed such that they can safely undergo robotic dentistry. To improve their feeling of control, the patient is ideally not restrained in movement beyond their head being positioned within a headrest that minimises

head rocking and shifting movements. The chamber allows the patient to be able to move their hands and arms without placing themselves at risk of contact with the robot.

The use of a chamber is made possible by the increasingly compact size of precise industrial robots, such as the Meca500 by Mecademic [225]. These are less visually confrontational, more suitable for small workplaces, and reduce the level of surrounding environmental uncertainty during procedures. This can assist the robustness of sensors that rely on direct line-of-sight, which could be obstructed by the patient. However, like a massage or physiotherapy, this position limits the visibility of the patient's face to check their emotional state during procedures and presents the need to track other physiological signals, such as the heart rate, to monitor their experience. Although the forward posture may increase the likelihood of the tongue resting in frontal regions of the mouth, the robot may be able to softly push it away the tongue with suitable force with non-cutting sides of the instrument to gain access to the hidden locations of the mouth. Patient compliance may be assessed in this step to ensure that they are not producing a strong reaction force on the instrument. For more non-compliant patients, a tongue guard attached to a mouth prop may be appropriate measure to ensure easier access to the teeth and gingivae.

This setup is almost a "one-size-fits-all" solution for all types of dental robot autonomy. Specifically, the flipped patient position makes it difficult for shared-control haptic operator control (e.g. hand-guided). This is not considered a point of concern as other forms of assistive autonomy, namely remotely operated systems such as the da Vinci robotic platform, are well suited to this design where the medical professional is no longer operating hands-on at the operative site. Unfortunately, skipping this form of autonomy limits the ability for dentists to experience the capabilities of a dental robot first-hand. However, if the shared-control design setup was the desired choice, the dentist would likely retain majority of the responsibility and barriers for autonomous dental robots would remain high. In particular, higher risks of collision

will remain as the robot would need to operate in an open field in close contact with another or multiple other dynamic nearby persons. Instead, the restriction to the dental environment promotes safety to the dentist and patient by simplifying the operative field, along with other benefits to reduce disease transmission. Moreover, this focuses the operator and the robot's safety management practices on the patient. For example, a dentist can step in if needed to move the robot's joints or manually disconnect the end effector after pausing or stopping autonomous control and opening a door to the chamber for direct access.

For this design to be possible, the robot must still be able to navigate through the small oral cavity and avoid collisions with soft tissues, such as the tongue, gingivae, cheeks, and lips. It must also be able to respond to movement of any hard tissues, such as of the mandible, loose teeth and the whole head, with the potential presence of body fluids such as blood impeding vision of teeth. A preliminary analysis was conducted to evaluate the impact of sideways head rotations for the risk of instrument collision for varying headrest positions and patient postures (Appendix A). The pivot point locations were adjusted to simulate a patient resting the back of their head against a headrest in supine, a patient seated upright with a headrest in front or behind their head, and a patient in prone posture with a frontal headrest. The initial analysis suggests that the seated posture is most optimal, shortly followed by the proposed prone posture, when compared to the likelihood of collision from a side head rotation in supine posture. However, it was visually determined that the seated posture was most ideal for operating in back regions of the mouth and the prone posture was best suited to front regions of the mouth. Nevertheless, the seated posture may be less naturally restraining to head movement depending on the angle of the patients head in the headrest, compared to a lying down posture, necessitating further analysis for its application for safer dental robot procedures.

3.5 A Workflow Modification

At a minimum, changes to the dental setup would involve the replacement of the headrest on an adjustable dental chair in a prone position. This headrest could have an opening like a massage table that was built with a customised slot to fit a virtual reality (VR) headset. The patient could have the headset fixed in place to avoid major head movements, with or without the straps over the back of the head, which the patient should be told how to remove in an emergency. Benefits of having a fixed VR headset could be to solely protect the patient's eyes during procedures but could aid in oral health awareness and distraction techniques. The inactive head movement during use of the VR headset could help minimise effects of motion sickness from latency-related technical challenges, along with further capabilities of eye-tracking [226, 227]. This could help detect the state of the patient during the technique or if they have removed themselves from the headset. Ideally, the robotic chamber would be relatively small and portable such that it could be positioned below the headrest of the dental chair when in use. Further, if it were to be positioned on a table, it would need to be relatively lightweight. To lessen this burden, the robot should be removable to lighten the load for manoeuvring the chamber. Adaptability of the possible positioning of the patient and robot in dental practices could increase adoption of dental robot systems.

To integrate recently developed dental digitisation systems into dental robotic procedures, a new workflow is proposed (Figure 3.8). In preparation for a dental robot procedure, a 3D model of the internal structure of the patient's mouth can be generated with scanned markers. These markers may be on a mouth prop that is used for visual tracking or linked to a passive tracking arm for localisation and model registration. A non-contact intraoral scanner, such as the CEREC Primescan, creates a 3D digital impression of the dental arches (Figure 3.8, Step 1). The scan data provides the potential for analysis and diagnosis of oral health and the ability to generate pre-programmed instrument paths, either manually or using

automated methods and based on the patient's anatomy (Figure 3.8, Step 2). This contrasts to dental implant robots including Yomi which require knowledge of the internal structure of the jawbone from radiographic records. Once the patient is ready (Figure 3.8, Step 3), the instrument paths should be checked and approved, depending on the level of autonomy.

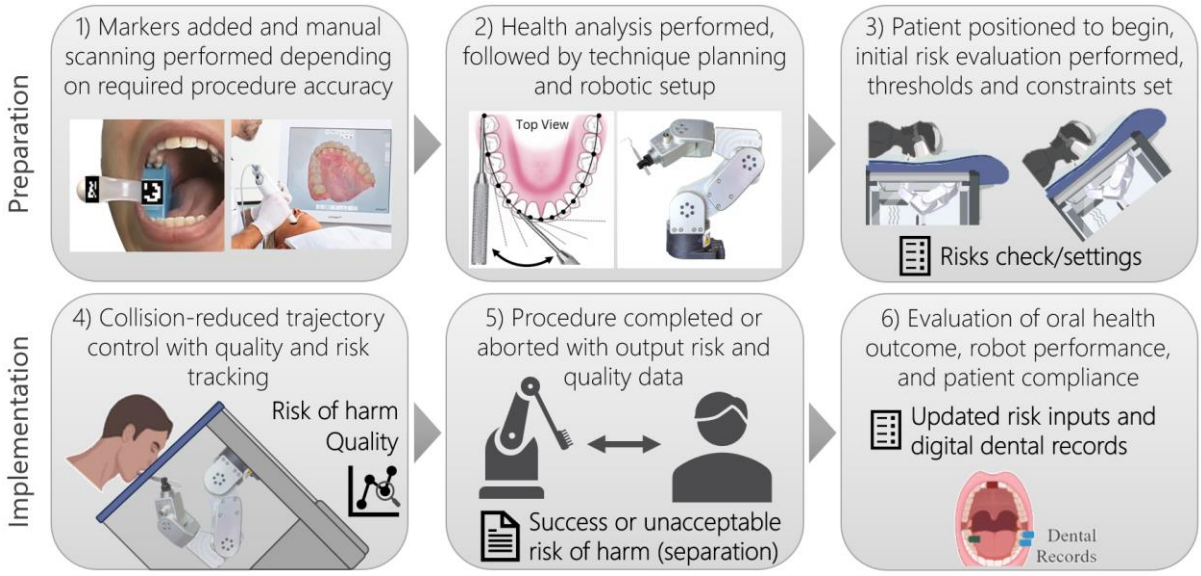

Figure 3.8. Potential workflow for an autonomous dental robot system to execute a cleaning procedure. *Preparation steps:* 1. Intraoral scanning of the patient's dental arches before a procedure or with a mouth prop that has necessary markers or a tracked chain linkage for improved mouth localisation; 2. Digital oral analysis of the intraoral scan by the dentist or developed algorithms to select targets and or create paths appropriate for the robotic operation; 3. Patient is positioned in the chosen posture and constraints to safe operation are defined for tracked quantities. *Implementation Steps:* 4. Robot performs a controlled technique while navigating around oral structures and tracking quality and risk parameters; 5. Robotic procedure is completed or halted based on risk measures and an assessment of the procedure performance is recorded; 6. The patient's oral health status is recorded using digitised dental records to track progress for future evaluation. Adapted from Deaker *et al.* (2023) [146, 220].

Due to the large number of hazards and unacceptable risks present in the complex and dynamic dental environment, an autonomous dental robot solution is not yet accepted and there are large barriers to entry for robotic device manufacturers. To mitigate these hazards, redundancy measures and safety protocols with the ability to detect changes in the environment and intervene before harm occurs is critical. Therefore, procedure quality and risk tracking are

important to ensure patient safety (Figure 3.8, Step 4). Critical aspects of procedures need to be constantly assessed to ensure the robot and environment are safe to avoid stopping the procedure prior to completion (Figure 3.8, Step 5). Quantitative data from the procedure can also be stored to inform future dental procedures to assist customisation of dental robot techniques for the patient and the type of procedure (Figure 3.8, Step 6). Integration with 3D models can enhance dental records for patients and reduce reliance on standard dental arch schematics that do not match the patient's anatomy.

It is important to note that the accuracy of intraoral scanners can be impacted by poor angulation, location of the mouth, starting point of scanning, and scanning technology employed [151, 228, 229]. Often, the accuracy of the first scanned quadrant is high and usually decreases when completing a full arch [228], similar to mobile robot localisation challenges [130]. The learning curve and accuracy for different intraoral scanners can vary between devices [228, 230]. Potential research could be carried out to determine whether automated robotic control of intraoral scanners can improve the accuracy of digital models. Additionally, if scans can be performed by the robot, it could divide the procedure into each quadrant of the mouth and scan the relevant sections as they are needed. This would suit robotic procedures that use a mouth prop to locate and track the dental arches. The controlled chamber environment with the patient facing down could help to minimise the effects of changes in ambient light from the surroundings. The dental robot systems should be made aware of the inaccuracies and capabilities of the individual scanner devices to best adapt and enhance the quality of the procedure for higher precision techniques.

3.6 Proposed Autonomy-Risk Levels

Increasing levels of automation is expected to reduce operator awareness and demand greater levels of safety for robotic systems to be accepted and trusted [199]. Given that there is

reduced available operator awareness, accepted autonomous procedures should be able to be operated by individuals with varying expertise and minimal impact of risk to harm. This aligns with the extension to allow non-specialised medical assistants to monitor and react to robotically assisted surgical equipment as proposed in International Electrotechnical Commission's IEC 80601-2-77 [156]. Professional operators present the least risk to operation and are ready to identify hazards and implement safety measures, and thus require the least amount of robot awareness [231]. In contrast, qualified operators should recognise related expected hazards [231]. Trained operators and educated users should be aware of the processes for safe operation, while informed users should only need to be aware of expected behaviour and know how to initiate an emergency stop, which results in the highest risk of harm without advanced robot awareness [231].

While unable to eliminate risks of autonomous dental robots through design practices, risk management systems should be integrated to assess and help mitigate risks to an acceptable level before and during operations of defined autonomy. Therefore, dentistry requires increases in robotic system risk awareness for each level of autonomy to counter the losses in operator awareness. This thesis introduces new levels of risk awareness and autonomy for medical robots that includes the minimum requirements for robotic system risk awareness and the corresponding minimum experience of the supervising operator (Table 3.2). The expertise of robot operators range from professionals, such as dentists, to those that are qualified or trained on a restricted range of services such as dental therapists and hygienists, and users who are educated or informed specifically on the robot's operation [231]. At the most advanced level of autonomy, Level 5.5 "Full Risk Awareness and Autonomy", the robot is required to accurately measure, predict and quickly recover from all foreseeable risk states for a selected procedure and setup.

Table 3.2. Proposed levels of robot autonomy based on minimum robot operator qualification with the relevant system risk awareness from manual and robotic assistance to full robot autonomy.

Level of Autonomy	Level	Operator Control	Description
Professional Operator Education: A dental professional trained as a specialist with knowledge in dental robot safety, performing risk management and problem solving in case of changes, and evaluations of dental robot performance.			
Manual	0	Dental clinician in control	Dental clinician performs tasks and decision making
Robotic Assistance	1	Dental clinician operates a haptic or remote robot	Dental clinician maintains continuous control of the system and the robot assists (e.g. with precision)
Task Autonomy	2	Dental clinician supervises individually created tasks	An automated task is created, initiated and supervised by a dental clinician for the robot
Conditional Autonomy	3	Dental clinician supervises pre-planned tasks	Automated planned tasks are selected, approved and supervised by a dental clinician for the robot with estimated risk feedback measurements for procedure safety based on instrument control
Qualified Operator Education: A dental or medical professional trained in dental robot risk management and able to adjust, monitor and appropriately respond to workflows, patient activities and critical environmental states to avoid harm.			
Conditional Risk Awareness and Autonomy	3.5	Qualified operator supervises pre-planned tasks	Conditional autonomy supervision with a qualified operator to manage the patient and the state of the oral cavity with automated robot risk management for instrument-control procedure safety
Trained Operator Education: A safety operator trained to carry out and recognise normal and abnormal operation of a dental robot to recover from unsafe operation, and to manage patient responses during dental procedures to avoid harm.			
High Autonomy	4	Trained safety operator supervises automated dental robot procedures	Robot can make decisions but under the supervision of a trained safety operator that monitors the patient's response to the procedure, with estimated risk feedback measurements for safety state of the dental environment and automated robot risk management for instrument-control and the dental environment procedure safety

Educated Operator Education: An operator or patient trained in the steps and possible uses of dental robot operation and informed of emergency practices and the acceptable behaviour or activities to carry out around the robot.			
High Risk Awareness and Autonomy	4.5	Trained operator or patient supervises automated dental robot procedures	High autonomy supervision with a trained operator or patient with automated robot risk management for instrument-control and the dental environment procedure safety
Informed Operator Education: An operator or patient pre-informed on the basic operation of a dental robot and methods to deal with simple problems, such as discomfort or fear.			
Full Autonomy	5	Informed patient or operator initiates automated dental robot procedures	An informed user that receives feedback on recommendations to improve their cooperation and behaviour around the dental robot with automated robot risk management for instrument-control and the dental environment procedure safety
Guided: An operator or patient guided on the basic operation during setup and the procedure by the dental robot system.			
Full Risk Awareness and Autonomy	5.5	Robotic system stepping a user through how to use it without previous training	Full Autonomy where the user is guided cooperate with the dental robot with automated robot risk management for instrument-control, the dental environment and patient safety
The table is divided by the operator control levels that describe the minimum acceptable levels of education for the operator using a dental robot at those levels. These have been adapted from Mollbach *et al.* (2020) [231]. The described levels of autonomy were modified and expanded on from Yang *et al.* (2017) [185], presented in Figure 3.3, to include relevant risk management practices for autonomous dental robots progressing towards full autonomy.			

Developed dental robots for implant surgery operate at low levels of autonomy that require highly experienced operators and planned instrument paths. By comparison, cleaning and diagnostic dental services are suitable for risk-reduced or risk-managed higher levels of autonomy with integrated monitoring systems. For a dental robot, such as ChartBot, the system would begin to operate at a lower level of autonomy with greater expert supervision before increasing to higher levels of autonomy with supervision by a risk-aware robotic system. To manage the dynamic risks of the dental environment, dental robots would ideally be able to carry out a form of "traded control" between the different levels of autonomy [232]. This would help to accommodate for increased risks of a procedure performed on different patients, thereby returning more responsibility to the operator and improving their operator awareness. The criteria for traded control should be managed by a risk monitoring system whose criteria for transitions between the forms of autonomy would be pre-determined. Where these transitions are automated, it presents an example of adaptive automation where the supervision system dynamically allocates tasks between the operator and the robot [198].

3.7 Discussion

For traditional medical robots, patients under general anaesthetic act as the object while the surgeon and robot are synchronised. An automated robotic system in dentistry requires human-robot collaboration with the conscious patient, which significantly increases the required safety without even considering the proximity to vital anatomy. Further, the current defined levels of autonomy for medical robots, presented earlier in the chapter (Section 3.2, Figure 3.3), are only concerned with advancing technological development. Successful implementation of dental robots, such as through the proposed series of dental robot systems (Chapter 2, Section 2.5) and the proposed levels of robot autonomy, should involve low pre-processing times and a short learning curve to ensure high efficiency.

To increase patient safety, a prone-like patient orientation is proposed with a frontal headrest and a small window through which the robot would access the mouth. A prone-like posture reduces the risk of quasi-static collisions with a strong robot arm and prevents choking hazards among other potential benefits. The new design can increase the patient's perceived control which is expected to reduce their fear and aversiveness to dental treatment [233]. The proposed workflow aims to reduce the reliance on radiographic imaging of patient jaw localisation, while ensuring sufficient accuracy. Moreover, the use of a 3D digital model and intraoral imaging removes the need for complex computer vision through a dental mirror. The design of the proposed dental robot system is discussed in the following section with reference to the Hierarchy of Controls that is used as a method to mitigate design-related risks.

3.7.1 Hierarchy of Controls

The safety of the proposed design can be assessed for its effectiveness using the 'Hierarchy of Controls'. This framework has been used as a strategy for risk prevention and control for other medical devices, such as medical device nano-biomaterials [234], as well as the safety of healthcare facilities [235]. Elimination of hazard sources is discussed with reference to the dental robot design, followed by substitutions provided by the reorientation of the patient. Although usually less effective for human operation, it is believed that engineering and administrative controls can play a significant role in the safety of autonomous robots. This is because automated systems, unlike those that are human operated, can be designed to comply with planned processes and requirements.

3.7.1.1 Elimination of Hazard Sources

While the introduction of the robot to the dental setup inherently adds risks opposing the "elimination" control method, the prone position design removes a number of risks associated with ingestion and fluid suction, and thereby eliminates the need for a second robot arm to mimic the tasks of a dental assistant. This reduces the risk of collaboration with an

assisting operator or second robot arm during robotic dental procedures, while the patient can also freely move away from the robot if desired. Moreover, there is potential to physically increase the distance between the patient in the chamber to eliminate the robot from the patient's proximity if the robot is on a linear guide track. Alternatively, it may be safer for the dental instrument to be disconnected from the robot end effector in the case of an error or emergency. However, with advancements in communication between devices and automated risk management processes, it will become possible to integrate with other robots to assist in activities, such as fluid suction, retraction, spray and visualisation using cameras or lighting.

3.7.1.2 Risk Reduction by Substitution

The shift in patient position substitutes risks associated with the safety of fluid ingestion with potential patient discomfort from pressure on the upper chest and face. Upon contact, a conscious patient that senses pain should be able to move away, creating a more transient collision with the robot and reducing the impact. This replaces the high probability of quasi-static collisions that can result from the more supine patient posture with a back headrest. Although the new patient posture is not suitable for haptic shared-control procedures, the system will require minimal change in setup between patients for increasing autonomy, while still allowing remote operation.

To minimise risks in the dynamic system, the robot system could transition to a lower level of autonomy to complete a procedure with a higher level of operator supervision by traded control. This would occur when high-level procedure risk is perceived alerting the system that the robot is not accepted to continue high level autonomous operation. In such situations, it may be appropriate for the dental practitioner or trained operator to take over control to perform the procedure remotely. Remotely operated robots currently involve a larger learning curve for clinicians, particularly with the introduction of new surgical instrument designs, adding another barrier to their acceptance and usage in medical applications [236]. Compared to manual

COVID-19 test sampling at 18±5.1 seconds, an average remote robotic sampling time was halved at 9±4.1 seconds [164]. These were carried out with a rotary Stewart platform with a ring of rods for actuation to ease operator learning challenges, however, improvements in their position tracking is necessary for most dental techniques (Figure 3.9) [164, 237]. Alternative technologies have since been developed including the 3D mouse devices, such as the SpaceMouse by 3Dconnexion and the more advanced Inverse3 by Haply Robotics, to control robot movement in 3D [238, 239].

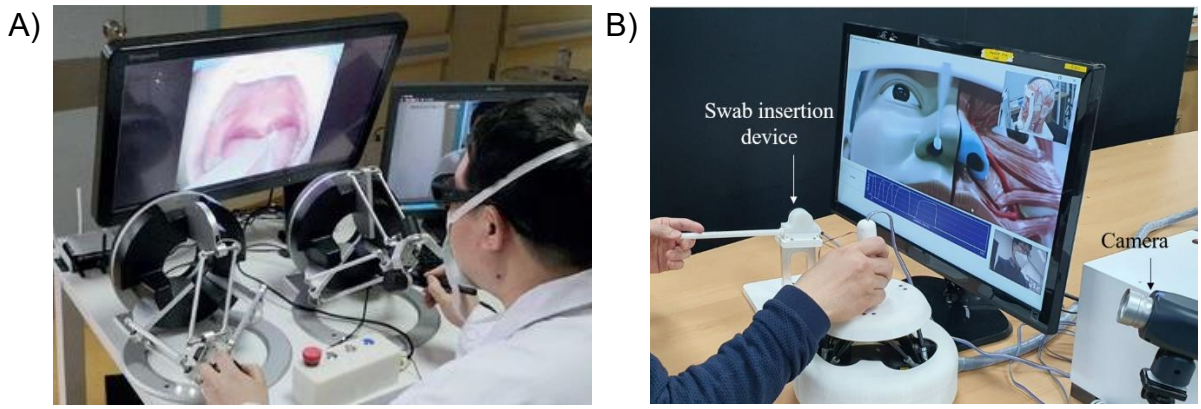

Figure 3.9. Remotely operated COVID-19 test robot studies using rotary Stewart platforms for control: A) Mouth swab [164]; B) Nasal swab [237].

There are a number of design considerations for patient safety and procedure quality. A robot with redundant joints (more than six joints) can be developed [69], which may be able to reach the target points with more available instrument orientations. In this way, the redundant joints could remain inactive unless they are needed to ease computation by limiting the number of solutions. The added weights and sizes of instruments to the robot arm end effector should be considered for the robot's accuracy, positioning and change in inertia. While a smaller robot, such as the Meca500, has a limited reach and working volume compared to a larger robot, it reduces the risk for nearby personnel, making it more suited to small workplaces and easier for the patient to exit its reach. A weaker robot could be substituted for procedures that are low in precision and accuracy, with a potential position feedback loop to improve its performance. Furthermore, a remote or supervising dental expert may be accessible to

troubleshoot errors or mitigate detected hazards before they are a concern in order to remain operating at high autonomy.

3.7.1.3 Engineering Risk Controls

Physical barriers can be used separate visitors, staff and the patient from the robot environment. The robot chamber follows the traditional robotic system design to limit unpredictable interaction with nearby personnel [66], limiting the potential interaction to be between the robot and the patient. Containing the robot creates a more predictable operative environment and reduces uncertainty by limiting the number of possible interactions and collisions during procedures. The headrest also creates a physical barrier to protect other facial features, including the eyes of the patient, and limits the robot's movement to the opening through the headrest. The robot base's position relative to the mouth opening can prevent direct contact of the robot links with the patient. Additionally, a physical barrier over the mouth opening could be closed to inhibit unauthorised or unsupervised use until the patient is confirmed to be in the correct position for operation. This can also be closed while the robot performs tasks within the chamber to carry out disinfection or tool changes.

As dental diagnostic and cleaning techniques can allow lower precision tracking than dental implant techniques, facial and oral opening visual tracking systems may be sufficient for localising the expected positions of the jaws for lower risk tooth brushing, intraoral imaging, and intraoral scanning techniques. However, some techniques will still require relatively high accuracy which may be provided through scanned visual marker localisation on a mouth prop or contact surface detection techniques with visual feedback. These localisation methods could be repeated when uncertainty is detected from a force-feedback dental instrument. Risk of movement in the mouth prop could be reduced by moulding it to their jaw like a mouth guard for sport. To make this more cost effective, it could be made reusable for the same patient in future visits. Speed and separation monitoring with patient tracking, as well

as power and force limiting measures, may be employed to minimise likelihood of a high force impact that could result in harm.

3.7.1.4 Administrative and Protective Risk Controls

To achieve patient safety with high autonomy, the hazardous situations such as mistakes in decision-making or negligence, such as poor instrument calibration, patient tracking or awareness of the patient's state, must be detected so harm can be mitigated appropriately. Without this, the robot will continue to be the responsibility of the operating clinicians and procedures will remain at low levels of autonomy [35, 61, 240]. To achieve automation of techniques, the robotic systems need to be designed with added risk awareness to increase the safety of higher autonomy and to gain acceptance from clinicians. To manage this, verified supervision systems should be introduced to observe patient risk during dental robotic procedures. This supervision system should be able to execute an emergency response to the robot or transition the robot to operator control so that procedural risks can be reduced to an acceptable "safe" level before it continues.

So that the procedure is initiated with a low expected risk, specific patient inputs may need to be identified prior to a procedure, such as head mass and size range, pain threshold, and expected compliance. There should be visual alerts to the operator on the quality and risk level throughout a procedure with recommendations to further improve the safety of the procedure. To improve the physical protection provided by the headrest, the headrest size should be adjustable or interchangeable for different patients. Mouth props to limit mandible movement during procedures and reduce instrument injuries could be designed like a mouth guard and fitted with a sensor for tracking or movement detection. Lip retractors, tongue guards and eyeglasses may be required to reduce risk of collisions with oral and facial features. Finally, robots that are not waterproof may require a protective cover, however the weight of the cover should be considered, given the allowable payload of the robot to maintain high accuracy.

3.7.2 Conclusion

Increasing autonomy has the potential to directly increase accessibility to dental services, particularly in rural areas, if the robots can be operated autonomously with non-specialised personnel or remotely by dental experts. By breaking down the development of dental robots into a series with increasing capabilities, risk barriers can be minimised for investment. Despite developments in safety mechanisms, research gaps exist for tracking of patient risk for human-robot interaction in confined and complex environments, particularly at higher levels of autonomy. Further investigation into safety mechanisms is required to determine whether they can provide a sufficient level of patient safety for the large variety of dental procedures on patients of different ages and experiences. These safety measures should be tailored to identified hazards and their hazardous situations to ensure that incorporated safety features effectively minimise the risk of harm to the patient. The following chapters of this thesis explore the need to develop risk management methods to develop dental robot safety. This will begin with an analysis of likely dental robot hazards.

Chapter 4: Risk Management Framework

4.1 Summary

Numerous limitations of the traditional dental setup were predicted to be mitigated through the new proposed design setup for dental robots in Chapter 3. This chapter analyses the success of the new postural dental setup in reducing the potential of patient harm. Outstanding hazards are highlighted as aspects that must be managed for patient safety. Risk management for a non-specific dental robot setup is described in order to track the presence of a critical hazards and assess patient safety throughout procedures. The framework begins with a risk supervision system that evaluates the safety of the instrument, environment and patient to operate a dental procedure for fast risk decision-making. This would then combine into a risk management network to estimate causal factors for active risk reduction during procedures. These aim to heighten hazard situation awareness such that autonomous dental robot developers can evaluate their robot safety and focus on designing high quality procedures.

4.2 Background on Risks and Hazards

The IEC 80601-2-77 standard includes dental treatments by dentists as medical procedures on the boundary of surgery, despite it not falling under the definition of surgery by WHO, as it requires "incision, excision, manipulation or suturing" while the patient is usually under anaesthetic for pain control [156]. Advanced risk awareness can reduce the chance of human and robot error during robotic dental procedures. Supervising analyses of system risks can help to detect skill-related errors of the robot, similar to the dentist checking for skill-based human errors [240]. By optimising the dental postural setup for patient safety with risk awareness, dental robots may be able to achieve higher levels of autonomy while minimising risk to the patient. Integrations with risk tracking systems for high level robot situational awareness may be effective in estimating and predicting the presence of high-risk hazards during dental procedures to limit the likelihood of harm.

Harm is typically preceded by the series of compounding hazardous situations, which can be represented by domino theory (Figure 4.1A) [241]. These can represent missing robot commands that constitute a "slip in action" or "lapse in memory" caused by the human error inputs, code programming or data transmission issues [240]. One or more latent risks or hazards, such as error or negligence, can lead to: a "near miss" incident or error with no harm; an 'adverse event' where there is harm; or an 'accident' where the event is unexpected and harmful [35, 95]. The effectiveness of risk controls can be represented by another accident causation model described as the 'Swiss cheese model' (Figure 4.1B) [242]. This model depicts the importance of effective safeguards to prevent an undesired event occurring with potentially unacceptable risk. Redundancy may be achieved by closing or minimising gaps ("holes") in multiple layers of the Swiss cheese model, which can assist to build safer and more robust systems against high-risk events.

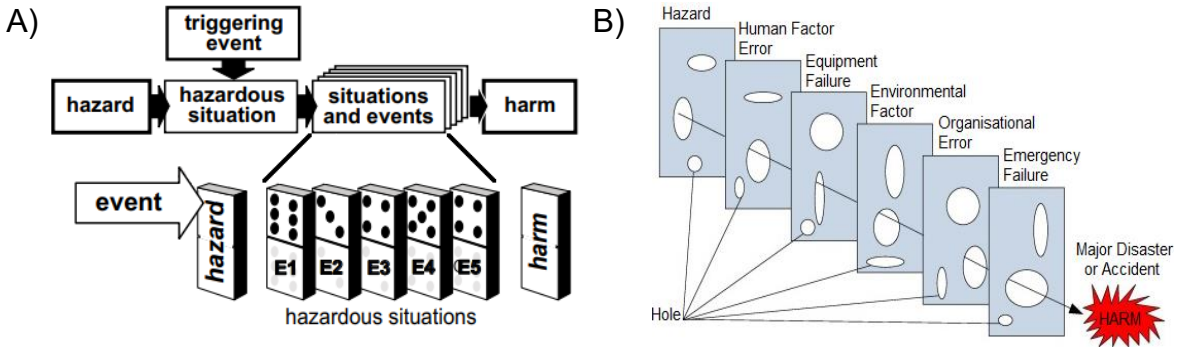

Figure 4.1. Hazard pathways: A) domino theory; and B) Swiss cheese model [241, 242].

Medical devices must account for all hazards using a risk matrix to ensure their risk level is acceptable in both normal use and failure modes. As according to the ISO 14971 Risk Management international standard, risk matrices are calculated by multiplying estimates of the probability of risks and their severity (Figure 4.2) [243, 244]. In this system, a risk rating value of 10 or above is considered to represent an unacceptable risk, whereas lower numeric results are considered acceptable risks. Medical devices must exhibit and maintain an acceptable risk to benefit ratio throughout the product life cycle, which are tabulated and tracked in a large Hazard Traceability Matrix (HTM) [155, 241]. Risk mitigation of unacceptable hazards is achieved by either adding risk controls and reductions to decrease their probability, or by eliminating the source of risk, and re-evaluating its success from residual risk assessments [243]. This is necessary as medical device safety requires the elimination or reduction of harm to patients as far as possible to an acceptable level [35].

Probability	Value
Improbable	1
Remote	2
Occasional	3
Probable	4
Frequent	5

Severity	Value
Negligible	1
Minor	2
Serious	3
Major	4
Critical	5

Probability \ Severity	1	2	3	4	5
1	1	2	3	4	5
2	2	4	6	8	10
3	3	6	9	12	15
4	4	8	12	16	20
5	5	10	15	20	25
			ACC	C ACC	N ACC

Figure 4.2. Semi-quantitative risk matrix calculated from the estimated probability and severity of risks with the six key stages of the ISO 14971 risk management process [241, 243, 244]. The probabilities are scaled from between 0–1 (or estimated based on the descriptor) to multiply with the severity rating and produce the risk matrix table with risk priority number (RPN) outputs in the range of 1–25. ACC = Acceptable; C ACC = Concern for Acceptance; N ACC = Not Acceptable.

Risk mapping models inform the HTM to describe and tabulate risk rating hazard assessments that are then used to inform design choices and work instructions for medical devices [245]. The most common methods used for medical devices include: the preliminary hazard analysis (PHA); failure modes and effects analysis (FMEA) for product reliability; and fault tree analysis (FTA) [246]. PHA and FMEA are risk tabulation methods that are often used to carry out analysis of prospective adverse events to propose appropriate corrective measures (Figure 4.3A,B) [35]. The accuracy of these methods improves with the development of a more mature product that has undergone system design and testing. FMEA assessments include severity, occurrence and detection as risk factors for the identified failure modes to calculate their risk priority number (RPN) [247]. Other methods like root cause analysis (i.e. FTA) are usually retrospective (Figure 4.3C) [35].

A) Preliminary Hazard Analysis (PHA)

Identifier	Operational Mode	Hazard	Causal Factors	Effects	IRAC	Recommended Action	FRAC	Risk	Comments	Status

IRAC = Initial Risk Assessment Calculation, FRAC = Final Risk Assessment Calculation

B) Failure Modes and Effects Analysis (FMEA)

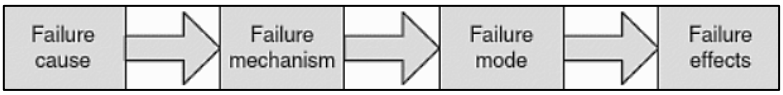

Process function requirement	Potential Failure Mode	Potential effect(s) of failure	S	Potential cause(s)/ mechanism(s)	O	Current process controls	D	RPN	Recommended action(s)	Responsibility and target completion date	Action taken	New S	New O	New D	New RPN

S = Severity, O = Occurrence, D = Detectability

C) Fault Tree Analysis (FTA)

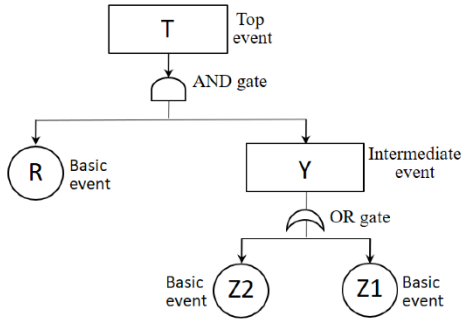

D) Event Tree Analysis (ETA)

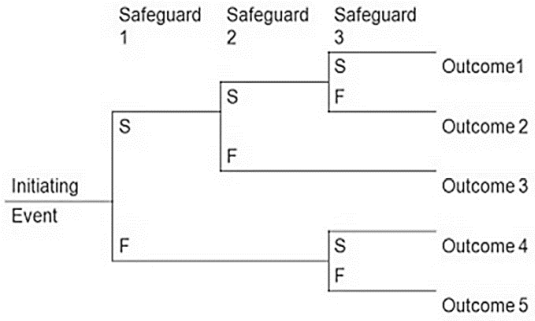

E) Sequentially Timed Events Plotting (STEP)

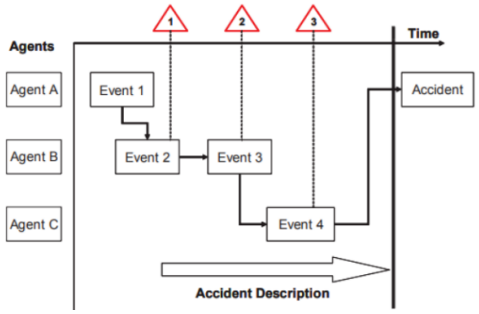

F) Tripod-Beta Bowtie

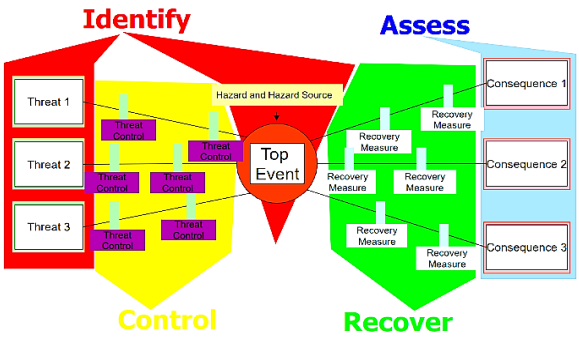

G) Markovian Decision Process (MDP)

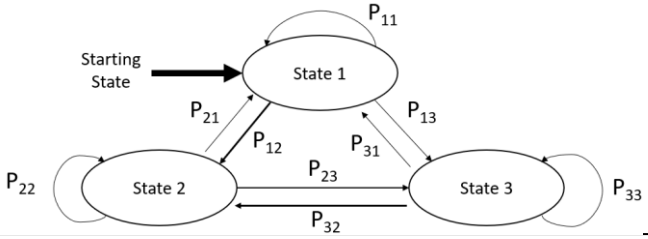

Proceeding State

$$\begin{array}{c} \text{Initial State} \\ \end{array} \begin{array}{c} \\ S_1 \\ S_2 \\ S_3 \end{array} \begin{bmatrix} S_1 & S_2 & S_3 \\ P_{11} & P_{12} & P_{13} \\ P_{21} & P_{22} & P_{23} \\ P_{31} & P_{32} & P_{33} \end{bmatrix}$$

S = State, P = Probability of a State Transition

Figure 4.3. Hazard pathways to model potential events that can lead to harm or failure: A) Preliminary Hazard Analysis (PHA); B) Failure Modes and Effects Analysis (FMEA); C) Fault Tree Analysis (FTA); D) Event Tree Analysis (ETA); E) Sequentially Timed Events Plotting (STEP); F) Tripod-Beta Bowtie; and G) Markovian Decision Process (MDP) [248-253].

Other standard methods for hazard mapping are Event Tree Analysis (ETA), Sequentially Timed Events Plotting (STEP), and the Tripod-Beta model that includes assessments of consequences to map the paths taken to recover from a hazard event (Figure 4.3D–F) [251, 254]. The Markovian Decision Process (MDP) describes a sequence of possible states for a system, like a finite state machine, that can be represented by state diagrams described by probabilistic transitions between each of the states (Figure 4.3G). MDP models have been used to model task sequences in shared human-robot environments, however the number of states can rapidly grow [255].

Fail-safe designs and operations can reduce the likelihood and severity of harm for people in the case of failure or malfunction [256]. This is necessary for robotic systems that rely on the use of complex software and must operate smoothly to limit the likelihood of harm whenever a failure occurs [257]. Simplified systems are more easily defined and segregated for analysis of associated risks [258]. These systems are usually designed with direct lateral influences as hierarchical cause-effect relationships, predictable outcomes and localised risks related to its subsystems [258]. In contrast, highly integrated systems have indirect and unobvious cause-effect relationships which affect system predictability for decision making potentially leading to large system-wide risks or consequences [258]. According to the FDA, redundancy and fail-safe features, feedback mechanisms and alerts should be designed into critical components of systems for improved reliability [259]. The IEC 80601-2-77 describes the safety of medical robots to be a combination of known mechanical and invisible or insensible hazards for the robot and medical device system (Table 4.1) [156].

Table 4.1. IEC 80601-2-77 major hazards for robot safety and medical device safety customised for a cleaning dental robot (created from [156]).

Mechanical Hazards	Safety Aspect	Objects Involved	Hazardous situations	Cause(s)	Incident(s)
Unintended collision	Medical Device	Robot end effector (dental instrument) in the mouth	Unintended and unexpected movement; Uncontrolled trajectory; Loss of speed control	Unexpected soft tissue movement of the head or oral cavity; Incorrect model or coordinates in space; Wrong robot arm dimensions or calibration	Damage to oral cavity soft or hard tissues; Unexpected abrasion or cutting of tissues in the mouth (soft or hard)
	Medical Device	Robot and human (patient body and medical staff)		Failure of safeguard functions and emergency management issues; Robot arm joints extended too close to the patient's mouth; Robot reaches a singularity and performs unexpected arm rotations; Improper reaction by monitoring human operators; Wrong instrument dimensions on robot arm	Trapping, crushing, shearing, pinching, or entanglement by the robot; Robot or the patient's teeth could cut or bruise the face
	Robot	Robot and other items		Performance degradation or poor quality of motion control; Wrong instrument dimensions on robot arm	Mechanical damage or harm
	Robot	Robot itself			
Unintended contact	Robot	Robots and other medical devices	Creation of new electrical, thermal, mechanical and other functional connections	Failure of safeguard functions; Capacitive coupling leakage and electromagnetic disturbance	Electrical, thermal, mechanical damage or harm
	Robot	Between surgical instruments			
Invisible and insensible hazards	Robot	Robot and other items	Unintended and unexpected energy generation and transfer (e.g. escalated temperature of the	Inability to detect hazard; Failure of safeguard functions; Side-effects from other safeguards (e.g. covering the system for sterilisation or other purposes traps heat around robot)	Harmful energy transfer (e.g., leak current, excessive heat damage); Electric shock; Toxicity of material; Infection of microbe; Radiation
	Medical Device	Robot and human (patient body and medical staff)			

			robot during operation)		
Broken attachment	Robot	Robots and other items	Surgical instrument not properly fixed to the robot; Robot movement despite disconnected instrument	Poor design (strength) of mechanical interface; Improper fixation of instrument to robot;	Crushing, shearing, pinching, or entanglement by the surgical instrument; Mechanical damage or harm
	Medical Device	Robot and human (patient body)		Instrument damaged or worn out (surpassed its life cycle); Disconnected instrument left within oral cavity	Broken or sharp components could penetrate soft tissues, lodge between teeth, or become swallowed or inhaled
Lack of data information transfer	Robot	Robot and human (operator)	Information essential to perform surgery is degraded	Poor robot-human interface; Lack of communication mechanisms	Errors and misinformation; Incorrect surgical technique; Incorrect surgeon response
	Medical Device	Robot and human (patient body)	Missing, poor or delayed data for analysis or tracking (poor vision)	Incorrect mouth model; Misidentified health state of tooth; Incorrect procedure performed;	Unneeded treatment or viable tooth structure damaged, broken or extracted

A dental robot to be sold in the US as a medical device requires FDA approval through the de novo, Premarket Notification (510k) or Premarket Approval (PMA) pathway [259, 260]. The de novo classification process is used for new low to moderate risk devices (Class I–II) with no substantially-equivalent legally marketed predicate medical device available for comparison [261]. However, only 10% of surgical robots have had to apply by the de novo pathway [165]. Most surgical robots, including the assistive dental robot Yomi, successfully applied by 510k as a moderate risk device (Class II) which would involve providing evidence of substantial equivalence to another approved surgical robot in order to reduce the time and cost to market [165]. High risk devices (Class III), which could include dental robots operating at higher levels autonomy, will likely necessitate the use of PMA with clinical trials to prove their product's medical benefits and safety for a given application to ensure it overcomes any associated risks, increasing costs to commercialisation [165, 260, 262]. Similar to the FDA, the European Union (EU) Medical Device Regulation (MDR), updated in 2017 for higher transparency, requires that each medical device receives a certificate and CE marking from their notified body after conformity assessment audits given their level of risk [187, 260].

In Chapter 3, a new dental setup was proposed where the patient lies face down in a prone-like position during a procedure. In this setup, the robot is positioned underneath the patient and is contained in a chamber. A small robot such as Meca500 was suggested to be suitable that has the capacity to operate in a small environment. Changing to a forward-leaning position has a number of benefits that minimise risk. Here, potential modifications to increase patient safety are assessed for a diagnostic and cleaning robot as an entry level autonomous robot. A supervision framework is then developed for dental robot risk management to minimise effects of the domino theory and Swiss cheese model for dental robot hazard pathways. Where possible, the framework simplifies challenges outlined by the complexity of the dental robot system, as highlighted by the functional connectivity map (Section 2.4, Figure

2.7). Where complexity is unavoidable, building redundancy into safety measures is critical to mitigate the occurrence of high-level risks.

4.3 Analysis of Potential Patient Harm

To improve the level of safety and confidence in a dental robot system and to minimise potential failure points, the complexity of the system should be reduced as much as possible. This section analyses the potential benefits in terms of risk probability of the risk reductions included from the Hierarchy of Controls for the postural dental setup. The standard risk matrix was used to perform the dental robot hazard analysis (Figure 4.2, Table 4.2) [244]. The probability levels were assigned based on the percentage of relevant errors to those reported and the Visual Analogue Scale (VAS), which is the most accepted method to measure dental pain, from Thusu *et al.* (2012) and Canakci *et al.* (2007) [9, 93]. This scale assigns a score of '0' for no pain or discomfort, through to a maximum of '100' for the worst pain or discomfort imaginable [9, 263, 264].

Table 4.2. Risk severity and probability descriptors and values with the dental robot hazard rating risk matrix.

Severity			**Probability**		
Value	***Descriptor***	***Method of Recovery***	***Value***	***Descriptor***	***Rel. %****
1	Negligible	No intervention required	1	Improbable	≤ 0.5
2	Minor	Self-treatment	2	Remote	≤ 2.0
3	Serious	Timely treatment	3	Occasional	≤ 15
4	Major	Surgery	4	Probable	≤ 20.0
5	Critical	Immediate intervention (life-threatening)	5	Frequent	> 20.0

*= % of errors/VAS (not of total procedures)

Risk Matrix		***Severity***				
		1	2	3	4	5
Probability	1	A	A	A	A	C
	2	A	A	A	C	N
	3	A	A	C	N	N
	4	A	C	N	N	N
	5	C	N	N	N	N

Key: N = Not acceptable (orange box); C = Concerned acceptance (orange outline); A = Acceptable (grey outline).

A total of sixteen forms of potential dental harm to the patient have been identified (Table 4.3). As no sources of harm have been eliminated, the severity of each remains fixed. Each risk was rated and the change in hazard probability between the current dental setup and the proposed potential dental setup was determined. It should be noted that injuries around the neck are at risk of air entering the deep neck spaces and large vessel involvement, with possible haemorrhage and or thrombosis [125]. Also, the introduction of harmful pathogens and bacteria can result in infection, while some patients are at risk of allergic reactions to materials used in procedures [35, 265].

Table 4.3. Change in system harm from robotic introduction with a safety-focused design. Estimated current probabilities determined using Thusu *et al.* (2012) and Canakci *et al.* (2007) [9, 93].

Ref	Expected Potential Harm	Severity	[1]Current Probability	[2]Potential Probability	Change in Risk Rating	Justification for Potential Probability
H1	Discomfort	Negligible	Occasional (1.64%)	Occasional	A = A	Easier to incorporate distraction techniques without impacting direct operator vision (e.g. VR).
H2	Pressure sores	Minor	Remote (0.50%)	Remote	A = A	There is potential for a robot to perform procedures faster with more precision so that the patient has less time in the operative chair.
H3	Operative dental bleeding	Minor	Occasional	Occasional	A = A	Inter-operative and intraoperative inconsistency can be reduced by robotic instrument control.
H4	Operative dental pain (e.g. gingival sensitivity)	Minor	Occasional (14.9 VAS for probing)	Occasional	A = A	Locations of the instrument where there is excess patient movement can be recorded and used to predict future patient movement at those locations.
H5	Ingestion of debris (crown, tooth, bridge, filling)	Negligible	Occasional (2.44%)	Remote	A ▼ A	The altered patient posture will reduce likelihood for particles to fall into or close to the throat. Potential to only use a circular high-volume suction device around the mouth for forward-leaning postures.
H6	Disease transmission between patients (infection control incidents)	Serious	Remote (1.64%)	Remote	A = A	The chamber can help to reduce the probability of disease transmission. The chamber may be thoroughly cleaned of blood, saliva and debris, and then sterilised with a combination of mechanical and chemical cleaning, followed by autoclaving,

								chemical or plasma sterilisation, between procedures.
H7	Disease transmission between patient and dentist (infection control incidents)	Serious		Remote	A	=	A	The reduced workload for a dentist can provide energy and time to carry out infection control practices. The robot can assist in cleaning or inspections. The chamber physically separates the patient and dentist, and all aerosols are contained in the chamber.
H8	Radiation exposure and electric shock	Serious	Remote	Remote	A	=	A	Safety standards are available for X-ray exposure and electrical instruments in wet environments. The dental robotic system is designed for lower risk procedures that do not depend on radiographic scans (i.e. for marker or target tracking localisation and 3D models).
H9	Hazardous liquid splashing into eye(s)	Serious	Remote (0.60%)	Remote	A	=	A	The headrest adds an additional physical barrier between the robot and the patient that can be designed to be stronger than safety glasses.
H10	Dental technique errors (e.g. damaged tooth viability, including WSTEs)	*Serious*	*Remote* (WSTEs at 1.79%)	*Occasional*	A	▲	*C*	Presence of dental errors relies on the quality of diagnosis, pre-planned or autonomous paths and tooth localisation, that are prone to human errors and limited by the AI vision capability. The robot is a not sentient device but could be trained to perform dentistry, such as by advanced reinforcement learning methods.

H11	Inhalation of debris or inhalation or ingestion of liquids	Serious	Remote (1.14%)	Remote	A = A	The altered patient posture will reduce likelihood for particles to fall into or close to the throat.
H12	Inhalation or ingestion of sharp and dangerous components (e.g. burs, scalpel blades)	Major	Remote (0.70%)	Remote	C = C	The tracked procedure can monitor visual changes to the dental instrument and keep record of components used in the mouth. Potential to only use a circular high-volume suction device around the mouth for forward-leaning postures. Tracking of the instrument orientation, and liquid velocity, must be performed to avoid spraying liquids, such as water, projecting towards the back of the mouth and throat.
H13	Adverse reactions (anaesthetic, pain control, antibiotics, material allergy etc.)	Major	Occasional (3.98%)	Occasional	N = N	Monitoring systems to measure vital signs can be used to indicate the need for an emergency response. Patients in a more prone position are closer to the recovery position than those in supine.
H14	Medical emergencies (vasovagal, epilepsy, hypoglycaemia etc.)	Major – Critical	Occasional (5.52%)	Occasional	N = N	The reduced workload for a dentist can provide energy and time to focus on safety for high-risk patients and procedures.
H15	Internal impact collision with tissue damage (laceration, sharps, bruising and burn)	Major	Occasional (6.86%)	Probable	N ▲ N	Dentist cannot directly see inside the mouth visually without a camera if the patient is in prone. The system is dependent on collision avoidance control for a potentially strong robot that holds a variety of sharp and non-compliant dental instruments.

								Without a person in control, risk and model tracking should be assessed to minimise chance of patient injury.
H16	External impact collision with tissue damage (laceration, sharps, bruising and burn)	Major	*Remote* (1.94%)	*Improbable*	C	▼	A	Chamber around the robot reduces the risk of the patient colliding with the strong robot. The chamber mouth opening could be closed while the patient is being prepared for the procedure. The headrest can protect the face as a physical barrier between the robot and the patient.

Key: [1]Current system design with patient in supine-like position on their back; [2]Proposed innovative setup; N = Not acceptable (orange box); A = Acceptable; ▼ = Reduced risk; ▲ = Increased risk. Highly uncertain risk estimates in *italics*.

4.4 Risk Management Framework Design

To understand the level of safety for a system, the risks must be quantified and measured. To do so, an automated independent safety monitor is proposed for dental robots in the form of a framework to automate risk management and provide situational and environmental awareness (Figure 4.4). This 'Risk Supervision System' follows the structure for Endsley's Situation Awareness Model (Figure 4.4A). In this model, Endsley *et al.* (1995) introduced the decision-making processes from the perspective of a person, beginning with perceiving the status, attributes, and dynamics of the environment in a volume of time. The data is then integrated to give meaning or understand the environment, including their significance to any goals and expected accuracy, deviations and patterns, before finally estimating states for decision making [266].

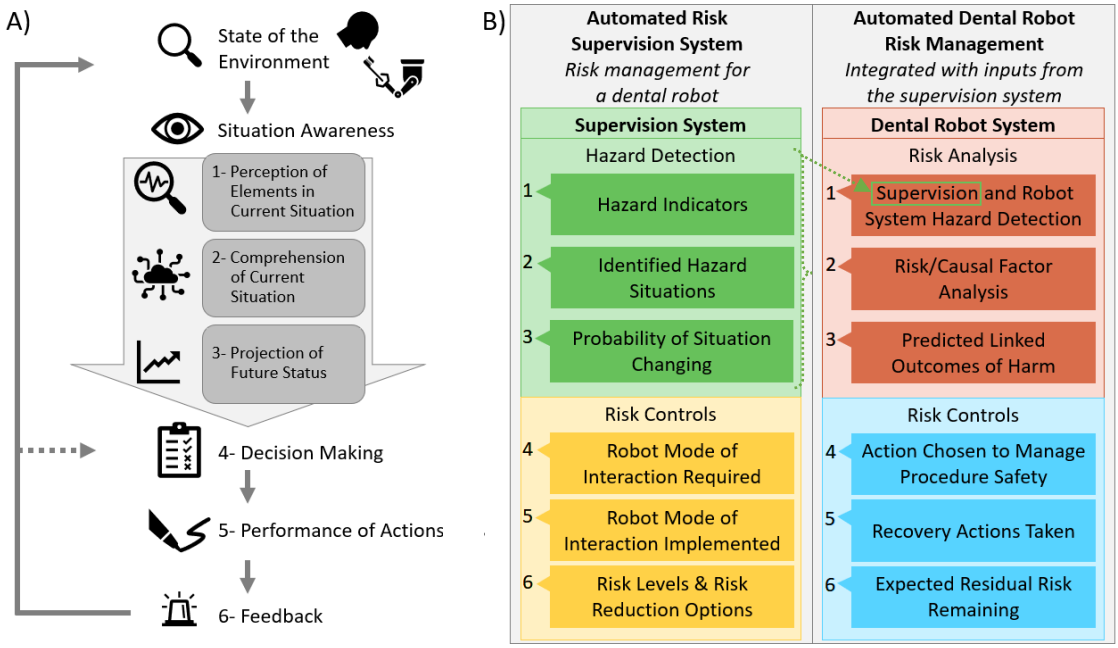

Figure 4.4. A) The internal structure of the Endsley's Situation Awareness Model [266]. B) Dental robot risk management system with a parallel supervision system model for hazardous situation awareness with its layered design inspired by Endsley's model, including hazard detection and defining the safe operating modes for a dental robot. The advanced risk management model includes the analysis and recovery measures for risk and causal factors of dental procedures. The supervision and dental robot risk management levels are labelled with corresponding numbers to the situation awareness model levels.

The different components of the situation awareness analysis model have been linked to the stages of risk analysis from hazard detection to risk controls (Figure 4.4B). A parallel risk management model was designed to allow the supervision system to track, assess, detect and respond to high risk and hazardous situations without the additional complexity of determining the contributing risk factors. The supervision system, therefore, acts solely as an automated independent safety monitor, which is "equipped with means for context observation" informed by sensors and "able to trigger safety interventions" [267]. In effect, the system can quickly respond to high-risk situations before knowing the exact cause of an error for decision making. This is particularly important for higher levels of automation with less human input. The automated risk management system model aims to lead to the development of "self-supervised" autonomous dental robots.

The concept of a safety monitoring has been considered in surgical and dental procedures, but is often considered a fault-tolerant approach that is used to assess quality over ensuring the safety of a procedure, particularly when reliant on force or visual feedback of a collision or harm [74, 207, 267]. Instead, the supervision system is designed to warn for changes in likelihood of risk. The supervision performs context observation informed by sensors and triggers safety interventions before harm is expected to occur, similar to the addition of an alarm module to alert surgeons when the difference is greater than the predefined tolerant range from the preoperative plan for dental implantology [268]. Future developments of the automated dental robot risk management can incorporate analysis of causes of harm to mitigate identified higher risk levels before a safety intervention is triggered (Figure 4.4B), which is necessary for the development of successful high and full autonomy dental robots.

4.4.1 Proposed Risk Supervision System

Assessment measures for safety have been broken down into three supervisory system blocks or "subcomponents" that include the procedure block, the observer block and the patient

block (Figure 4.5A,B). The blocks are responsible for the safety of the dental instrument technique, the stability of the dental operative environment, and the compliance and response of the patient. Their role is to monitor high-risk hazardous situations that could cause harm during dental procedures. The robot system is then expected to have its own overlapping supervision capabilities that focus on the quality and performance of the robotic procedure in normal operation and during emergency responses, highlighted by supervision block exclusions (Figure 4.5C). By dividing the risk management responsibilities between multiple supervision systems, the overall system can be simplified and have multiple levels of redundancy for safety, similar to the Swiss cheese model (Figure 4.1B).

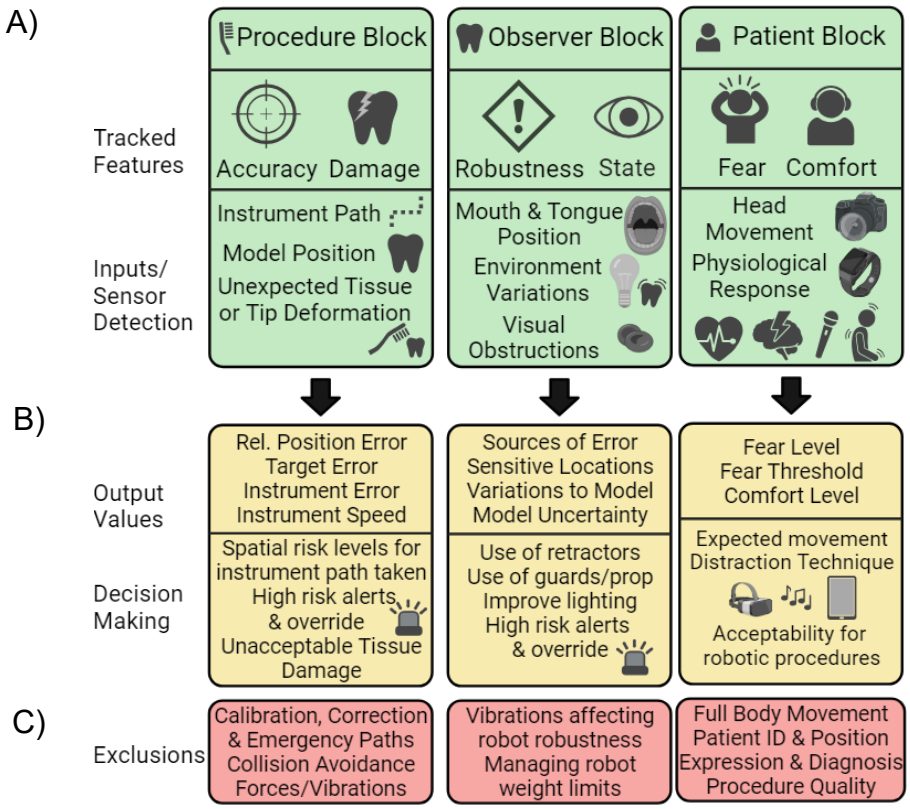

Figure 4.5. Risk supervision system blocks for automated risk management where the remaining exclusions would act as inputs for the robot system design. A) Tracked features of each block are labelled followed by the relevant inputs from the environment sensors to achieve it. B) Output values can be used to carry out safety-related decision making. C) Exclusions from each of the blocks are relevant aspects of the dental environment that can improve safety but rely on the design and setup of a dental robot.

4.4.1.1 Perception of Environment Hazards

The detection of hazards may combine current technologies, such as visual guidance systems, with physical dental safeguards that protect soft tissues or hold the mouth open to assess the safety of the operating instrument in the oral cavity. These technologies can be combined to create "interpreted data" (ID) from the environment to assess states, attributes and system dynamics in a given time. The interpreted sensor data can assist the identification of latent risks of hazardous situations before it results in patient harm. Critical aspects should overlap with calculations made by the robotic system for safety through redundancy. Examples of possible sensor detection systems for the supervision systems are provided (Table 4.4), together with their importance for dental robotic safety.

Table 4.4. Automated risk management inputs from sensors used by the supervision system blocks with the potential redundancy for safety provided by the robotic system.

System Input	Sensor Detection Systems	Robot System	Safety
Procedure Block			
Instrument path	• Visual guidance system marker tracking and known instrument type (speed thresholds, position constraints)	• Robot joints angles or positions calculating the relative instrument position • Joint limits and singularity management	Known relative position of the instrument to the oral cavity to recalculate safe locations and paths
Relative model position	• Visual guidance system marker tracking linked with intraoral scan • Passive multi-link arm tracker attached to pressure-sensitive mouth prop	• Mouth position from camera vision, marker position or from multi-link arm tracker	
Unexpected tissue or tip deformation	• Probability model of head tissue contact depth (patient jaw parameter inputs) • Patient head scan data used to calculate contact with instrument • Camera computer vision of depth into tissue to estimate force • Access to instrument force measurements from robot or a digitised instrument	• Measure and manage forces on instrument, ideally with a 6-axis force sensor • Possible estimated pressure on tissues from contact area based on direction and location along instrument (i.e. from a torque-force sensor)	Alerts to check the calibrated instrument position and to correct paths if required
Observer Block			
Mouth and tongue position	• Camera computer vision from outside the oral cavity • Mouth prop pressure and orientation sensors (with or without tongue guard)	• Localisation of mouth model and force tracking • Orientation of sharp tip away from potential tongue location	Data for observing the tongue position and location of the mouth relative to the initial position
Environment variations	• Oral images taken overtime for changes in properties of the oral cavity from its initial appearance (observing the reflectivity of the mouth, i.e. moisture and saliva)	• Robot to track trajectory for collision avoidance accounting for instrument shape, weight and vibrations on potential force of impact with a moving jaw	Data for observing for the presence of excess saliva or water in the mouth, and unexpected

	• Repeated intraoral images and scans to compare changes in appearance of location in the mouth		cheek, gingivae, jaw or tooth movement
Visual obstructions	• Check for poor camera vision and lens clarity	• Check camera sensors for low image quality	If poor vision or obstruction, cameras need to be cleaned from debris
Patient Block			
Jaw movement and presence of blood	• Track of mouth opening for instrument procedure via computer vision or marker tracking (if no mouth prop)	• Tracking instantaneous and potentially future head and jaw movement • Emergency protocol plan (paths for instrument to exit the mouth if required) • Proximity sensor or laser curtains to ensure distance (of hands) from robot arm	Data for tracking and predicting jaw and head movement for a procedure to indicate patient compliance; Presence of blood may indicate sensitivity of gingivae
Head movement	• Pressure sensors on headrest • Visual guidance marker • Passive multi-link arm tracker • Oral images taken overtime for changes in presence of blood around gingivae from initial appearance		
Physiological response	• Galvanic skin resistance (sweat) sensors • Heart rate, blood pressure and body temperature sensors • Hand grip strength and hand movement tracking • Eye tracking with VR headset system • Expression difficult tracking with computer vision (less possible with chin rest or headrest)	• Patients may be cleared prior to using a robotic dental system and observed closely during initial procedures by the operator. Patients should be trained on how to exit safely from the robot procedure.	Data for estimating the patients state of mind during a procedure (i.e. stress, fear and discomfort)

4.4.1.2 Hazard Comprehension and Projection

Interpreted sensor data (Table 4.4) can be evaluated to determine the severity of identified relevant hazardous situations for each supervision block. By tracking the severity of hazardous situations over time, the likelihood of a hazard occurring can be determined and abated using different measures depending on the supervision block (Table 4.5). To account for public aversion to harm by a robot, the output risk matrix ratings of "concern" were also included as important forms of harm to mitigate [244]. The potential for dental technique errors (H10), which depends on operator supervision and planning methods for the dental procedure, has been excluded from the supervision systems as they are designed to focus on safety, rather than technique quality, except where it results in physical patient harm.

Table 4.5. Hazardous situations that can be detected and managed from sensor measurements (interpreted data) from the dental environment to avoid harm.

No.	Interpreted Data	Hazardous Situation to Detect	Relevant Hazard(s)	Harm to Avoid
Procedure Block				
ID1.1	Motion of instrument and tip	Poor collisions and control during procedure	Instrument laceration or force impact hazard	*H15* Internal impact collision with tissue damage
ID1.2	Position of instrument handle through the mouth opening	Inappropriate collisions and motions of instrument handle, such as with the cheeks, lips or other teeth		*H16* External impact collision with tissue damage
ID1.3	Relative instrument movement around constraining oral tissues	Unsafe movement of instrument at locations towards patient oral features prone to high impact on collision		
ID1.4	Location and rotation of instrument around sensitive oral features	Holding instrument in a relatively unsafe orientation and location around soft oral tissues prone to laceration		
Observer Block				
ID2.1	Mouth opening	Jaw opening too narrow for instrument and motion of procedure	Instrument laceration or force impact hazard	*H15* Internal impact collision with tissue damage
ID2.2	Tongue position	Tongue in unsafe location for procedure that obstructs access to operative site		*H16* External impact collision with tissue damage
ID2.3	Vision quality	Poor camera vision of the inside of the mouth and components to assess any changes in their appearance or quality (e.g. lighting or obstructions)	Adverse reaction (contamination); Instrument laceration or force impact hazard; Patient position (choking) hazard	*H6/H7* Disease transmission *H9* Hazardous liquid splashing into eye(s) *H16* External impact collision with tissue damage *H12* Inhalation or ingestion of sharp and dangerous components

				H15 Internal impact collision with tissue damage
ID2.4	Liquid volume in mouth	Unsafe amount of liquid (saliva and water) in the mouth with or without debris	Patient position (choking) hazard	*H1* Discomfort *H5* Ingestion of debris *H11* Inhalation of debris, or inhalation or ingestion of liquids
Patient Block				
ID3.1	Patient compliance to movement requests	Patient non-compliant (moving excessively, continuously closing mouth or unresponsive)	Compliance hazard	*H15* Internal impact collision with tissue damage
ID3.2	Procedure length vs breaks	Long procedure time or lack of breaks for patient		*H1* Discomfort *H2* Pressure sores
ID3.3	Sensitive dental sites or oral locations	Sudden jolting movement expected at operative sites with high sensitivity and blood indicating weak tissues, harm or pain	Compliance and adverse reaction hazard	*H3* Operative dental bleeding *H4* Operative dental pain *H13* Adverse reactions
ID3.4	Patient physiological response	An undesirable large change in physiology may indicate an adverse event or change in stress level (i.e. from GSR, heart rate, blood pressure or body temperature sensors)	Adverse reaction or emergency health hazard	*H13* Adverse reactions *H14* Medical emergencies

4.4.1.3 Hazard-based Decisions and Action Controls

The results from the hazardous situation interpreted data should be compared to a defined criteria or threshold to determine whether the risk is acceptable or unacceptable for the procedure to continue. The combined supervision block risk outputs can then be used to inform a hazard state diagram. A state diagram was made with three levels to describe the detected hazard risk state of the system (Figure 4.6A). To qualify for a transition out of Hazard State 1, the patient should appear comfortable and not stressed with an acceptable patient block risk output. Hazard State 3 is for normal operation of the dental robotic procedure with acceptable risk outputs for all supervision blocks. When a high-risk output is detected, the system transitions to Hazard State 2 if it is a manageable dental environment (low observer block risk output), or Hazard State 1 otherwise.

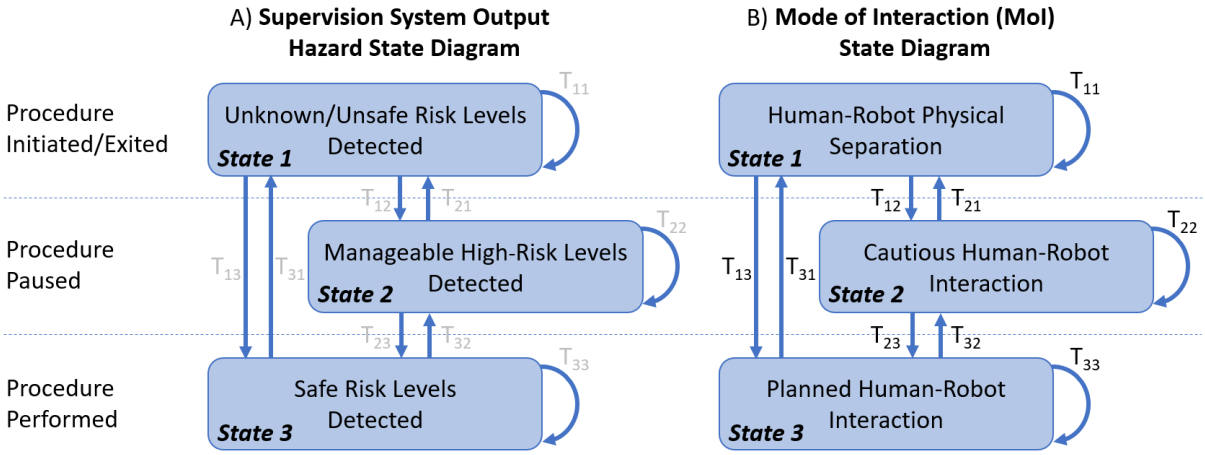

Figure 4.6. Simplified three-state Markovian Decision Process diagrams for: A) Supervision system hazardous situation risk output states for probability of patient harm (Hazard States); and B) Modes of Interaction (MoI) to define the accepted form of human-robot interaction (HRI) depending on the measured supervision system risk state.

The supervision system hazard state levels defined by the supervision block decision making have been designed to directly relate to the acceptable mode of robot interaction (Figure 4.6B). To simplify control of a dental robot, three Modes of Interaction (MoI) were identified for system operation: 1) human-robot separation; 2) cautious human-robot interaction; and 3) planned human-robot interaction performing the dental procedure. The risks

for the robotic procedure increase from MoI State 1 to State 3 (state transition, T_{13}) and must correspond to a decrease in perceived supervision risk for the identified hazards. To transition to a higher MoI State, the system must be at the same or higher Hazard State. This decision making is independent of the degree of dental robot autonomy.

The risk supervision system outputs can be curated to be of interest between values of 0 to 10. These values can be used to define the acceptable mode of interaction for the robot (Table 4.6). To safely perform a procedure in State 3 for planned interactions, the risks for all aspects of the procedure should be minimised to a manageable level. This has been assigned a threshold of 8/10. An increase in risk based on instabilities detected in the environment from the observer block should result in a transition to State 2 for a cautious interaction. Finally, where the patient appears fearful and non-compliant, the patient block should detect high risk and require a transition to State 1 for separation between the patient and the robot.

Table 4.6. Modes of interaction related to the supervision block states for operation of a dental robot and supervision block ID output risk thresholds.

<table>
<tr><th rowspan="2">Mode of Interaction (MoI)</th><th colspan="3">Supervision Block ID Output Range and Details for MoI</th></tr>
<tr><th>ID1 (Procedure)</th><th>ID2 (Observer)</th><th>ID3 (Patient)</th></tr>
<tr><td>State 1: Human-robot separation</td><td>>10
Procedure evaluated and recreated</td><td>≥8
Dental environment instability</td><td rowspan="3"><8
Patient appears comfortable and not too stressed</td></tr>
<tr><td>State 2: Cautious human-robot interaction</td><td>8 – 10
Procedure in review</td><td rowspan="2"><8
Ideal dental environment for operation</td></tr>
<tr><td>State 3: Planned human-robot interaction</td><td><8
Performing safe procedure</td></tr>
</table>

The robot would need to comply with the output MoI requirements to ensure a safe operative environment for the patient. Each MoI State defines the accepted types of interactions and describes the transitions between them by their need in terms of patient harm and the system's design control options (Table 4.7). In State 3 with a procedure in operation, any harm or hazards detected that increase the system risk may cause an emergency robot response (T_{32})

and then separation between the robot and patient (T_{21}) if required. The probabilities of transitions between states can be measured and tracked over time, along with the probability distribution or proportion of time for remaining in State 3 and the speed of transitions to the accepted MoI State for compliance to the reported Hazard State. The probability distribution of the states may be calculated following a procedure using the probability transitions to converge on the system's equilibrium state from iterative calculations.

Table 4.7. Automated risk management inputs from supervision system blocks and redundancy for the robotic system safety.

No.	MoI State	Transition	Transition Condition	Potential Harm	Control Options
S_1	Human-robot separation	T_{11}	Unsafe to approach patient while in hazard state	Low since patient separated from robot and the dental instrument end effector, unless patient is non-compliant	• Autonomous or manual instrument dismount • Zero-gravity robot control separation • Patient removed by distance to the robot or a barrier • Controlled emergency exit (L1-L5) • Halted procedure and robot fixed in place (E-stop)
		T_{12}	On testing the patient's response to an approaching or nearby robot		
		T_{13}	Safe to start procedure		
S_2	Cautious human-robot interaction	T_{21}	Unsafe to remain near patient (emergency exit)	Medium-high depending on hazards detected, patient movement, instrument type, relative instrument position and controlled robot motion (emergency exit trajectory)	• Manual robot remote control or hand-guiding procedure (L1) • Robot in cautious mode where the procedure is paused, and the instrument tracks the patient (L2-L5)
		T_{22}	Safe to remain near patient with automated procedure paused		
		T_{23}	Safe to continue procedure (risk reduced or system recovery)		
S_3	Planned human-robot interaction	T_{31}	Safe conclusion of procedure (no transition if unsafe level detected)	Medium-high dependent on accuracy of hazard detection and relative patient-instrument position or movement	• Autonomous or pre-programmed robot control (L2-L5)
		T_{32}	Unsafe hazardous situation detected		
		T_{33}	Safe to continue procedure		

Key: MoI = Mode of Interaction; Traditional robot autonomy levels: L1 = Assistance; L2 = Task; L3 = Conditional; L4 = High; L5 = Full.

4.4.2 Proposed Risk Management Model

The development of an automated risk management system is necessary to manage the dynamic risks of the complex dental robot environment in order to develop higher levels of autonomy that can implement risk controls to create a safe and efficient dental robot. The proposed framework for a dental robot involves the development of risk awareness using the combined outputs from the supervision and robotic system to diagnose the presence of hazards (Figure 4.4B). This is challenging as causal factors may have overlapping characteristic risk measures for a given hazardous situation, rendering the need for large arrays of possible causes that need to be distinguished for effective risk recovery. The development of the framework is outlined in Appendix B, along with calculations of severities, risk ratings and relevant ratios.

The framework was developed into a risk management network (RMN) model (Figure 4.7). The defined layers begin with the supervision system block outputs, along with measurements taken by the dental robot system (Level 2, Figure 4.7). Within each block, the interpreted data used to define the risk level can be linked to a number of risk factor groupings (Levels 3–4, Figure 4.7). These groups aim to manage the extensive number of causal factors that could result in the detection of the relevant hazardous situation (Levels 4–5, Figure 4.7). Further, to simplify decision making processes, the most important causal factors and recovery methods can be prioritised to maximise patient safety during high-risk situations (Levels 5–6, Figure 4.7). The potential cyclical nature of the risk management network is generated from the potential to estimate the supervision system risk outputs by taking a bottom-up approach from known risk factors. This creates an added benefit of assessing the safety of a dental robot system prior to an operation or before resuming a procedure.

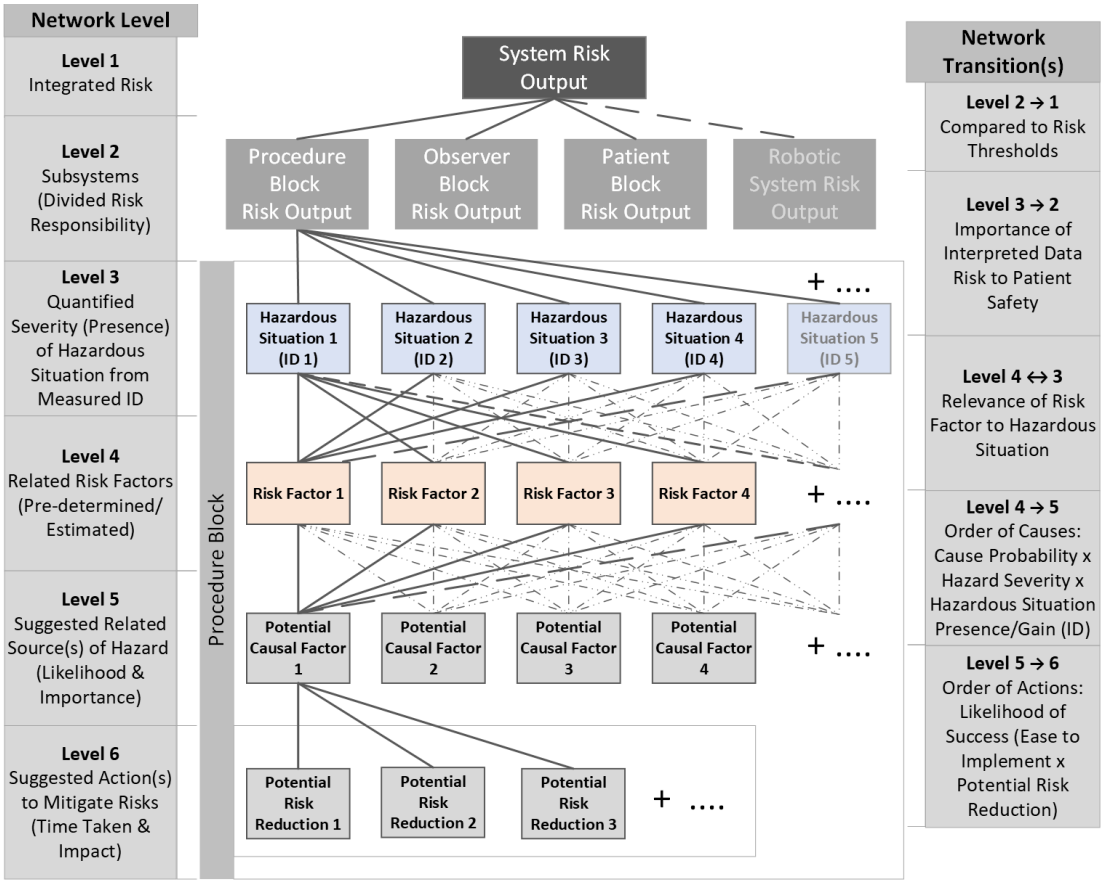

Figure 4.7. Risk management network (RMN): Combined supervision block network (cyclical-middle-&-out) with the defined network levels and methods of transitioning between them. The internal structure of a supervision block is displayed. An additional robotic system risk output is included for specific robotic system safety measurements.

Numerous factors can influence and help to predict the success of a dental procedure. Potential major predictor risk variables for robotic dental procedures that relate to the technique, operative and patient factors are categorised into twelve risk factor groups, regarding the procedure preparation, operative environment, operative procedure, and patient's reaction to the procedure (Table 4.8). Increasing the number of known factors can reduce the uncertainty of the dental robot system before and during procedures. These risk factors can amplify or deflate the severity (or importance) of the supervision system risk outputs depending on the procedure, instrument or the level of robot autonomy.

Table 4.8. Risk factor categories grouped as potential predictor variables affecting risk to assess procedure safety and carry out procedure risk management.

Category	Technique Risk Factors	Operative Risk Factors	Patient Risk Factors
Procedure Preparation	*RF1.1 Anatomical Challenges* • Patient mouth: opening size, tongue size, and presence of diseased tissue • Tooth properties: tooth spacing, morphology, malocclusion, mixed dentition, missing teeth, and mobile teeth affected by periodontal disease • Dental arch shape: width, arch form, Curve of Spee, and curve of Wilson	*RF1.2 Instrument Handle* • Handle properties: size (width and diameter), angle of axis (relative to instrument tip) and compliance • Soft tissue avoidance requirements (cheeks/lips) • Instrument control: distance to last robot joint, orientation limits, robot reach and payload limit	*RF1.3 Patient Position* • Headrest size and comfort • Patient posture • Head rotation (pivot point) • Eye protection
Operative Environment	*RF2.1 Instrument Tip* • Properties: size (working end area), compliance, sharpness, tip wear, and angle for operation • Tracking: calibration, and localisation of operative site • Technique: ease and efficiency of tip actuation, speed setting, and vibrations, heat produced, and cooling required (water volume speed or air pressure)	*RF2.2 Oral Tissue Resistance* • Instrument: size (handle width) • Patient mouth: opening size and tongue size, bite strength, tissue fragility • Movement and compliance: oral tissue flexibility (cheek or lip), mandible jaw, patient head (depending on its mass and the patient's strength), and soft headrest cushioning • Patient awareness: likelihood to react to pressure (age and experience factors), pain thresholds	*RF2.3 Stress or Fear* • Annoyance or discomfort • Tissue sensitivity • Dental pain • Previous experience • External factors • Patient awareness: distraction techniques involved and their effectiveness, and pain threshold

Operative Procedure	*RF3.1 Instrument Control* • Pressure: technique forces and pressure required, and robot strength (force and torque) • Accuracy: sensor resonance, waterproof properties, temperature range and force limits • Motion: robot movement control, singularities, and trajectory plan • Movement and compliance: patient head, dental arch jaw, and oral tissues (tongue) • Speed: procedure efficiency, and maximum robot speed limit	*RF3.2 Operative Site Location* • Localisation: head of patient, dental arch scan accuracy and registration, jaw of dental arch site, instrument calibration accuracy, and instrument tip localisation accuracy • Accessibility: position along jaw, depth below gingival margin, side of dental arch, tongue position, sensitivity, and accuracy of robot control • Camera visibility: quality, blurring or obstructions	*RF3.3 Patient Compliance* • Patient perception: vibrations, heat, liquid volume in mouth • Movement: opening size (opening and closing), head rotation and tongue • Annoyance and discomfort • Stress and fear • Cooling technique: risk of water projecting to the back of the mouth or throat
Patient Reaction	*RF4.1 Patient Movement* • Robot control: achievable relative instrument movement and rotation, maximum speed limit of robot, and robot reach limit • Patient mouth: opening size, and tongue size • Movement: speed of head or jaw movement, angle of mouth rotation • Tracking: blurring and quality of camera vision, quality of position tracking system	*RF4.2 Adverse Reaction or Emergency* • Physiological response: measures, sensor robustness and data analysis accuracy • Camera visibility: quality, blurring or obstructions • Volume of water, blood or swelling of tissues in the mouth • Patient condition: biting or mouth closing, patient movement, and changes to expected “active consent” hand grip pressure sensors	*RF4.3 Annoyance or Discomfort* • Patient perception: vibrations, heat, noise, and smell • Technique: procedure time, procedure efficiency, and use of oscillating instruments • Patient awareness: distraction techniques involved and their effectiveness, jaw opening pain (trismus), previous experience, and pain threshold

4.4.3 Integration with a Dental Robot

In accordance with the proposed autonomy-risk levels (Section 3.6), the three proposed supervision system components take a step to close the gap to the next higher level of autonomy (Figure 4.8). The procedure block should be integrated at Level 3 to confirm risk awareness for an intermediate stage, Level 3.5 “Conditional Risk Awareness and Autonomy”, that can be operated with a qualified trained operator as opposed to a required dental expert (Table 3.2). The observer block may be integrated at Level 4 “High Autonomy” with a trained safety operator to be ready for Level 4.5 “High Risk Awareness and Autonomy” with the potential of self-supervision for experienced patients. At a minimum, the patient block should be applied at Level 5 towards the development of Level 5.5 “Full Autonomy with Risk Awareness”. These supervision systems are designed such that they are only analysing the safety of the dental technique, while not providing expert medical advice on the diagnosis or technique decision making. The use of autonomous dental robots will ease the required level of training for complex hand-guiding and remote collaborative techniques, thereby help to focus the clinicians’ tasks towards in order to focus on patient safety during procedures, as well as technique and setup efficiency and infection control between procedures.

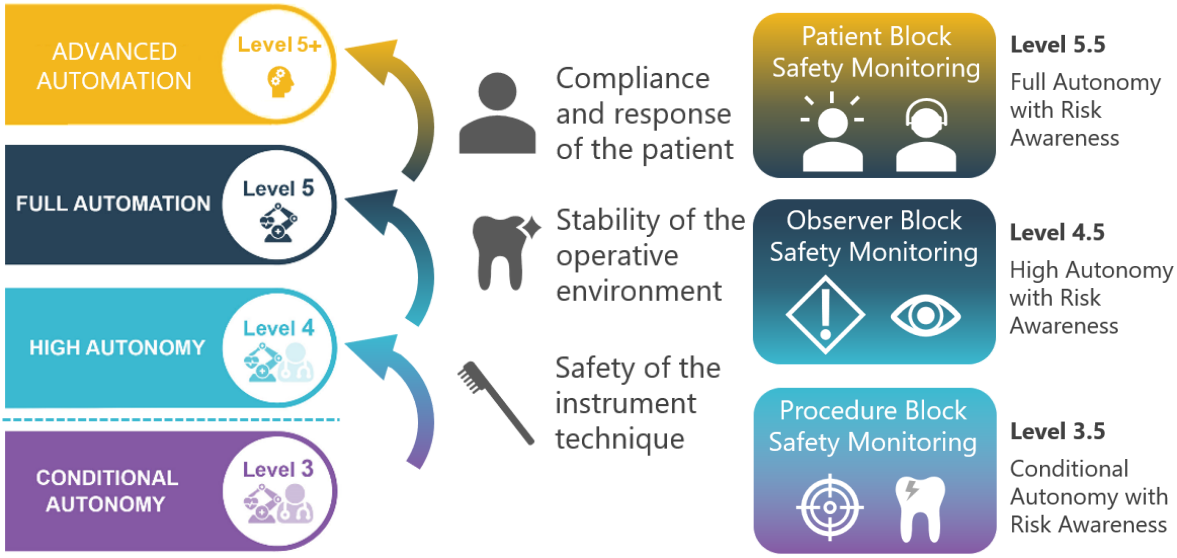

Figure 4.8. Integration requirements to progress to the higher levels of autonomy beyond the conditional autonomy "glass ceiling" to satisfy changes in operator awareness towards improving patient access to dental services. Added levels for monitored risk awareness: Level 3–4 Transition: Level 3.5 procedure block; Level 4–5 Transition: Level 4.5 observer block; Level 5–5+ Transition: Level 5.5 patient block (input levels from [57]).

For Class II dental robots, 510k is the cheapest and least time-consuming path to approval in the US and was introduced to encourage the development of innovative medical devices [269]. Like Yomi, this pathway was even used for the da Vinci robot surgical instruments that claimed to be substantially equivalent to laparoscopic instruments [262]. The cost of 510k pathway is a total of ~US$33,500 in FDA fees, which is 15% of the cost for the De Novo classification request at a total of ~US$171,500 in FDA fees in 2025 [270]. For future Level 4 and Level 5 medical robots, it is anticipated that they will need to follow the PMA pathway as a high-risk device (Class III) at a cost of US$550,000 in fees to the FDA [165, 270]. Manufacturers that apply for PMA can use their extensive validation through clinical trials to be pre-empt from state products liability laws [260, 262]. Additionally, the increased costs of PMA are expected to increase barriers to entry for other similar medical robots, opening the door for potential high-risk forms of investment, such as from venture capital, which benefit from the reduced likelihood of competitor products entering the market.

An important design consideration for the supervision systems is the ability to implement their use independent from a dental robot. This can be used to verify their quality in safety assessments of dental procedures performed manually before their application with a robot by integrating with computer vision, sensors and a guidance system like RoboDent, Navident or X-Guide. This can be observed visually where the supervision system only provides feedback for the robotic system and operators to interpret (Figure 4.9). Feedback received by the robot on procedure safety could be incorporated to improve its planned paths or autonomous control during dental procedures. When combined with advanced dental robot control, the risk supervision for full situational awareness should continuously track the risks in the dental environment, while taking into account the procedure, patient and observer blocks. As an example, a robot control system is presented with a Reinforcement Learning Framework since this method could directly receive rewards for following a safer path around the oral cavity (Figure 4.9B).

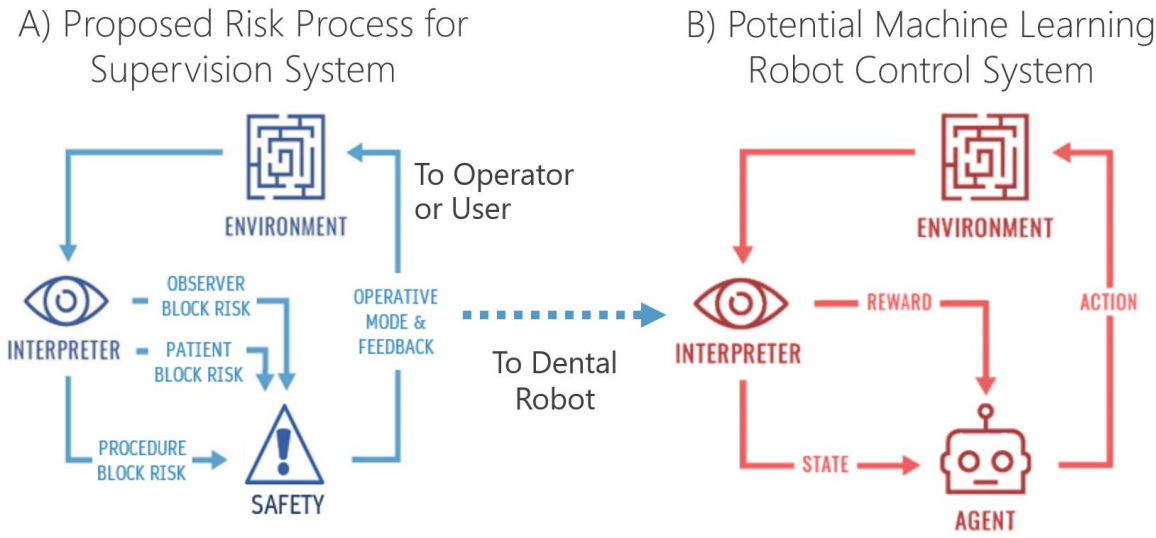

Figure 4.9. Potential dental robot system running in parallel to a supervision system: A) The supervision system blocks with defined transitions for measuring safety to inform patient safety levels; B) A potential robot system software design using a reinforcement learning model to train the robot to perform procedures using rewards for high quality operation [271].

Calculations for the maximum block risk output can be continuously evaluated to assess the state of the procedure over time and to compare the relative risks for each supervision

system component, similar to that of the procedure block with ID1.1–1.4 (Equation 4.1). The overall risk rating or safety at a given point in time over the procedure can then be computed as the maximum of the three supervision system blocks (Equation 4.2, Figure 4.9A).

Equation 4.1. $$R_{ID1} = \max\left([R_{ID1.1},\ R_{ID1.2},\ R_{ID1.3},\ R_{ID1.4}]\right)$$

Equation 4.2. $$R_{ID} = \max\left([R_{ID1},\ R_{ID2},\ R_{ID3}]\right)$$

To evaluate the acceptable mode of interaction (MoI) for safe procedure, the minimum requirements for each level can be represented using logical AND statements (∧) (Table 4.6). For the patient to enter the working envelope of the robot, the patient block must not present as a high risk (Equation 4.3). For cautious robot control near the patient, both the observer and patient block must not indicate high risk (Equation 4.4). Finally, all supervision blocks must not be high risk for the procedure to be performed (Equation 4.5). At a minimum, the acceptable MoI must be provided as feedback with additional warnings to the robot and the operator when the robot is uncompliant.

Equation 4.3. $$S_1 = (R_{ID3} < 8)$$

Equation 4.4. $$S_2 = (R_{ID2} < 8) \wedge (R_{ID3} < 8)$$

Equation 4.5. $$S_3 = (R_{ID1} < 8) \wedge (R_{ID2} < 8) \wedge (R_{ID3} < 8)$$

For autonomous medical systems, pathways for safety-related decision making must be well defined, unlike neural network AI system “black boxes” which have hidden layers of functions that make the decision-making process hard for humans to understand. Automated risk awareness is therefore needed for the system to ensure the decision pathways for safety are known and tracked. By incorporating transparent safety monitoring systems, the robot may take advantage of advanced robotic systems for technique-related decision making using rapidly improving AI algorithms, such as advanced machine learning methods. A robot’s

control system should be able to incorporate aspects of neural networks for control and functionality, such as a deep neural network with computer vision and reinforcement learning algorithms for motion planning decisions. Thus, the different dental robots developed can be assessed in their quality and safety by the supervision system components, while expanding the options of choice for robotic systems without putting the patient's safety at higher risk.

4.5 Discussion

Dental hazard risk analysis highlighted outstanding unacceptable risks for dental robots as medical devices. These were present even with the design for safety carried out for the downward-facing patient positioning with the robot contained in a chamber. Of the sixteen likely forms of dental harm, three major unacceptable residual risks for an autonomous dental robot were determined, including: adverse reactions; medical emergencies; and the potential for an internal high impact collision with tissue damage. Additionally, two areas of concern were identified, which were the potential dental technique errors and the risk of sharp component inhalation. Current assistive robots with direct human operator control, as well as task and conditional autonomy, are more accepted to operate in the high-risk environment where clinicians are willing to take on the responsibility of maintaining the safety of the patient [165]. The identified unacceptable risks prevent the development of an autonomous dental robot as a medical device and the classical hazard analyses based on current standards are not yet designed to manage complex HRI [76]. This necessitates the development and implementation of safety-focused supervision systems for tracking hazardous situations to reduce the likelihood of harm inflicted by a dental robot for patients.

The supervision system has been designed to operate for all stages of autonomy. This was considered important as safety sensors with identified redundancy should be incorporated for medical robots, along with speed limits, particularly when using strong and accurate

industrial robots. This should enable robots operating at full autonomy to mimic the necessary sensorimotor skills of an expert surgeon [185, 272]. For this reason, a similar model to the situation awareness model of a human operator by Endsley *et al.* (1995) was developed for hazard and risk analysis decision making for dental robot risk management. This led to the development of the RMN for dental robots which begins with the hazardous situation with fixed risk severity, then the relevant risk factor groupings and the likelihood of present causal factors (Figure 4.10). The residual risk assessment should evaluate instantaneous risk to estimate changes in the future safety level of the system.

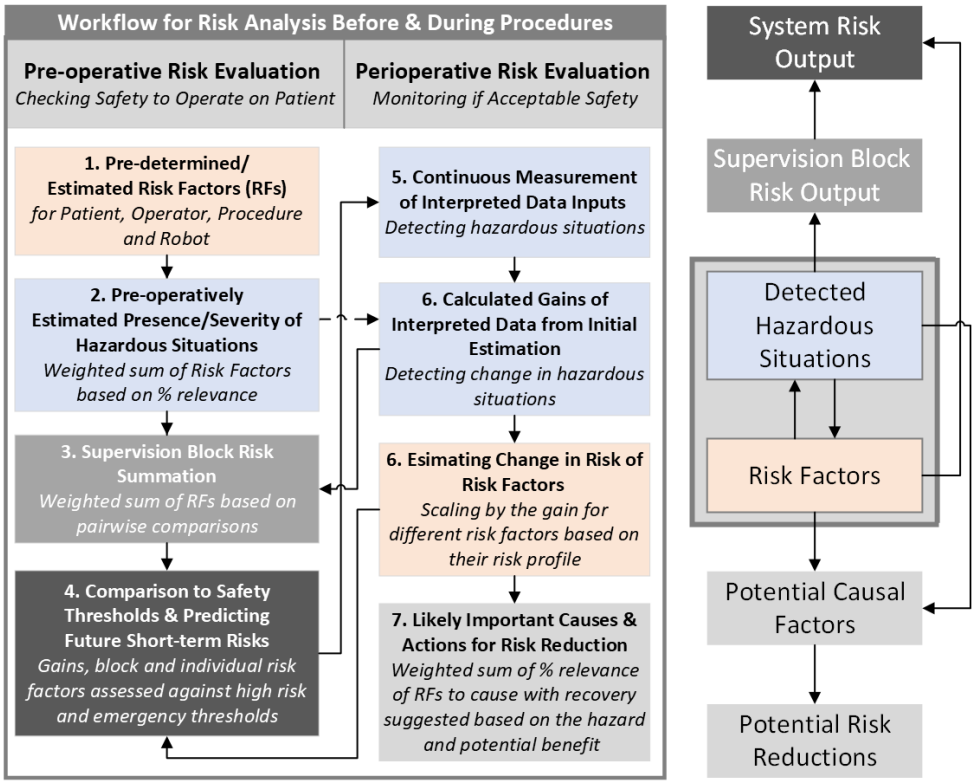

Figure 4.10. Risk analysis workflow for the risk management network (RMN) for risk evaluations of supervision blocks.
Pre-operative evaluation: Estimated relevant risk factors identify likely hazardous situations to predict the risk output of blocks and the system. *Perioperative evaluation:* Measurement gains of tracked hazardous situations are adjusted and evaluated to estimate the block and then system risk output. Measurements are also returned to the risk factors to confirm the prominent risk factors acting on the system.

According to Guiochet *et al.* (2016), classical hazard analysis methods have not been adapted for the complexity of human-robot interaction [76]. Developers of robotic system perception tend to include a wide variety of sensors and measurements in order to improve the robot's awareness of its surroundings with cost as the major limiting factor. For example, the feeding robot was designed with temporal and visual features using RGB-D camera, microphone, joint encoders, current sensors, fabric-based tactile skin sensors and force-torque sensor and classified by a neural network [273]. Nevertheless, effective and purposeful integration of sensors is necessary for effective cost and risk management for medical robotic systems. Analysis of surgical parameters and robot decision making was assessed by Yan *et al.* (2022) towards the development of a collaborative vascular interventional robot to predict guidewire insertion states using force feedback with a human-machine mapping and trust evaluation model [274].

To develop the complete risk management network, specific analysis of causal factors and their necessary risk reductions must be performed. This may require the use of decision-making methods, such as the Analytical Hierarchy Process (AHP), which manages multiple criteria to reach a goal calculated by pairwise comparisons [254]. This could simplify analysis for causes of risk and their recovery actions to be prioritised with respect to their likelihood, importance, effectiveness, ease to implement, time taken, and impact on risk reduction. The AHP method was utilised by Chung *et al.* (2024) to solve complex decision making from qualitative or quantitative inputs for a chemical experiment risk evaluation that included the relative rating the importance of hazardous situations [247]. This analysis should be assisted by fault tree analyses of risk pathways. These have been used to map causes of hazardous situations for a biopsy robot involving wrong needle positioning and image processing errors [272].

The dental robot should not rely on the supervision system to diagnose the direct cause of a hazardous situation, particularly as many overlapping factors are likely to have created the high-risk environment [35]. This acts as a benefit to the supervision system structure as there is reduced pressure on knowing the reason for an error condition. As long as the sensors can detect a hazardous state, the maximum level of instantaneous risk is reached even if the cause of error or hazard cannot be determined. This is believed to be similar to how surgeons and dentists operate in an emergency as the root cause is often analysed after detection and response to a hazardous situation or adverse event. However, refinements to the weightings of different risk factors and related causes factors for different procedures, instruments, patients and setups can improve the accuracy of suggestions to recover from risk before impacting the progress of the procedure.

For the verification of the hazard analysis methods, an additional layer for the identified potential forms of patient harm (Section 4.3) is proposed to sit above the hazardous situations layer of the risk management network (Appendix B.3, Figure B.4). Using the defined severity for potential patient harm, the accuracy of the risk output measurements from the supervision blocks can be evaluated (Appendix B.3, Equation B.5). An additional benefit of this system is that the risk management framework has been developed as a standalone system that is independent from a dental robot, such that it does not require force sensors that are commonly used for collision detection. Therefore, risk measurements can be performed during tracked manual techniques by dental clinicians using standardised guidance tracking systems for further verification for hazardous situation measurements. This is important as verification and validation of the risk detection methods for the supervision systems should be undertaken with patients in current dental procedures before they are accepted for robotic dental procedures. However, investigations should be carried out in simulation to assess the design of the specific methods of detection and to estimate their effectiveness to detect high likelihood of harm.

Chapter 5: Risk Supervision Methods

5.1 Summary

For a dental robot system, it is essential that measurable latent safety risks are tracked and managed to an acceptable level over the course of a procedure, before they develop into high-risk and potentially unsafe conditions. This chapter involves the development of procedure block methods to analyse the location of an instrument, including its tip and handle, in and around the mouth for to assess the safety of a dental procedure. Data required for these measurements would be collected by instrument and patient tracking sensors to be interpreted for potential high risk unsafe control or collisions. By identifying hazardous situations using procedure safety measurements, these procedure block measurements represent the first stage of risk awareness for an autonomous dental robot in order to ease the responsibilities of the operator to ensure a safe operative procedure under task and conditional autonomy. These represent detailed methods for small-scale localised separation monitoring in the oral cavity.

5.2 Introduction

Over the past decade, there has been an increasing uptake of assistive and remotely operated robots in the medical industry [60]. This was initiated by the da Vinci robotic platform [62, 63], which has made way for assistive guidance robots, like Yomi by Neocis and NaoTrac by Brain Navi [167, 275], task and conditional autonomous orthopaedic surgical robotic systems, such as the TSolution One knee replacement robot by THINK Surgical Inc. [276], and now COVID-19 testing robots [157, 158, 162]. In the dental industry, commercialised haptic implant robots are controlled by an operator so that they can actively assess safety and directly prevent hazardous situations [167]. Other new dental implant task-automated robots with patient tracking currently heavily depend on clinical supervision for patient safety [59, 186, 277]. There is great potential for the adoption of autonomy in the dental industry with numerous benefits to both patient and dentist wellbeing (Chapter 1), although patient safety remains a significant barrier for the potential adoption of autonomous dental robots. Safety frameworks are therefore an essential component of dental robot design.

Cleaning and general check-ups are essential components of dental health that, due to their relatively low risk compared to surgical procedures [35], have great potential to be performed by safe autonomous robots. Cleaning procedures involve removing supragingival deposits above and along the gumline on teeth, or more challenging subgingival deposits below the gumline [278, 279]. Dentists use probes and other instruments to determine the depth of gingival pockets, the presence of plaque or calculus, and to test for bleeding as a feature of inflamed tissues (Figure 5.1A). Manual charting techniques are used to create a "map" of the patient's mouth to guide scaling and root planing procedures, which can be a challenge for dentists and a potential source of error during dental procedures [278, 279]. Regular cleaning is essential to control periodontitis (Figure 5.1B). Common oral sites that require cleaning include interdental locations (between teeth), along and below the gumline on teeth (on the

gingival margin and in dental pockets), and in crevices or cracks on chewing surfaces of teeth (large dental fissures) [280]. These regions are often challenging for dentists and patients to clean and could benefit from precise and force-controlled robotic automation.

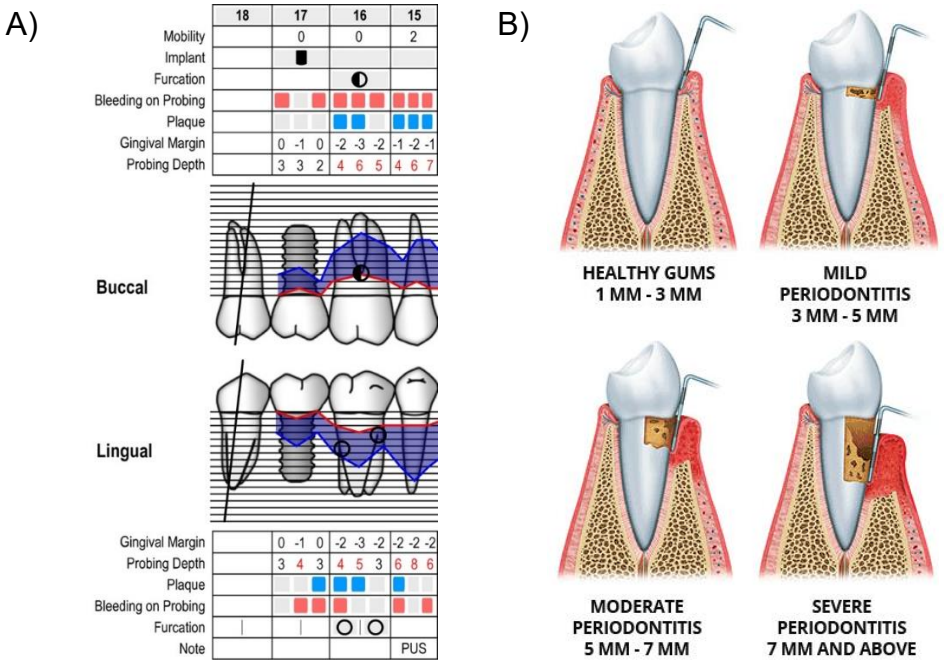

Figure 5.1. Charting with a periodontal probe: A) Recording of depth measurements (in mm) of periodontal pockets; and B) Stages of gum disease with inflammation of the gingiva and receding alveolar tooth sockets [281, 282].

Dental procedures can be uncomfortable or painful for patients [9, 263, 264], increasing the risk of injury, and their repetitive laborious motions are a leading contributing factor of musculoskeletal diseases for dentists from poor workplace ergonomics and the use of oscillating instruments [104-106]. In addition, high patient fear and anxiety increases the intensity and duration of their dental pain [283]. Dental clinicians require significant training to fully develop the required motor skills to operate through the limited mouth opening with a restricted view of the operative space [284]. Dental errors including laceration with sharps, bruising burns, or tooth fractures, can result from the use of dental instruments around alert and mobile patients [93]. The relative movements of a dental instrument by an operating robot must be monitored and assessed for potential unexpected fast and unstable control to minimise the

presence of high-risk situations that are more likely to result in patient harm, particularly when sharp oscillating instruments are used.

A key aspect to consider for safe instrument movement in robot design is its accessibility between the lips and through the oral cavity. The oral opening can be likened to a port through the abdominal wall required for laparoscopic surgery, and which causes motion inversion and the 'fulcrum effect' (Figure 5.2A) [284]. In general, dental instruments are oriented in line with the curvature of dental arches to avoid forces from soft tissues affecting force feedback from the operative site to the clinicians' hands. However, due to instrument tip angled design and vision challenges, dental instruments may be rotated towards the cheeks to locate the target site at the optimal angle while evading impact with the opposing dental arch (Figure 5.2B).

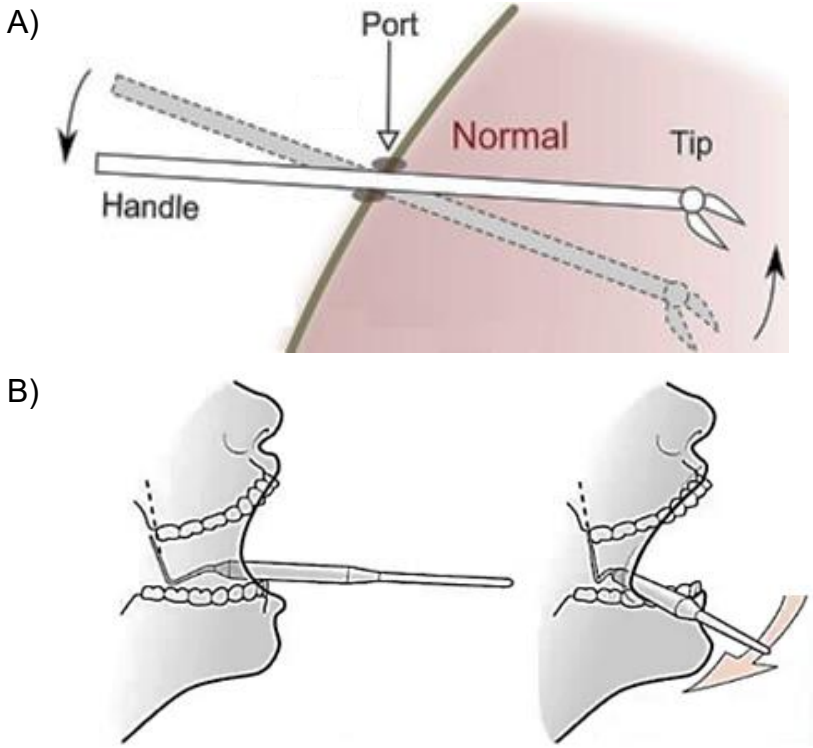

Figure 5.2. A) Instrument motion inversion caused by the 'fulcrum effect' for a laparoscopic surgery through a port in the abdominal wall [284]. B) Rotation away from the dental arch curve to reach a location in the mouth [285].

Anatomical variations in patients can also influence the safe range of instrument movement within the oral cavity. Dental arches can be classified by: the size; width as being narrow or wide; and arch shape along the biting surface, known as the occlusal plane (Figure 5.3A) [286]. The accessibility of operative sites at the back of the mouth and the path taken to reach them can also be affected by the curvature of the jaw in the sagittal plane, known as the curve of Spee (Figure 5.3B), as well as curvature in the frontal plane at the back of the mouth (curve of Wilson). These two occlusal curves combine to represent a near spherical shape (the sphere of Monson) and estimate each tooth's root angle of inclination [287, 288].

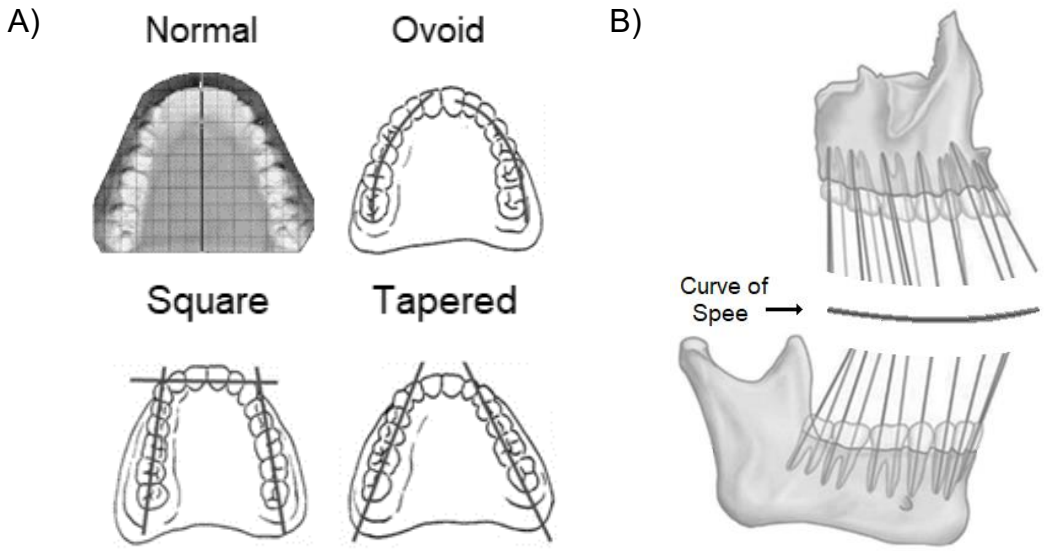

Figure 5.3. A) Common dental arch forms in the transverse plane [289, 290]. B) Inclination of teeth showing the curve of Spee in the sagittal plane with estimated orientations of the tooth roots [288, 291].

Careful control of instruments and frequent assessments of risks are essential for an autonomous dental robot. A supervision system must undertake an automated independent safety monitoring and decision process which can take information from the dental environment to adapt its safety measurements that are responsible for detecting hazardous situations. In Chapter 4, a supervision system was proposed that included a procedure block, an observer block and a patient block. This chapter aims to develop the procedure block for a supervision system by providing risk awareness to the dental robot system. This risk awareness

system incorporates tracking and assessing instrument movement, the patient's mouth, and the potential for harm based on the position of the instrument within virtual models (Figure 5.4).

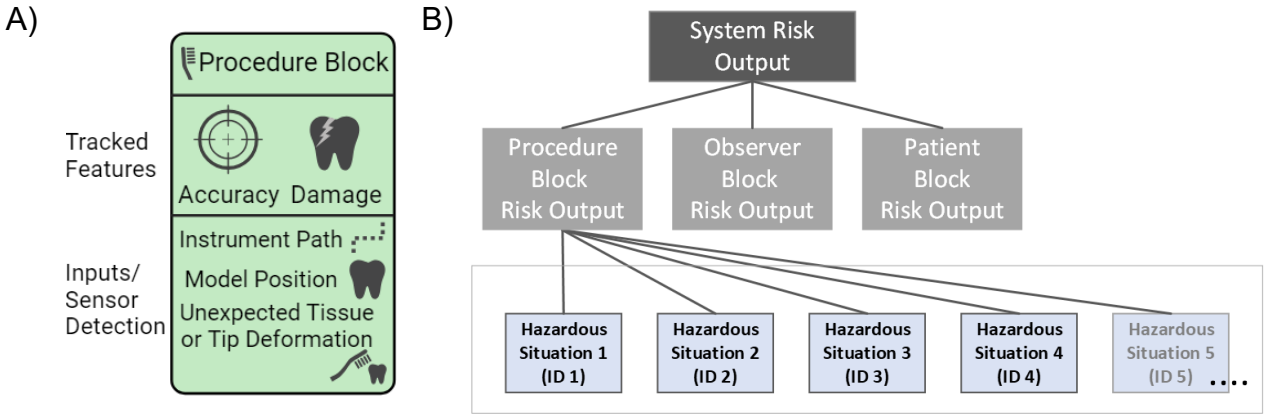

Figure 5.4. A) Features and measurements for Procedure Block safety tracking (component from Figure 4.5, Section 4.4.1). B) Supervision system components of the Risk Management Network framework (RMN) for detected interpreted data informing hazardous situations to estimate system risk output (component from Figure 4.7, Section 4.4.2).

5.3 Methods

Four separate detection methods for the defined procedure block measurements (ID1.1–1.4) that were proposed in Chapter 4 are described with reference to the oral tissues involved (Figure 5.5). The relevant tissues are identified as either hard or soft and the distance of penetration into tissues is considered an important parameter, as is the motion of the instrument tip relative to the top of each tooth (occlusal point) and its instrument handle entry point into the mouth. Each method is addressed in this chapter to progress towards the development of a supervision system for autonomous dental robots, so that patient safety is maximised through redundancy and barriers are reduced for their implementation. Transparent and transferrable understanding between dental clinicians, patients and engineering roboticists is critical for safety measures, therefore the measurements of the procedure block represent physical and estimated distance measurements from important features in the mouth.

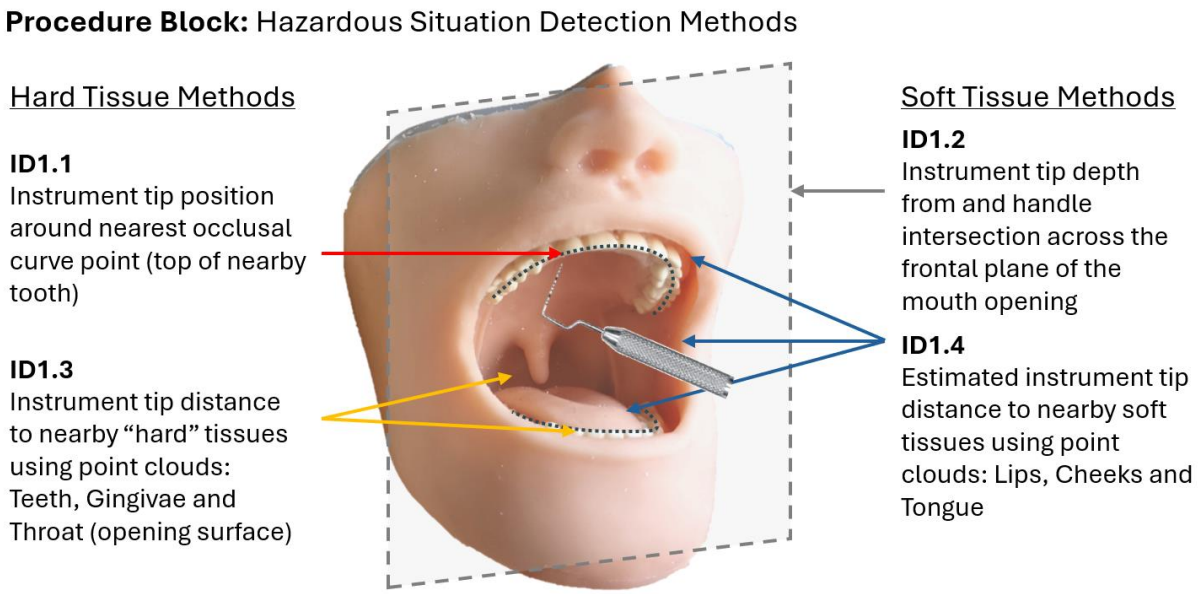

Figure 5.5. Proposed methods to measure the identified procedural hazardous situations with each side identified by the type of relevant oral tissues and the rows as performance of instrument tip movement in relation to safety (top) and the estimated distance to or deformation of oral tissues (bottom) (based on Chapter 4, Table 4.5). Occlusal curved profiles (OCPs) on each dental arch are represented by dotted black lines.

For a given instrument tip and its orientation, the procedure block safety measurements were carried out using intraoral scan data and tissue point clouds from a full head model scan to estimate the risk of harm to hard and soft oral tissues. The first two methods (ID1.1–1.2 as per Chapter 4, Table 4.5) are performance-based which can be used to compare motions of the tip around the teeth and the instrument's location through the mouth opening. The next two methods (ID1.3–1.4 as per Chapter 4, Table 4.5) are collision-based and measure the position of the instrument tip in relation to the expected locations of virtual hard and deformable soft tissue surfaces around the mouth. These measurements aim to estimate the instantaneous and near-future risk levels when coupled with limits or thresholds for assessment. The spatial measurements were mapped to the ID output risk ranges for the different risk levels (Table 5.1).

Table 5.1. Equivalent raw interpreted data variable inputs as distance measurements mapped to output risk range thresholds for their risk levels.

Detected Risk Level	**ID Output Risk Range**	**Raw ID Variable Input Distance Ranges (mm)**					
		ID1.1	*ID1.2**		*ID1.3**		*ID1.4*
			x, z	y	*x, y*	z	
Low	<0	<0	<20	<30	>5	>10	>5
Acceptable	0 – 8	0 – 8	20 – 36	30 – 60	-3 –5	2 – 10	-3 – 5
High	8 – 10	8 – 10	36 – 40	60 – 70	-5 – -3	0 – 2	-5 – -3
Unacceptable	>10	>10	>40	>70	<-5	<0	<-5
Key: ID = Interpreted Data; *Raw data conversion varies depending on axis							

5.3.1 Generating a "Patient" Scenario

To simulate the targets for a dental mode, intraoral scans were carried out on a silicone local anaesthetic (LA) head model available from OneDental (Castle Hill, NSW Australia) using a CEREC Primescan by Dentsply Sirona (Charlotte, NC United States). Dental arch analysis was carried out to find a curve following the tops of the teeth of each arch used to represent occlusal curved profiles (OCPs, Figure 5.5) in MATLAB. The 25 target points in each quadrant for a PCPNT12 periodontal probe by Novatech (Chicago, IL United States) were selected following assessments of locations with the highest change in model surface normal vectors, particularly along the gingival margin (gumline). Instrument frames of reference for each target utilised the tangent of the nearest occlusal curved profile point as an estimated ideal instrument handle rotation that would minimise the likelihood of a soft tissue collision in the mouth, as published in Deaker *et al.* (2023) [220]. The positions of the intraoral scans were registered to their positions on a full scan of the head model using Iterative Closest Point (ICP) and Coherent Point Drift (CPD) methods. These methods are detailed in Appendix C.

5.3.2 ID1.1 Instrument Tip Position around a Tooth

The tip motion distance measurement assesses the tip's depth into the dental arch and towards the gingivae. Knowing expected values and motions for the instrument tip around teeth, this aims to allow for comparisons to the expected motion of the instrument around the oral cavity for a given technique. The position of the instrument tip was assessed with respect

to a tooth's cross section along the occlusal arch curve (Figure 5.6). At each curved profile location, a cross-sectional plane was used to define the position of the instrument tip in the local space around the tooth, where the x_b axis is directed towards inside the mouth, y_b axis represents the offset from the plane (e.g. uncertainty) and z_b axis indicates the proximity to the gingivae or depth into the pockets from the occlusal surface (Figure 5.6).

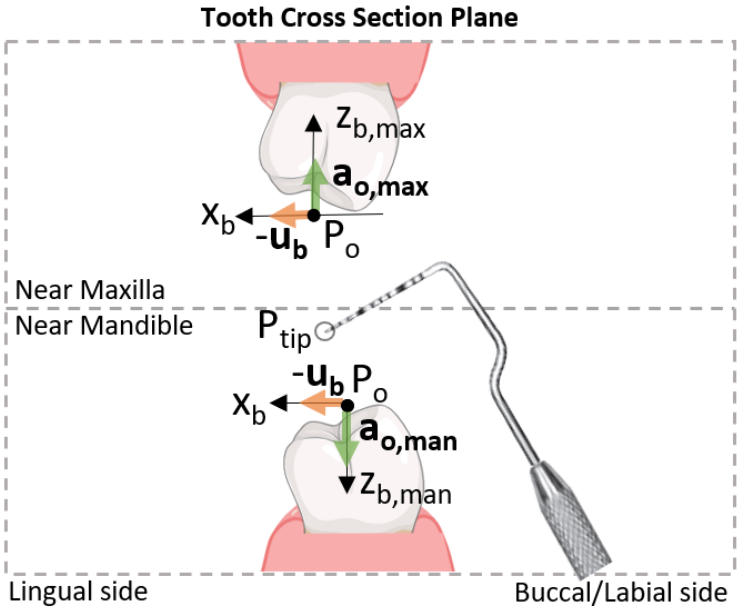

Figure 5.6. Cross section of open dental arches with axes x_b, y_b and z_b where the position of the instrument tip is nearest the occlusal curve point (P_o) of the mandible. This point represents the transition from buccal to lingual points for this model.

A unit vector, $\boldsymbol{u_b}$, pointing outwards to the buccal side of the tooth was calculated from each occlusal curve point. This was calculated using the cross product between the tooth angulation vectors, $\mathbf{a_o}$, and occlusal curve tangents, $\mathbf{t_o}$, (flipped in Quadrant 2 and Quadrant 4) such that the tangents pointed to the left for the maxilla and right for the mandible in the head model's x-axis (Equation 5.1). The nearest occlusal curve point, P_o, for an instrument's tip, P_{tip}, was found using the *dsearchn* function in MATLAB and was used to calculate the vector to the tip location (Equation 5.2). The components of each axis were calculated using the dot products for the relevant directions of the tooth cross section plane axes in x_b and z_b (Equation

5.3). Points from the plane in the y_b were calculated as larger when offset in the direction of the sides and back of the mouth (aligned with the occlusal curve tangents).

Equation 5.1. $$\boldsymbol{u_b} = \frac{\mathbf{a_o t_o}}{|\mathbf{a_o t_o}|}$$

Equation 5.2. $$\boldsymbol{d_b} = \mathrm{P_{tip}} - \mathrm{P_o}$$

Equation 5.3. $$\boldsymbol{d}_{1.1} = \left[-\boldsymbol{u_b} \cdot \boldsymbol{d_b},\quad |d_{b,y}|\left(\frac{\mathbf{t_o}}{|\mathbf{t_o}|} \cdot \frac{\boldsymbol{d_b}}{|\boldsymbol{d_b}|}\right),\quad \frac{\mathbf{a_o}}{|\mathbf{a_o}|} \cdot \boldsymbol{d_b}\right]$$

5.3.3 ID1.2 Instrument Oral Cavity Entry Position

Adjustments of the instrument tip position and orientation alter the entry through the oral cavity which is measured from the centre of oral opening between the maxilla and mandibular dental arch incisors. This is an important consideration as frequent unnecessary contact with the patient's soft tissues around the operative area could increase distress, harm to the tissues from excess friction, and potential for bruising. To avoid this, the distance from the central opening point for the entry of the instrument can be limited to reduce the potential for unintended contact between the robot's instruments and the soft tissues in the patient's oral cavity. This can in turn reduce the chance of altering the end effector force sensor readings. The position and orientation of the instrument tip was used to define the orientation of the instrument handle through the mouth opening (Figure 5.7), which was published in Deaker *et al.* (2023) [220]. A frontal plane with x_f, y_f and z_f axes was introduced to the opening mouth entrance, which the instrument handle would pass through to reach a target point.

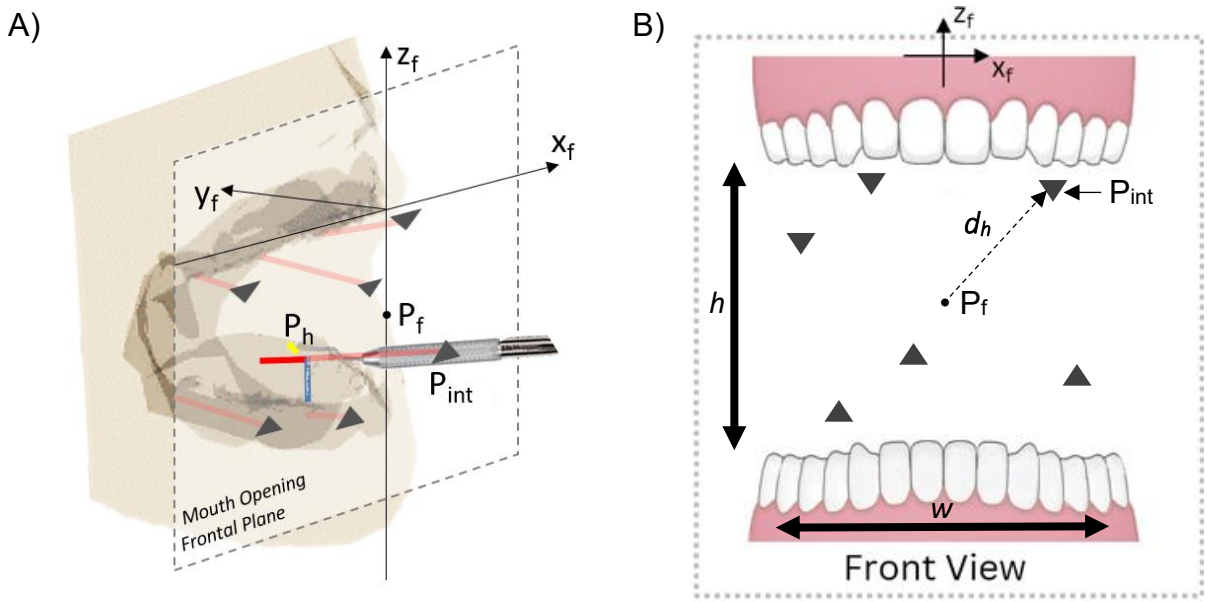

Figure 5.7. A) The handle x-axis intersection points on the frontal plane, P_{int}, is denoted by triangles for the maxilla and mandible dental arches. The centre of the mouth opening point, P_f, is offset away from the front teeth. B) Front view of an open mouth showing the distance from the centre opening of the mouth to an intersection point, d_h. The mouth opening dimensions for height, h, and width, w, are indicated.

The intersection points for the instrument's handle with the frontal plane, P_{int}, were calculated using the tip x-axis vector, $\mathbf{n_x}$, at the handle point, P_h, to account for the tip offset length (Figure 5.7A). The orientation of the frontal plane was defined by a normal vector, $\mathbf{n_f}$, pointing into the oral cavity (in y_f) that was calculated by the cross product of the direction from the bottom to the top incisor with the positive x-direction (Equation 5.4). The centre point of the mouth opening, P_f, was calculated as the average of the occlusal curve points at the centre front of each arch, x = 0, at an offset distance, d_f = 10 mm, from between the front incisors of the maxilla (*max*) and mandible (*man*) in the direction of the normal vector, $\mathbf{n_f}$ (Equation 5.5). The intersection points for different target locations, which had a handle-to-tip offset of 10 mm (the length of the periodontal tip markings), were computed using the *line_plane_intersection* function in MATLAB in 3D for the output distance x and z measurements (Figure 5.7, Equation 5.6) [220, 292]. A distance vector between the central entrance point and the handle intersection point on the frontal plane was calculated for the y-direction in the frontal plane (y_f).

Equation 5.4. $$\mathbf{n_f} = \left(\mathrm{P_{o,}}_{max@\mathrm{x=0}} - \mathrm{P_{o,}}_{man@\mathrm{x=0}}\right)[1 \quad 0 \quad 0]$$

Equation 5.5. $$\mathrm{P_f} = \frac{\mathrm{P_{o,}}_{max@\mathrm{x=0}} + \mathrm{P_{o,}}_{man@\mathrm{x=0}}}{2} - d_f \frac{\mathbf{n_f}}{|\mathbf{n_f}|}$$

Equation 5.6. $$\boldsymbol{d}_{1.2} = \left(\left[\mathrm{P_{int,x}} - \mathrm{P_{f,x}},\ (\mathrm{P_h} - \mathrm{P_f}) \cdot \frac{\mathbf{n_f}}{|\mathbf{n_f}|},\ \mathrm{P_{int,z}} - \mathrm{P_{f,z}}\right] - 20\right)\left[\frac{1}{2}, \frac{1}{5}, \frac{1}{2}\right]$$

The distances were included in the total distance measurement when greater than 20 mm in each axis direction. These risk measurements were scaled down (Equation 5.6), given that the cheeks are flexible up to a displacement of 20-30 mm outwards and that expected maximal mouth opening is in the range of 40 to 60 mm [293-298], to give a rating out of 10 at a distance of 40 mm from the centre of the mouth. However, the y-axis indicates the difficulty to retract or manipulate the instrument based on its depth into the oral cavity. To improve from works published in Deaker *et al.* (2023) [220], acceptable entrance zones for the instrument's handle were distinguished between the back teeth and front teeth (at the junction between canine and first premolar) as circular zones with a 20 mm radius and a 30 mm radius from the centre of the frontal plane, respectively (Figure 5.8).

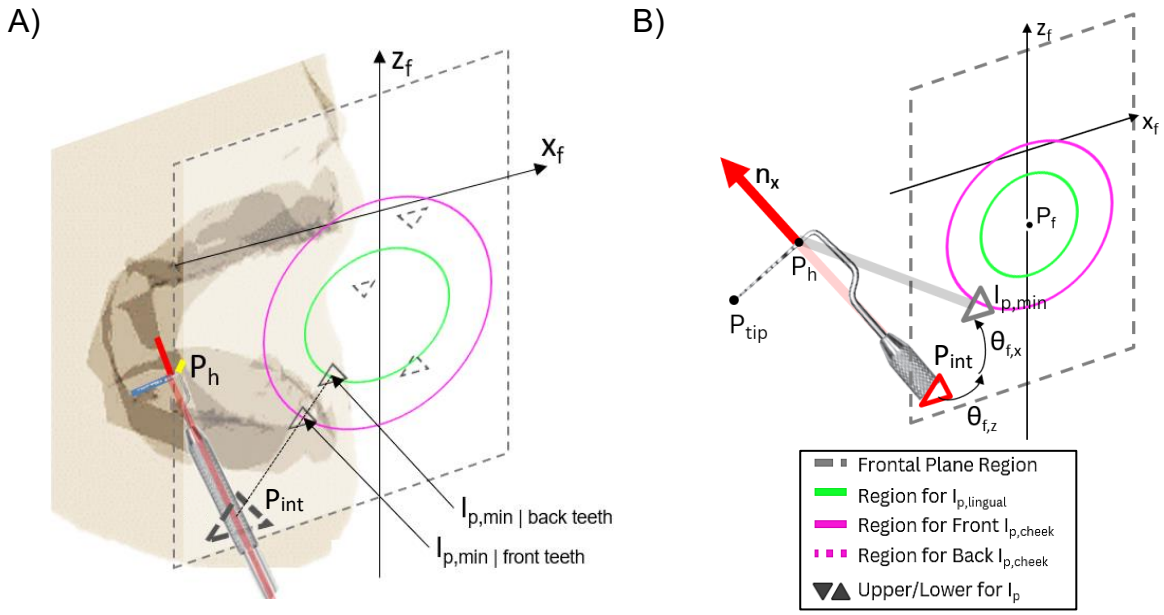

Figure 5.8. A) An example instrument intersection point (P_{int}) outside its zone of the frontal plane with x_f and z_f axes. Its minimum intersection point ($I_{p,min}$) along the boundary of the acceptable entry zones: the larger magenta zone for front teeth; and the smaller green zone for back teeth. B) Suggested angles of rotations for an instrument with a frontal plane intersection point (P_{int}) outside its boundary to its minimum intersection point ($I_{p,min}$) inside the front teeth boundary in each axis (θ in x_f and z_f).

Euler angles, $\theta_{f,x}$ and $\theta_{f,z}$, about the x_f and z_f axes were calculated between the ideal intersection point for instrument handle control, $I_{p,min}$, and the instrument handle's intersection point, P_{int}, from the tip handle offset point, P_h (Figure 5.8B), using the angle between two vectors formula (Equation 5.7, Equation 5.8). The sign of the angles were flipped using sign() where the instrument handle intersection was behind the angled frontal plane. The final intersection positions were recomputed for risk assessment by rotating the instrument handle axis direction using *rotx*() and *rotz*() functions in MATLAB.

Equation 5.7. $$\theta_{f,x} = \cos^{-1}\left(\frac{(I_{p,min}-P_h)_{y,z}\cdot(P_{int}-P_h)_{y,z}}{\left|(I_{p,min}-P_h)_{y,z}\right|\left|(P_{int}-P_h)_{y,z}\right|}\right)\text{sign}(P_{f,z}-P_{int,z})$$

Equation 5.8. $$\theta_{f,z} = \cos^{-1}\left(\frac{(I_{p,min}-P_h)_{x,y}\cdot(P_{int}-P_h)_{x,y}}{\left|(I_{p,min}-P_h)_{x,y}\right|\left|(P_{int}-P_h)_{x,y}\right|}\right)\text{sign}(P_{int,x}-P_{f,x})$$

5.3.4 ID1.3 Tip Distance to Hard Oral Tissues

Movement of the instrument in the oral cavity can result in planned or unplanned collisions with hard tissues based on the size of the mouth opening or orientation of the instrument. For dental diagnosis and cleaning techniques, this should only occur on the surfaces of the teeth and below the gingival margin on the hard tooth surface probing for periodontal attachment and the presence of subgingival calculus. The surfaces used to estimate the risk of likely hard tissue collision of ID1.3 include the teeth and gingivae from intraoral scans, and a virtual throat entrance surface (Figure 5.9). The throat entrance acts as a hard tissue feature "wall" positioned behind the back teeth since the instrument should not enter the throat. To increase the resolution of the tooth surfaces, the teeth from the intraoral scan models were manually sectioned away in Blender and then imported into MATLAB as a triangulation. In this way, the tooth sectioned intraoral scans only needed to be down-sampled by skipping over 50 points for ICP and CPD registration methods in MATLAB.

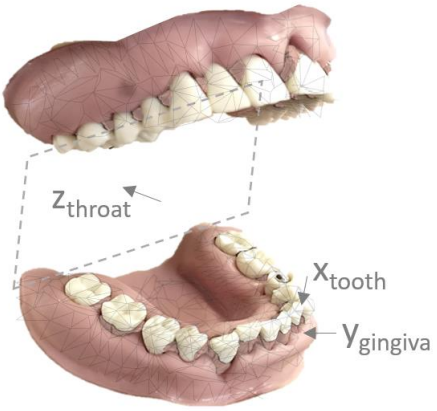

Figure 5.9. Virtual hard tissue surfaces of the oral cavity including the teeth and gingivae models collected from intraoral scan data, along with a "wall" to be positioned behind the back teeth for the entrance of the throat. The distance from or depth into the hard tissues is representative measurements for ID1.3.

The sectioned tooth model points were matched to the nearest points of the lower resolution intraoral scans using the *dsearchn* function and transformed using the registration results from the CPD Method for the points and ICP Method for the surface normal vector. To create separate point clouds for the gingivae of the initial intraoral scans, the tooth point indices

were found using the *ismember* function to be removed from the intraoral scans. Additional points of the teeth that were missed were found by a moving region of interest (ROI) with a volume of 7x7x4 mm^3 centred at each arch's occlusal curve points from [5:5:50] to allow for the greater height of the gingivae near the back teeth. Since the arch point clouds were already rotated, the ROI was rotated in the x-axis by the angle, θ_a, between the mean tooth angulation for each arch, $\bar{\mathbf{a}}_{\mathbf{o,arch}}$, and the vertical direction for the maxilla of [0 0 1] and the negative vertical vector for the mandible of [0 0 -1] (Equation 5.9). Points found inside the ROI were found using the *inpolyhedron* function [299], which were then removed from the gingivae point cloud model.

Equation 5.9. $$\theta_a = \cos^{-1}\left(\frac{\bar{\mathbf{a}}_{\mathbf{o,arch}}}{|\bar{\mathbf{a}}_{\mathbf{o,arch}}|} \cdot \begin{bmatrix} 0 & 0 & \pm 1 \end{bmatrix}\right)$$

A throat wall point cloud surface was created in Blender with the Blender knife tool to increase point resolutions and imported into MATLAB. The normal surface vectors for all point clouds were designed to be pointing into the oral cavity region. Nearest point searches were performed for each point cloud (PC), $P_{n,PC}$, at each instrument tip position, P_{tip}, with the *dsearchn* function. The dot product was performed with the nearest point's surface normal vector, $n_{s,n}$, such that the distance, $d_{n,PC}$, would produce an increasing negative distance as the instrument is pulled away from the tooth surface (Equation 5.10). This distance measurements become positive when the tip is near or inside the tissue surfaces (Equation 5.11).

Equation 5.10. $$d_{n,PC} = \left(P_{n,PC} - P_{tip}\right) \cdot \frac{n_{s,n}}{|n_{s,n}|}$$

Equation 5.11. $$\boldsymbol{d}_{1.3} = \left[d_{n,PC=1} + 5,\ d_{n,PC=2} + 5,\ d_{n,PC=3} + 10\right]$$

5.3.5 ID1.4 Tip Distance to Soft Oral Tissues

Soft tissues around the mouth can be more flexible and can often deflect under pressure, providing a greater workspace for operating in the oral cavity. However, repetitive or prolonged

exposure of contact can result in soft tissue injury. Point clouds to assess the movement of the instrument near or into soft tissue regions can estimate the extent of contact, deflection or potential harm to those tissues, and therefore the risk of harmful collision can be estimated from excessive displacement. The internal oral surfaces for soft tissue distance measurement of ID1.4 include the lips, cheeks and tongue (Figure 5.10). Sectioning the structure for the inner oral cavity surfaces was performed in Blender in Edit Mode. These were for the left and right cheek, maxilla and mandible lips and the tongue using sectioned components from the silicone LA head model. The cheek models were extended upwards to allow for larger mouth openings. Any sections with low point resolutions were increased in resolution using the Blender knife tool, such as for the extended cheek regions.

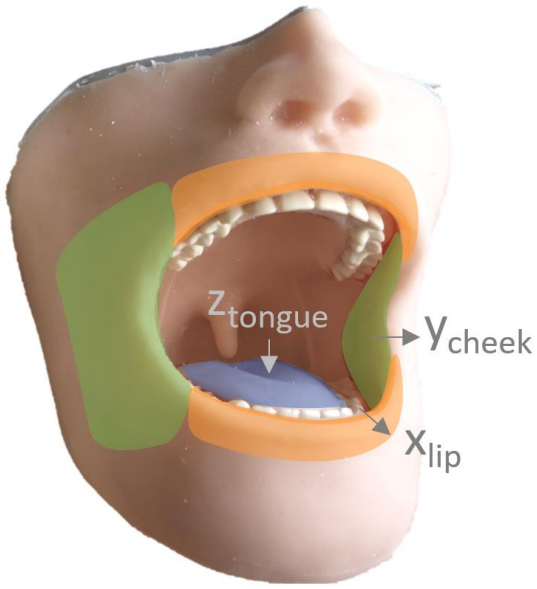

Figure 5.10. Sectioned silicone LA head internal surfaces for the soft tissue model with measurement directions of increasing risk to represent virtual depth into inner oral surfaces. The inner lip surface is orange, the cheeks are green, and the tongue is blue to represent the x, y and z measurement directions, respectively.

Similar to the throat "wall" feature, internal oral surfaces of soft tissues were imported into MATLAB and positioned as point clouds around the dental arches. Nearest point searches for each instrument tip location were carried out to these surfaces (Equation 5.10) and the

output distance measurements to the respective point clouds, $d_{\mathrm{n,PC}}$, were designed to become positive when the tip is near or passing into the soft tissue surfaces (Equation 5.12).

Equation 5.12. $$d_{1.4} = \left[d_{\mathrm{n,PC=1}} + 5, d_{\mathrm{n,PC=2}} + 5, d_{\mathrm{n,PC=3}} + 5\right]$$

5.4 Results

5.4.1 Patient Scenario and Registration Analysis

The general shape for intraoral scans were observed as a surface mesh in MATLAB (Figure 5.11). The low-resolution surface meshes fill the unmapped open space within the dental arch allowing for easy recognition of whether the arch is right side-up or upside-down relative to the mean arch height in the z-axis. By identifying the arch as either maxillary or mandibular, the analysis could be tailored to the upside-down orientation of the maxillary arch. Since intraoral scans of the maxilla are exported from the intraoral scan in the upside-down positions, this assessment can work for different dental arches.

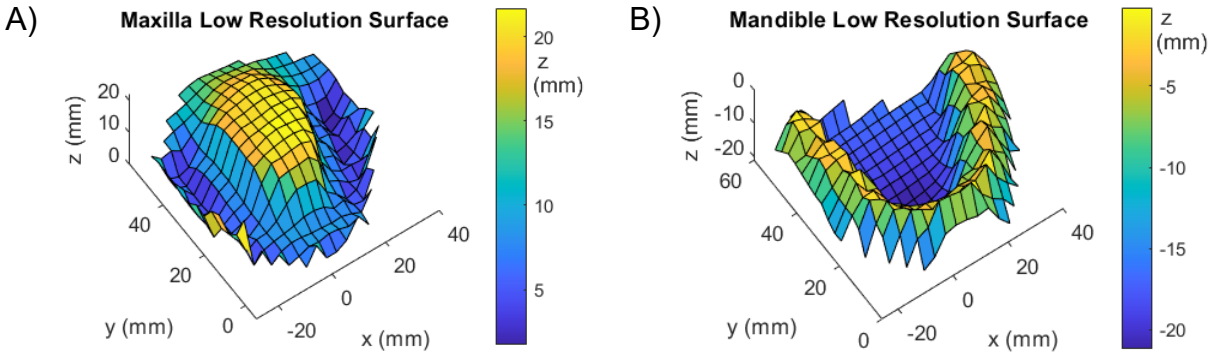

Figure 5.11. Low resolution surface meshes from the surf function for the dental arches: A) the maxilla and B) the mandible.

The intraoral scan data arches were found to be slightly rotated in the z-axis, resulting in a reduced number of data points around the top right region (i.e. points 9, Figure 5.12). From the calculated occlusal curve positions, the width of the maxilla was 52.5 mm was found for the distance between points 1 to 9 (Figure 5.12A). The mean depth was 47.2 mm (42.7 mm for points 5–9 and 51.7 mm for points 1–5). For the mandible, the width was 53.7 mm, and the mean depth was 43.8 mm (38.5 mm for points 5-9 and 49.0 mm for points 1-5) (Figure 5.12B).

For the silicone LA head model, the calculated occlusal curve profiles follow the arch curvature as desired but had to be adjusted for regions that lack data points. The final occlusal curve profiles can be observed in the side view to follow the dental arch curves (Figure 5.12C-D). Between the means of the two middle occlusal curve centre points of each dental arch, the height of the opening was calculated for the digital head model as 48.9 mm.

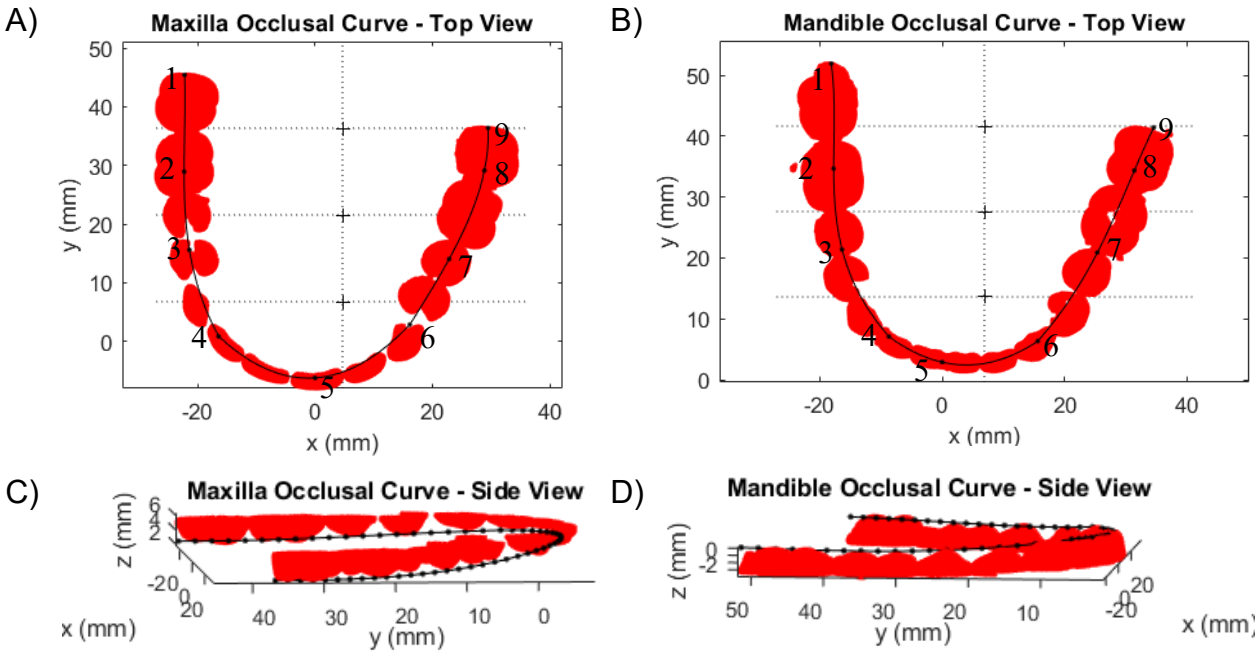

Figure 5.12. Top view of the dental arches for A) the maxilla and B) the mandible. The shape-defining curve points are labelled from 1 to 9 for the 8 sections and the centre front point. The red high density point clouds represent the intraoral scan top tooth sections used for calculating the occlusal curved profiles. The orthogonal side views of C) the maxilla and D) the mandible are shown with their occlusal curves that resulted from splines performed between the 9 points of each arch.

The two registration methods, ICP and CPD, were assessed in MATLAB. The ICP method performed best in millimetres, however its translation was slightly offset in the z direction to the sectioned head model arches with root mean square errors (RMSE) 2.78 mm and 2.65 mm for the maxilla for the mandible, respectively (Figure 5.13A). In contrast, the CPD method performed slightly better and registered the intraoral data to the head model with RMSEs of 2.57 mm and 2.62 mm when converted into units of meters and was used to translate the intraoral scan data (Figure 5.13B). The ICP method provided a useful simplified output

transformation matrix which could be used to rotate the mean surface normal vector of each target point and the occlusal curve profiles (Figure 5.13). This was equivalent to ZYX Euler rotations of [-5.88°, 0.39°, -10.70°] and [-7.73°, 0.48°, -35.63°] for the maxilla and mandible, respectively. The use of the ICP caused the occlusal curve to be slightly offset in the z-axis from the teeth. The occlusal curve tangents were calculated pointing to the back of the mouth for each arch quadrant and the average tooth angulation vectors were directed into the tooth from the occlusal plane (Figure 5.13A). The 100 selected targets and their rotated surface normal vector are spread over the dental arches with 25 points in each quadrant (Figure 5.13B).

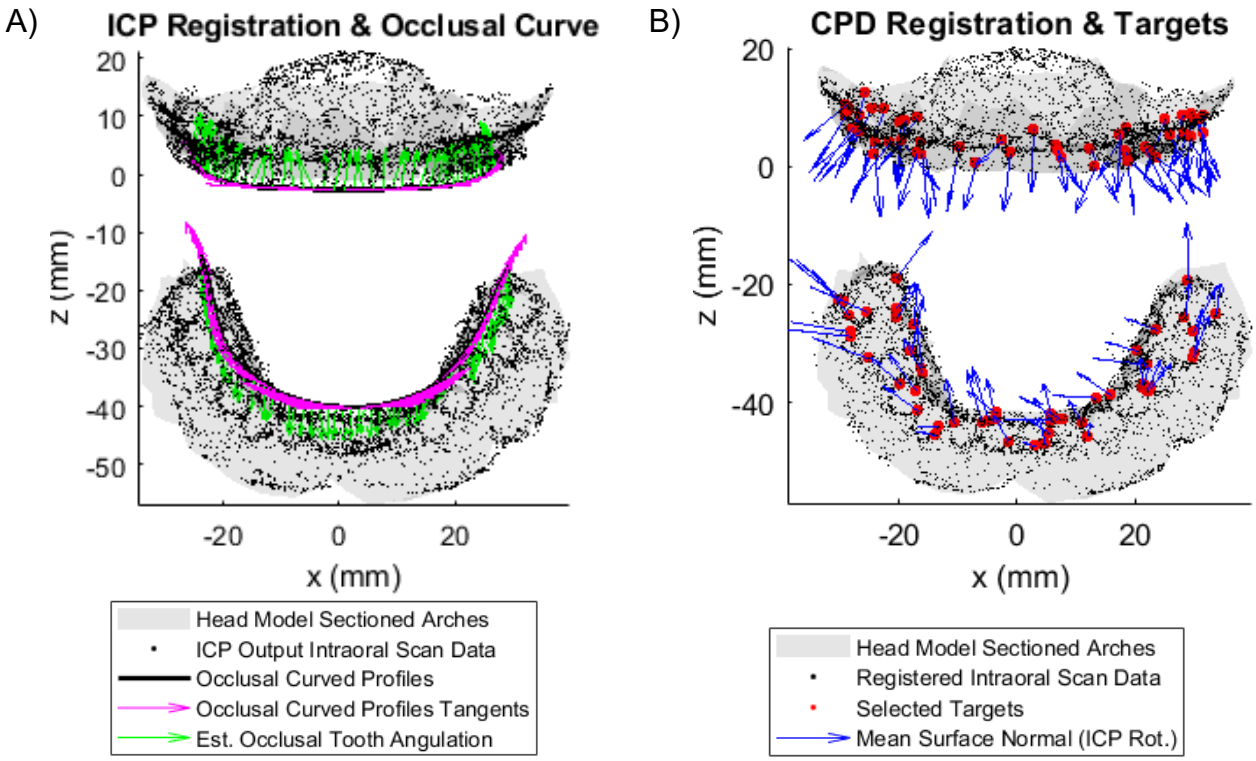

Figure 5.13. Intraoral scan data registration to sectioned head model arches. A) The ICP method with the occlusal curved profiles and vectors rotated using the output ICP transformation matrix. B) The CPD method with the mean surface normal vector of the selected target points also rotated using the ICP rotation matrix (displayed in blue).

Each target point (in red) was matched to its nearest occlusal curve point (in black) (Figure 5.14). The occlusal curve tangent (in magenta) was placed at the corresponding target point and is shown to point to the sides and then to the back of the mouth for each quadrant

when moving from the front to the back of the mouth. Target points inside the occlusal curved profiles represent lingual targets, while those on the outside represent buccal targets.

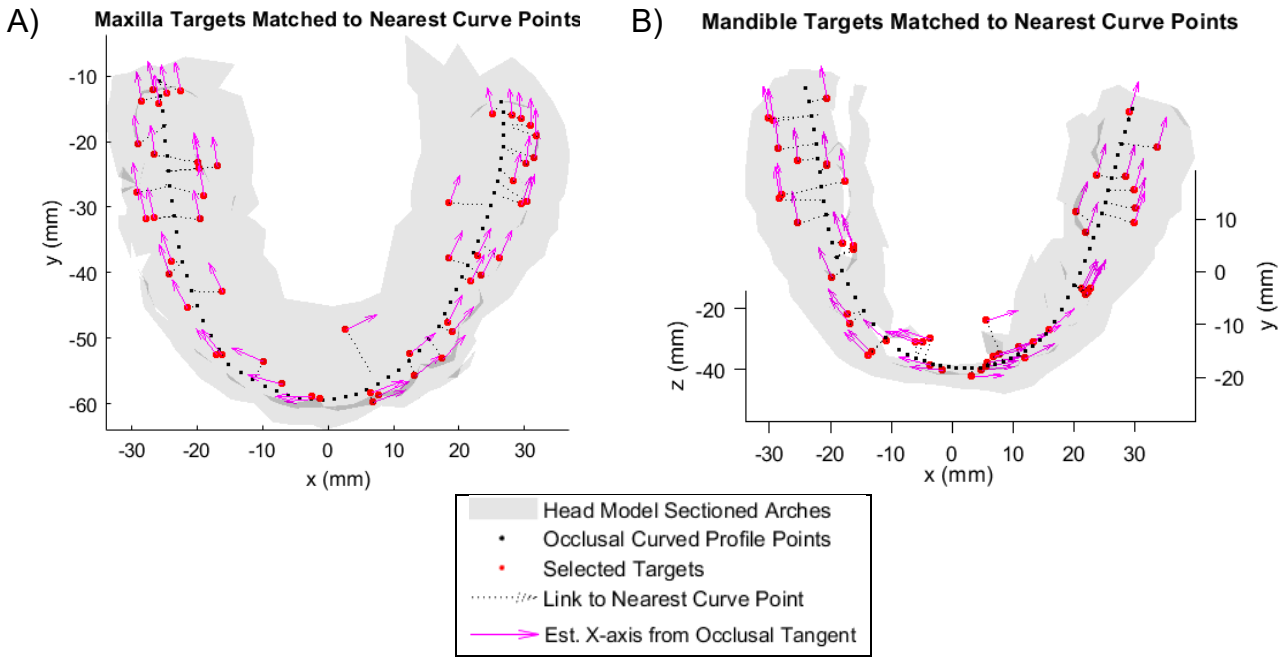

Figure 5.14. Assignment of targets in red (T_{pt}) to nearby arch curve profile points in black (P_o) for A) the maxilla and B) the mandible dental arches. Their matched profile tangents (in magenta) to estimate the x-axis of frames of reference is placed at each target.

The plot transform axes of target points (Figure 5.15B) can be seen to align in the expected directions of the target's axes vectors (Figure 5.15A). As planned, the x-axis Euler angle oscillated around 0° for the maxilla targets and 180° for the mandible targets (Figure 5.16A). The peak Euler angle according to the Kernel distribution in the y-axis was -5.65° for the maxilla and -40.45° for the mandible, while in the z-axis, there was a peak at 100.27° with local peaks at an angle away of +62.80° and -40.60° (Figure 5.16B-C). The distribution's peak expected rotation of the dental instrument for the targets was 24.46°, which had a standard deviation of 23.94° (Figure 5.16D).

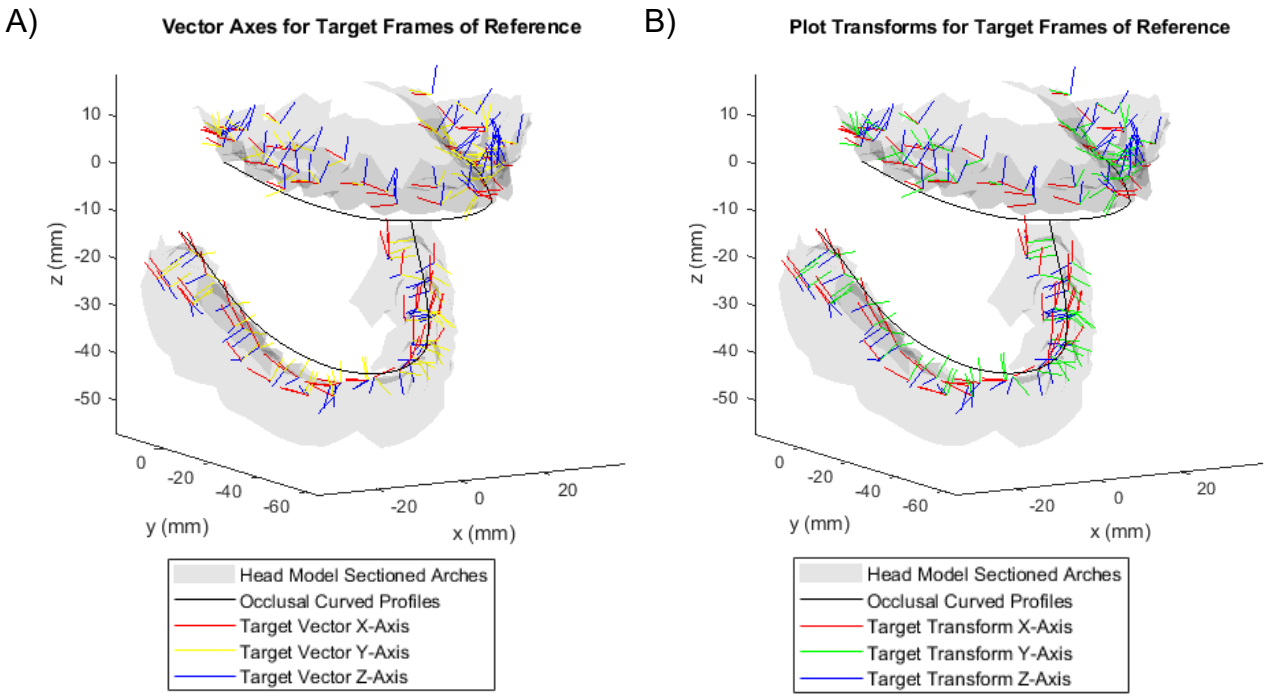

Figure 5.15. A) Vector axes for target point frames of reference. B) Plot transforms defined by Euler angles for each target point.

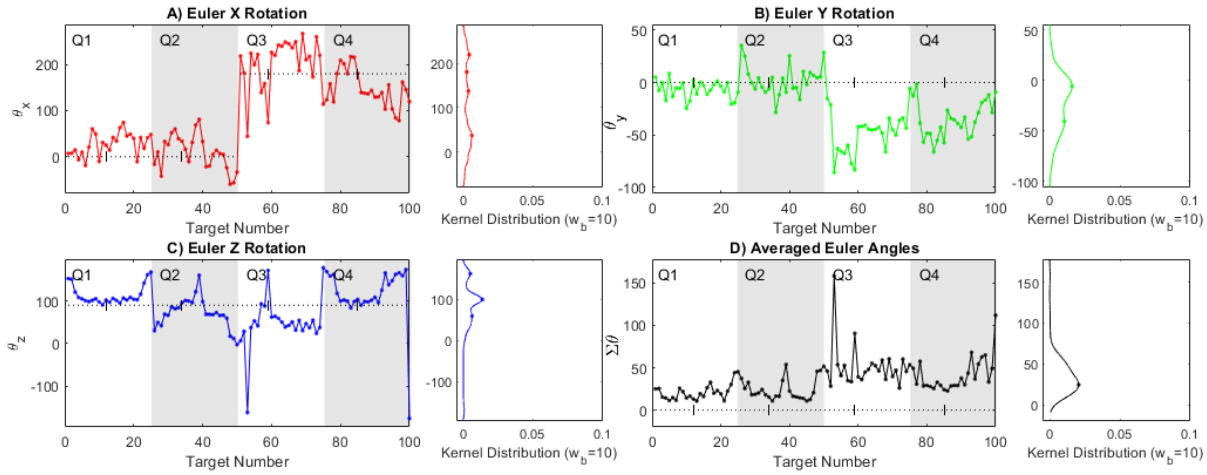

Figure 5.16. Euler angles for the plot transforms at each target point across each quadrant with the probability distributions (bandwidth, w_b). Units are in degrees.

The results for the orthogonal offset instrument handle frames of reference also show the x-axis vector (in red) pointing in a similar direction to the matched occlusal curve tangents (Figure 5.17). The tip direction z-axis (in blue) represents the opposing direction to the surface normal vector of each point, which represents the direction of offset for the instrument handle from the target point. These frames of reference define the instrument tip locations for safety measurements undertaken for the performance block (ID1.1–4). The tip target locations were

ordered as starting from the maxilla centre front of the arch, then passing through the lingual targets to the back of Quadrant 1 and returning through the buccal targets to the front of Quadrant 1. This was then repeated for the other three quadrants.

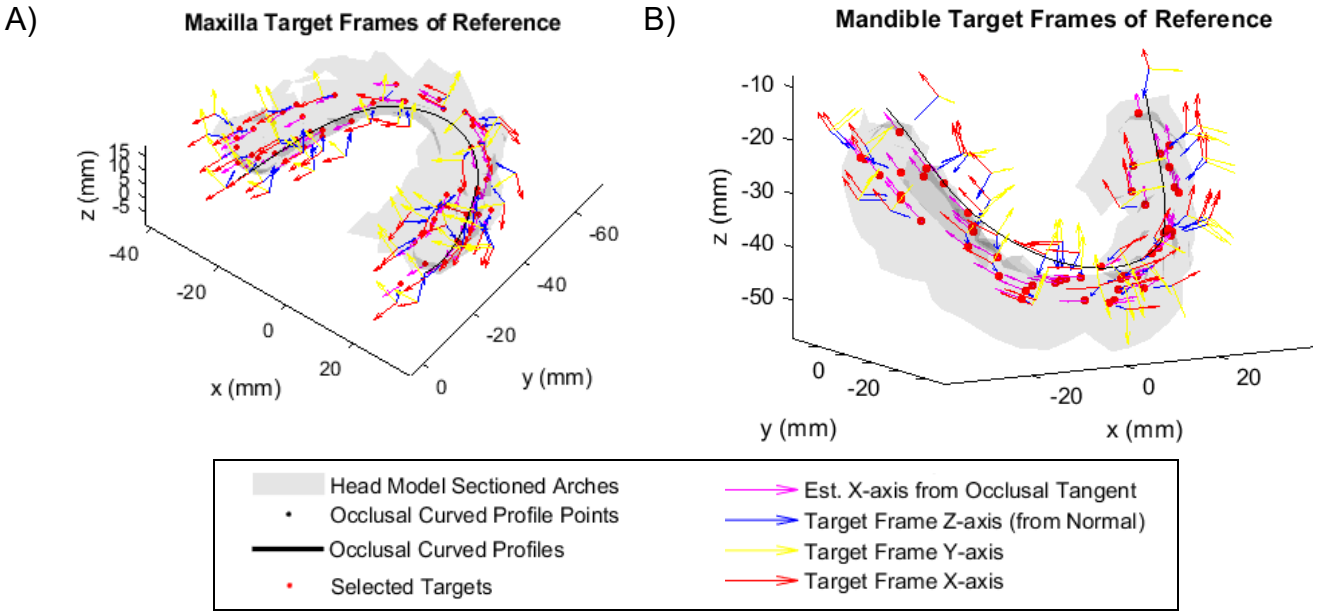

Figure 5.17. Offset instrument handle frames of reference for targets of A) the maxilla and B) the mandible with their occlusal curved profiles.

5.4.2 ID1.1 Instrument Tip Position Risk

Instrument tip position around the nearest occlusal curve point (P_o) was measured for each target location. Measurements for ID1.1 were taken in the tooth cross section planes (Figure 5.18A,B) and a comparison was included to target points that were offset on the maxillary arch by [4,4,4] and on mandible jaw by [4,4,-4] (Figure 5.18C,D). Measurements for the distance the lingual and buccal directions (in orange) and the distance into the arch along the tooth angulation direction (in blue) varied between either side of the occlusal curve (Figure 5.18A,B, Figure 5.19A,C). Their values increased in the x-component in Quadrant 1 and Quadrant 4 after their shift to the left side of the head model (Figure 5.18C,D, Figure 5.19A), while their values across all quadrants increased in the z-component after the shift into their relative dental arches (Figure 5.18C,D, Figure 5.19C). The variation in y-offset increased for the maxillary arch targets with the shift towards the back of the mouth (in green) (Figure 5.18C,

Figure 5.19B). A large offset from the plane cross section in y_b at target point 35 shows the target is positioned behind the back teeth (Figure 5.18A, Figure 5.19B).

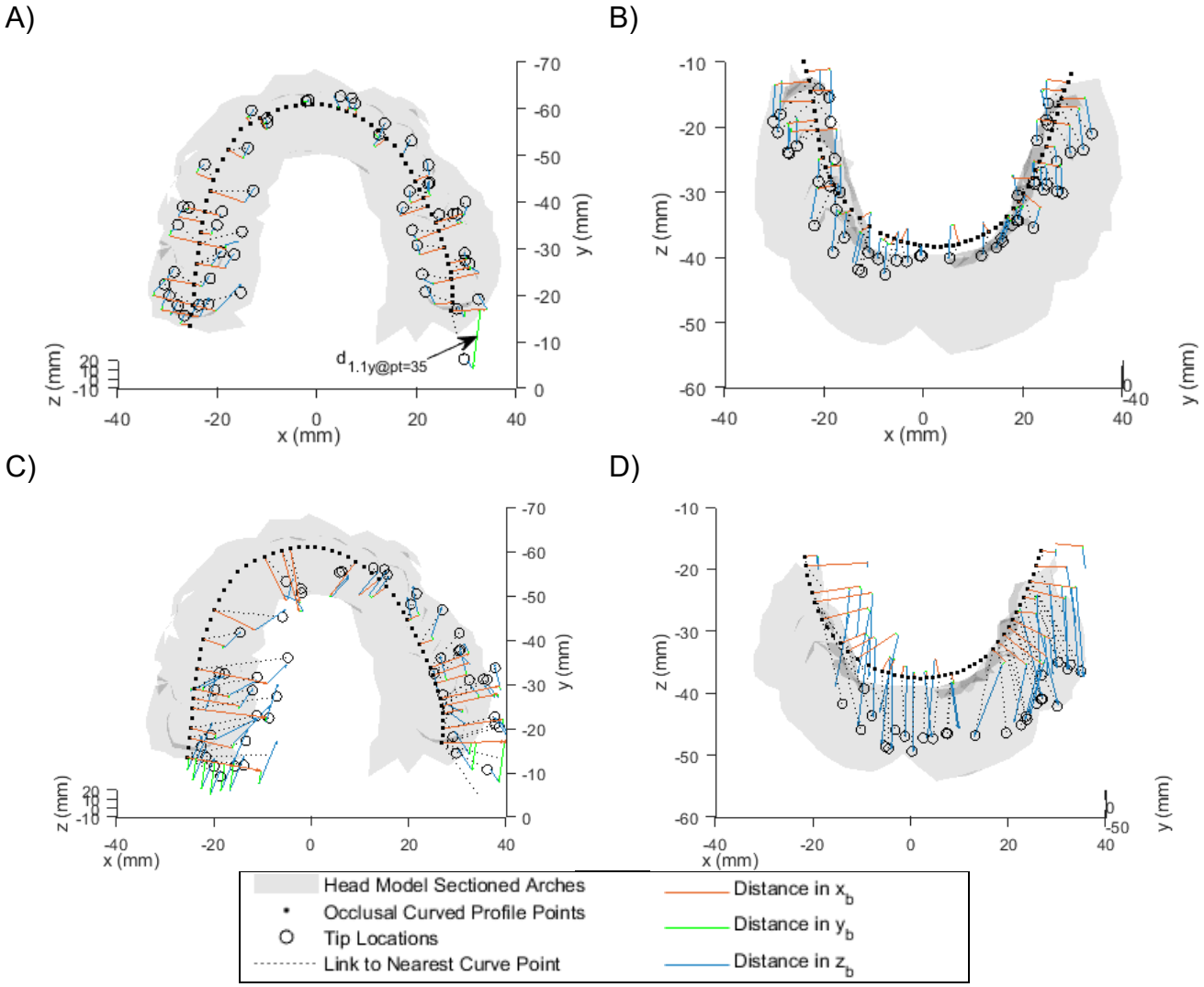

Figure 5.18. Distances from the nearest occlusal curve point (P_o) in the tooth cross sectional planes (in x_b and z_b) with offset from that plane in the y_b direction for the dental arches: A) the maxilla and B) the mandible. Distances from the nearest occlusal curve point for poorly localised target points: C) Targets shifted on the maxillary arch by [4,4,4]; D) Targets shifted on mandible jaw by [4,4,-4]. Lines to the target points are shown in the local reference frame of the nearby occlusal curve point.

The transition between the relative lingual and buccal locations is represented by the $d_{1.1x}$ graph (Figure 5.19A). These align with the denoted transition points of each quadrant (I symbol), showing that the instrument was positioned on the lingual side of the teeth on entry and buccal side on exit. Point 35 at the back of the mouth, at the transition between being

lingual to buccal targets in Q2, had a large difference of greater than 10 mm in $d_{I.1y}$ to the expected value near 0 mm (Figure 5.19B). The maximum risk of each component is recorded as the risk output for ID1.1 (Figure 5.19D), that highlights the regions where it is expected locations where the instrument will have more difficulty exiting from the mouth in an emergency, which are more lingual, deeper down the sides of the teeth or offset from the nearby occlusal point plane towards the back of the throat. Overall, the shifted target points had an average risk output of 10, compared to 6/10 for the initial locations around the gingival margin Figure 5.19D.

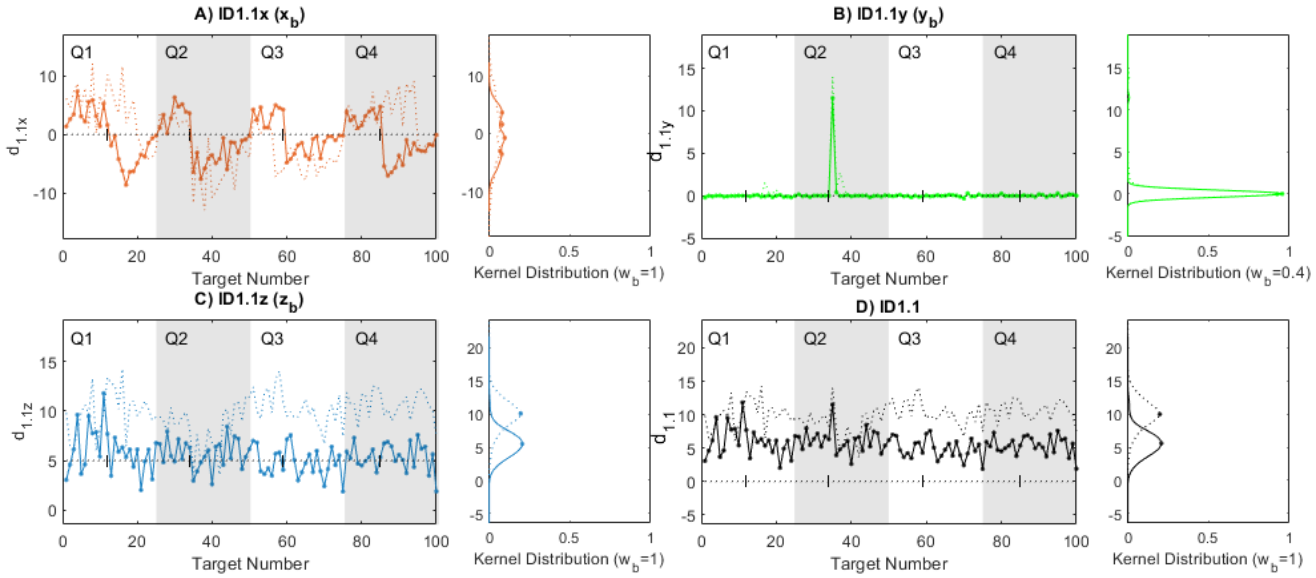

Figure 5.19. Risk measurements for ID1.1 in the A) lingual-buccal plane (x_b), B) offset from the expected nearby tooth cross section plane (y_b) and C) depth down beside the tooth (z_b). D) Maximum of each of the components as the final risk output. Probability distributions are shown for each plot (bandwidth, w_b). Units are in mm. Risk measurements from the nearest occlusal curve point for poorly localised target points represented by dotted lines.

5.4.3 ID1.2 Instrument Handle Position Risk

The silicone LA head model arches had an oral opening that was 53 mm in width and 49 mm in height. The frontal plane is presented with the intersection points of the maxilla and mandibular targets of the front of the mouth (Figure 5.20A) and the back of the mouth (Figure 5.20B). Targets with intersection locations outside the acceptable regions are displayed in black

markers (▲). Rotations of the instrument at the target locations can improve the risk of oral tissue collision with the model (Figure 5.21A,C-D), where the intersection locations are within the acceptable regions for front teeth (magenta) and back teeth (green) (Figure 5.20C,D).

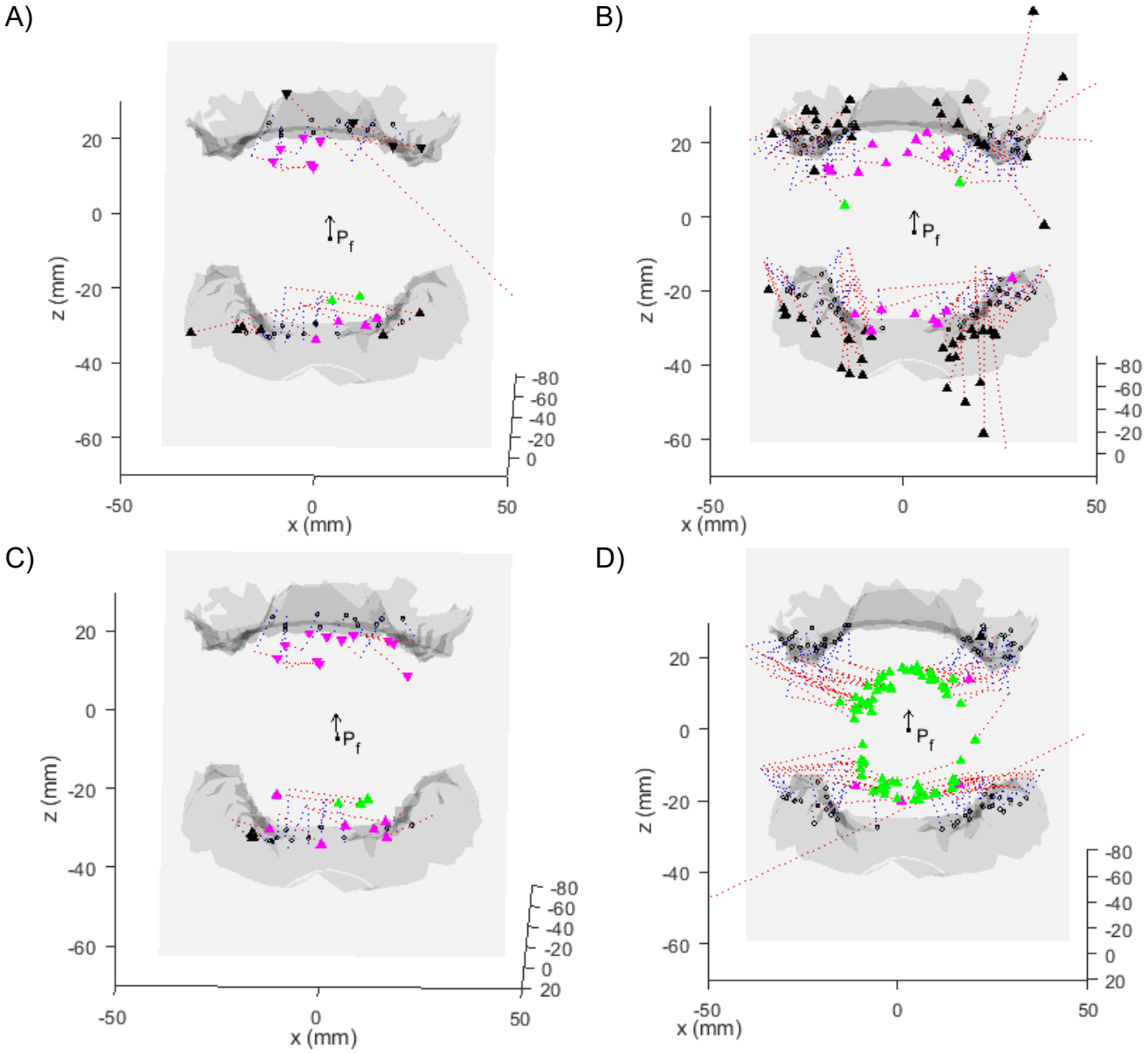

Figure 5.20. Intersection points of the instrument handle for A) front and B) back teeth targets on the frontal plane. Improved intersection points following rotations of the instrument for C) front and D) back teeth targets. The centre of opening is denoted by P_f with its normal vector directed into the oral cavity. The tip-to-handle offset frame is shown by a blue dashed line. The handle offset to the intersection point shown by a red dashed line. Maxilla handle intersections have a ▼, while mandibular handle intersections have a ▲, which are colour coded to their entry zones, which are either the larger magenta zone for front teeth or the smaller green zone for back teeth.

The depth of tip movement into each quadrant while moving through each target point is depicted by the changes in $d_{1.2y}$ (Figure 5.21B). This only reached a maximum risk of 6.31/10 as this is an indicator of the difficulty to operate or remove the instrument from the mouth, rather than a measurement of the risk of collision. The magnitudes of $d_{1.2x}$ and $d_{1.2z}$ represent increasing risk of the instrument handle as it moves towards the sides of the mouth entrance. Rotations of the instrument improved the outputs for these risk measurements, shown by the shift in the kernel distribution peaks (Figure 5.21A,C). The improvements provided by the rotations are shown by the dotted line for the maximum ID1.2 output for each target point (Figure 5.21D).

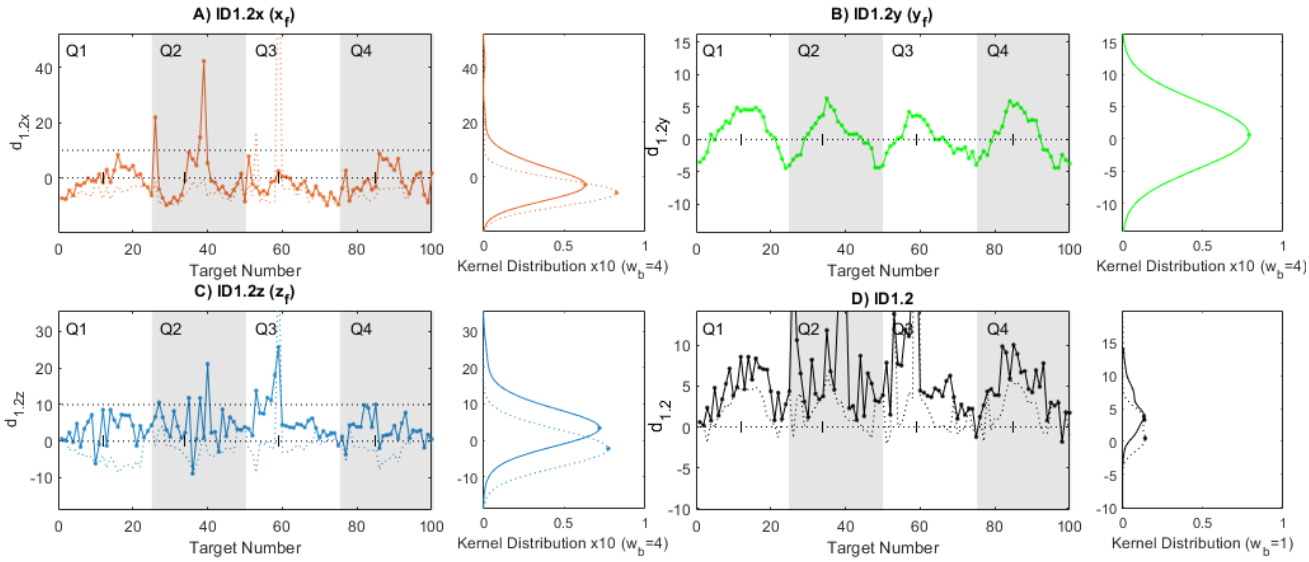

Figure 5.21. Risk measurements for ID1.2 in the frontal plane: A) x_f axis for movement side-to-side of the instrument handle at entrance to mouth; B) y_f axis for depth into mouth; and C) z_f axis for vertical movement of the instrument handle at entrance to mouth. D) Maximum of each of the components as the final risk output. Probability distributions are shown for each plot (bandwidth, w_b). Units are in mm. Risk measurements on the frontal plane for improved instrument rotations of target points represented by dotted lines.

5.4.4 ID1.3 Virtual Hard Tissue Risk Distances

Each model was imported into MATLAB and their point clouds were created for the virtual hard tissues and the throat surface was reoriented (Figure 5.22A,B). The sectioned tooth model was used to remove data points of the intraoral scan to output sectioned gingival data points. An additional 62 points of the dental arches were found and removed from the gingival surface model using the moving ROI method (37 in maxilla and 25 in mandible) (Figure 5.22C).

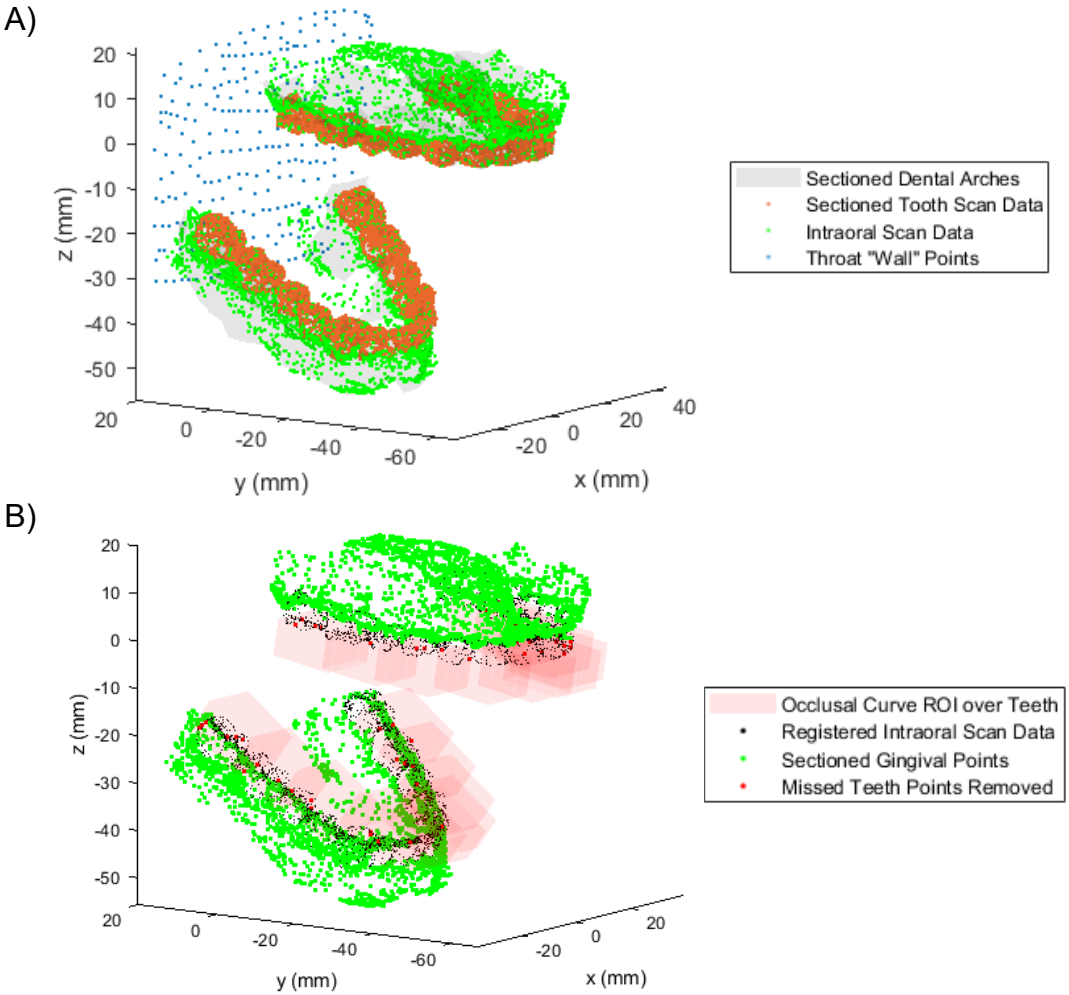

Figure 5.22. A) Imported simplified tooth point cloud with higher resolution registered to the head model with the intraoral scan data (to be cropped for the gingivae point cloud) and the throat entrance cover ("wall"). B) Cropped intraoral scan data to find gingival surfaces including the patches to remove missed tooth points.

Measurements for ID1.3 were taken for the target locations and a comparison was included to target points that were offset on the maxillary arch by [4,4,4] and on mandible jaw by [4,4,-4], similar to ID1.1 (Figure 5.18C,D). As expected, most tip locations are close to the tooth and gingival surfaces (Figure 5.23A,B, Figure 5.24A,B), however these increase with shifts by 4 mm in the head model axes in each direction of the targets (Figure 5.23C,D, Figure 5.24).

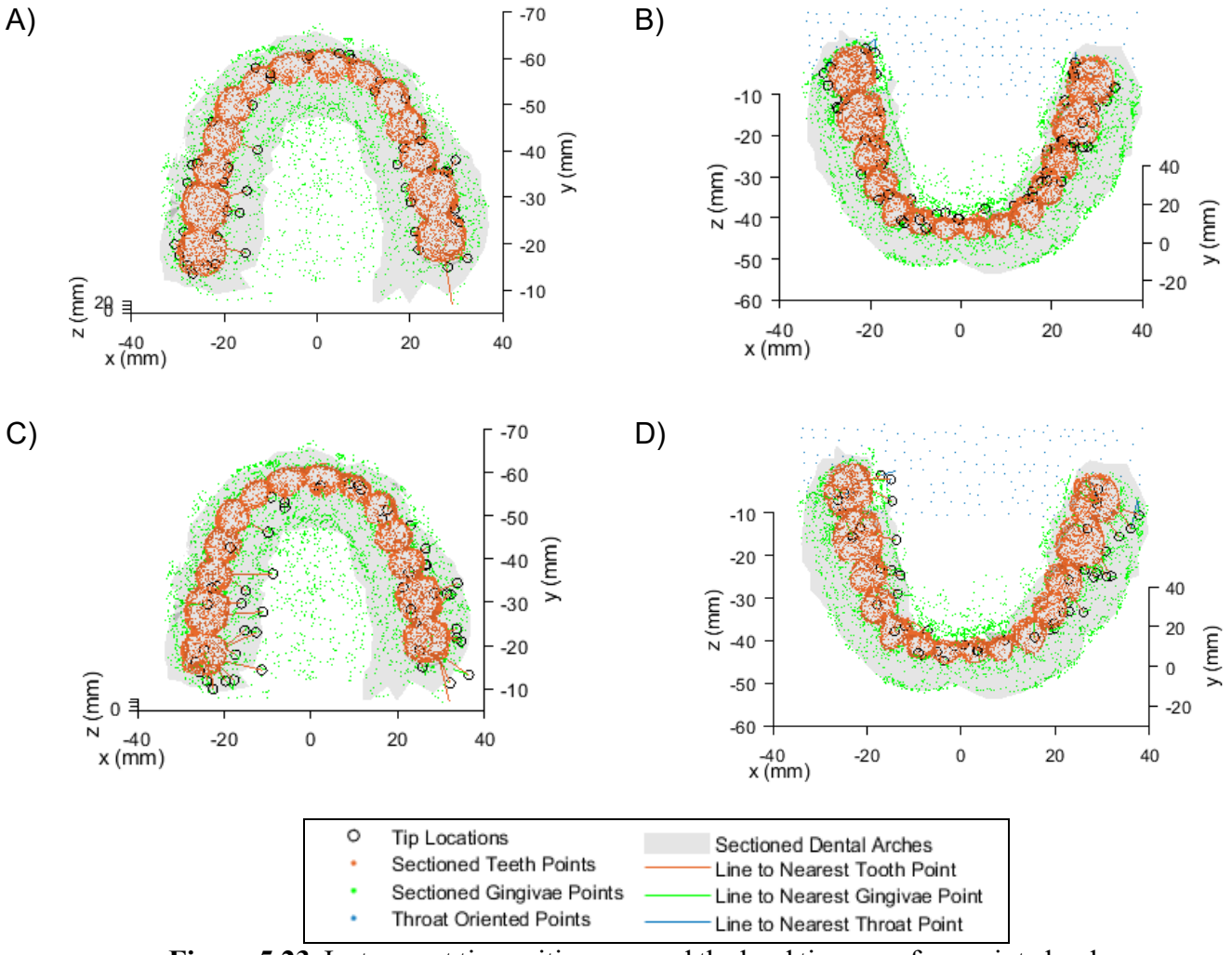

Figure 5.23. Instrument tip positions around the hard tissue surface point clouds for the dental arches: A) the maxilla; and B) the mandible. Distances from the nearest hard tissue surface point for poorly localised target points: C) Targets shifted on the maxillary arch by [4,4,4]; D) Targets shifted on mandible jaw by [4,4,-4]. Lines are shown between points and the nearby surface. Only targets within 10 mm to the throat were used to show the line to the nearest throat point.

Since the selected points are on the arches (or gingivae) from the intraoral scan, the distribution of the results for $d_{1.3x}$ and $d_{1.3y}$ are as expected around 5/10 (Figure 5.24A-B). Similar to ID1.2 (Figure 5.21B, D), the depth of tip movement into each quadrant while moving through each target point is depicted by the changes in $d_{1.3z}$ with positive peaks occurring around the back of the mouth (at quadrant transition points) for the mandible targets (Figure 5.24C). The peak maximum risk outputs for ID1.3 increased to 8.06/10 for the shifted target locations with respect to the hard oral tissues.

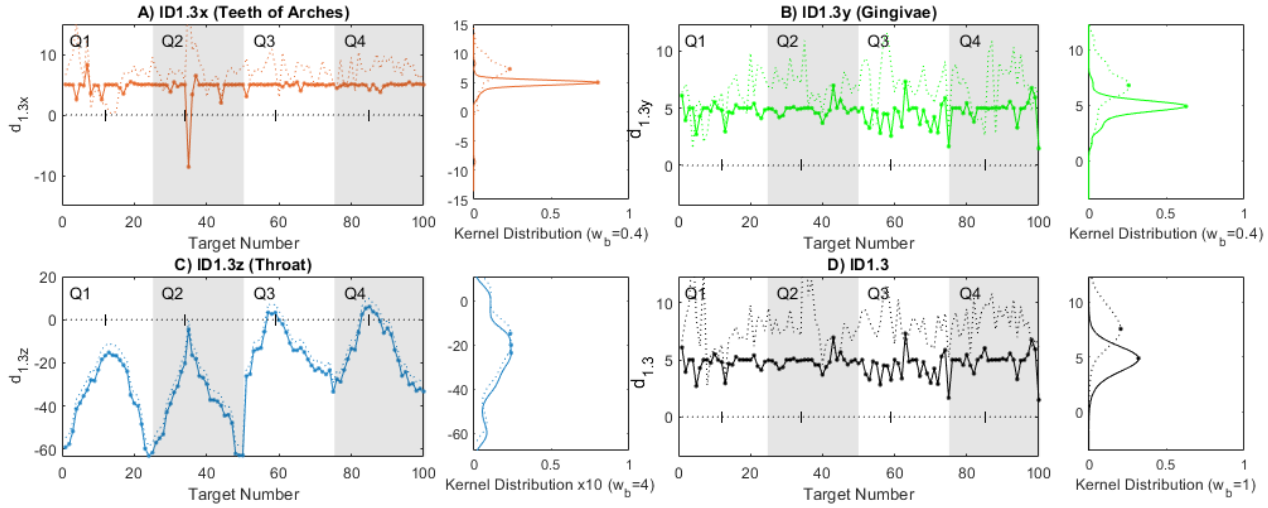

Figure 5.24. Measurements for ID1.3 for: A) the distance away from the nearest tooth surface point; B) the distance away from the nearest gingival surface point; and C) the distance away from the nearest throat surface point. D) Maximum of each of the components as the final risk output. Probability distributions are shown for each plot (bandwidth, w_b). Units are in mm. Distances from the nearest hard tissue points for the poorly localised target points represented by dotted lines.

5.4.5 ID1.4 Virtual Soft Tissue Risk Distances

The surfaces for the lips, cheeks and tongue were imported into MATLAB to measure the virtual depth of the instrument tip into the tissues (Figure 5.25A). Measurements for ID1.4 were taken for the target locations with the comparison to target points that were offset on the maxillary arch by [4,4,4] and on mandible jaw by [4,4,-4], similar to ID1.1 and ID1.3. For the planned and shifted tip locations, the nearest soft tissue features are highlighted by the lines to points at risk (Figure 5.25B,C).

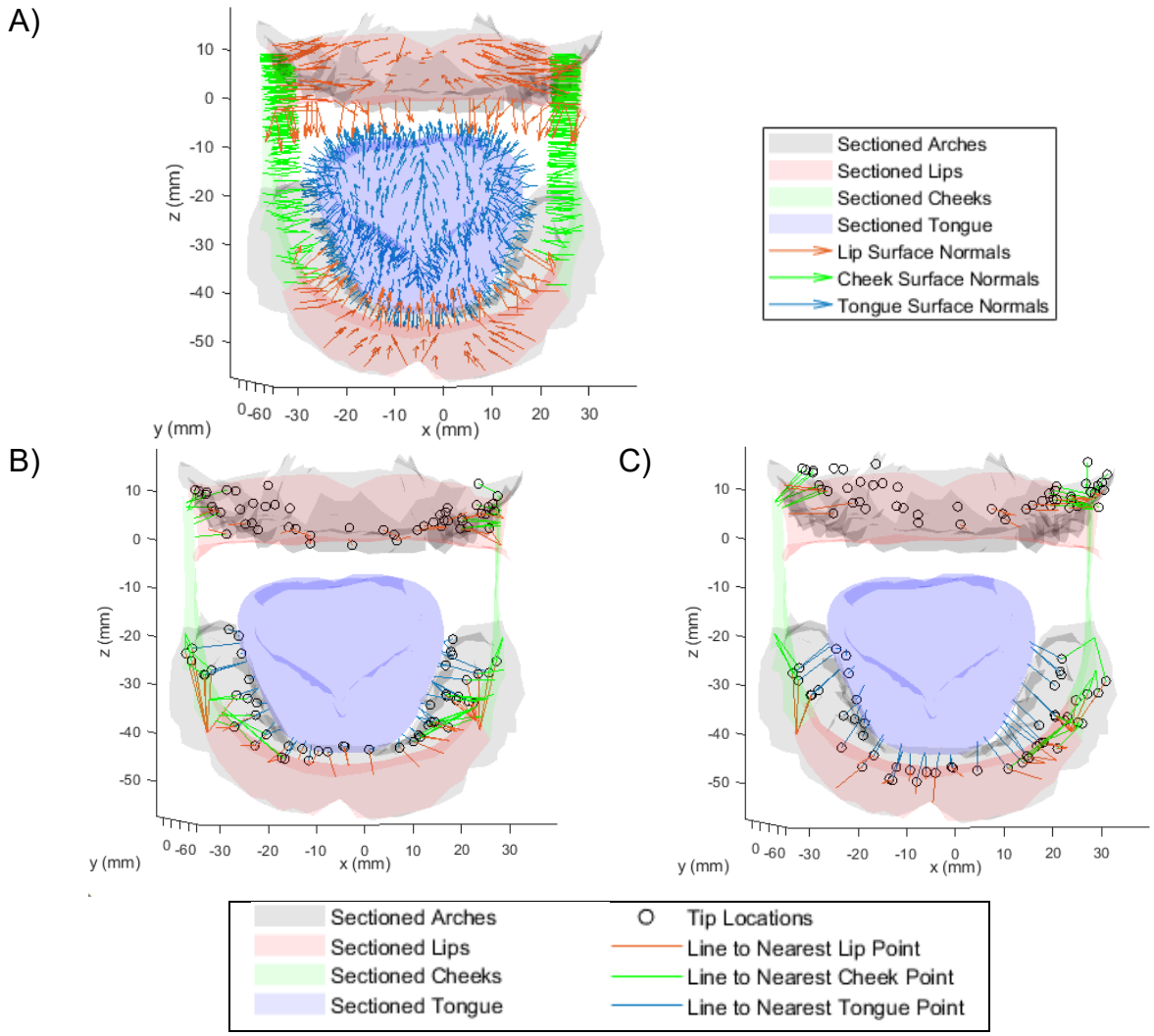

Figure 5.25. A) Soft tissue surfaces for the lips, cheeks and tongue shown positioned around the arches with their surface normal vectors pointing in the direction of reducing risk (out of the surface). B) Distances from the nearest hard tissue surface point to the planned target points. C) Distances from the nearest hard tissue surface point for poorly localised target points (shifted on the maxillary arch by [4,4,4] and shifted on mandible jaw by [4,4,-4]). Lines are shown for points within 10 mm of the nearby surface.

Back and front tip locations are furthest from the lips and cheeks, respectively, shown by minimums in risk at transition points or between quadrants (Figure 5.26A,B). Lingual locations of the mandible (Quadrant 3 and Quadrant 4) are closest in proximity to the tongue in its flat position (Figure 5.26C). On average, the shifted target points were found to be further from the soft tissue surfaces (Figure 5.26D), except in the distance to the left side cheek of the head model (Quadrant 2 and Quadrant 3) (Figure 5.26B). The region with the lowest risk furthest from soft tissues were the maxilla lingual tip locations of Quadrant 1 and Quadrant 2 (Figure 5.26D). Across all the target locations, the peak maximum risk outputs for ID1.4 reduced to -2.56/10 for the shifted points from a value of 1.53/10 with respect to the soft oral tissues.

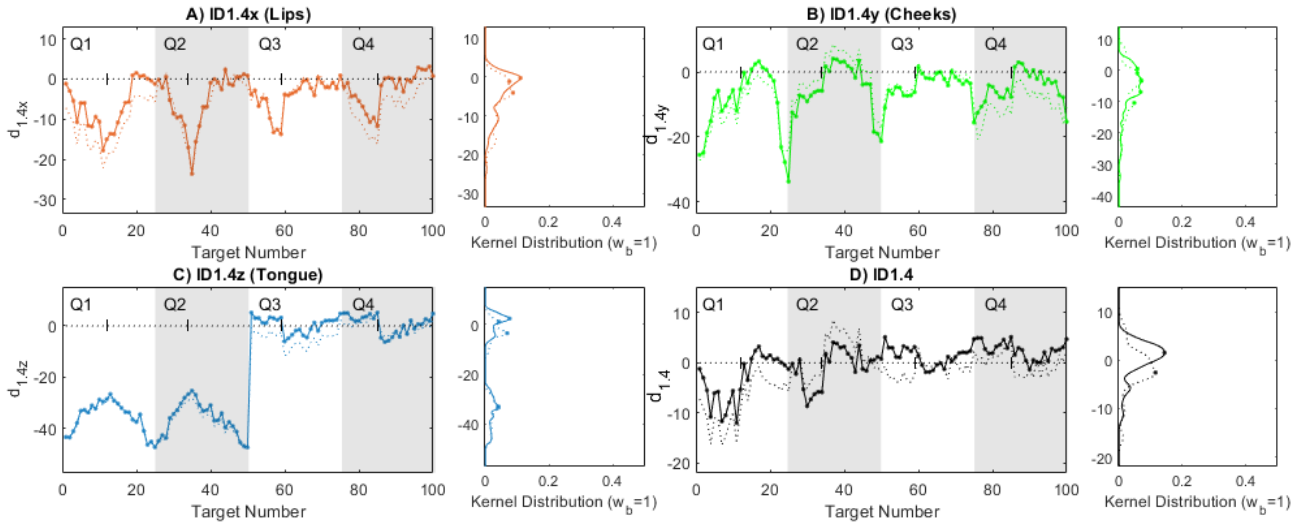

Figure 5.26. Measurements for ID1.4 for: A) the distance away from the nearest lip surface point; B) the distance away from the nearest cheek surface point; and C) the distance away from the nearest tongue surface point. D) Maximum of each of the components as the final risk output. Probability distributions are shown for each plot (bandwidth, w_b). Units are in mm. Distances from the nearest soft tissue points for the poorly localised target points represented by dotted lines.

5.5 Discussion

The risk distance measurements from ID1.1 to ID1.4 can help to identify the changing risk levels of different target locations in the oral cavity. This was a first step in verifying the capability for a procedure block supervision system to detect high risk hazardous situations. Triggered high risks can be used to promote the robot to recover to a safe level with or without the assistance of an operator to improve safety performance and avoid harm. The estimated quantitative spatial measurements encompass the risks involved in the position and orientation of the instrument within the oral cavity during dental techniques in a way that can be understood by both dentists and roboticists. These safety measurements can be carried out during tracked dental procedures to assess their safety over time, as well as prior to a procedure for virtual pre-programmed dental techniques to assess their level of safety.

The methods for ID1.1–1.2 rely on the occlusal curve which should be checked with a visual assessment prior to a procedure. In contrast, ID1.3–1.4 rely on the position and shape of intraoral scan data and soft tissue surfaces. A benefit of the four procedure block methods is that there is breakdown of different risks for redundancy of safety, of which some experience overlaps in their results despite undertaking different methods of measurement in different frames of reference. This was shown by the similarities in trends over the target point plot risk components. Additionally, the instrument tip path in the tooth cross sectional planes aims to eliminate the challenge of comparing motions for teeth at different orientations within the mouth, thereby allowing for comparisons between the motion of techniques on similar tooth structures.

In standard separation monitoring, operators approach the robot's workspace, and the robot assesses the distance to the person before continuing their chosen task (Figure 5.27A) [300]. In the context of the instrument risk measurements, the perspective shifts from that of the person to the robot. These collaborative systems are usually designed to detect the presence

of a whole person by heat radiation or their physical appearance from other non-critical objects in the environment to improve robot efficiency using longer range sensors [300, 301]. At small ranges in the oral cavity, distance separation detection is increasingly difficult to perform. The chosen design of the procedure block risk measurements is beneficial as it can be used to distinguish the relative risk of important dental features, such as the types of oral tissues and important points of reference, and includes the depths into their respective axes or virtual deformation of their tissue surfaces.

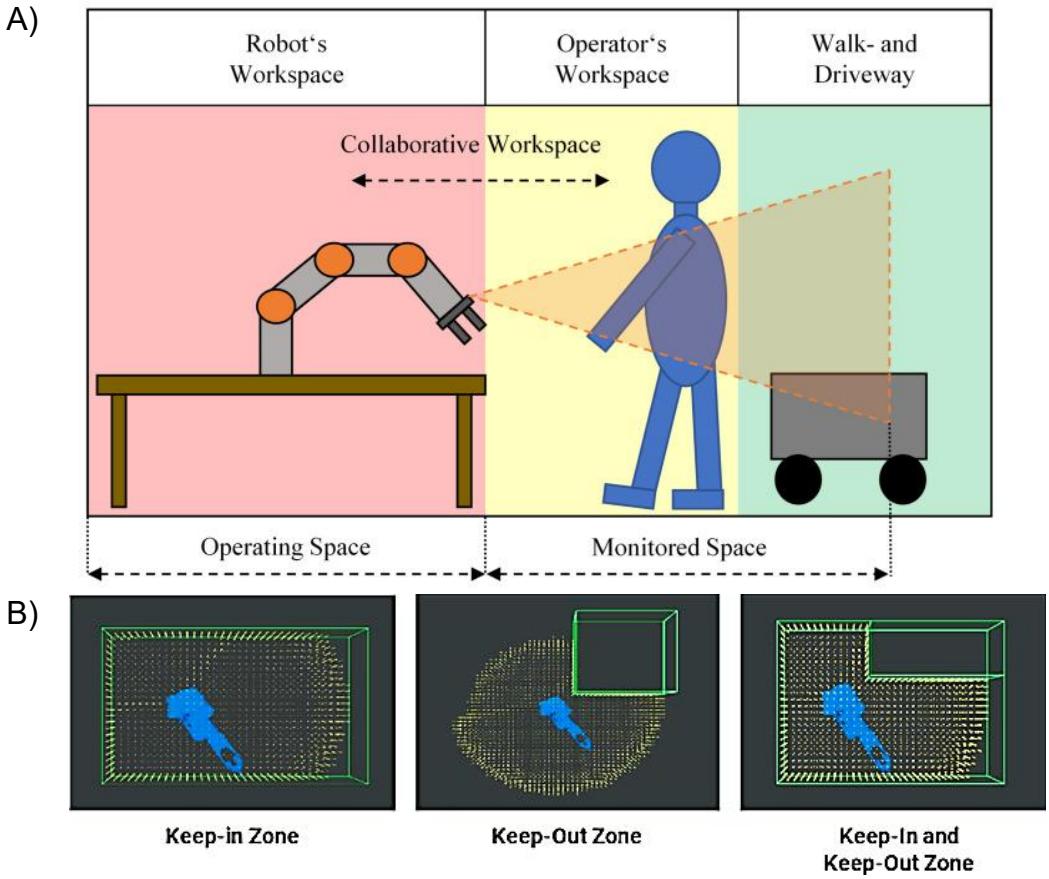

Figure 5.27. A) Workspaces around a robotic application for separation monitoring including the robot's workspace (red), and operator's workspace (yellow) and free space (green) with a variable range of distance that is monitored [300]. B) Illustration of robot joint safety constraints: a keep-in zone (left); a keep-out zone (middle); and a keep-in/keep-out zone (right) [302].

The hard and soft oral tissue surfaces can be likened to keep-out zones suggested by Moel *et al.* (2022) for robot joint control constraints [302] (Figure 5.27B). The robot safety constraints were defined as potentially dynamic volumes that prevent the robot from movement

into recognised zones of risk and maintains the robot joint within a recognised safe zone based on the initial and detected state of the robot [302]. The oral tissue models were also designed to be adaptable to patient movement for the position of the dental arches. This was achieved by dividing the model into separate point clouds for the different tissue types such that they could be layered and allow for a dynamic mandible jaw. Similarly, soft tissue features of ID1.4 can be positioned around a patient's custom intraoral scan to reduce the need for whole head scans. Although the model used a flat tongue resting on the mandibular arch, it can be repositioned based on visual feedback from tracking to provide a more accurate risk output estimate.

The procedure block methods' simple design makes them dependent on the accuracy of intraoral scans and their localisation during procedures. The registration methods to position the intraoral scans for the head model had root mean square errors in the range of 2.57-2.78 mm. However, based on the visual plot, the CPD method seemed to have an accurate representation of the points. The apparent errors may be a result of the lower resolution of the imported sectioned head model arches used for registration. Also the current methods do not account for the shape or compliance of the instrument as the target reference frames were designed for a thin handle with a right-angled tip working end and its depth into the oral tissues was estimated based on the virtual depth from the surface. An angled instrument working end is likely to further alter the available orientation of the instrument when operating at the back of the mouth with the presence of the opposing dental arch.

The developed procedure block safety assessments aim to make a step towards good practice of patient safety in dentistry. Supervision system measurements could be a useful tool to provide evidence of the true sources of error during dental procedures, while bringing patient safety to the forefront of discussions. Indemnity or professional liability insurance that protects the clinician during practice and after retirement is recommended to last at least six years after

the clinician has stopped working, independent of the period of time worked [303, 304]. This is because complaints and allegations of negligence can be filed years after the treatment was provided [304-307]. Delayed claims are more complex and expensive to defend or settle, since it can be difficult to remember a specific treatment with the lack of dental records [304]. The addition of tracked safety measurements could provide vital objective information and reduce assumptions made during investigations, especially when combined with 3D models of the patient's anatomy [96].

Improvements to the verification of safety measurements and assessments should include assessments of instrument paths around the mouth, extending from the current static model at specific target locations. This is important as locations below the tongue can present with low risk although the path to reach the target would present high risk of harm. Moreover, these risk methods could be extended to other locations of the instrument to create a map of risk over the instrument, which could assist in determining the safest orientation for its position within the mouth. The directions of reducing risk can be calculated for the locations of the hard and soft tissues of ID1.3–1.4. These could be used to assess the path of least risk for an emergency exit from a given location inside the mouth. This acts in contrast to the risk measurements of ID1.1–1.2 which estimate the risk to exit the mouth in an emergency. Together, the measurements could be used to determine if the safest course of action is to leave the instrument in the mouth or to perform an emergency exit in a high-risk event.

Limitations of the procedure block risk measurements may be accounted for in the design of the supervision system observer block by visually assessing the compliance of the instrument tip and oral tissues in the environment. The observer block should be designed to monitor the power and force limiting safety methods of dental procedures by focusing on the velocity limits for the instrument during dental procedures with the potential to carry out force estimation measurements. This would need to incorporate virtual assessment methods akin to a

speed, power and force monitoring and limiting systems, but its capabilities should not depend on the use of a dental robot for its verification. For instance, the measurements can make use of the rates of change in procedure block spatial measurements to assess the safety of the instrument's relative movement to the identified important dental features. Further, this should account for the instrument sharpness and orientation in the oral cavity.

Digital dental arch analysis was performed on the intraoral scans of the silicone LA head model. This analysis of the dental arches made efforts to account for anatomical variations in size, shape and curvature of the dental arch models. These aim to move towards the development of dental techniques which should be defined by a patient's oral health through digital visual analysis. Initial instrument Euler angles at the targets were also calculated. Larger values in angle offset from the start position could also be associated with higher risk as it may be more challenging for the robot to reach those positions for accurate performance. Analysis of robot system capabilities could be added as a fourth block for robot system risk output (Figure 4.7, Chapter 4).

Future verification methods that use tracking of the dental model using CT scan data, such as those for visual guidance system or the Yomi passive robot arm, may require the intraoral scans to be registered to the position of the tracked model. To achieve a very low RMSE that is more reflective of the accuracy of registration, both the digital CT and intraoral scan models would require higher resolutions such that all their points in close proximity. It should be noted that the high RMSE score could have been amplified by the soft silicone gingivae of the head model. Due to the division of specific oral tissues, it is possible to include the tracking of each to evaluate the risk in a more dynamic environment. Facial or mouth recognition camera systems could be used to achieve this. Customisable virtual tissue features, that can be adjusted in size and position for different patient anatomies, minimise the need for the creation of patient-specific digital models all the oral tissue surfaces beyond that of the

dental arches. The simplification to measure the amount of penetration into the “inflexible” digital models for soft tissues features reduces the need for high power computing and complex tissue modelling while still assessing the extent of a collision or contact by an instrument.

The comprehensive procedural risk assessment by spatial mapping aims to increase awareness safety considerations for robotic operation during dental procedures. These can act as an extension to standard separation monitoring to include virtual model contact monitoring. This estimate of the risk of harm from deformation of the soft tissues limits the need for complex deformation analysis which takes time and requires higher computational power. This is important as it is valuable to prioritise the use of an accurate scan of the dental arches for dental techniques, even though the scans also had to be reduced in size for registration. Further methods will need to be developed for the observer and patient blocks of the supervision system. Testing in a simulated environment is needed to evaluate the robustness of the spatial risk measurements by observing for the presence of false positives and negatives.

Chapter 6: Simulated Dental Robotics with Risk Tracking

6.1 Summary

This chapter presents a virtual simulation environment for dental applications in Unity that assesses procedure risks spatial measurements, pertaining to the location of a dental instrument around the mouth, in comparison to the likelihood of a collision, an indicator of high risk. The simulation environment was designed to perform initial verification testing of the patient block supervision system for tracking real-time spatial risk assessments. For verification, collisions between the dental instrument and a head model are measured using a force-torque sensor in a dynamic dental environment using pre-programmed paths for various dental instruments, including an intraoral camera, sonic toothbrush and periodontal probe. Experiments are undertaken with passive and active simulated head and jaw movement.

6.2 Introduction

Autonomous dental robots need to perform safe dental techniques while tracking and moving with the patient at an acceptable speed, accuracy and dental instrument. Achievable robot arm solutions must account for its reach, position constraints, and rotational limit constraints for its link lengths and number of joints [69]. This becomes more difficult for compact robots that are ideal for dental applications as they appear less confrontational and are more suitable for small workplaces with human interaction. An example of this is the ~$20,000 AUD 6-DOF lightweight Meca500-R3 (v8.3 firmware) that costs at 4.5 kg with a maximum rated payload of 500 g and 0.005 mm precision repeatability which can allow it to create fine movements of dental instruments in its limited working envelope (Figure 6.1A) [225]. The six rotating joints have functional states of $J_1 \perp J_2 \parallel J_3 \perp J_4 \perp J_5 \perp J_6$ with specific joint ranges (Table 6.1). Frames of reference for each joint can be described by the modified Denavit-Hartenberg (D-H) parameters (Table 6.1), while the location of the Tool Reference Frame (TRF) can be defined for different end effector instruments (Figure 6.1B).

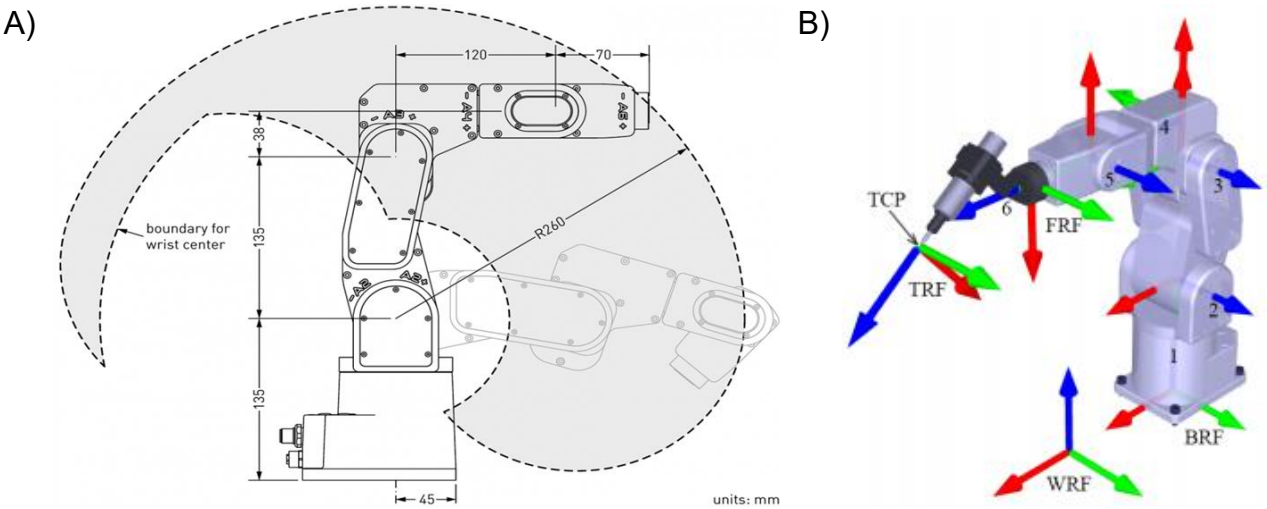

Figure 6.1. A) Meca500 robot reference frames and numbered joints with the Tool Reference Frame (TRF), World Reference Frame (WRF) and B) the working envelope [225, 308].

Table 6.1. The Meca500 joint limits and its modified D-H parameters based on the robot's dimensions and joint frames (Figure 6.1). The a_i and α_i represent link length and link twist, while d_i and θ_i are link offset and joint angle. The immobile base is considered joint 0.

Joint	**Joint Limits**		**D-H Parameters**			
i	***Min (º)***	***Max (º)***	***α_{i-1} (º)***	***a_{i-1} (mm)***	***θ_i (º)***	***d_i (mm)***
1	-175	175	0	0	θ_1	135
2	-70	90	-90	0	$-90 + \theta_2$	0
3	-135	70	0	135	θ_3	0
4	-170	170	-90	38	θ_4	120
5	-115	115	90	0	θ_5	0
6	-36,000*	36,000*	-90	0	$180 + \theta_6$	70

*Joint 6 is limited by the presence of wires to electronic sensors on the robot end effector.

As with human arms, robot arms and the dental instrument end effector can be positioned to work in a left- or right-handed manner, i.e. in an elbow (or wrist) up or down configuration [69]. The point of transition between changing configurations is known as a singularity which presents a challenge for robotic control depending on the robot's joint and link structure. For the Meca500 arm, transitions passing near three types of singularity, namely the wrist, elbow and shoulder singularity, can cause sudden fast movement and pausing of the robot end effector. These occur when changing the robot configuration state, such as when joint 5 aligns with joint 1 (or 3) (Figure 6.2A), when the arm is completely stretched (or bent) (Figure 6.2B) and when flipping joint 5 (Figure 6.2C). Singularities for joint 5 and 3 occur when the angle passes over 0° or -72.43°, respectively. Jolting movements caused by passing through singularities should be avoided, especially in cases where the robot is not in a chamber, to limit the occurrence of unexpected collisions. This is particularly important when there are unsuspecting nearby persons and users that need to gain trust and confidence in the autonomy of the robotic system.

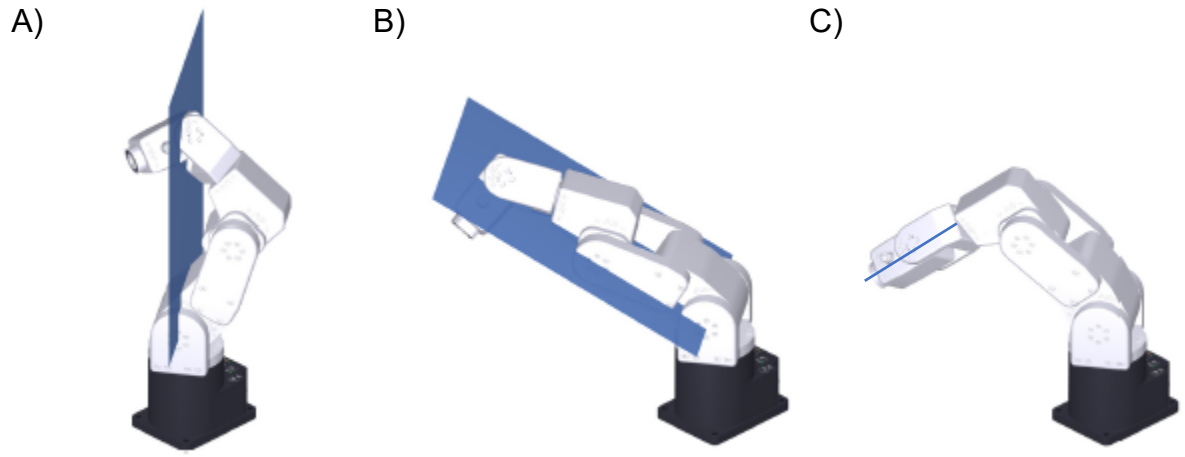

Figure 6.2. Three types of robot singularities shown for the Meca500 robot arm: A) Shoulder singularity where joint 5 is positioned vertically above joint 1; B) Elbow singularity at full reach from joint 1 to joint 5; and C) Wrist singularity where link 5 and link 6 are aligned [309].

Control of robots in a dynamic dental environment is challenging when accounting for movement of the head in three axes, including flexion and extension, rotation side-to-side and lateral bending [310]. Without a mouth prop, there is an additional risk of mandible movement, such as from the mouth closing, chewing or biting on an instrument [311], which could result in excess force applied between the instrument and the patient's oral features. Some patients already have a limited mouth opening, from normal 40–60 mm to less than 35 mm [293-298], which restricts the amount of movement and visibility for automated dental procedures and can cause patient pain and discomfort [293]. The use of safety monitors tend to be considered a fault-tolerant approach [267]. Systems that rely on force-feedback for safe control and compliance of the robot end effector have to cause a collision to detect a surface and in the process can cause unwanted harm [74]. Unlike force-feedback detection, the supervision system with high spatial risk awareness should be able to estimate the risk of harm like a "near miss" (a hazardous situation incident) without the event of minor or adverse harm [35].

This chapter explores the potential implementation of the game engine, Unity, for the simulation of normal and abnormal use of the Meca500 robot in a dynamic dental environment. A head model was used that allowed for side-to-side head rotation and opening and closing jaw

movement. Robotic applications are carried out to simulate dental techniques on the head model with an intraoral camera, sonic toothbrush and periodontal probe. The success of the dental instrument to carry out pre-programmed paths are observed from robot joint and singularity calculations, force measurements and risk calculations. The procedural risks from simulations are compared to the force sensor measurements in Python to assess the potential of risk tracking records to be used to assess high risks for the position of the instrument in a model mouth. The procedure block risk spatial measurement methods (ID1.1–1.4) were transferred from MATLAB (Chapter 5) and recreated in Unity (Figure 6.3).

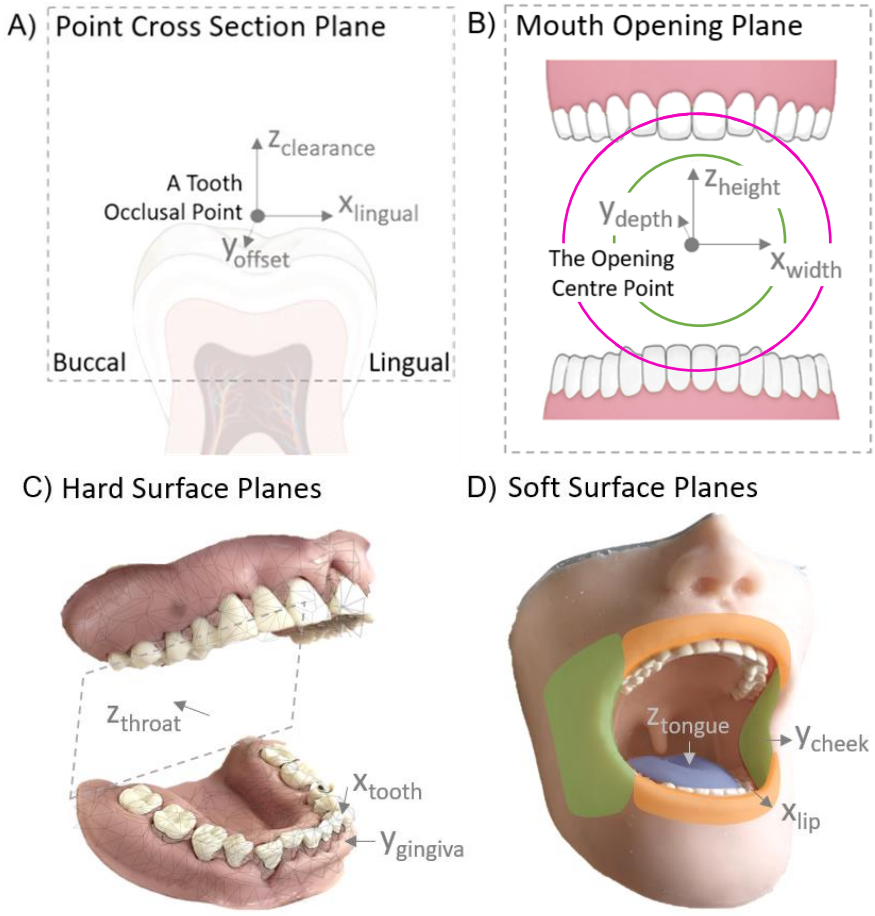

Figure 6.3. Procedure block measurement diagrams (Chapter 5) for interpreted data (IDs) with respect to dental features: A) ID1.1 axis frame for the position around a tooth occlusal point viewed through its cross section. B) ID1.2 axis frame for the instrument intersection through the frontal plane. C) ID1.3 distance measurements relative to nearby hard tissues including the teeth, gingivae and virtual throat "wall". D) ID1.4 distance measurements relative to nearby hard tissues including the lips, cheeks and tongue.

6.3 Methods

6.3.1 Dental Environment Setup

6.3.1.1 Dental and Robot Models

The physical dental environment was set up with the 2.27 kg silicone LA head model positioned in front of the Meca500-R3 robot end effector (Figure 6.4A). The head side-to-side rotation is released by loosening a hex screw lock to the metal support rod. The maxillary arch is fixed relative to the skull, while the mandibular arch is suspended in the silicone and can flex. To recreate the environment in simulation, the head model STL file from Chapter 5 was imported into Blender. The full head model scan was split into two halves for the maxilla and mandible such that the simulation could produce separate rotations of the dental arches with their respective head model features. The head model was split in Blender in Edit Mode using a horizontal cut below the maxillary arch and all dental arch points were cut away in each half to be replaced by the intraoral scan arch models in Unity. Models were smoothed and coloured in Blender using the UV mesh feature and imported into Unity with its material image file (Figure 6.4B). The instruments were held by a 3D printed connector at joint 6 (Appendix D.1).

A) B)

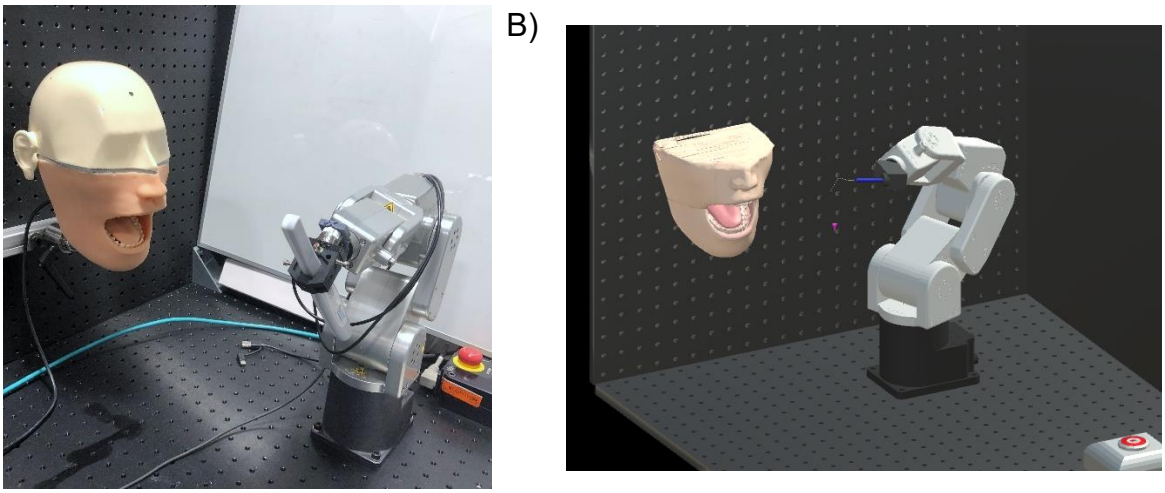

Figure 6.4. A) Physical setup with the silicone LA head model and Meca500 robot holding the intraoral camera on perpendicular optical breadboards. B) Unity virtual scene setup with the virtual periodontal probe with the coloured split head model, a sectioned tongue and intraoral arch model scans in Unity.

Mecademic provides the robot's properties which are described in a unified robotics description format (URDF) file [312]. The virtual robot model was imported into Unity using the *URDF Importer* package by Unity Technologies from GitHub (Figure 6.4B). The Meca500 robot was connected to the computer via an Ethernet cable and the computer's ethernet connection was configured to the robot's static IP address by manual assignment [308]. A Transmission Control Protocol (TCP) connection was established to connect directly with the robot by a TCP client re-written from python code to C# for Unity. Using the *GetJoints* command, the angle of the simulated robot joints produced by Mecademic's internal inverse kinematics solver was called each frame to update position of the simulated robot's joints and its end effector with the dental instrument.

To assess the percentage closeness to joint limits and robot singularities, four cost functions were designed for the Meca500 as potential robot system risk outputs. For the joint limits, this was measured as the difference of the joint angle to the midpoint ($\theta_{i,j,mid}$) divided by the joint range (Equation 6.1). Three cost functions measured the relevant joint angles and positions relative to the three types of joint singularity as a percentage (Equation 6.2, Equation 6.3, Equation 6.4), where the reach distance (d_{reach}) was 260 mm with additional inputs from the D-H parameters (Table 6.1).

Equation 6.1. $$f_{c,lim,j} = 100\left(1 - \frac{(\theta_{j,max} - \theta_{j,min}) - 2|\theta_j - \theta_{j,mid}|}{\theta_{j,max} - \theta_{j,min}}\right)$$

Equation 6.2. $$f_{c,shoulder} = 100\left(\frac{d_{reach} - \sqrt{a_2^2 + a_3^2}\cos\left(\theta_2 + \theta_3 + \tan^{-1}\left(\frac{a_3}{d_4}\right)\right) + a_2\sin(\theta_2)}{d_{reach}}\right)$$

Equation 6.3. $$f_{c,elbow} = 100\left(1 - \frac{d_{reach} - d_{5|2}}{d_{reach}}\right)$$

Equation 6.4. $$f_{c,wrist} = 100\left(1 - \frac{|\theta_5|}{\theta_{5,max}}\right), \quad where\ \theta_{j_5,max} = 115^{o}$$

6.3.1.2 Force-Torque Sensing Device

A force-torque sensor was connected to the robot end effector to measure the occurrence and impact of head model collisions. The Nano17-e force-torque sensor from ATI (9105-TW-Nano17-E, serial code FT22324, SI-12-0.12 calibration). This robot was considered suitable for dental applications as it has sensing ranges of at least ±12 N and ±120 Nmm in each axis (Figure 6.5A), a mass of 9.07 g and is small in size (17 mm diameter and 14.5 mm height) [313]. The sensor hardware was set up with a NI USB-6259 DAQ (194021D-01L) by National Instruments for analogue-to-digital conversion (Figure 6.5B). A differential connection for data acquisition (DAQ) was chosen to minimise effects of sensor drift. The colour-coded strain gauge sensor wires were connected to selected DAQ terminals (Figure 6.5C,D). From an ATI power supply (FTIFPS1), the sensor's input and ground (red cables) were connected to (+5 Volts, pin 96) and digital ground (D GND, pin 94), while its twisted shielding was connected to analogue input ground (AI GND, pin 30).

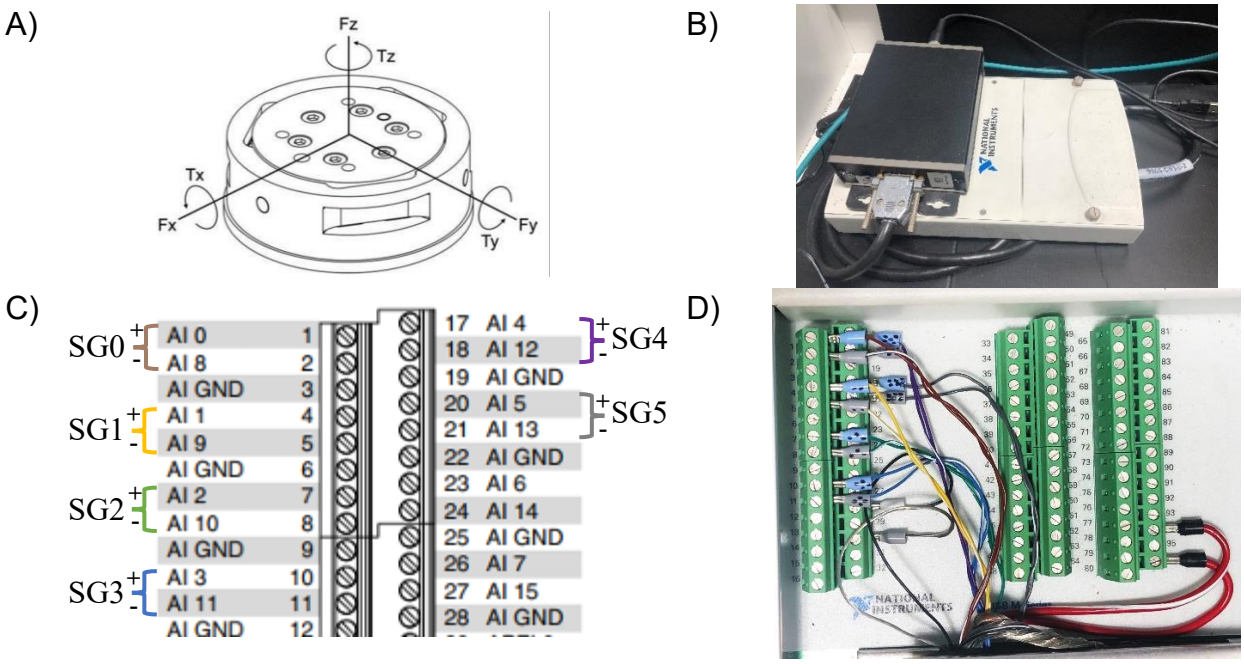

Figure 6.5. A) Nano17-e sensor force and torque axes and directions in x, y and z [314]. B) Sensor hardware with the power supply (black box) and NI USB-6259 DAQ (grey container). C) Negative and positive DAQ pin terminals for different coloured strain gauge (SG) wires to create a differential connection [315]. D) Force-torque sensor wires connected inside the DAQ.

Since Unity is a game engine, the development of a TCP server was restricted to connecting to the force-torque sensor directly. There is also limited support for National Instrument devices in C#. To overcome these challenges, a TCP server was built in Python which was designed to collect, transform, encode and stream data to a subscribed client in Unity. The *nidaqmx* package was imported in python to connect to the sensor analogue input channels. The raw data was transformed using the transformation matrix for the calibrated sensor. The transformed data were encoded by "utf-8" and sent to the Unity client.

6.3.1.3 Orientation Sensing Device

An Attitude Heading Reference System (AHRS) sensor, VectorNav VN100 (VN-100S-CR), was used to track movement of the head model during the dental application. The sensor was mounted below the jaw of the head model (Figure 6.6A,B). This sensor is accurate up to 2.0° in heading and 0.5° in pitch and roll with a resolution of 0.001° and range of ±2,000°/s [316]. The output data ranges from ±180° in heading and roll, and ±90° in pitch (Figure 6.6C). The head was positioned upright with the lock screw released to allow slight manual head rotations (Figure 6.6B). Orientation data was collected via USB using a serial port in Unity with a baud rate of 230400. The sensor heading (z-axis) captured side-to-side rotations of the head, while its pitch (y-axis) was oriented to capture depression and elevation of the mandible.

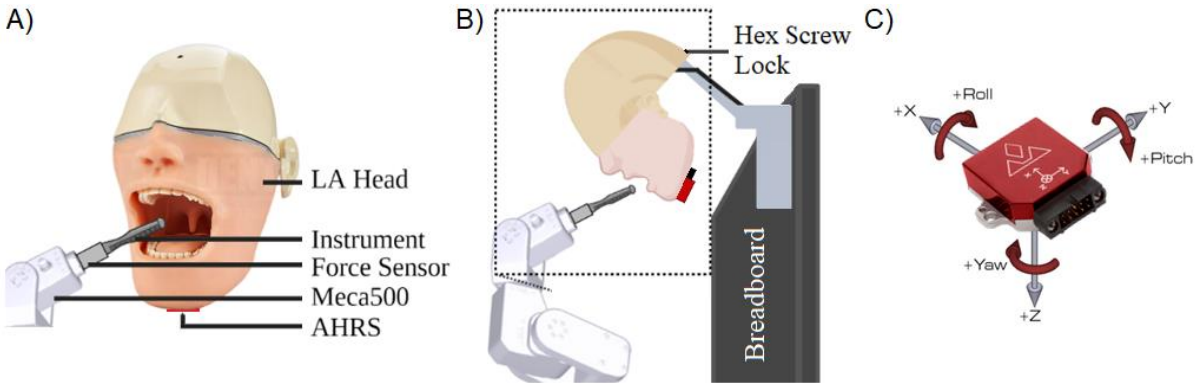

Figure 6.6. A) General setup for the OneDental LA head model with an orientation sensor. B) Setup with the AHRS sensor positioned under the jaw. C) Axes of rotation for roll (x-axis), pitch (y-axis), and heading or yaw (z-axis) [317].

6.3.2 Unity Measurements

The Unity visualisation system is set up using a series of "gameobjects" with internal scripting and rendering components. The models imported into the virtual environment are represented visually as 3D objects, while others can be created directly in Unity. A gameobject, named the "reference tip", was created to with three "child" gameobjects. The first child was designed transparent in appearance to indicate the distance travelled into the model along the on 3D pre-programmed planned paths. The second was opaque and used to identify the chosen location for the instrument tip during dental technique simulations for its planned action performed offset from the planned paths. The third had no visual 3D properties ("empty") and defines the offset position and orientation of the instrument's handle. To perform risk supervision of robotic dental procedures in simulation, the spatial risk measurement methods ID1.1–ID1.4 were recreated in Unity (Figure 6.3). Their outputs were used to define the Hazard State risk level of the system, which should be used to inform the acceptable robot mode of interaction during the procedure.

6.3.2.1 Procedure Block Risk Measurements

For ID1.1, occlusal markers representing the centre of a tooth's occlusal plane point were added to the top of each tooth and labelled according to the FDI numbering system (Figure 6.3A). These were added as child gameobjects of their respective dental arch so that they would follow movements of the tracked dental models. ID1.1 was calculated by finding the distance from the closest marker in each of its axes to the relevant instrument reference point (Figure 6.7A). The *InverseTransformPoint* function was used to convert the points position into the occlusal marker's axes. Since Unity uses a left-hand rule for axis frames, the y-axis for $z_{clearance}$ was manually aligned with the tooth's longitudinal axis and the z-axis for $x_{lingual}$ was pointed towards the centre of each arch (Figure 6.3A, Figure 6.7B).

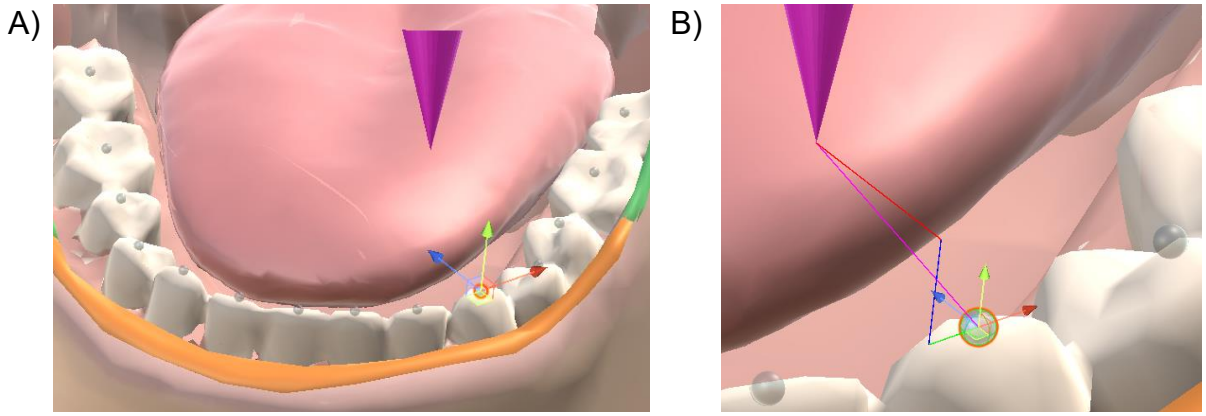

Figure 6.7. A) Occlusal markers positioned around the tops of the dental arch teeth with the oriented axes shown for Tooth 33 (x in red, y in green and blue in z). The reference tip's closest occlusal marker is selected. B) ID1.1 measurements from a tip reference point (the magenta cone object) depicted using DrawRay ordered and coloured to replicate the right-hand rule axes with red, green and blue DrawRay lines from MATLAB (x, y and z axis measurements).

For ID1.2, a frontal plane object was created with a Unity cube gameobject in the simulated environment with a thickness of 0.01 mm. The *LookRotation* function used the average y-axis and z-axis incisor teeth occlusal markers to reorient the frontal plane to the centre front of the mouth, and their average position was used to position the plane centrally at the front of the mouth entrance. The frontal plane was defined as a mask layer and had an inbuilt box collider to detect ray casts extending along the instrument's handle direction to assess its intersection with the frontal plane (Figure 6.8). Intersections with the box collider were found using the *RaycastAll* function with the selected layer. The *InverseTransformDirection* function was used to convert the frontal plane vector to the intersection point into the frontal plane axes for the x_{width} and z_{height} (red and blue lines in Figure 6.8, Figure 6.3B). The distance of the ray cast was used to measure the handle's perpendicular depth, y_{depth}, into the mouth from the frontal plane (a component of the green lines in Figure 6.8, Figure 6.3B).

A) B)

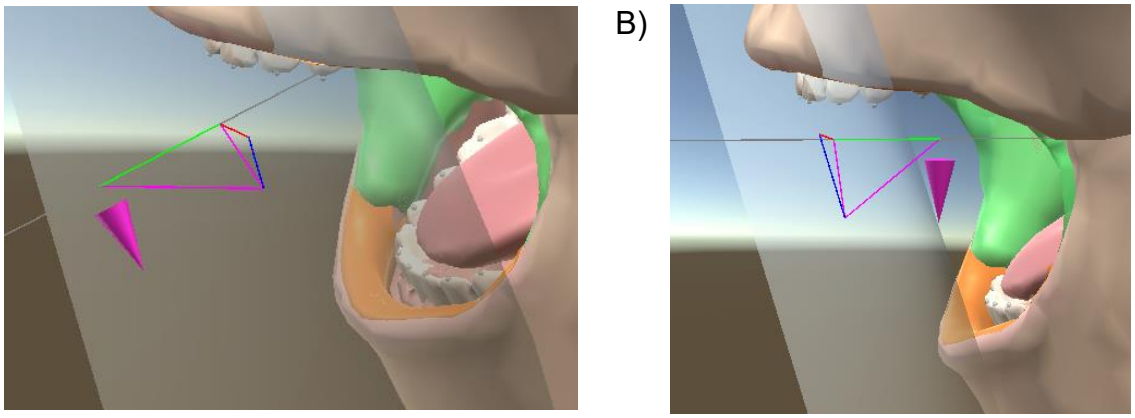

Figure 6.8. Frontal plane (grey surface) oriented to the front of the mouth opening with a tip reference point (the magenta cone object): A) oriented pointing upwards behind the frontal plane; and B) oriented pointing straight in front of the frontal plane. The grey DrawRay line presents an offset line in the direction of a handle for an instrument. ID1.2 measurements are represented by the red, green and blue DrawRay lines.

In Blender, the dental arches were sectioned into tooth and gingivae models. The objects for the hard and soft surface meshes were imported and attached to the halved head model sections in the 3D environment. These were grouped so that the maxilla teeth and gingivae, throat wall and maxilla lip only move with the maxilla head model. The other objects were added as children inside the mandible section, such as the tongue, to follow side-to-side movement of the head and have additional rotations with the movement of the mandible. This was considered appropriate for experimental testing for a tongue resting at the bottom of the mouth. However, future methods could rotate the tongue child object independently using this structure. The meshes were modified to enable “Read/Write” in Unity to gain access to the mesh vertices from script. The nearest vertex of each tissue surface and its normal vector were found to calculate the distances for ID1.3 and ID1.4 (Figure 6.9). The dot product between the reference point and the closest mesh vertex vector and the surface normal vector was used to confirm the position relative to the surface.

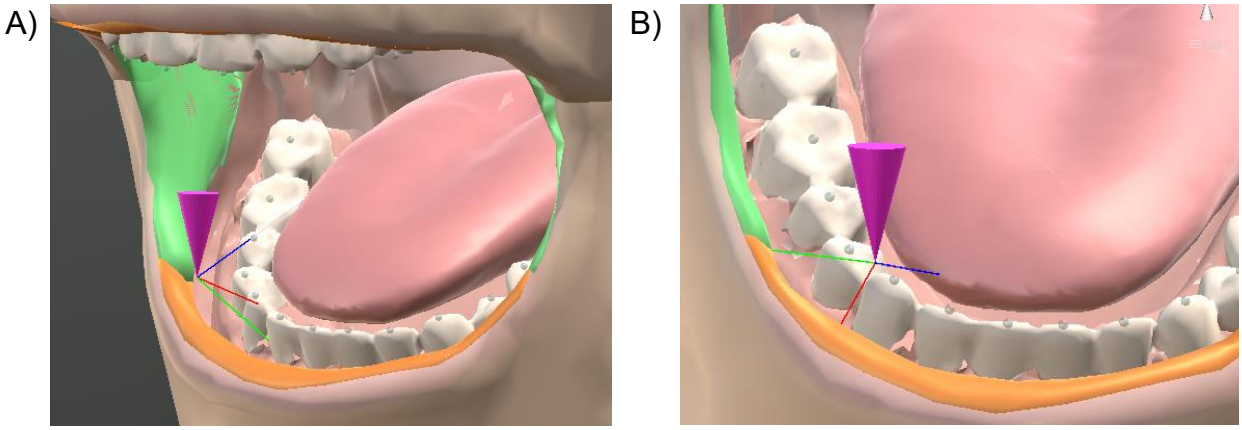

Figure 6.9. A) ID1.3 measurements where the DrawRay lines represent the closest tooth vertex (red line), the closest gingivae vertex (green line) and the closest throat wall vertex (blue line). B) ID1.4 measurements where the DrawRay lines represent the closest lip vertex (red line to orange surface), the closest cheek vertex (green line to green surface) and the tongue vertex (blue line).

6.3.2.2 Risk State Model for Risk Level Supervision

The risk controller was built with a Unity Animator component that operates as a State Machine. The tracked variables for the procedure block risk measurements were used as conditions to determine the probability of patient harm as recognised by three Hazard States. These were combined into a single value by taking the maximum of ID1.1–1.4 at a given time. The state machine replicates the simplified three-state Markovian Decision Process diagrams from Chapter 4 (Figure 4.6A), where outputs for the other supervision system, namely the observer and patient block (ID2–ID3), were included for completeness of the state transitions. Where the risk outputs are successful in estimating the safety of the system, these levels can be renamed as the Hazard State levels.

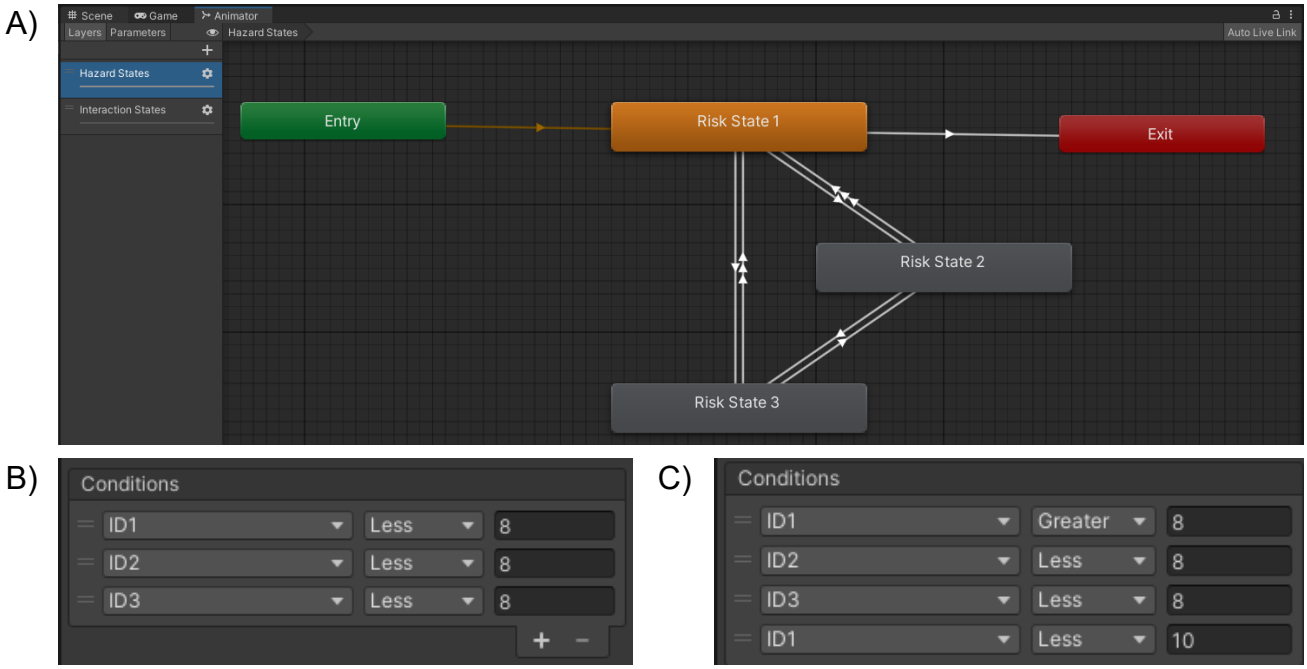

Figure 6.10. Unity Animator state machine for hazard states. A) MDP designed to output the supervision system hazard states with changes in measured risk. Supervision system sample transition conditions for: B) Hazard Risk State 1 to Hazard Risk State 3 with all interpreted data as "not high risk" (<8 in value). C) Hazard Risk State 1 to Hazard Risk State 2 with observer and patient interpreted data as "not high risk" (<8 in value) but high risk for procedure safety (8–10 in value).

The system was designed to begin at the unknown or unsafe risk level "Risk State 1" and transition to "Risk State 3" with known safe risk levels where the ID1 risk was required to be less than a value of 8 (Figure 6.10A,B). Risk State 2 was entered if the ID1 was greater than 8 (high) or less than 10 (Figure 6.10C). The system would return to Risk State 1 if the ID2 or ID3 were greater than 8 (high) or if ID1 is greater than 10 (Figure 6.10C).

6.3.3 Experimental Setup

6.3.3.1 Instrument Settings

For the robot end effector, the instrument tip position and orientation were set using the *SetTRF* command. The chosen 3D printed connector held the instruments at an offset rotation of 45° from the default tool reference frame at joint 6 (Appendix D.1). The TRF position was configured as (14.9,-36.1,89.7,45,-90,0) and confirmed using the Mecademic Web Interface, where the first three parameters were converted for the local position of the instrument tip on

the virtual end effector (eef_v) from the Unity workspace by $\left(x_{TRF} = -y_{eef_v}, y_{TRF} = -x_{eef_v}, z_{TRF} = z_{eef_v}\right)$.

6.3.3.2 Robot Control Settings

To react quickly to patient movement, the proportional acceleration and angular velocity limits were set to 25% for the *SetJointAcc* command and 15% for the *SetJointVel* and *SetCartAngVel* commands for joint and cartesian motion. The cartesian linear velocity was set to 105 mm/s by the *SetCartLinVel* command. The maximum speed was set to allow the robot to quickly retract the instrument out of the mouth to a distance of separation in one second. These values were calculated using the dimensions of the robot arm, the planned robot end effector design, the maximum permissible forces applied by collaborative robots around the face, and the Meca500 robot properties (Appendix D.2). The *MoveJoints*(0, -30, 35, -20, -5, -70) command was initially called to position the robot for the simulated techniques. This was used to avoid beginning at a wrist singularity at the zeroed joint position.

6.3.3.3 Technique Simulation Paths

In Unity, paths were manually programmed in 3D using the Bézier Path Creator package [318]. Each path curve was created with the Path Creator Script by positioning multiple waypoints in 3D where the shape of the curve between the points was smoothed using the directional control points and oriented by adjusting the roll angle of each waypoint (Figure 6.11A). Three dental paths were designed in Quadrant 4 and tailored to have a straight lower risk path over the occlusal surface (Figure 6.11B), a higher risk path going to the back of the mouth near the cheek (Figure 6.11C), or follow the side profile of the teeth while angled towards the side of the tooth (Figure 6.11D).

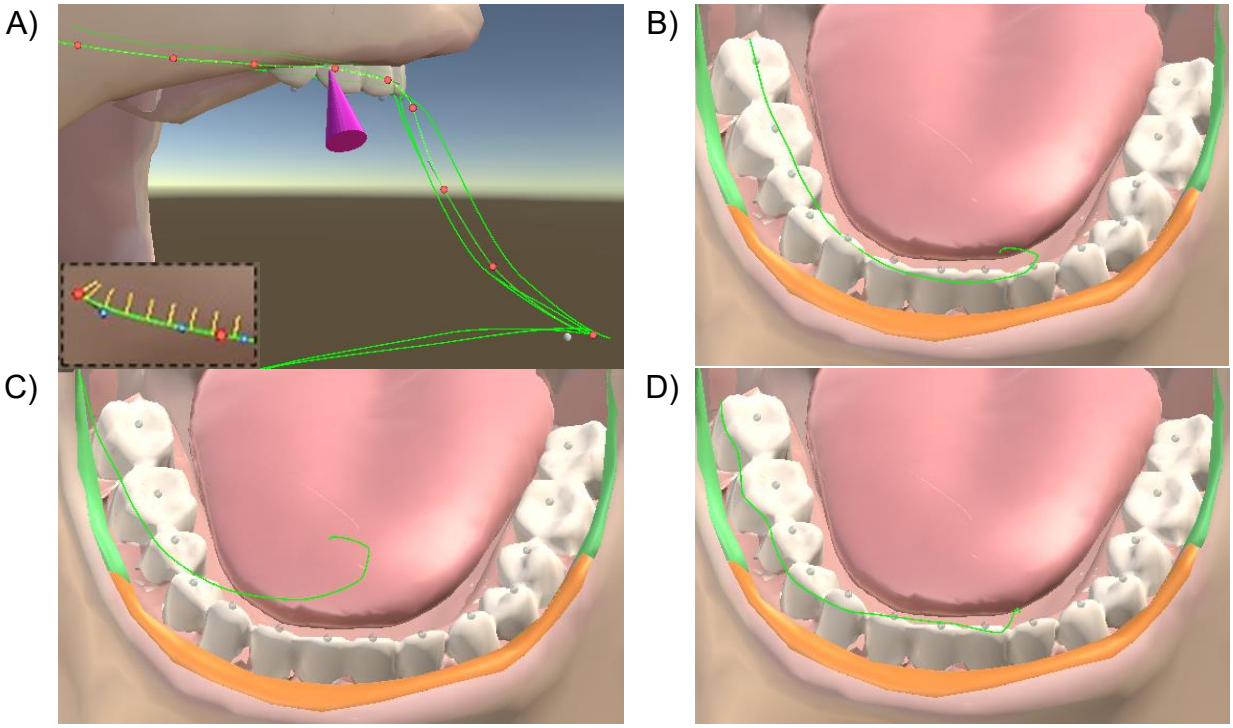

Figure 6.11. A) Diagram of path (green) followed by the reference tip (in magenta) in "run" mode made manually with ten waypoints (red dots), direction control points (blue), and roll angle pointers (yellow). Front view of dental 3D paths created in Quadrant 4: B) a straight lower risk path over the occlusal surface; C) a higher risk path going to the back of the mouth near the cheek; and D) a path matching the side profile of the teeth while angled towards the side of the tooth.

A Path Follower Script was added to the reference tip gameobject such that it would follow the curve with a set speed when the virtual simulation was run with its forward direction (z-axis) pointing in the direction of travel (Figure 6.11A). The paths were set to "Reverse" so that the reference tip will enter and exit along the same path. The distance travelled was reset once the path returned to the start position (waypoint 1) at two times the length of the path. The reference tip position could be reset to the start by setting the distance travelled to zero.

6.3.3.4 Reference Tip Position and Rotation

The global position and orientation of the reference tip's opaque child gameobject (*ref*) was sent to the Meca500 robot to be followed using the *MoveLin* command for Mecademic's internal inverse kinematics solver [308]. For this command, the reference transform was converted from Unity's left-hand rule to the robot world reference frame (WRF) (Equation 6.5,

Equation 6.6). Unity Euler angles sent to the robot were shifted to between -180° and 180° and limited to ±15° in each axis from reference tip's starting rotation to minimise the impacts of sharp turns in the paths preventing end effector movement. The *MoveLin* command was called each frame to update the position of the end effector (*eef*) to match the position of the reference location. Dental environment testing with the orientation sensor and robotic setup testing were performed to confirm that the data sent to the robot correctly informed the reference position and rotation for varying positions of the head model (Appendix E.1).

Equation 6.5. $$\boldsymbol{p}_{eef} = \left(p_{ref}(z), -p_{ref}(x), p_{ref}(y)\right)$$

Equation 6.6. $$\boldsymbol{r}_{eef} = \left(r_{ref}(z), -r_{ref}(x), r_{ref}(y)\right)$$

6.3.3.5 Experimental Test Cases

Test cases were chosen to use available dental instruments for simulated robotic dental application (Table 6.2). The technique simulations used 3D paths created in Quadrant 4 of the mouth (lower right quadrant). These included intraoral imaging (or scanning) with a ProDENT intraoral camera (PF740), sonic brushing by the head of a Colgate sonic toothbrush (Pro Clinical 250R), and charting (or dental exploring) using a Single Use periodontal probe (S2006). The ProDENT intraoral camera was designed to follow the paths at an offset distance ~10 mm. The position of the reference tip child gameobject (in opaque) were modified for the sonic toothbrush and periodontal probe paths to simulate their technique motions. The sonic toothbrush was supplied with 2.3 V, drawing a current of 0.26 A from a POWERTECH DC regulated power supply (MP-3840). The head model can move in response to the motion of the instrument (passive mode), or it can be moved manually (active mode). Each path, defined as lower or higher risk, was planned to be repeated five times while collecting data of spatial risk measurements and object transforms from Unity, the robot for joint feedback, angular rotations of the head and jaw from the AHRS, and force data from the force-torque sensor.

Table 6.2. Test setup to assess procedure block risk measurements using pre-programmed planned paths that simulate dental techniques. Simulated active model movement is applied manually, and rotations are sent to the simulation.

Test Case (Index)	Simulated Technique Path	Dental Instrument	Simulated Model Movement	Path Risk Level
T1	Intraoral imaging and scanning	ProDENT intraoral camera	Only passive head and jaw movement	Lower Risk
T2			Only passive head and jaw movement	Higher Risk
T3			Active head movement	Lower Risk
T4			Active jaw movement	Lower Risk
T5	Sonic brushing	Sonic toothbrush head (turned on)	Only passive jaw movement	Lower Risk (ProDENT path with circular oscillations)
T6	Charting and probing	Periodontal probe	Only passive jaw movement	Lower Risk Modified Path (occlusal/buccal-side tooth exploration with vertical instrument motion)

6.3.3.6 Speed and Motion Simulation

The reasonable path speed for the dental instruments around the model was considered as 5 mm/s along the 3D paths. As mentioned, the intraoral imaging path followed the designed paths at an offset distance with the reference tip (*tip*) and its child gameobject (*ref*) remaining in the same location throughout the simulated technique. In contrast, the periodontal probing simulation used Unity's *Raycast* feature to detect the reference tip's distance from the virtual tooth model and shift the child reference position to the "hit point" surface of the virtual tooth. Moreover, a circular motion for sonic brushing was created by using a set angular velocity (ω) of 10° per game frame count (n_f) with an amplitude (A) of 5 mm and the reference object's right and forward unit direction vectors ($\boldsymbol{u}_x$, $\boldsymbol{u}_z$) (Equation 6.7). While active technique motions were performed for the sonic toothbrush or periodontal instrument, their path velocities were halved to 2.5 mm/s.

Equation 6.7. $$\boldsymbol{p}_{ref|tip} = \boldsymbol{p}_{tip} + \boldsymbol{u}_{x|ref}\frac{A}{2}\sin(\omega \cdot n_f) + \boldsymbol{u}_{z|ref}\frac{A}{2}(\cos(\omega \cdot n_f) - 1)$$

6.3.3.7 Periodontal Probe Localisation Method

To ensure sufficient accuracy of periodontal probing, the thin periodontal probe reference point was manually dragged in the virtual environment to a selected mandible dental arch feature of the front teeth on the head model. The position of the head was then adjusted in the virtual environment to match the physical model. Three other locations were used to confirm the relative position of the physical head model (Appendix E.1, Figure E.4). This head model position was used for test case T6.

6.3.3.8 Data Capture and Analysis Methods

The Python server was activated for the connection to the force-torque sensor and the orientation sensor was connected by USB prior to running the simulation in Unity. Once the robot was connected, its position was reset using *MoveJoints* and the position of the reference

tip was provided to position the end effector connection in front of the model head. Once in position, the respective dental instrument was attached. The simulated technique was then activated, and the data was set to record in Unity.

The sequence of code in the simulation passes the reference pose as an input from Unity that defines the robot's target pose (Figure 6.12). The spatial risk measurements are measured and tracked in Unity for the updated instrument tip pose based on virtual environment where the head position is updated by tracking feedback data from the orientation sensor and the robot's end effector is positioned by rotating the relevant joints by their output angles. Finally, the Unity virtual environment receives data on the forces and moments from Python to be recorded at the same time points. The virtual and physical dental environments for the test cases are presented in Appendix E.2. A Unity *streamwriter* was used to export data as text files from the robot, sensors and simulated scene for analysis in Python.

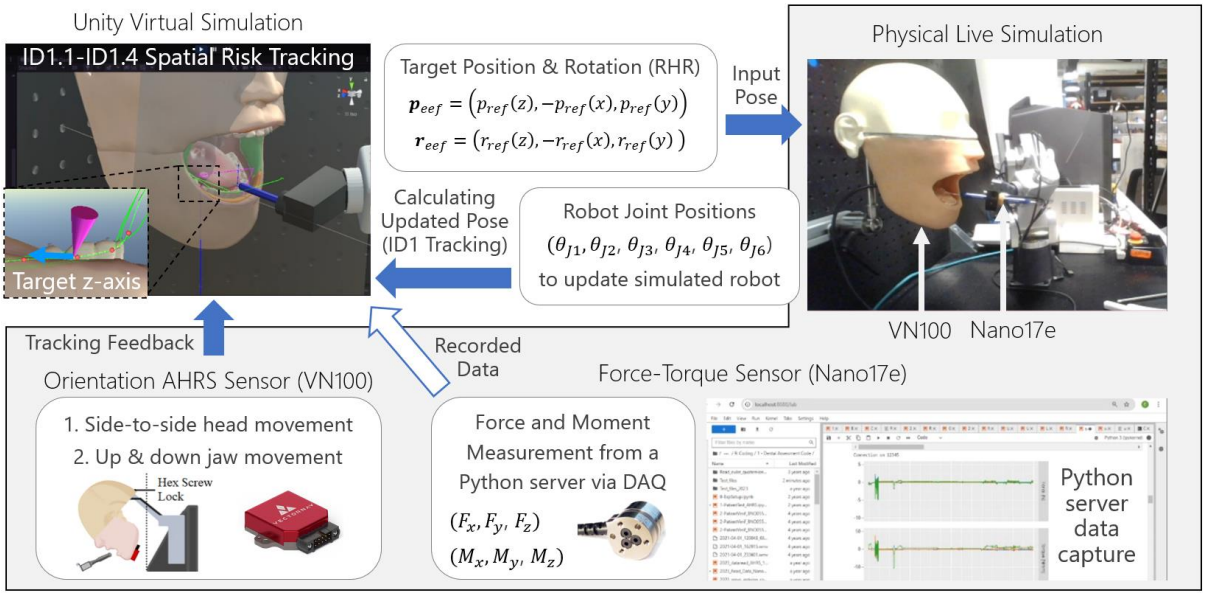

Figure 6.12. Hardware-in-the-loop used for the simulation with pseudocode to show the sequence of the code executed from Unity, along with those returned from the robot and the orientation and force sensors.

Dental robotic forces on the instrument were considered low for 0–0.5 N (yellow), medium for 0.5–2 N (orange), high 2–3 N (pink) and unacceptable for >3 N (white) for the defined risk levels with their corresponding ID output and raw ID variable inputs (Table 6.3).

To manage a risk averse dental robot, the medium accepted reported forces aim to encompass the expected forces for manual charting, brushing and ultrasonic scaling from up to under 2 N [319-324]. Forces over 2 N were considered high risk, although these can occur during dental techniques [324-326]. Additional steps were taken to mitigate the occurrence of false positives. For ID1.1 measurements while away from the teeth, the x-values were ignored ($d_{1.1z} < -8$) to minimise effects from the angled jaw opening and y-values were scaled down by 1/5 ($d_{1.1z} < -10$) given that the approximate distance between tooth occlusal points is 10 mm.

Table 6.3. Colour-coded risk levels for the risk output ranges and total force ranges with equivalent raw spatial interpreted data inputs (Table 5.1).

Detected Risk Level	**ID Output Risk Range**	**Raw ID Variable Input Distance Ranges (mm)**						**Total Force (N)**
		ID1.1	*ID1.2**		*ID1.3**		*ID1.4*	
			x, z	*y*	*x, y*	*z*		
Low	<0	<0	<20;	<30	>5;	>10	>5	<0.5
Acceptable	0 – 8	0 – 8	20 – 36;	30 – 60	-3 – 5;	2 – 10	-3 – 5	0.5 – 2
High	8 – 10	8 – 10	36 – 40;	60 – 70	-5 – -3;	0 – 2	-5 – -3	2 – 3
Unacceptable	>10	>10	>40;	>70	<-5;	<0	<-5	>3

Key: ID = Interpreted Data; *Raw data conversion varies depending on axis

The approximate intervals of each cycle were estimated, and time series data analysis was undertaken to align and combine the repeated paths from the simulated dental techniques. To maintain the shape of the data, Dynamic Time Warping (DTW) was incorporated to get an approximated shape of the reference tip position data while managing the time shifts between repeated path cycles. This was achieved using the Soft-DTW weighted barycenters that minimises the sum of squared distances to the time series of a data set [327]. To align the original cycle data of the repeats, an iterative Pearson coefficient calculation was performed to shift the data into alignment. Based on the changing Pearson coefficient, the relative positions of the curves were shifted by adding and removing data points to the start or end, to maintain the length of the dataset. The number of indices, and the direction, used to shift the data were recorded for each test case cycle. All data variable cycles for that test case were aligned using

the shifted indices count determined using the reference position data. Finally, to minimise the loss of high peaks present in the data, the maximum range was used to combine the aligned cycle data and produce the highest ranged curve output as a single maximum cycle.

6.4 Results

6.4.1 Tracked Path Position

The six instrument reference paths were plotted in 3D space (Figure 6.13). The difference in the position in the lower and higher risk straight ProDENT intraoral camera paths can be observed with the higher risk being pushed back towards the throat (Figure 6.13A). The low risk camera paths that were altered by active movement show the result of the side-to-side head rotation or and elevations of the mandible jaw (on mouth entry and exit) during a single cycle (Figure 6.13B). The sonic brushing reference path copied that of the camera instrument, with the additional circulating movement of the reference object as it moved along the occlusal surfaces of the teeth inside the mouth (Figure 6.13C). Finally, the periodontal probe instrument path, which was modified to pass around the buccal side of the dental arch, displays a charting-like action produced by the Unity *Raycast* virtual surface detection method (Figure 6.13D). The data produced in this chapter for T1-T6 has been colour coded to match the colours of paths shown in Figure 6.13.

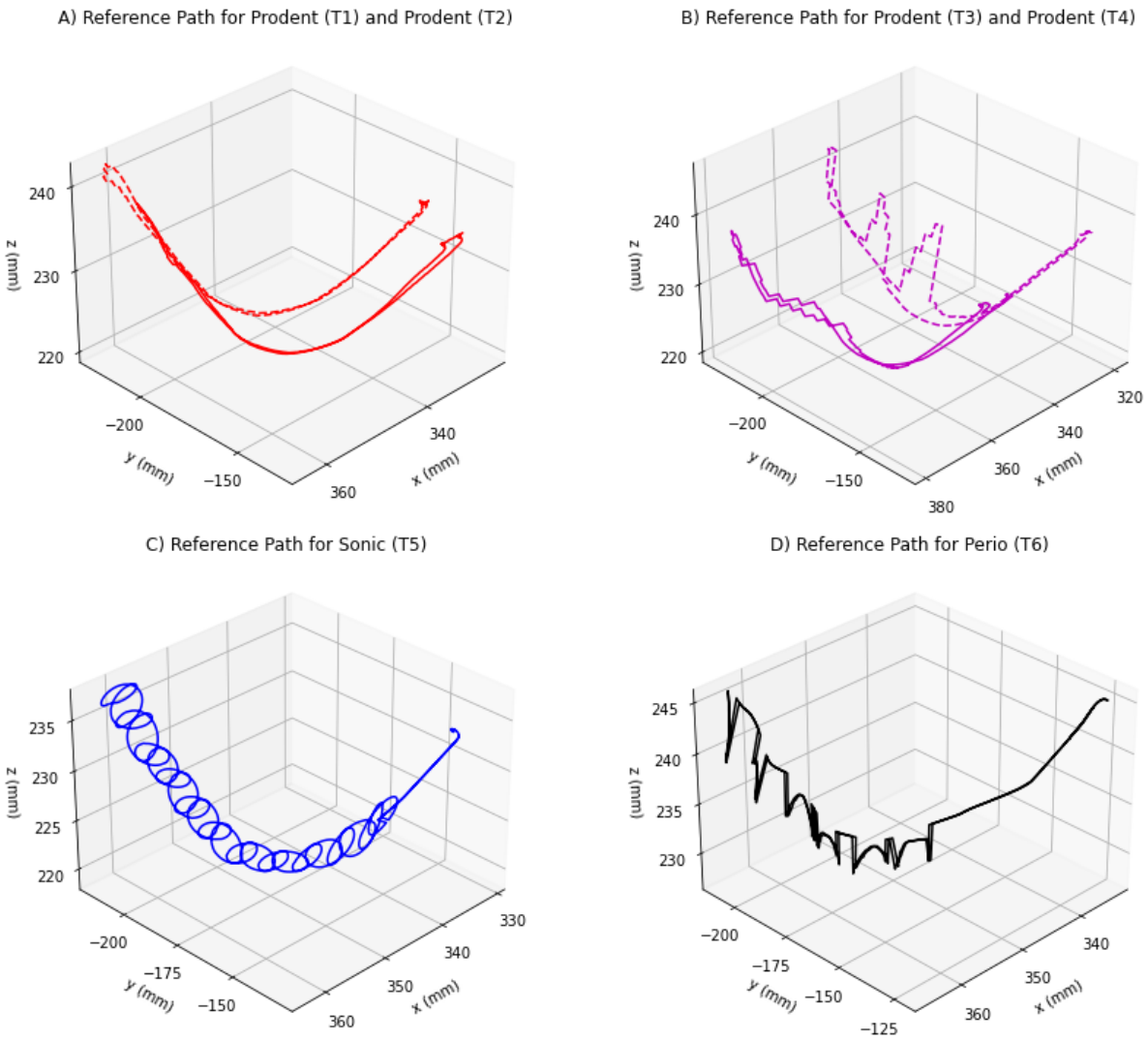

Figure 6.13. Instrument tip reference paths showing the 2nd cycle of motion in 3D space: A) Lower risk (-) and higher risk (--) straight paths for T1 and T2, respectively; B) Actively modified lower risk straight ProDENT camera paths with side-to-side head rotation (-, T3) and jaw rotation (--, T4); C) Sonic toothbrush lower risk path for T5; and D) Periodontal probe path for T6.

The instrument tip' position for each path is presented (Figure 6.14), which was captured in Unity by rotating the virtual robot joints in simulation based on feedback from the robot using *GetJoints*. This displacement between the position of the reference object and the instrument was usually between less than 10 mm (Figure 6.15). On average, the robot was able to follow the general position of the reference paths (Figure 6.13). However, the path data appear to experience spatial aliasing and latency due to under sampling of the trajectory, or lost

data points from communications of joint feedback. This is particularly obvious for the motions of the instrument for the sonic brushing and periodontal probing (Figure 6.14C,D).

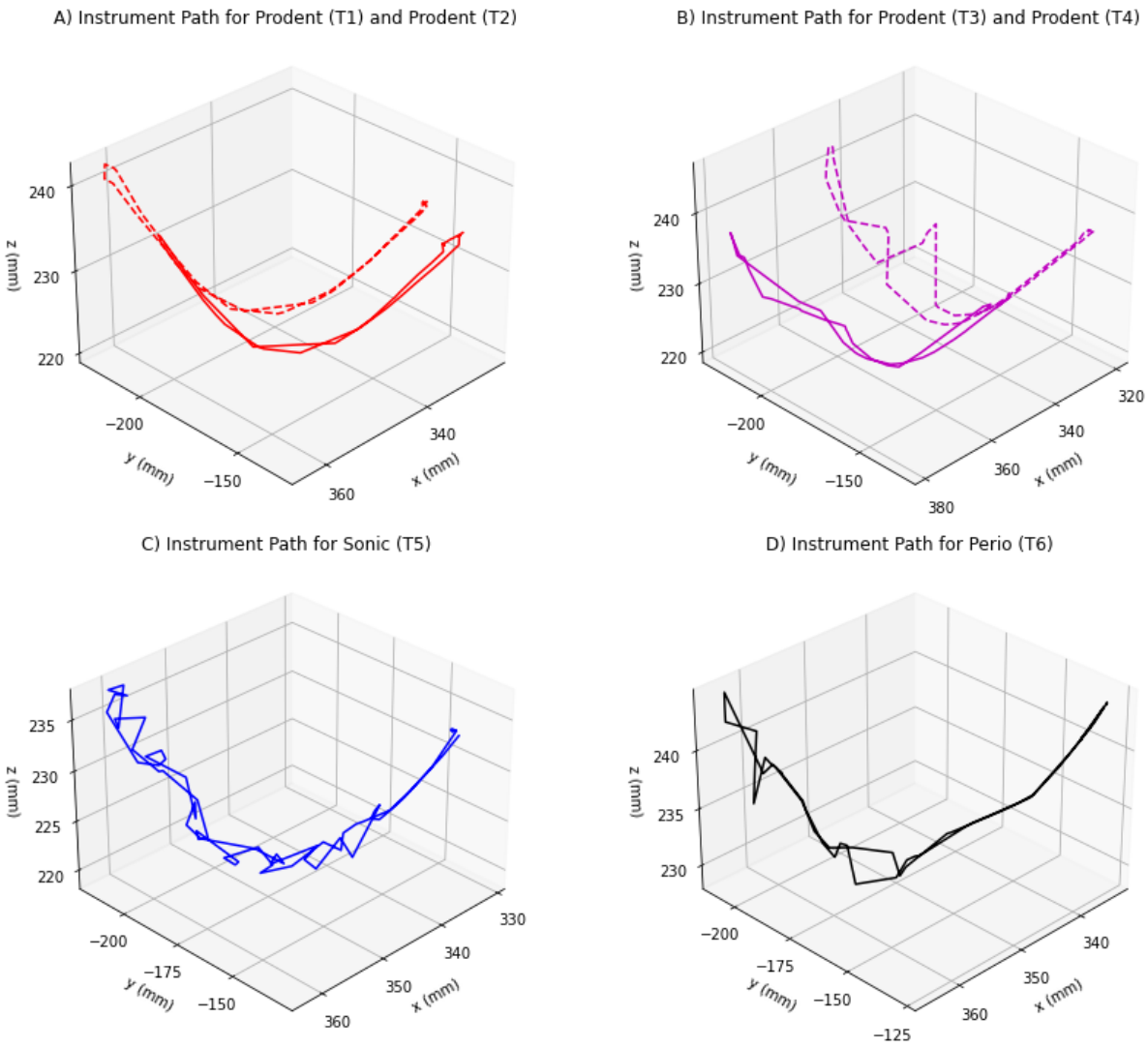

Figure 6.14. Instrument tip paths performed with the robot showing the 2nd cycle for motion in 3D space: A) Lower risk (-) and higher risk (--) straight paths for T1 and T2, respectively; B) Actively modified lower risk straight ProDENT camera paths with side-to-side head rotation (-, T3) and jaw rotation (--, T4); C) Sonic toothbrush lower risk path for T5; and D) Periodontal probe path for T6.

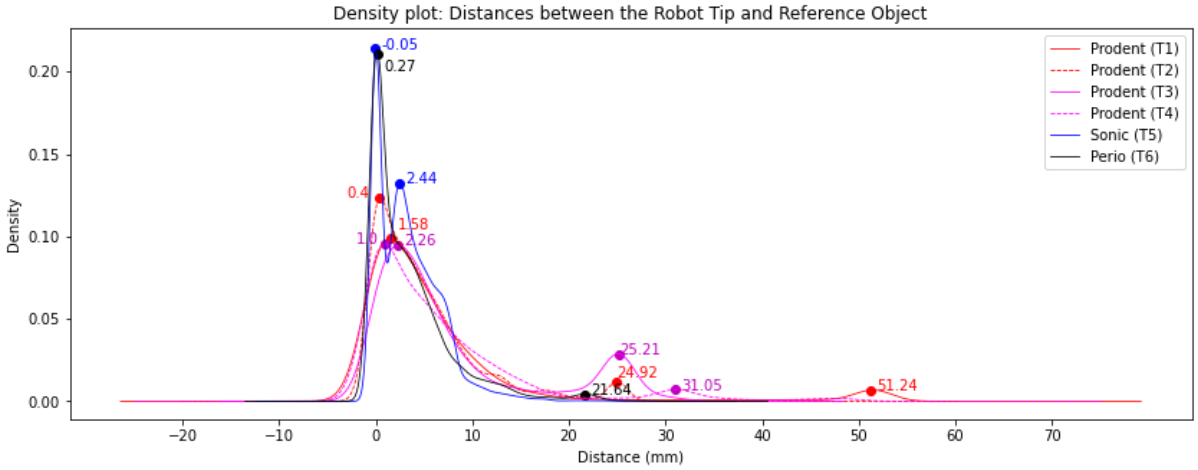

Figure 6.15. Density plot of the distances between the instrument tip and the reference tip point for each test case.

6.4.2 Robot Joint Assessments

The joint angles for robotic techniques show movement away from its joint limits during a cycle, except for Joint 3. Joint 1 uses 14% of its large range in motion, while Joint 2 uses 38% of its smaller range of motion. Joint 3 approaches 85% of its joint angle limit during a cycle, using 49% of its maximum range of -135°–70°, shown by the trend towards the darker zones in the chart (Figure 6.16C). Joint 5 initially started very close to its joint limit of -115° at a minimum of -99.23° and only rotated to a maximum of -49.00° (T2, Figure 6.16E). Similar to the joint limits, the closeness to each of the robot joint singularities was assessed. During each cycle, the proximity to the shoulder and wrist singularities began low and increased to 50–60% (Figure 6.16G,I). However, the robot started very close to the elbow singularity at approximately 95%, but this decreased during motion into the mouth to 40–70% (Figure 6.16H). Also, it can be seen that the elbow singularity directly opposed the other Meca500 robot singularities as the robot's end effector position moved toward and away from its maximum reach.

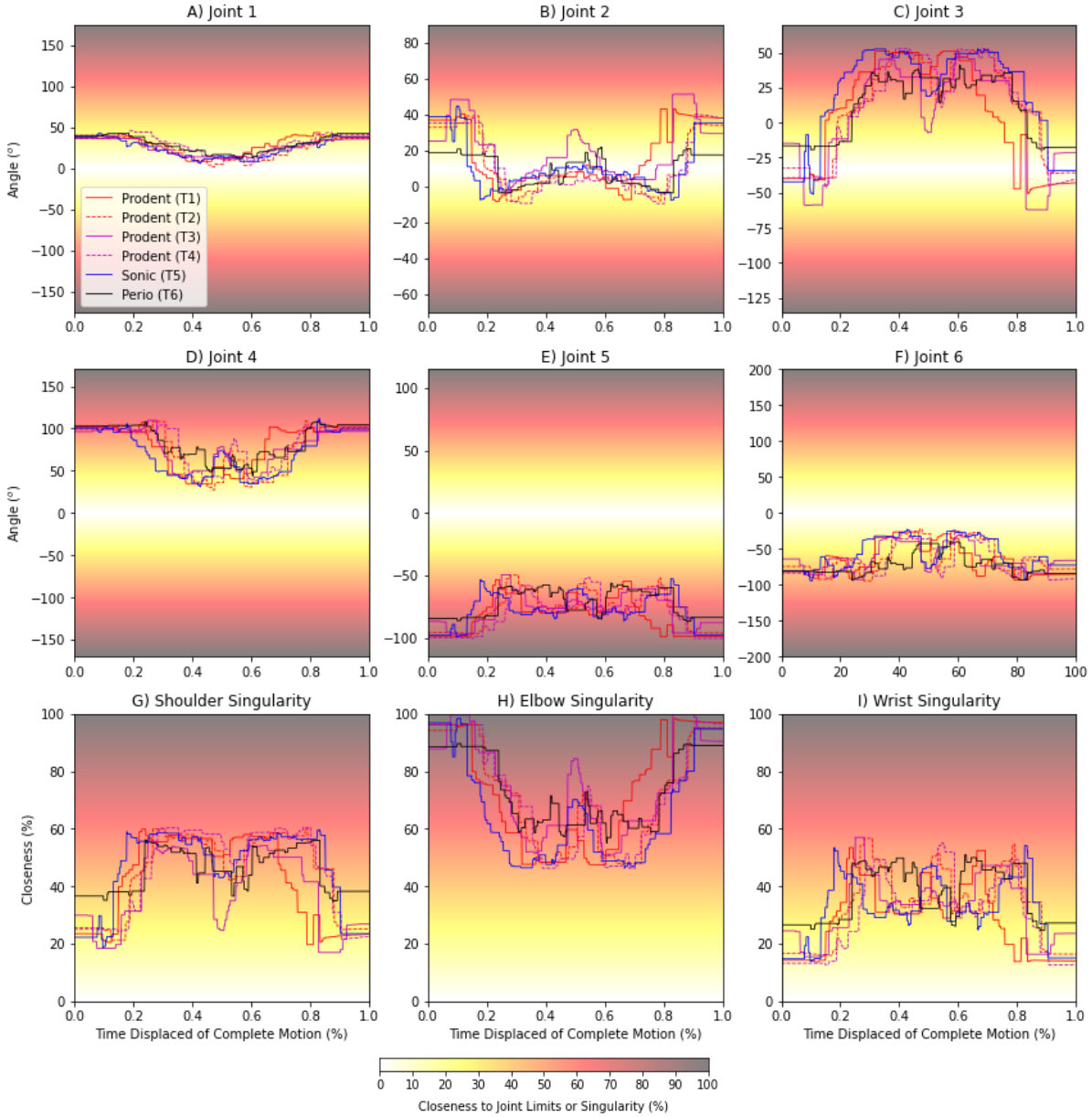

Figure 6.16. Robot joint angles over time for paths with five cycles for the Meca500 6-degree-of-freedom robot arm: A) Joint 1; B) Joint 2; C) Joint 3; D) Joint 4; E) Joint 5; and F) Joint 6. Closeness to joint limits is shown by a colour gradient in the background where 0% is at the midpoint between joint limits (white) and 100% is the joint limit (dark red).

6.4.3 Time Series Data Analysis

Analysis of the instrument path cycles was carried out using an iterative approach using the Pearson Coefficient and the mean cycle path output from the soft DTW for the reference tip's x-axis position data in space. The mean DTW curve was plotted against each cycle curve to show the unaligned overlapping time series data (Figure 6.17A). The DTW method was able to successfully extract the location of the mean path independent of time, however, it could not

accurately replicate the shape of the data. By shifting the indices of the position data, the data was aligned with the mean DTW curve and each other (Figure 6.17B). The direction and number of indices shifted was used to align the other datasets for the relevant test case.

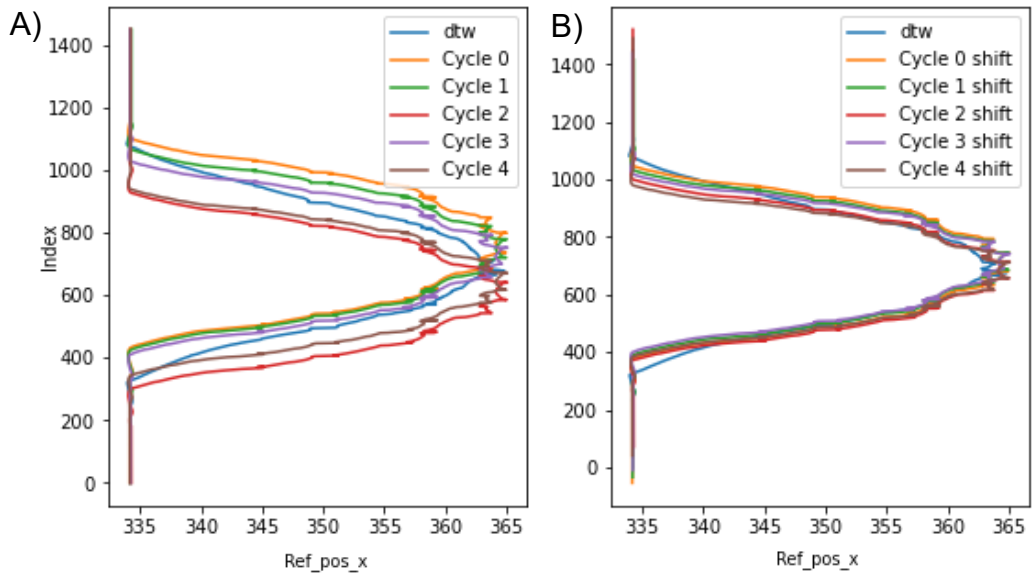

Figure 6.17. Time series analysis process with x-axis reference tip position data of the periodontal test case (T6), as performed for each test case: A) Unaligned cycle paths with the Dynamic Time Warping (DTW) mean curve output; B) Alignment of cycle paths to DTW mean curve with Pearson Coefficient maximisation with a tracked number of indices required to shift each array.

Sample outputs for the resulting alignments of the total force output data are presented for cycles of the periodontal probe test case, T6 (Figure 6.18). In some cases, the five repeats were not completed which were mostly attributed to poor localisation, such as the apparent drift in sensor heading. There were three good cycles for active head rotation and four cycles for active jaw rotation. A low pass filter with a cutoff frequency of 0.2 Hz was used to smooth high frequency data for the sonic toothbrush. To compare progress of the different procedures, the time data for each of the maximum output cycles were scaled to match the test case that was performed the earliest (T4) (Figure 6.19).

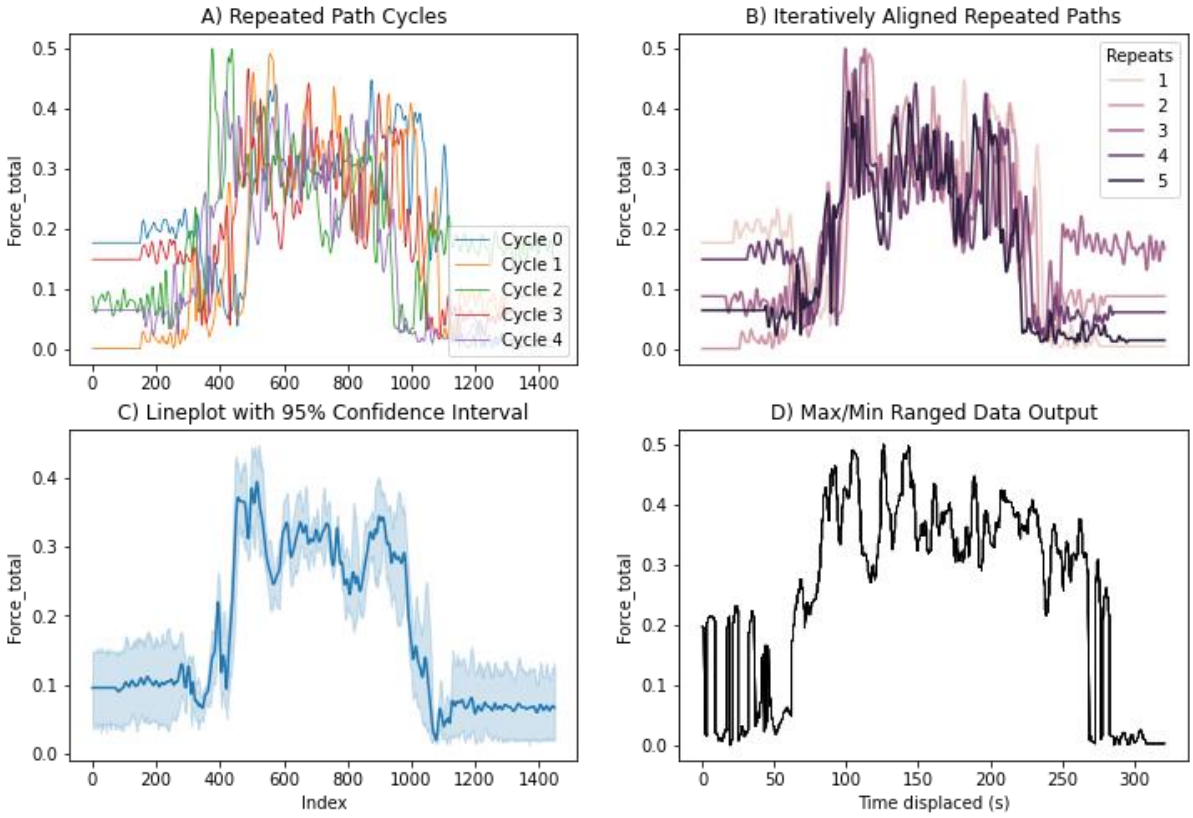

Figure 6.18. Time series data analysis for cycle curve outputs of the periodontal probe data test case (T6): A) Unaligned cycle path force data; B) Aligned using the output number of indices to shift from alignment of reference tip x-axis position data; C) Seaborn lineplot of force data (95% Confidence Interval). D) Maximum range of data kept for the highest ranged curve output of aligned cycle path data (relative to a selected starting value).

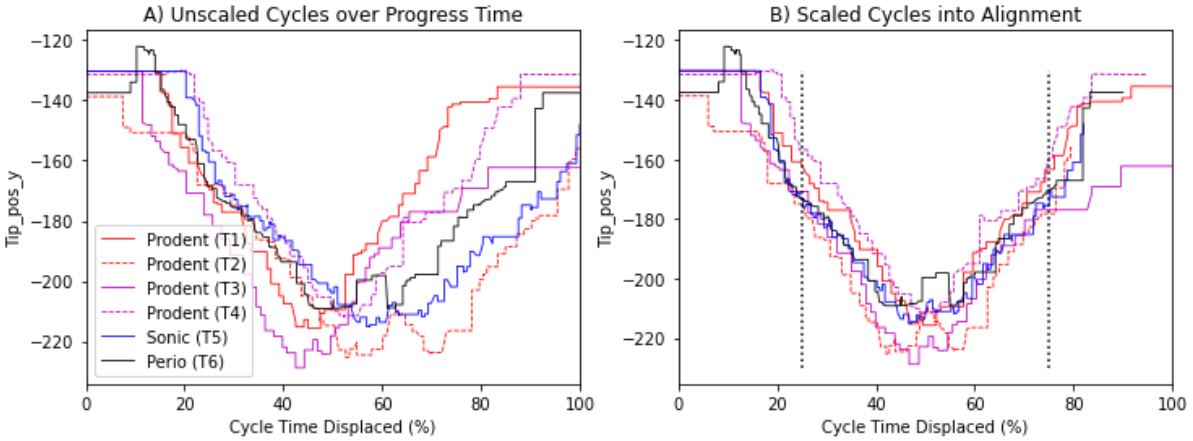

Figure 6.19. Maximum range cycle outputs compared and scaled into alignment with ProDENT test case T4. A) Unaligned cycle paths across the test cases shown with the y-axis instrument tip position data. B) Manually aligned cycles with dashed black lines represent 25% and 75% of cycle time displaced for reference.

6.4.4 Passive and Active Model Movement

The rotations of the head model and its mandible jaw were recorded and used to update the position of the models in Unity. The maximum range rotations of the cycles were combined from time series data analysis for each test case (Figure 6.20). The lower risk ProDENT test case (T1) experienced three peaks in angular rotation at 33%, 50% and 74% (1.97°) as a result of the force applied on the head model by the instrument (Figure 6.20A). Downward pressure applied by the intraoral camera on the dental arch caused slight corresponding jaw depression rotations with peaks at 33%, 48–54% (-0.27°) and 72% (Figure 6.20B). By comparison, the higher risk path test case (T2) experienced lower mean head rotation of 0.69° (reduced by 0.29°) with lower peaks at 26–37%, 49% (1.26°) and 66%, and a high sudden additional peak at 2.41° (44–45%) (Figure 6.20A). The highest jaw rotation was 0.46° (42–44%), with small peaks at 22% and 55–57% (Figure 6.20B). The more flexible periodontal instrument (T6) had caused minimal change in the position of the jaw (Figure 6.20B).

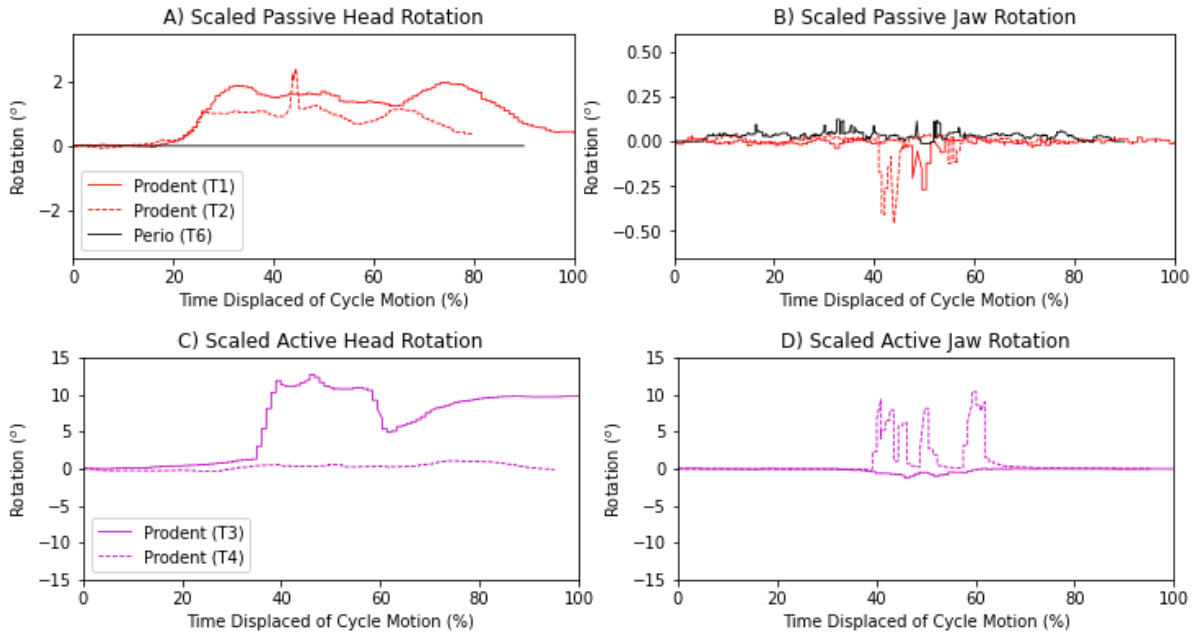

Figure 6.20. Scaled time series analysis output for model rotation feedback measured by the orientation sensor (re-zeroed at the beginning of the cycle). Passive movement test cases: A) Head rotation; and B) Jaw rotation. Active and passive movement test cases: C) Head rotation; and D) Jaw rotation. No orientation data was collected for the sonic instrument test case (T5).

An active head rotation of 11.38° was maintained from 39–56% of the procedure in the ProDENT test case T3 (Figure 6.20C). A passive head rotation is expected to have caused the additional peak at 47% (12.67°) from pressure applied by the instrument. Following the active rotation, the angle of the recorded head rotation returned to a difference of 5.35° (61%) before increasing back to 9.76° (87%) (Figure 6.20C). This may have resulted from errors in calculations or drift from the sensor. The tracked AHRS heading data results over time is presented in Appendix E.3. For this reason, all orientation data excluded for passive sonic brushing and jaw rotations were re-included for the periodontal probing. The ProDENT test case T4 experienced a maximum upward jaw rotations of 10.38° with four peak regions at 41–43%, 45%, 51% and 60–62% (Figure 6.20D).

6.4.5 Force Measurements

The total forces on the instrument for each test case are displayed by their maximum range cycles (Figure 6.21). Without smoothing, the maximum forces measured with the ProDENT instrument were 2.19–2.31 N (T1, peak at 3.19 N in last cycle, 48–50%), 4.77 N (T2, 42–44% and 55%) and 4.75 N (T3, 47–50% and 55%) (Figure 6.21A-C). The head rotation test case had an additional small peak at 1.62 N (T3, 58–62%) (Figure 6.21C). The highest forces occurred when there was active jaw rotation (T4), which had a high peak maximum force of 31.80 N (49–52%) with other peaks at 29% and 40% (Figure 6.21D). The high force resulted from an additional collision between the head model and the end effector holder (or the top of the instrument) with the head model maxillary arch or lip (Appendix E.3). Excluding the sudden high force contacts, the camera forces ranged from 0.5–1 N (Figure 6.21A-E). Furthermore, sonic toothbrushing had a maximum force of 1.87 N (49–52%), increasing from 0.93 N at 33% and reducing to 1.45 N at 58% (Figure 6.21E), and the total forces remained at low ranges between 0.2–0.55 N for the periodontal probe (Figure 6.21F).

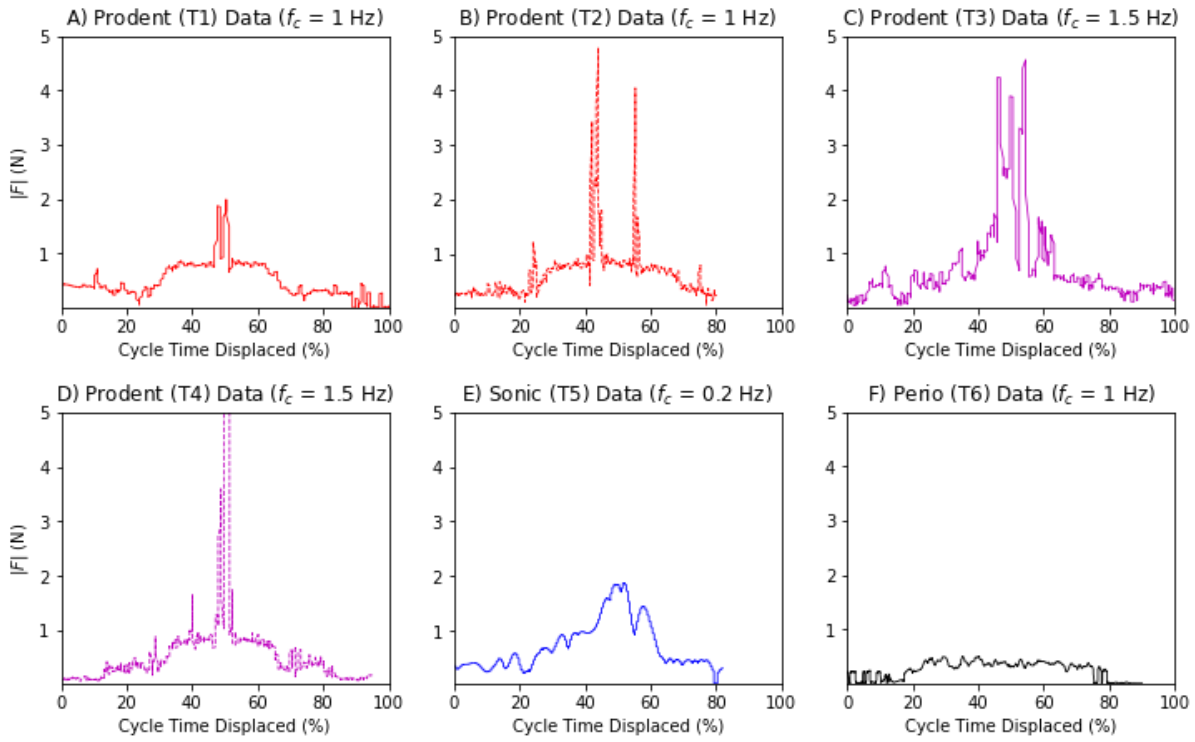

Figure 6.21. Scaled time series analysis output for total force (N) over a single path cycle. ProDENT test cases: A) Lower risk path and passive model (T1); B) Higher risk path and passive model (T2); C) Lower risk path and active head model (T3); and D) Lower risk path and active jaw model (T4). E) Sonic test case with a lower risk path and passive jaw model (T5); F) Lower risk periodontal probe instrument with passive jaw model (T6). Cutoff frequencies (f_c) used to smooth the force data are indicated.

Boxplots are presented to compare the acting component forces during the middle half of each path cycle (Figure 6.22). The forces were largely influenced by the measurements in the z-axis which represent the horizontal forces acting on the side of the instrument (Figure 6.22D). The higher risk path (T2) had higher median forces acting on the instrument compared to the lower risk path (T1) in the vertical and horizontal directions. However, the median force in the x-component was lower with outliers appearing at 3–3.5-fold higher, indicating a sudden change in force along the instrument's handle (Figure 6.22B). The active side-to-side head movement (T3) and jaw rotation (T4) produced similar median force outputs in all components to the lower risk path (T1) with maximum outlier at a similar or higher value than the higher risk path (T2). The sonic test case (T5) and the periodontal test case (T6) experienced a more even distribution of forces without outliers (Figure 6.22).

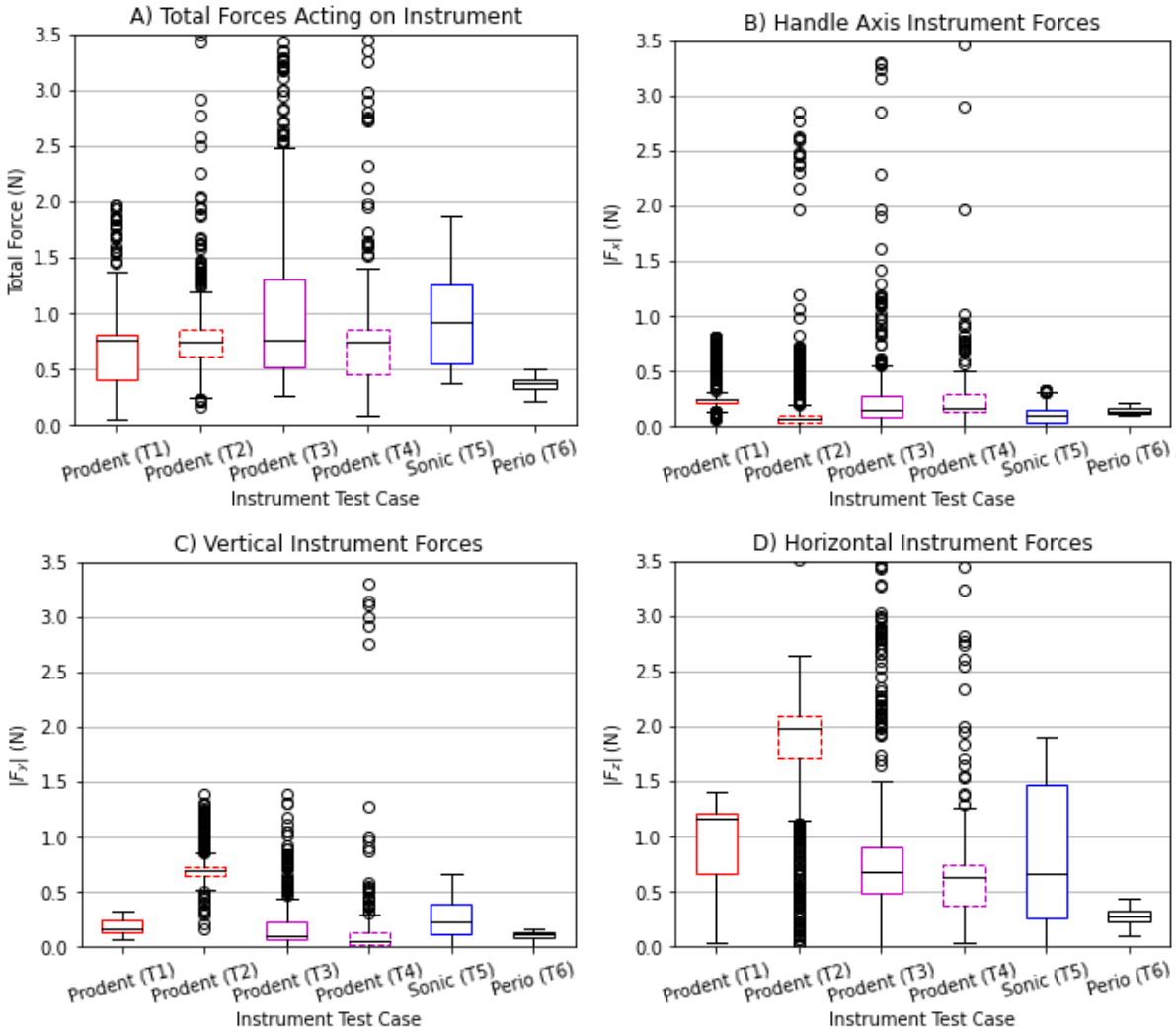

Figure 6.22. Forces in the middle third of each path cycle for each test case (y-axis limit of 3.5 N): A) Total force; B) Force along the x-axis of the instruments handle; C) Force in the y-axis for vertical forces acting on the instrument; and D) Force in the z-axis for horizontal forces acting on the side of the instrument. Directions of the forces acting on the instrument are depicted in Appendix D.1.

Vertical forces acting in the instrument's y-component better represent the forces transferred from instrument tip to the dental arch for the simulated technique, rather than the cheek, side of the tongue and mandibular jawbone behind the dental arch. The estimated technique forces were generally below 0.25 N for the ProDENT test cases (T1, T3 (upper quartile) and T4 (excluding outliers)) and the periodontal test case (T6) (Figure 6.22C). The estimated force on the teeth from brushing was only up to 0.66 N. Higher risk paths and active rotations produced higher forces on the dental arch with outliers up at 1.40 N (T2–T4) (Figure

6.22C), where there were also sudden peaks in active jaw rotation (T4), measuring up to 11.71 N, although not visible on the chart.

6.4.6 Spatial Measurements

Post-procedure visual analysis was carried out to assess the position of the instrument tip with respect to the important dental features identified for the simulated dental techniques (Figure 6.3). This data was produced by converting the procedure block spatial risk measurements for ID1.1–1.4 into their raw input distances (Chapter 5, Section 5.3). The ID1.1 axis frame shows the position of the instrument tip with respect to the top of the nearest tooth (tooth occlusal point) through its cross section (Figure 6.3A, Figure 6.23). As expected for an intraoral camera, the position of the ProDENT was above the nearest tooth by 5–10 mm (T1, Figure 6.23A).

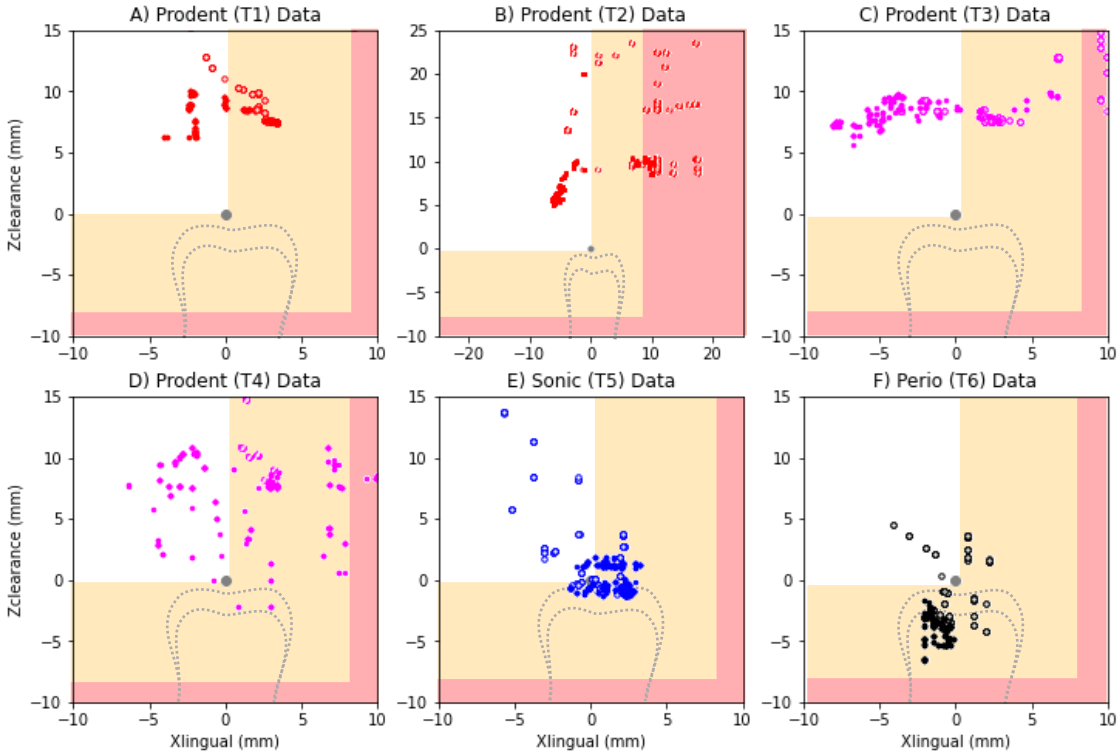

Figure 6.23. The relative positions of the instrument tip around its nearest occlusal point (grey marker) for ID1.1 risk measurements. ProDENT test cases: A) T1; B) T2; C) T3; and D) T4. E) Sonic test case (T5); and F) Perio test case (T6). Solid markers represent markers around the back teeth (the middle third of each path cycle). Regions: Low risk (white); Safe risk (orange); High or unacceptable risk (pink).

Positions for the higher risk path shift away from the tops of the teeth at up to 25 mm in clearance and 20 mm in width (T2, Figure 6.23B). The side-to-side head movement produced a 2-fold increase in width, which was caused by the robot's limited speed to correct its position with the detected movement (T3, Figure 6.23C). Active jaw movement resulted in the greatest spread of points relative to the nearest tooth surface of the back teeth (T4), especially when compared to the localised sonic toothbrush test case (T5), with some points below the occlusal curve point which represents mean top surface location of the teeth (Figure 6.23D,E). The periodontal instrument tip is shown to be acting on the buccal side of the teeth ($x < 0$) and below the occlusal point ($z < 0$) around the back teeth (Figure 6.23F). The unexpectedly close locations of the points to the centreline of the tooth may represent interdental contacts along the sides of the teeth and be influenced by the flexibility of the probe.

Procedure block risk measurements on the frontal plane for ID1.2 shows the instrument's axis intersection point varying over a cycle for each test case (Figure 6.3B, Figure 6.24). The radius of intersection for the intraoral camera and sonic test cases extended beyond the back teeth zone (green) in all cases. However, the instrument intersection remained approximately 5 mm away from the front teeth zone limit (magenta) (Figure 6.24A-E). As this is the approximate radius of the instrument handle, it is estimated that contact with the cheek would have restricted movement beyond the higher limit. Therefore, the instrument handle could be improved by re-orienting its axis to remain within the smaller zone to horizontal contact with the model tissues, such as the cheeks (Figure 6.22D).

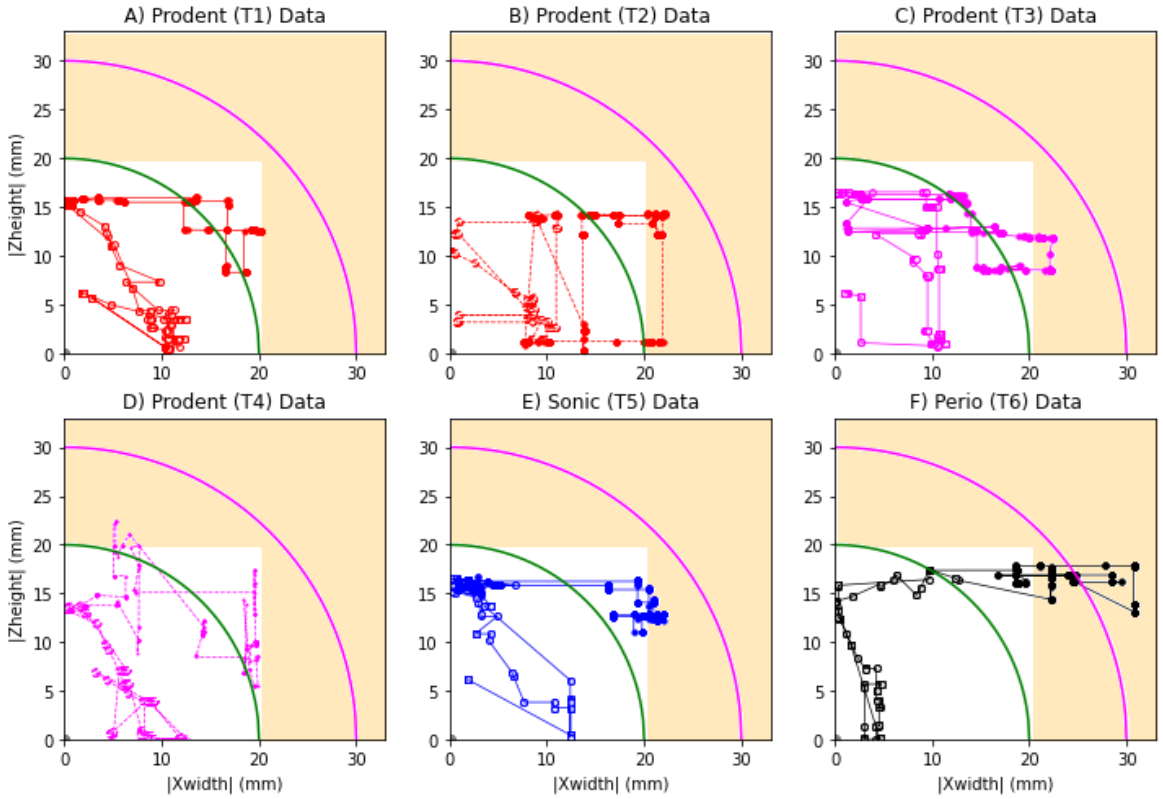

Figure 6.24. The intersection points of the instrument's handle axis with the frontal plane for ID1.2 risk measurements (adjusted back to raw data inputs). Magnitude relative to the centre point presented as a quarter of the frontal plane with the boundaries of the acceptable entry zones: 30 mm radius for front teeth (magenta); 20 mm radius for back teeth (green). ProDENT test cases: A) T1; B) T2; C) T3; and D) T4. E) Sonic test case (T5); and F) Perio test case (T6). Solid markers represent markers around the back teeth (the middle third of each path cycle). Regions: Low risk (white); Safe risk (orange); High or unacceptable risk (pink).

The different path taken around the sides of the teeth for the periodontal probe test case created a different shape of the intersection points, compared to the other test cases. This caused a higher shift in data points at the back of the mouth beyond the 30 mm radius (Figure 6.24F). The thinner width of the instrument was expected to minimise the presence of horizontal forces despite extending past the higher limit of the frontal plane (Figure 6.22D).

Distance risk measurements for ID1.3 of the Procedure block (Figure 6.3C) were used to compare the position of the instrument during ProDENT techniques and between the sonic and periodontal instrument test cases (Figure 6.25). In general, the instrument tip remained

close to the teeth and gingivae throughout the sonic and periodontal test cases (Figure 6.25B,D). Closing the mouth produced closer distances to or contact with the teeth and gingivae (Figure 6.25A,C). The two detected virtual throat wall contacts along the higher risk path (T2, Figure 6.25E) correspond to the detected forces on the instrument and rotations of the model from 42–45% and 55–57% (Figure 6.20A,B, Figure 6.21B). Further, the close contact to the throat wall for active head rotation matches the relatively high force region, reported from 47–55% (Figure 6.21C). The four peak regions in active jaw rotation (T4, Figure 6.21A,C) can be observed with changes in the distance to the teeth and gingivae (Figure 6.20D).

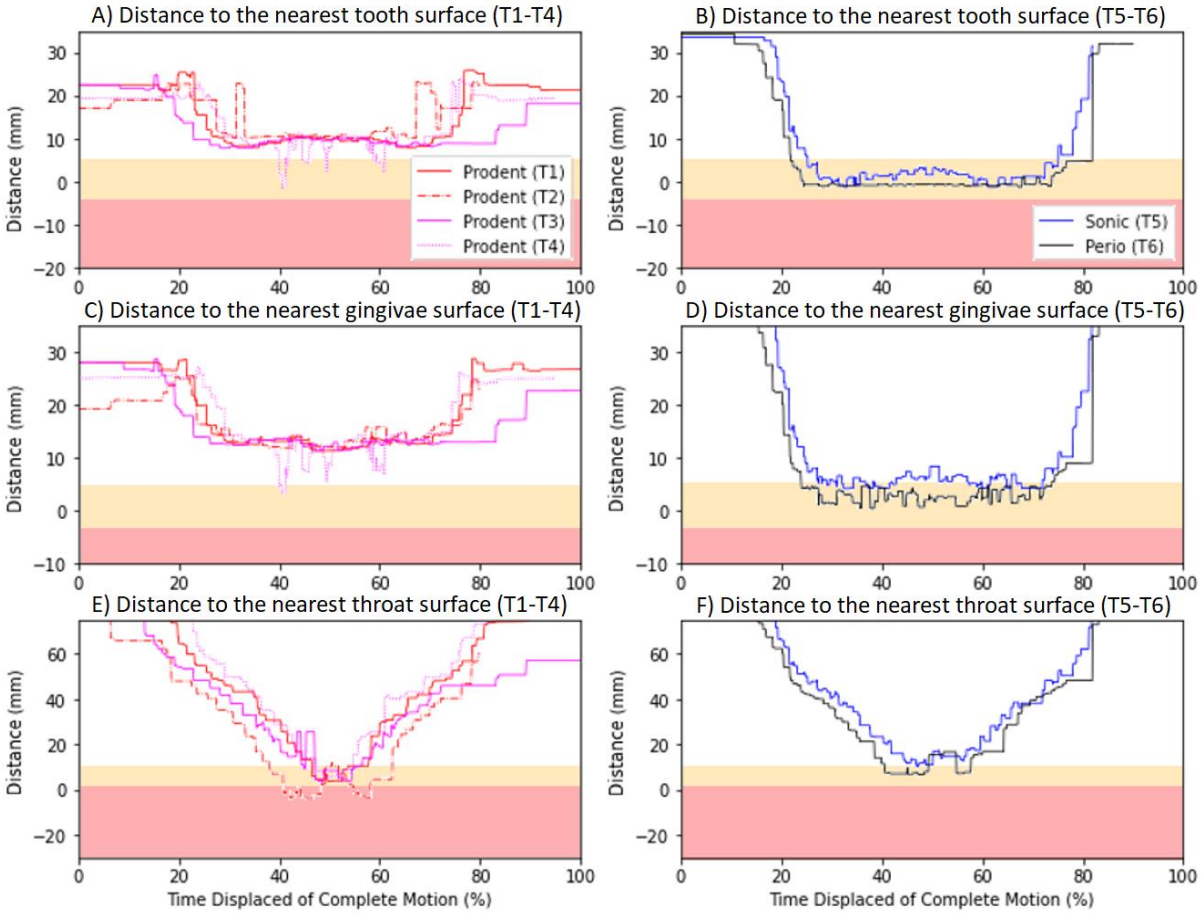

Figure 6.25. Scaled time series analysis output for distances to hard tissue dental features for ID1.3 risk measurements (adjusted back to raw data inputs). Distances to the teeth (A, B), the gingivae (C, D) and the throat wall (E, F) for the ProDENT and non-ProDENT test cases, respectively. Regions: Low risk (white); Safe risk (orange); High or unacceptable risk (pink).

The estimated ID1.4 distance risk measurements to soft oral tissues for the Procedure block (Figure 6.3D) were also observed between the test cases (Figure 6.26). As expected, the sonic toothbrush and periodontal probe tips were closer to the lips upon entry and exit of the mouth than the ProDENT intraoral camera (Figure 6.26A,B). However, the ProDENT instrument approached closer to the cheeks while at the back of the mouth, reaching a minimum where the instrument would have been in contact due to its radius of approximately 5 mm (Figure 6.26C). Active head movement produced the closest distance of the instrument tip to the cheeks, while active jaw rotation was closest to the tongue at approximately 60% of the path cycle (T3 and T4, Figure 6.26C,E). Finally, the oscillating sonic toothbrush tip experienced the closest distance to the tongue (Figure 6.26F).

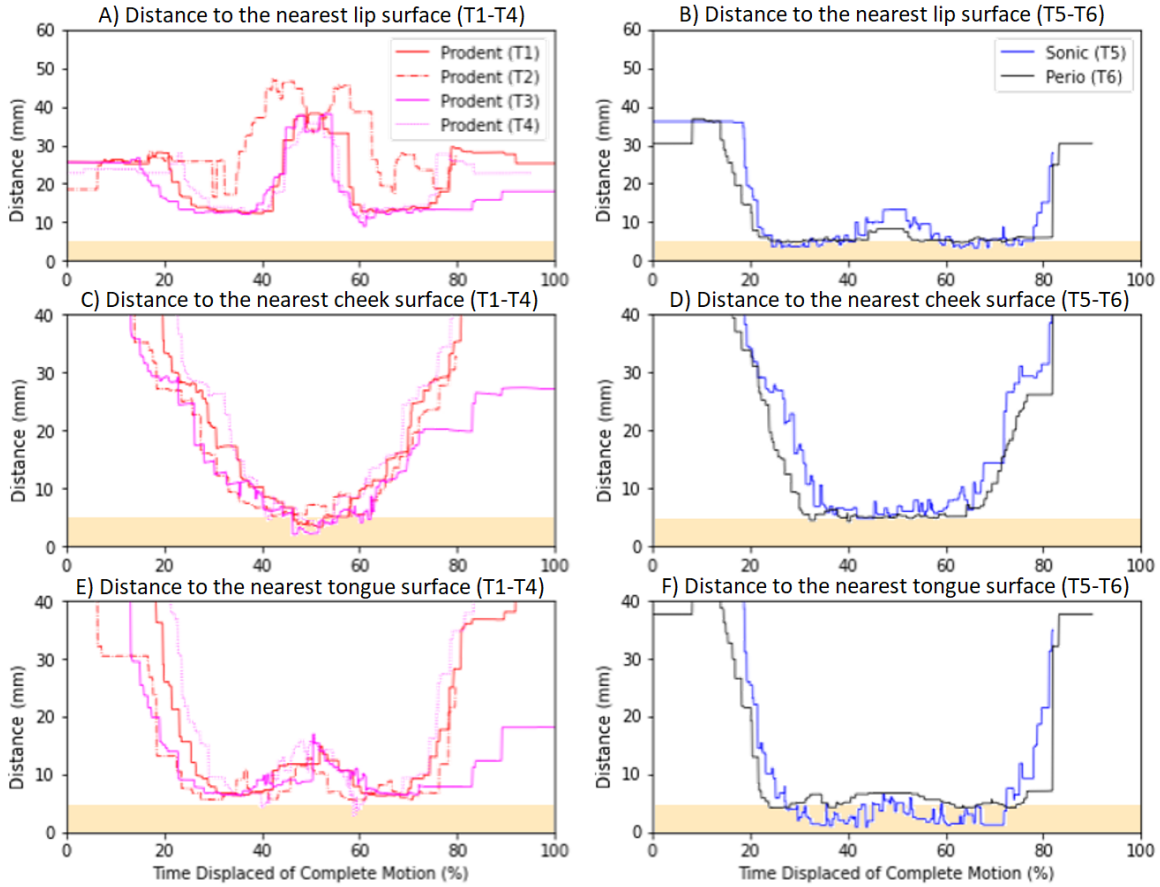

Figure 6.26. Scaled time series analysis output for estimated distances to soft tissue dental features for ID1.4 risk measurements (adjusted back to raw data inputs). Distances to the lips (A, B), the cheeks (C, D) and the tongue (E, F) for the Prodent and non-Prodent test cases, respectively. Regions: Low risk (white); Safe risk (orange); High or unacceptable risk (pink).

6.4.7 Forces and Risk Outputs

For procedure block supervision system verification, the force measurements were compared to the risk output measurements of ID1.1–1.4. In the lower risk ProDENT test case (T1), risk data for ID1.1–1.2 showed transitions into high risk levels where there was a sudden increase in force measured (Figure 6.27A-C). The higher risk path experienced transitions to the unacceptable high risk and force regions, including ID1.3 (Figure 6.27A-D). The paths were found to present relatively low risks to the soft oral tissues; however, this did not account for the width of the instrument (Figure 6.27E). For ID1.1 and ID1.3, the risk outputs were higher for periodontal probing than sonic brushing (Figure 6.27G,I). Whereas the ID1.4 risk output was higher for the sonic brushing which operated close to the tongue (Figure 6.27J). The combination of ID1.2 appears to best estimate the presence of high forces for all test cases except for the flexible periodontal instrument (Figure 6.27A,C and Figure 6.27F,I). However, the ID1.1 and ID1.3 well approximate the timing of higher forces for the camera instrument, but ID1.1 may inaccurately represent the force level on the instrument (Figure 6.27A-B,D).

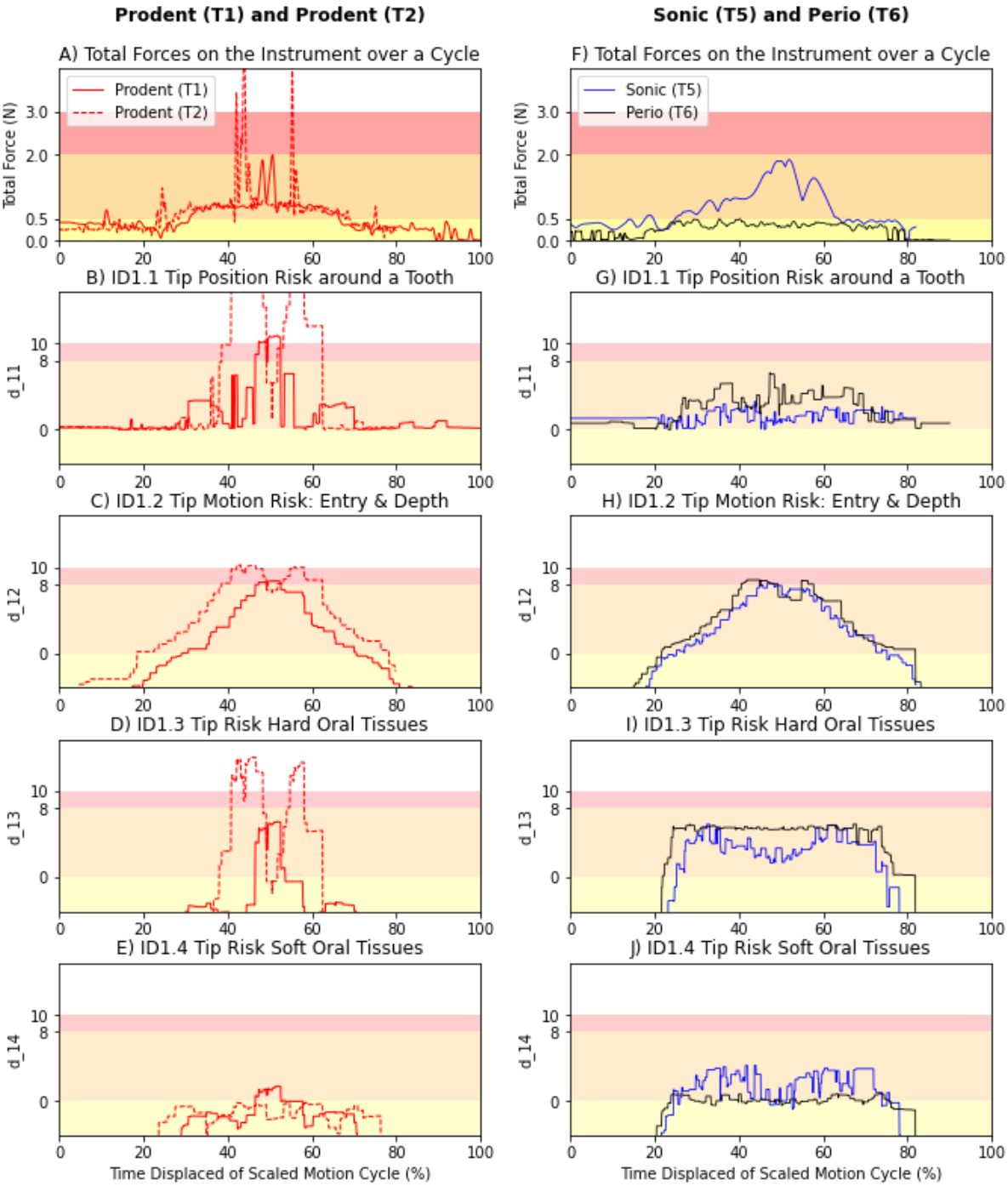

Figure 6.27. Measurements taken with passive model movements over the lower and higher risk paths using the ProDENT instrument (T1-T2, Left Column A-E) and lower risk paths with the sonic and periodontal instruments (T5-T6, Right Column F-J). A/F) Total forces on instrument. Spatial risk measures: B/G) ID1.1 risk output; C/H) ID1.2 risk output; D/I) ID1.3 risk output; and E/J) ID1.4 risk output. Regions: Low risk or force (yellow); Safe risk or force (orange); High risk or force (pink); Unacceptable high risk or force (white).

The force and risk outputs for the lower risk path test cases using the ProDENT intraoral camera were analysed for the addition of active model movement. The ability for the robot arm to track the head resulted in minor changes to the risk outputs between the active and the passive test cases (Figure 6.28). The side-to-side head movement caused the most variability in ID1.1 (Figure 6.28B), although there was a slight increase to the risk to the soft oral tissues at the centre of the path (Figure 6.28E). By comparison, the jaw movement produced slight increases in the risk outputs for ID1.3 and ID1.4 at ~40% and ID1.1 also at ~60%, compared to the passive model test case, which corresponds with movements in the jaw (Figure 6.28G,I-J, Figure 6.20D). Under active movement, the risk outputs could not be used to estimate the magnitude of force for contact between the head model and the instrument. Nevertheless, ID1.3 measured high risk and ID1.1 triggered an unacceptable high-risk output which can initiate an emergency exit of the mouth until risk levels are determined acceptable to continue on an adjusted path (Figure 6.28A-B, Figure 6.28F,G).

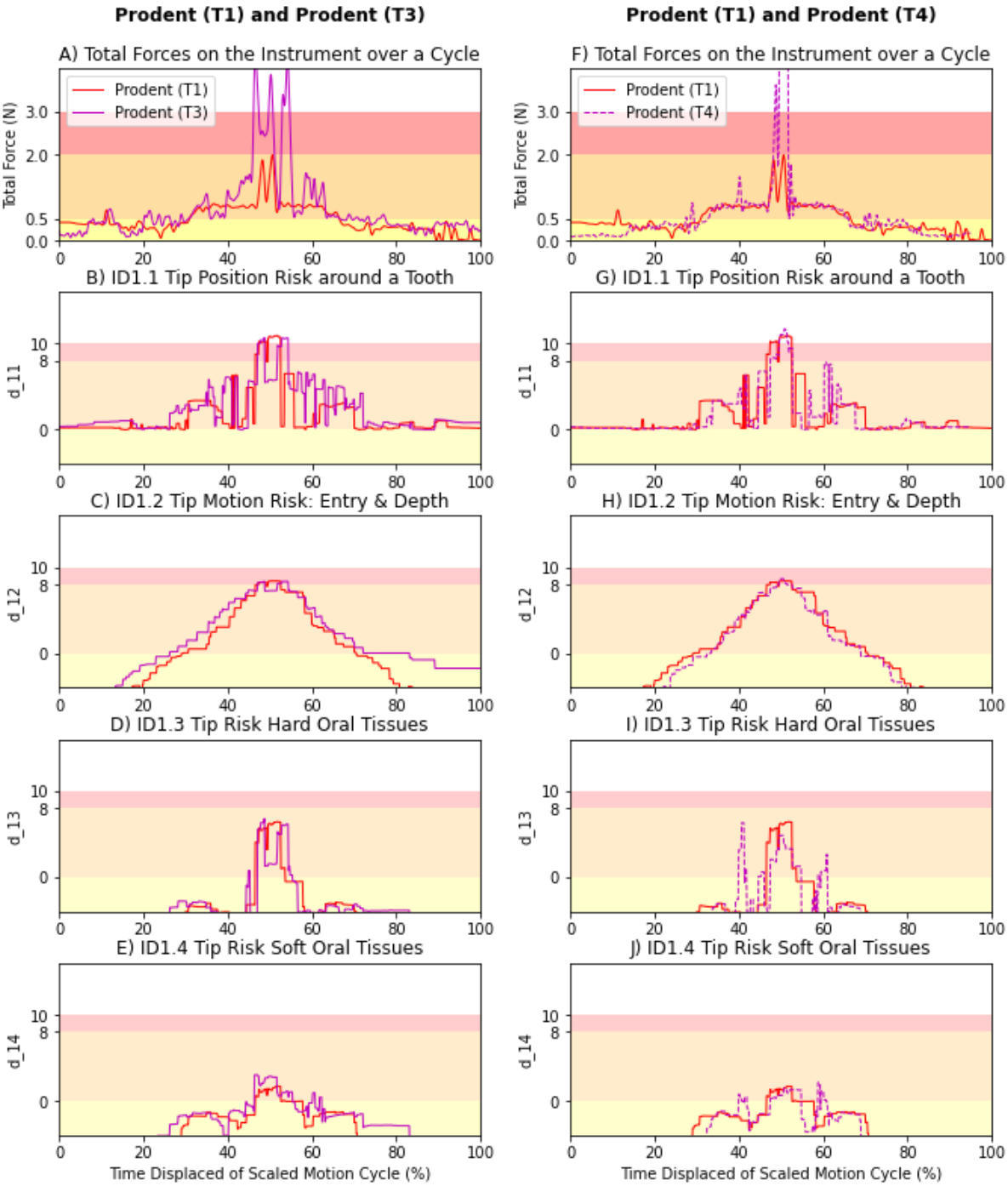

Figure 6.28. Measurements taken with the ProDENT instrument on the lower risk path for active model movements compared to passive model movement for: Head Rotation (T1, T3, Left Column A-E); Jaw Rotation (T1, T4, Right Column F-J). A/F) Total forces on instrument. Spatial risk measures: B/G) ID1.1 risk output; C/H) ID1.2 risk output; D/I) ID1.3 risk output; and E/J) ID1.4 risk output. Regions: Low risk or force (yellow); Safe risk or force (orange); High risk or force (pink); Unacceptable high risk or force (white).

6.5 Discussion

For robotic speed and separation monitoring, the distance from any detected surface controls the relative speed of the robot. This becomes extremely challenging to define for the complex dental environment, where a singular detected feature is insufficient to perceive the true safety of an operation. The spatial risk measures designed in Chapter 5 represent various forms of separation monitoring using measurements from important features and frames of reference to perform near real-time risk analysis of simulated dental procedures. A series of dental applications were carried out on a dynamic soft tissue head model that allowed for side-to-side rotation and jaw movement. In addition to orientation feedback, joint position and force data were collected from the robot and a force-torque sensor to assess the performance of the robot during dental technique simulations. Output force data was compared between the different techniques performed and then assessed against the developed procedure block supervision system risk measurements.

The forces produced on the instrument from contact with oral tissues usually remained between 0.5–1 N during the techniques. This is an ideal force range for dental techniques where forces during operations have been reported as between 0.049–1.32 N for manual charting and 0.5–1.34 N while using advanced instruments, such as a sonic toothbrush and ultrasonic scaler [319-324]. Higher simulated technique forces were reported up to 5 N, apart from active jaw movement which reported an unexpected high total force of 31.80 N. Dental technique forces have been reported to range from 0.86–10.35 N during manual methods [324-326]. High forces on the side of the instrument are assumed to have resulted from contact with the cheek during techniques, particularly for the wider instruments such as the ProDENT intraoral camera and the sonic toothbrush. Forces in the direction of the instrument's handle are likely to have been higher than expected due to friction of the silicone head model soft tissues, with the highest forces produced when in contact with the head model behind the dental arch. However, when

observing the forces in the y-direction, the amount applied by the sonic toothbrush and periodontal probe applications were low for standard dental techniques. Further testing and new dental robot paths should be developed for more accurate depictions of the dental instrument techniques.

The output forces were compared to each of the interpreted data spatial risk outputs. Sudden increases in force measured were usually associated with the timings and magnitudes of the risk data for high risk ID1.1 and 1.3 outputs, while the timing of high risk along the path was most related with the ID1.1–1.3 outputs. As expected, the risk of the ProDENT instrument path was low for the ID1.3–1.4 as the tip of the instrument was designed to not enter hard or soft tissues. However, this was not able to effectively capture the width of the instrument, and the head model was able to move away on contact, preventing any increases in ID1.4 risk outputs. Further testing will need to be carried out to evaluate the effectiveness of ID1.3 and ID1.4, given that the path and risk measurements of these experiments focused on tip's movement for expected dental procedures rather than abnormal scenarios. While there were false positive measurements for high risk periodontal and sonic toothbrush technique, the whole purpose for capturing the spatial risk calculations is to better understand the risk beyond what is measured in force feedback to avoid an unnecessary collision occurring. Moreover, as multiple risk assessments triggered high risk, this risk model presents safety through redundancy.

Other safety monitors with alerts have been investigated for their benefits to detect high risk. Zheng *et al.* (2007) considered the addition of an alarm module to alert surgeons when the difference is greater than the predefined tolerant range from the preoperative plan for dental implantology [268]. Wang *et al.* (2014) had a dentist perform real-time monitoring based on visual feedback from an optical tracking sensor that received light reflected during tooth ablation to ensure safe operation of automated crown preparation [207]. Sharkawy *et al.* (2020)

presented a multilayer feedforward neural network for human-robot collision detection to minimise the force of impact to an acceptable level [74]. Often the included safety measures or "safety skills" for robot operation are integrated into complex system architectures, such as that of a feeding robot and a walking assistance robot (Figure 6.29) [76, 273] [328]. This all-in-one architecture, encompassing additional functionalities or handling of lower risk errors to fine tune their operation, makes it difficult to identify the presence and function of significant safety features [171].

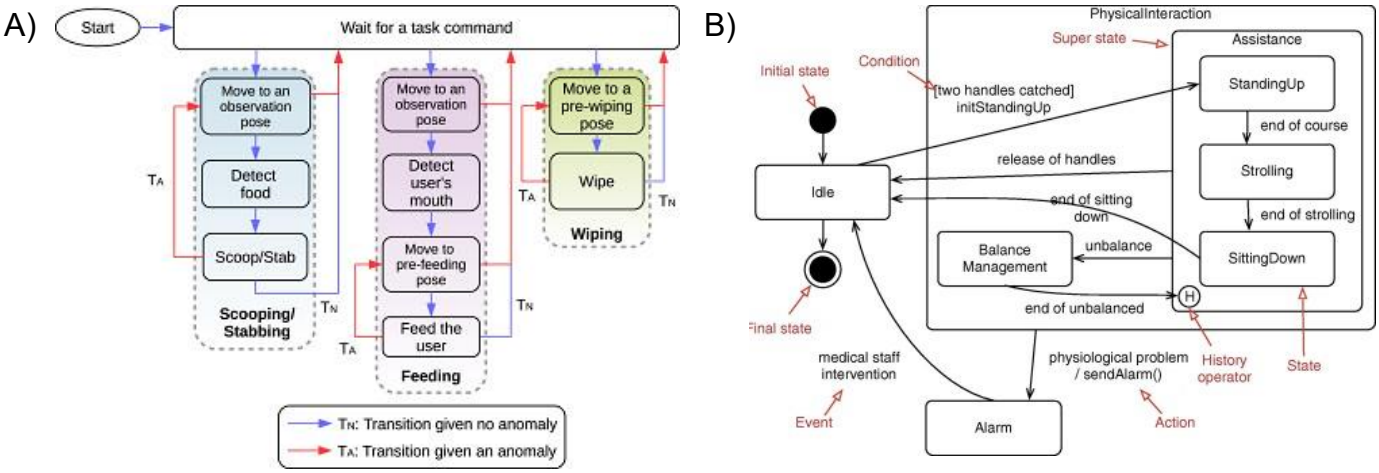

Figure 6.29. System architectures for assistive robotic systems: A) Finite state machine for a feeding robot providing meal assistance [273]; B) Simplified version of the state machine for the MIRAS walking assistance robot [76].

The complexity of system architectures and control algorithms for medical robots presents legislative and ethical barriers for their integration, especially when performing procedures on conscious patients [329]. Despite this, research and development into robotic applications around the eyes is underway to take advantage of advanced AI for precise instrument control. This began in 2019 with the first assistive robot for micro precision retina surgery, the Preceyes surgical system, introduced to Europe [329]. Since then, supervised robotic techniques for lash extensions on conscious patients have been developed [330]. These use lightweight instruments with magnetic connection that release when excess force is applied [330]. This safety mechanism could be effective for use with lightweight intraoral cameras and toothbrushes with potentially lower strength robot arms. These developments represent the

combination of a top down and bottom-up approach to develop medical robots for applications of the eye. This thesis follows this approach to supplement the research in surgical implant and restorative dental applications with a focus on lower risk diagnostic and cleaning procedures.

A benefit to the safety of dental techniques is the localised movement of the instrument during operation on a tooth. This enables the robot to be assumed as more static during an accidental contact, compared to other collaborative robot systems that are usually highly dynamic [331]. For large robot arms, particularly when operating in a confined space, the robot must be able to avoid contact along each of its links to operate safely with the expected level of accuracy required for procedures. Liang *et al.* (2021) developed a training algorithm to allow the robot to identify and then "remember" the presence of obstacles in its environment that can limit its motion using a learned neural network [331]. Other methods involve fault tolerant approaches to measure changes in the torque of individual joints upon impact which is only available on certain robotic systems [331].

To produce a more predictable and defined motion, linear control of the robot's position from the World Reference Frame (*MoveLin* command) was utilised in the simulation experiments. The compact Meca500 robot was able to sufficiently cope in the current setup to complete the paths of motion for the purpose of assessing the risk with the spatial measurements. Nonetheless, there seemed there was a limit where the Meca500 robot would not approach near a singularity. To improve performance, the starting position of the robot should be adjusted to move away from the Joint 5 angle limit and the elbow singularity. Additionally, the relative position of the head should be adjusted to move away from the Joint 3 angle limit during robotic techniques, which could have impacted the robot's ability to follow the reference object in Unity. Inverse kinematic solvers from robotics companies, including Mecademic, have been improving the ability for robots to overcome limitations and safely pass near singularities in recent firmware updates, such as for bent shoulder and wrist singularities

[225, 332]. However, to avoid the occurrence of singularities for the small Meca500 robot arm, varying patient postures could be recommended for the left and right quadrants of the mouth. If this were performed, it would suit the use of a mouth prop which could be fixed in space or integrated with an orientation sensor or passive arm tracking system to locate the patient's dental arches. This could also improve the accuracy of dental scanning techniques where there have been challenges in accuracy for scanning whole dental arches [228].

The relative speed of 5 mm/s is below the calculated limit for the larger diameter dental instruments (Appendix D.3), such as the ProDENT camera and sonic toothbrush. The reduced relative speed of 2.5 mm/s is more appropriate for the periodontal probe, although this is approximately 5-fold higher than the calculated speed limit for a tip diameter of between 0.4–0.6 mm (Appendix D.3). Fortunately, the flexibility of the S2006 probe instrument slightly reduces the risks of operation, but the need to exceed the limit to operate at a reasonable for a dental procedure highlights the importance of robot risk awareness. To ensure that the force-torque sensor did not contribute to further tip position uncertainty, preliminary assessment of the angle of the sensor under load was carried out with a laser pointer (Appendix D.4). For the Nano17-e, the measured sensor deflection only increased linearly at 0.376°/N, which was equivalent to 0.39 mm and 1.30 mm displacements for offset distances of 30 mm and 100 mm under a 2 N force loads, respectively (Appendix D.4). Future testing should be carried out to assess the flexibility of the dental instruments used in operations.

The drift of the orientation sensor may be influenced by heat, which could have resulted from being positioned inside the base of the silicone head model and having been turned on for a long period of time. However, since the use of an AHRS, such as the VN100, typically provides orientation estimates with respect to a global inertial frame (e.g. NED or Earth-centred), a transformation from the AHRS frame to the head model's local coordinate frame may have been necessary to ensure the data directly tracks the model motion. This should be

carried out before future experiments to enable the data to accurately interpret the motion of head or jaw movement within the context of the dental model. Furthermore, the sensor could be rotated by 90° to use the pitch and roll axes to improve the accuracy of the results, since the heading axis only being accurate up to accurate up to 2.0°, compared to the other axes at 0.5° [316].

An improved position of the head model could allow a wider range of possible instrument orientations. Current methods limited the angle of rotation in each axis to ±15° from the starting position. The highest force measurement during active jaw movement of 31.80 N, as a result of the additional collision with the instrument end effector holder. This could be managed by increasing the length of the instrument, decreasing the radius of the holder and performing multi-point instrument risk tracking, rather than only focussing on the tip of the instrument. A multi-point risk analysis could account for varying instrument sizes and shapes, with the overall calculated risk weighted to the locations with a small surface area, as well as the locations in close contact to hard tissues which could present a collision with a small surface area. Causes of spatial aliasing in the tracked feedback and latency to robotic movement for the position of the instrument tip should be assessed. This may have been caused by the reduced speed of the robot arm or the frequency of joint feedback received from the robot.

Poor tracking of the head movement using the orientation sensor could have impacted the results over time and limited the number of dynamic test cases performed. Alternative methods, such as navigation systems like Navident, could be utilised instead to limit effects of robot feedback delays. Future developments in the spatial risk assessments should assess the occurrence of false positives and false negatives for identifying near misses and high force impact. In this chapter, false positives were detected for ID1.1 and mitigated in analysis methods. This resulted from the change in methods from Chapter 5 where only one frame of reference was involved per tooth along the occlusal surface. In the future, a higher number of

reference frames can be included and will allow the instrument tip to be plotted in real time around the nearest occlusal point with its digital dental arch cross section. For post-operative analysis, the location and index of each reference frame in ID1.1 should be defined along the occlusal plane to recreate instrument techniques around a patient's digital intraoral scan models. These future methods will need to account for potential errors in dental surfaces to estimate probabilities of false positives and false negatives, while changes in code or the digital setup, including the reference frames, should be evaluated for their impact on the quality of risk tracking in various dental scenarios.

To improve future methods beyond the risk of the instrument tip, other locations along the instrument could be selected as additional points for ID1.1–1.4 risk measurements to provide a more detailed model of the risks associated with the instrument inside the oral cavity. It can be used to track the distance around the occlusal surfaces over the instrument in ID1.1 and be integrated into ID1.2 to capture the width of the instrument's handle through the frontal plane. This could enhance the awareness of the whole instrument's position around nearby hard tissues in ID1.3 and the estimated locations of soft tissues in ID1.4. This could directly inform the system of the size of the instrument tip and its contact surface area, as well as include a calibration step to confirm the instrument's flexibility. Whole instrument risk modelling could allow for more accurate of force prediction modelling, particularly for instruments that are more likely to contact the cheeks, such as the wider ProDENT. These additions may help optimise the orientation of the instrument in the oral cavity. Future methods should also involve exporting the raw interpreted data risk measurement inputs along with the output of the rotation of the instrument. From raw ID1.2 measurements, the path of the instrument in the frontal plane can be observed visually across the whole frontal plane in post-operative analysis. Finally, the location and orientation of the virtual "hard tissue" throat surface should be re-evaluated to ensure that accurate risk distance measurements are captured for ID1.3.

The outputs from the procedure block risk measures could be used to recreate dental procedures based on the systems performance for analysis, and lead to the development of "futuristic" dental records involving the tracked instrument path. Furthermore, the size of the mouth opening, origin, and rotation of the localised dental arches to show the patient's compliance and activities during procedures. These factors can add a layer of protection as objective evidence against liability accusations for practitioners, which is essential in dentistry [303-307], and for the patient's safety to avoid uncertainties in litigation proceedings for any malpractice. Additionally, digital records of robotic dental procedures could help dental robot manufacturers to develop a robot that can fulfill identified safety criteria for safe operation in a way that is traceable to avoid unknown litigation practices from the lack of standardisation for high autonomy collaborative medical robots.

Although efforts to measure the presence of singularities were included in this thesis, future work will need to be carried out for developing dental robot systems to manage and mitigate the impact of singularities to maintain smooth and expected instrument control. This will help them produce high quality dental techniques that are also safer. Future methods could take into consideration the cost functions for the singularities produced in this chapter, however, the functions are specific to the design of the robot arm. Future efforts could consider a passive limit of 80% for joints and singularities, depending on their available ranges of motion and pending improvements in firmware to mitigate this issue. The Unity simulation system could be reconfigured to operate with these improvements in future work and should include active use of the Unity Animator state machine to control the robot's modes of interaction and assess the effectiveness of risk tracking to avoid high force collisions.

Simulation testing needs to be performed in the other quadrants of varying shaped mouths and dental arches, as well as tongue positions, to compare environmental factors influencing the progress and safety of procedures. Moreover, further tests should be carried out

with active jaw movement without maxilla collisions to assess whether the risk measurements are indicative of the magnitude of force for contact between the head model and the instrument. In the future, these simulation models should be combined with observer and patient block safety assessments which will need to analyse changing rates of risk over time. Direct feedback from expert dental professionals on the specific risks should be recorded during simulated paths and compared to the captured risk outputs and accepted MoI decision of the supervision system. From there, the risk measures can be modified or fine-tuned from the raw ID inputs to allow higher angles of the instrument without unnecessary increases in the risk output measurements, thereby reducing the likelihood of false positives or false negatives [220]. These sessions can also help evaluate the values of inputs for the risk management network in order to evaluate the likely causes of the identified hazardous situations.

Tracking each of the identified risk measures in the virtual simulation and evaluating their output is needed to in order to validate the design of the risk supervision system for the procedure block. Future validation studies can be performed manually by dentists with visual guidance systems to evaluate the ability to detect changes in instrument risk, along with input from clinicians. If validated, these measurements could also be utilised to evaluate the safety of dental students in training. Despite limitations mentioned, the combined risk measures presented in this chapter were able to trigger high risk during high force collisions with the head model. This chapter presents a proof-of-concept for the development of risk-based spatial measurements that can be integrated into a safety monitoring supervision system for robotic dental applications. Together, the multi-dimensional risk supervision systems aim to assist progress towards dental robot automation by creating a risk-aware system for the design, development and testing of various patient-robot environmental setups and scenarios. Analysis of the speed of movement for the observer block, and optionally also the patient block, is the next step for the development of the dental robot supervision system.

Chapter 7: Discussion

7.1 Introduction

Increasing autonomy with dental robots has the potential to transform the dental industry by significantly improving the experience of patients and dentists and increasing accessibility to dental care. Dental robots with thorough risk management design have widespread benefits from bridging the urban-rural gap in dental professionals and increasing standardisation in procedures. For dentists, they can minimise the occurrence of MSDs, high stress, and disease transmission. Improvements in dental digitisation can reduce the likelihood of dental error from fatigue and miscommunication. In doing so, dental robotics present an opportunity to effectively mitigate the high prevalence of dental diseases around the world. To be successful, autonomous dental robots must be trusted to perform dental procedures while safely collaborating and interacting with its environment and conscious patients. The accuracy, affordability and safety of such systems needs to be proven and supported by regulatory institutions, dental practices, and the public.

There has been minimal change to the structure of dental clinics in recent history and the dental field tends to be slow to adopt new technologies [333]. According to Haidegger *et al.* (2019), research in digital medical technologies and integrations with remote robotic applications have not yet reached a critical point to significantly change traditional methods due to the expense, limited acceptance, and complex regulatory challenges [187]. In addition to the cost, a high learning curve is expected for remote and haptic systems as the dentists must be trained in the robots' movements and control, as well as their safety, maintenance and limitations. The cost of training and deployment of the dental care workforce has already been increasing to reduce misdiagnosis and improve access to cleaning and diagnostic practices [49, 113]. For Yomi, the assistive robotic system, dentists take a few weeks or approximately 20–30 cases to become well trained [333]. Calls for changes in the practice of dentistry that occurred during the COVID-19 pandemic in 2021 went beyond the need to introduce more digital devices to dentistry [334], prompting the need to "radically reform" the practice of dentistry from an interventionist model to a prevention-based system in order to manage future ageing populations [29].

To progress towards autonomy, this thesis proposed designs, methods, and safety frameworks for dental robots including the development of a supervision system to detect and reduce the likelihood of harm (Figure 7.1). The steps taken to the development of a safe dental robot presented below makes use of recent advances in dental digitisation, specifically intraoral scanning technology, that are especially facilitative for dental robotics. Methods in this thesis focused on procedure risk measurements of the instrument to evaluate the presence of high risk independent from robot control based on multi-dimensional spatial estimations. The innovative forward-facing dental setup proposed in this thesis plans to reduce the opportunity for unsafe quasi-static collisions, inhalation and ingestion, and can allow the patient to feel more in control during the robotic procedure. The dental robot chamber helps to develop and maintain a more

controlled environment for dental procedures which can aid the standardisation of techniques and analysis.

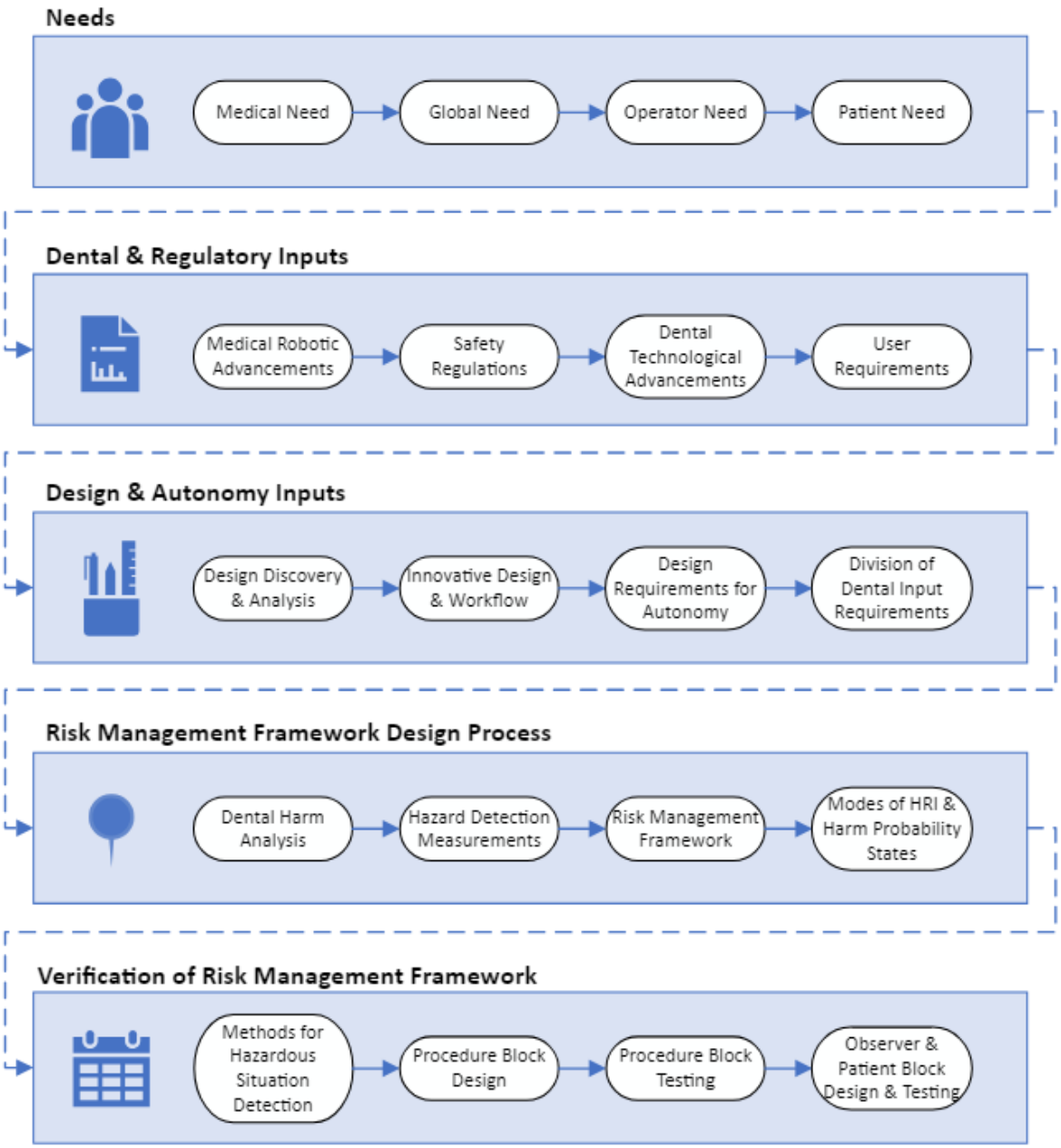

Figure 7.1. Steps taken towards the development of a dental robot risk management framework to improve robot risk awareness during procedures, involving user needs, design inputs and harm analysis. Future work includes further procedure block testing, and the observer and patient block design and testing.

Improvements to the inherent safety of the dental setup greatly reduce the risks to patients during procedures operated by robots. This thesis was designed to investigate dental

robot safety as the limitation to developing robot autonomy by overcoming barriers to the detection of high-risk situations in the complex dynamic dental environment. The combination of the dental robot design and the risk management network with inbuilt supervision systems aims to reduce complexity of dental robot systems to move towards development and enable safer transition to higher levels of autonomy to benefit dental practices and the community.

7.2 Developments for Dental Robot Safety

Safe design of an autonomous dental robot alone cannot ensure patient safety during dental procedures for higher levels of autonomy. Dental robots must be made aware of high-risk situations, particularly when the operator's situational awareness may be limited. It is believed that automation of risk management for hazard detection and analysis is necessary to develop system risk awareness and respond to high-risk states to limit the occurrence of harmful hazardous events. This thesis involved research towards the design of dental robot systems and the development of the dental robot supervision system to reduce the likelihood of harm during dental procedures by quantifying aspects of risk. Together, this research aims to overcome the "glass ceiling" for medical robot autonomy and promote safe operation of dental robots with reduced responsibility for supervising dental clinicians at higher levels of autonomy.

A representation of the new proposed dental robot setup is presented next to the traditional patient posture in Unity for visual comparison (Figure 7.2) [335]. The safety-focused design presents the patient positioned above the operating robot (Figure 7.2B). The developments in this thesis aim to create redundancy in safety by allowing the patient to gain the ability to retract away from the robot and minimising risks from inhalation and ingestion, while limiting the occurrence of unexpected interactions for the robot. This is important as dentists and patients should only need to be aware and trained on basic robot safety for safe

operation. Important hazardous situations were identified for dental robot supervision and their corresponding safety measures involving the dental instrument were established in this thesis. The supervision system's overall complexity was reduced by dividing major identified hazards between multiple supervision system blocks that were designed to facilitate greater robot system awareness with the reducing operator awareness at higher levels of autonomy.

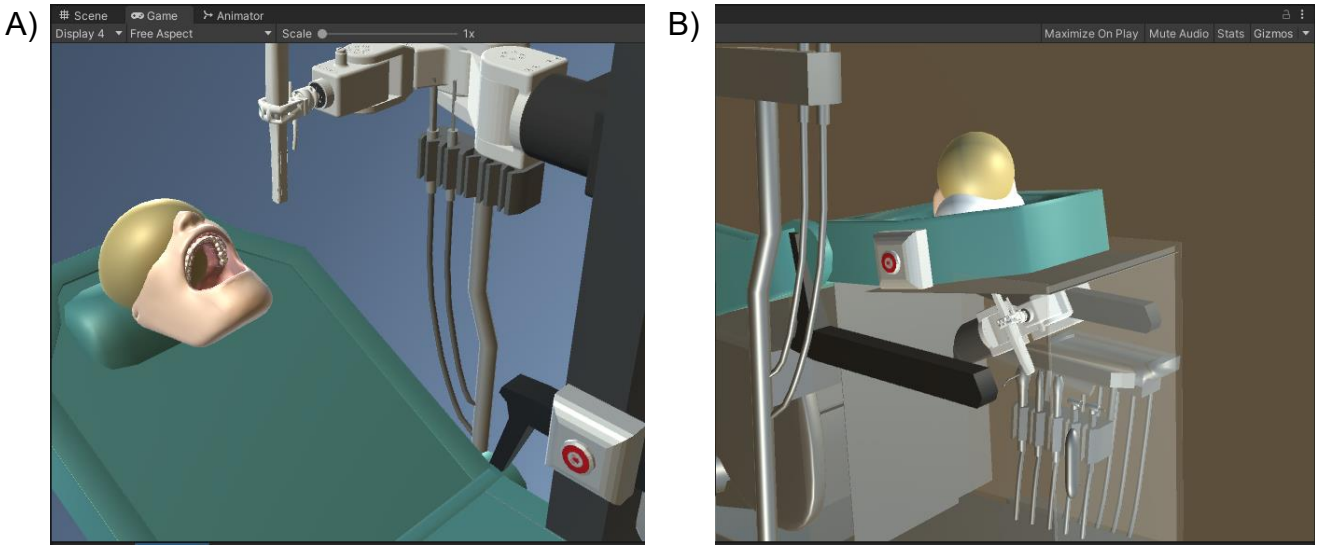

Figure 7.2. Unity virtual dental setup comparison of: A) the traditional dental setup with a dental robot above the patient; and B) the proposed dental setup with a patient in a prone or forward posture and the robot below in a chamber (made using objects from [335]).

This thesis envisioned autonomous robotic dentistry to include the robot, the dental instrument (procedure block), the oral environment (observer block), and the patient's experience (patient block). The procedure block proposed measures of physical distances to assess the instantaneous and planned risk level of dental instruments inside the oral cavity. The observer block was proposed to focus on the detection of the jaw opening, tongue position (with or without a tongue guard), presence of water and saliva, and the quality of vision. This can be used to manage the impacts from the narrow opening of the oral cavity, obstructions, image colour or resolution that could impact the measurements from cameras and other sensors which impact or limit the ability to monitor the safety of the instrument's movements in the oral cavity [141, 336]. Important risk measures for the patient block have been described as

tracking of the patient's compliance, the length of the procedure, the presence of sensitive locations in the mouth and the patient's state of mind from their estimated physiological response to the procedure.

The supervision system promotes the development of high-quality dental techniques. The division of risk management from procedure quality grants dental robots the ability to remain focused on high quality trajectory planning and patient motion tracking for optimising dental techniques as their main form of risk management. Previous systems developed for HRI experienced frequent inaccurate false positive detections with raw data, fixed boundaries and thresholding, which caused the shift towards advanced probabilistic analyses, dynamic thresholds and deep learning with lower rates of false positives [74, 337]. In contrast, this thesis proposes maintaining the use of the former for tracking risks during dental procedures by using specific dental feature frames of reference and important surfaces. In this way, the supervision system remains fully defined and can objectively assess repeatable risk measurements, adjusted for varying instruments and procedures. This means that robotic systems can safely include advanced "black box" control systems to create safe and efficient dental robots without publicly disclosing their internal intellectual property as proof of the safety of their system [338, 339]. Compliance with the dental robot supervision system can establish a method to standardise dental robot testing and create trust and understanding in the safety of dental robot systems for both operators and patients.

This thesis focused on the procedure block as the critical first step required to reach Level 3.5 "Conditional Risk Awareness and Autonomy" (Table 3.2, Figure 4.8) in order to have procedures operated by a qualified trained operator as opposed to requiring a dental expert. This block would need to be validated for different techniques at lower levels of autonomy with dental experts to ensure that the dentist expert is confident with its ability to identify unsafe instrument paths and positions within the oral cavity. Instrument risk awareness

will assist progression to Level 4 “High Autonomy” where the instrument path can be autonomously dynamically updated to meet the goals of the procedure. This trajectory-based decision making should be able to be supervised by a trained safety operator. By Level 4.5 “High Risk Awareness and Autonomy”, a validated observer block should also be in effect under educated operator or self-supervision. Level 5 “Full Autonomy” would include decision making for methods to improve the procedure and should update the informed operator or patient to put that into effect. At Level 5.5 “Full Risk Awareness and Autonomy”, the patient block should be in effect to assess the patient’s response to the robot as it guides them through the procedure for safe operation with emergency state detection mechanisms. The complete integration of all the supervision system blocks should allow for safe operation of the dental robot on patients for the higher levels of autonomy.

The goal of the designed supervision system is to mitigate harm by tracking the presence of critical hazardous situations and by performing safety-related decision making. This is vital for autonomous robots to function in a highly uncertain and dynamic dental environment on a conscious patient, especially when the use of a robot can reduce the dentist’s situational awareness of a procedure. Since each supervision system block can be applied for manual dental procedures, expected hazards can be better identified and included in risk management before the implementation of a dental robot, thereby overcoming traditional limitations of robotic development processes [76]. The supervision system risk measures set a baseline for patient safety and additional measures can be incorporated by the robot manufacturers to enhance patient safety further. The defined risk management network and structure of the supervision system ensures transparency for risk management. This contrasts to developing safety monitors for HRI systems which heavily rely on complex AI and deep learning (neural network) or machine learning approaches for safety assessments [76, 156].

7.3 A Roadmap Towards Robotic Dentistry

Virtual reality scenes can be developed to showcase a 3D perspective of the new robotic dental experience in order to improve dentist understanding and assess patient fear during simulated procedures with different setups (Figure 7.3). Patient and dentist feedback from simulated scenes can be used to inform design-related decision making to create less confronting patient setups and increase the willingness of patients to undergo robotic dentistry. This can also be used to explain and compare design choices of different dental setups for different dental procedures to lead to greater acceptance by dentists and patients. Additionally, VR simulated dental experiences could be used to help educate new users on important safety factors before undergoing robotic dental procedures and manage dentist and patient expectations. This is because the perceived safety of robots increases when a volunteer witnesses safe forms of human-robot interaction prior to their own interaction [83].

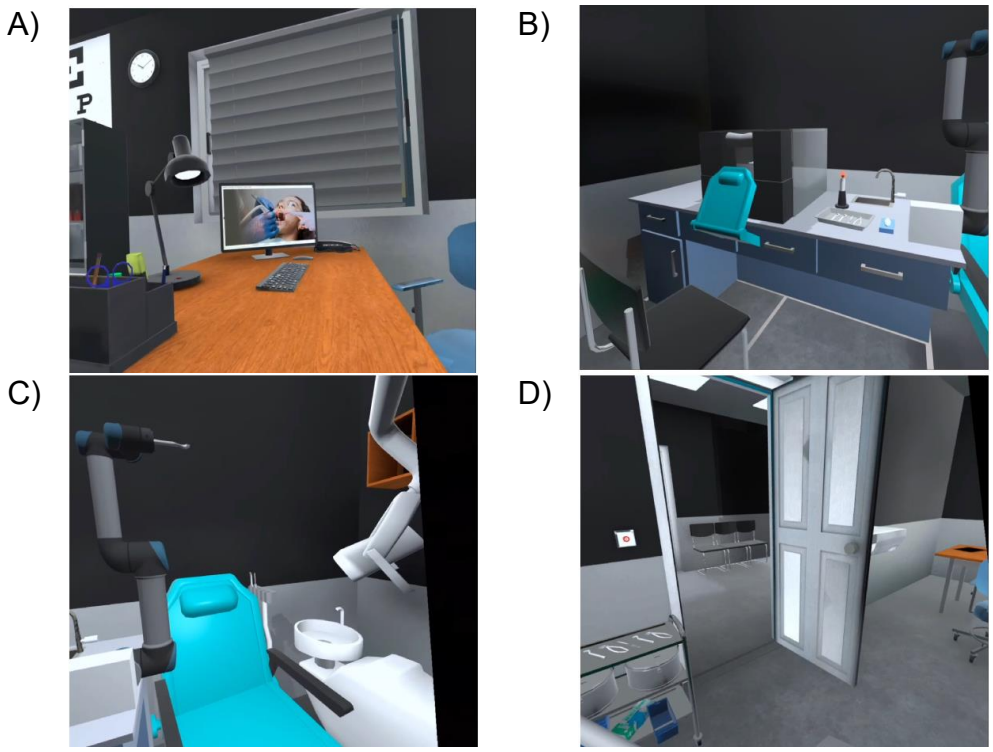

Figure 7.3. Unity hospital package with a dental setup developed for a virtual reality (VR) headset (made using [335]). A) 0° Viewpoint: Desk with screen to view operation; B) 90° Viewpoint: Forward posture setup with Meca500 in chamber; C) 180° Viewpoint: Supine posture setup with UR5 robot arm; D) 270° Viewpoint: Entry to dental office with instrument and equipment station.

Before dental procedures can be automated, VR experiences and assistive hand-guiding dental robots would help dentists to understand the current physical limitations and capabilities of robots. The use of these systems for dental technique tracking by dentists could build a model dataset to enable the development of imitation learning models for dental robots [276, 340]. However, as for Yomi, clinicians remain reluctant in uptake of the robots due to the high upfront cost, the associated learning curve, and any impacts on personnel and physical space, and their single functionality to only assist implant procedures at this time [333]. Currently, physicians are required to maintain the equipment and technological devices in their practice, which includes ensuring the systems are up to date and functioning properly, despite them not being a robotics expert [61]. For 510k Premarket Notification, the reported average time after submission for FDA approval in 2023 was 175 days, while the median was 85 days [341]. However, this varies depending on the category and the amount of difference to the predicate device [341]. However, the whole life cycle depends on the success of the medical device company to progress through all the stages of development (Figure 7.4).

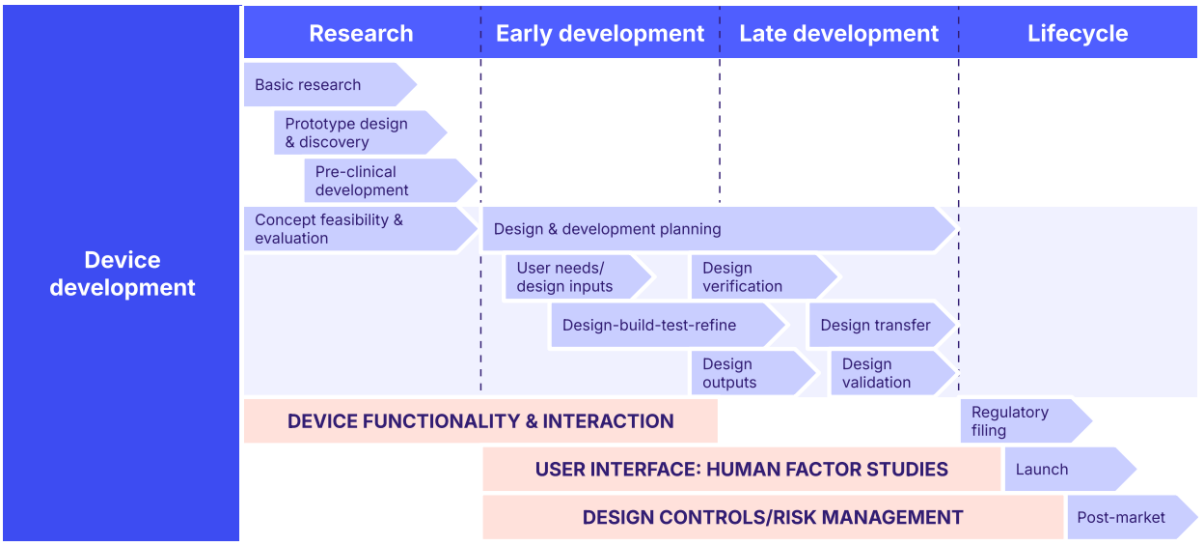

Figure 7.4. Medical device development timeline by the 510k Premarket Notification [341].

Without transitioning to remote operation, which is limited by capabilities in haptic feedback to clinicians and longer learning curves, an example of a potential assistive robot well

suited to assist a variety of dental procedures is the V01 robotic solution for arthroscopy by Convergence Medical Robotics. Its design includes fluid control, vision modelling and multiple gesture arms that can hold instruments (Figure 7.5A) [342], such as dental handpieces, suction and cameras for easy access and control by the dentist in the future. Although it is in early to mid-stages of development for arthroscopy [343], it would also need to apply for additional FDA approval through the relatively cheaper 510k pathway and perform testing before it is available as a low-level autonomy dental robotic platform. To use this setup, dentists and dental assistants would need to be trained on the normal use and abnormal use cases for the assistive platform, and how to manage the safe removal of all the instruments from around the patient in an emergency. This design would involve minor changes to the setup of a dental clinic, apart from taking up some physical space, since it would operate with the dentist over a supine patient. To mitigate barriers to uptake for arthroscopy, Convergence's business model proposes a consignment model where hospitals pay for usage without the high upfront capital costs for the robots [344].

A) B)

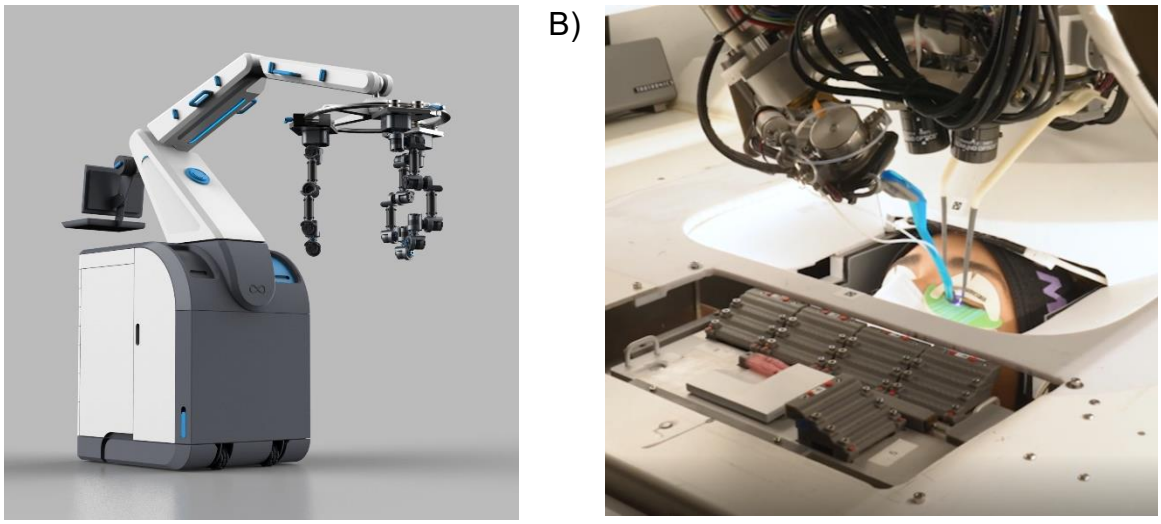

Figure 7.5. A) V01 Surgical Robot by Convergence Medical Robotics [342]; B) Lash extension robotic system by Luum [330].

Data from tracked manual and assistive dental techniques can lead to the development of advanced pre-programming software for automated and eventually autonomous dental

instrument trajectory generation. Integration of the proposed risk management framework could aid in the creation of autonomous robot trajectory decision making to improve instrument safety, as well as benchmarks and safety protocols to reduce ambiguity in the robot's capabilities and functions [187]. A starter autonomous dental robot could involve a simple magnetic end effector connection for larger blunt instruments, such as a toothbrush or intraoral camera. This could operate similarly to the lash extensions robotic application system that has two robot arms, one to separate the eyelashes and the second to apply the false lash and cure it in place with a light source (Figure 7.5B) [330]. The simple brushing or imaging dental robot could sufficiently reduce the required level of supervision, cost and risk such that any high force would dislodge the instrument rather than cause a high impact with the patient. The robot can be made aware of the connection or disconnection using a simple Hall switch, limiting the need for supervision by staff, as long as the robot arm is sufficiently weak or cannot make contact with the patient. This could be integrated with an available smartphone camera on a stand that can recognise the approximate location of the dental arches.

Where capabilities of autonomous techniques are limited or presented risks are high, the procedure could be facilitated through remote operation from trained clinicians. These could be integrated in the prone posture setup with the 3D mouse or pen devices, like the SpaceMouse and Inverse3, to control the robot end effector holding the dental instrument [238, 239]. By defining the future of dental robotics, systems can be built into teaching methods for dental students to minimise the need for retraining. As the proposed setup with autonomous dental robots is more likely to apply to simple cleaning techniques first, dental hygienists are most likely to benefit and therefore would need to consider the re-structuring of their clinics to provide autonomous robotic procedures. Dental practices that perform advanced restorative procedures will be able to follow by their example as autonomous techniques and risk awareness develops. Communications between practicing clinicians and dental robot

developers is necessary to ensure smooth integration of dental robots to manage the need for improved access to dental care globally.

7.4 Patient and Dentist Acceptance

7.4.1 Patient Comfort and Participation

The early exposure of technology, such as digital tools using automation and AI, to younger individuals is likely to enhance a positive perception towards the acceptance of robotic dental procedures [83]. In the US, the patient's level of education and standard of living was found to play a role in perceived acceptance of autonomous surgeries [345]. This contrasted to a recent study on the use of AI in dentistry for 511 patients in Saudi Arabia that found no significant effects for age and level of education [346]. In this study, patient-enhanced experience, personalized dental care and cost efficiency had the most impact on a patient's willingness towards advanced dental procedures [346]. The major focus on cost aligns with the previous study in the US where the acceptance jumped to 83% when the costs were halved for less complex procedures [59].

App technologies have begun to gamify good oral care practices in the home to increase participation and awareness of cleaning and diagnostic techniques using visual aids to highlight regions of the mouth to prioritise [336, 347, 348]. For example, OralCam provides deep learning data analysis for "self" examination of users' oral health using smartphones for mostly labial surfaces of teeth [336, 348]. Its dataset consists of annotated oral photos by dental experts, along with inputs of the patient's habits and oral sensitivity, to detect oral conditions and suggest appropriate preventative maintenance or necessary treatment [348]. Furthermore, the advancements in intraoral imaging and scanning have enabled dentists to present a coloured image or animation of the patient's own oral anatomy to improve their understanding of oral health [150-152], reducing the likelihood of miscommunication with patients and possible legal

action. The use of intraoral scanning for dental robots could also facilitate the use of the visual aids to promote safe collaboration with patients during robotic dental procedures.

It should be noted that a patient's fear and psychological response to pain can be influenced by potentially controllable situational and environmental factors (such as smell, temperature and noise), as well as behavioural or emotional factors from their personal expectations [9, 349]. For instance, audiovisual devices can distract patients and improve patient compliance [36, 350]. A lavender scent was also observed to have a calming effect on dental patients undergoing dental procedures [264]. For various dental techniques, the VAS score reduced by 20.47 ± 1.29 after smelling lavender over a procedure, compared to a decrease of 4.07 ± 2.87 for the control group [264]. Perceived pain and discomfort from hypersensitivity can also be reduced by adjusting properties of water sprays and instrument coolants to be closer to the temperature of the human body (e.g. piezo ultrasonic scaler) [351]. Furthermore, advancements in technology may allow for communication in the patient's native language, improving understanding and reducing anxiety [39].

The patient management will be is even more critical in the presence of a dental robot in order to not increase likelihood to react, impacting the progress of procedures. Therefore, since procedures themselves can trigger sensitisation of oral tissues, it is important to focus on increasing the patient's tolerance of the treatment while keeping them calm, comfortable and cooperative without excessive stress [350]. A patient that is uncooperative or has undue stress can produce erratic behaviour that creates an unsafe dental environment with a high risk of an unplanned collision or injury, such as biting down on an instrument controlled by the dental robot. This can harm the patient and risks damaging the instrument which can produce sharp broken components that can be ingested. Also, as treatment progresses, patients usually become more uncomfortable due to the level of noise and vibration [351]. To control the patient's able

to access the robotic dental procedures, it may be necessary to screen for appropriate patients while technology develops to account for uncooperative patients.

Patient block measurements will be vital to detecting the occurrence of patient discomfort to minimise or avoid progressing to a state of patient fear that can compromise their psychological health and wellbeing. The analysis of physiological sensor data can be helpful to estimate a patient's emotional state of mind, rather than relying solely on patient feedback during dental procedures where it is challenging for patients to speak. Proposed sensor measurements include heart rate, blood pressure, body temperature and muscle tension (e.g. electromyography, EMG) for stress and pain, galvanic skin resistance (GSR) response for the presence of sweat, and changes in respiratory rate and oxygen saturation for their ease to breathe in the chosen posture and headrest [264, 350, 352]. The indicators of the patient's physiological response can be combined with pressure sensors integrated into the headrest to detect the stability of the patient's head. Additionally, the type of hand motion and grip strength, and bite strength on the mouth prop, can indicate compliance, pain, fear and anxiety. However, external environmental factors, such as the weather, need to be accounted for to ensure reliability of the psycho-physiological data measurements [350]. Measurement of psychological data may be critical for dental robotics where the patient's face is obscured, limiting the ability to observe their facial expressions.

To inform, distract or manage patients, VR integrations could be used to motivate their cooperation by rewards, feedback and progression in a virtual scene or influence their psychological and behavioural state during procedures [353]. For example, a medical navigation app was used to help children undergoing medical procedures in order to reduce fear, while improving compliance and understanding [354]. Gamification in dentistry could help overcome societal fear and anxiety by distracting patients undergoing dental treatment from their stress, pain and discomfort [233, 355-357]. Despite these benefits, there has been

limited uptake in current practice [358]. This may be due to the size and weight of the headset causing discomfort or reducing the visual working field, along with the need to observe patient facial expressions and keep the patient immobile [358]. As such, these limitations should be mitigated through the development of the patient block that will be designed to monitor the state of the patient. This patient block should also more objectively evaluate the extent of stress instigated by the robot in the case of a malfunction or incident, thereby ensuring the patient receiving sufficient support in the case of potential physical and psychological impact [160].

7.4.2 Dentist Confidence and Adoption

In 2021, a survey of 570 dental students and professionals in Saudi Arabia by Abouzeid *et al.* was conducted to assess their awareness of robotics and AI in dentistry [359]. At an average of 62%, the majority of participants agreed to have knowledge of use cases, a positive attitude and a perception that robotics and AI can be beneficial [359]. Advancing to 2023 in India, 90.6% of a group of 161 dentists, with an average age of 30.17±9.18 years, found robotics and AI beneficial during the COVID-19 pandemic [360]. This study reported that 60.6% were willing to undergo robotic and AI treatment, if necessary [360], similar to the level of confidence in Abouzeid *et al.* (2021). Dental staff were the most confident in their knowledge and attitude, compared to interns, postgraduates, and private practitioners [360].

The adoption of dental robots would not only change the role of the dentist but also the dental assistant. The dental assistants are most likely to be involved in the management of the robotic equipment in dental practices. Similar changes have recently occurred with the introduction of CAD/CAM systems, digital radiography and 3D imaging devices, requiring dental assistants to take on a dynamic role of understanding the operation of the systems, along with their sterilisation and hygiene protocols for infection control [361]. Therefore, it will be important for the dental robot manufacturers to provide the necessary targeted training to both the dentist and dental assistants to ensure proper operation of their equipment.

The dental robot systems should be user friendly to ease training requirements and minimise stress for dental practices. This can also help to reduce the likelihood of errors from unfamiliarity and uncertainty, such as data-related errors from incorrect files or technical faults [362]. In addition, as the robots become more integrated into their practice, standard practice operations will begin to depend on their use and, therefore, will be vulnerable when they fail [362]. To manage this, the robots need to be robust to minimise the impact of technical malfunctions from disrupting procedures, negating the benefit of time saved from increased autonomy [362]. Access for dental practices to dental robots is likely to also depend on the robot manufacturer's business strategy to market. Dentists would be more willing to hire dental robots to reduce upfront implementation costs, while also needing clarity on the ongoing costs for maintenance [362, 363]. As a benefit to the risk of errors, digitalisation makes it easier and provides a source for sharing patient cases between dental professionals [362].

The use of dental robots may increase the willingness of dentists to acknowledge the occurrence of dental errors during dental procedures. The robot creates an additional degree of separation from the operation, limiting the likelihood of human error with good design and side effects of shame and embarrassment associated with the dentist being a "second victim" of the emotional harm from making a mistake [96]. This can help to create a culture of "unified dentistry" with proactive shared learning among dental practices to improve safety awareness of likely and rare dental errors and hazards [35, 96]. Further, this could involve the sharing of anonymous videos of the faults, as long as the patient and operators' privacy can be maintained. This is challenging to achieve in traditional supine postures as the video will require more editing to remove distinguishing facial features [364]. The proposed dental posture with the headrest physically blocks exposure to the patient's face within the operative scene, reducing the risks associated with safety breaches while capturing a highlighted success or incident. For preliminary assistive dental setups, deep learning models are in development for real-time

anonymization during complex and lengthy surgical procedures for both patients and healthcare workers [364].

The traditional levels of surgical autonomy indicate the change in role of the surgeon to be more "hands-off," rather than changes in their responsibility, where they are required to closely monitor the patient, the environment and the quality of automated procedures. The impact on their awareness becomes a greater concern as they become less involved with forms of decision making at higher levels of autonomy [156]. Dentists operating dental robots will need to be able to verify the consistency between the digital model and the patient's mouth to confirm the safety of their digital plans for a given procedure [362]. For this, repeat intraoral scans may be required between visits for specific techniques to manage changes to the patient's bone structure [362]. The potential dependence and requirements of the dental robot on the intraoral scanner accuracy should be considered in its path to market for the robotic manufacturer, potentially limiting the range of options for dentists and adding another upfront cost for dental robot integration.

Concerns in the transparency of previous medical robotics manufacturers for the safety of their devices was brought to light due to the dependence on self-reporting of incidents. In the US, there system requires hospitals to inform manufacturers of a device malfunction or adverse event involving their device, which should then be reported to the FDA by the manufacturer [365]. In 2014, 3697 reports involving the da Vinci system were received by the FDA dated from 1595 to 2012 [366]. As a result of the underreporting, the FDA threatened Intuitive with equipment seizures or fines, forcing Intuitive to make product corrections for allegations against the system and alter their marketing practices to accurately represent the outcomes from surgery [366]. To improve tracking and reporting of risk, the proposed risk supervision system should be developed prior or adjacent to the introduction of the dental robots into dental settings. This can help to provide a more objective analysis of the

performance of the path and robot in terms of patient safety, with less focus on the quality of the technique.

The absence of physical feedback may discourage some dentists from using advanced autonomous robotic systems, particularly after years of training to develop advanced proprioceptive skills. This may be due to concerns for the quality of their techniques without consistent practice or the fear of losing self-confidence and independence [362]. This was a concern for the uptake in use of surgical guides for drilling, although it increases patient safety [362]. Nonetheless, some dentists believe digital tools help refine their skills to produce high quality results [362]. With good visual feedback and robust risk tracking supervision systems, dentists are likely to desire autonomous dental robots for lower risk repetitive dental procedures, such as for charting and cleaning. This can in turn help to develop a more dynamic operative setting for dentists and dental assistants to improve their overall health and wellbeing.

7.5 Contributions

This thesis establishes a guide to begin the development of safe autonomous robotic dentistry for low-risk cleaning and diagnostic dental procedures to benefit dental practices. Design analysis of current technologies highlighted major barriers to patient safety and comfort. This thesis proposed that an altered patient posture, leaning slightly forwards or in prone, can lead to numerous benefits, such as the likelihood of quasi-static collisions, inhalation and ingestion of water and debris, dampen instrument vibrations to the patient's head and reduce the transmission of diseases. Despite these advantages, patient safety was identified as the main concern for the development of autonomous systems. A framework for the automated risk management of dental robots was designed that outlined the need for three supervision systems in terms of instrument safety (the procedure block), environmental stability (the observer block) and patient compliance (the patient block). These safety systems lead to the

creation of dental robot risk awareness in order to overcome the reductions in operator awareness for increasing levels of robot autonomy.

Supervision system developments identified significant hazardous situations for operation of dental robots on conscious patients. As the first step to situation awareness for robotic dental procedures, methods for analysing the safety of a dental instrument's position in the mouth were modelled to create virtual spatial risk measurements. These measurements represent the location of the instrument relative to relevant frames of reference and distances to identified critical dental features, such as the teeth, gingivae, throat entrance, lips, cheeks and tongue. The first two methods (ID1.1–ID1.2) are performance-based which can be used to compare motions of the tip around the teeth and the instrument's location through the mouth opening. In contrast, the next two methods (ID1.3–ID1.4) measure the position of the instrument tip in relation to tracked or expected locations of hard and deformable soft tissues of the mouth in order to estimate the risk of collision with a dental feature, as well as the amount of instrument or soft tissue displacement.

The spatial risk measurements can be a tool to understand the anatomical constraints of the oral cavity for a dental robot. ID1.1 distance measurements can be compared across different techniques to confirm the expected position of the instrument tip relative to a tooth of varying position in the mouth. By comparison, ID1.2 can assist instrument control to minimise contact with the sides of the mouth opening, and further, it can include the depth required to retract out of the mouth to the frontal plane during an emergency. The relative depth into the teeth and gingival pockets from ID1.3 can be used to assess whether a procedure is being carried out at an expected depth, while acknowledging that different instruments will produce varying deflection against the oral features. Finally, ID1.4 can indicate the potential impact with soft oral tissues for the instrument tip. Contact of this form may result in patient harm as instruments, including those for cleaning and diagnosis, can be relatively sharp.

To assess the designed risk management methods for instrument safety, the instantaneous risk measurements were carried out in simulation using a virtual dental environment. A dental setup was developed with a small robot arm and a head model that was linked to the simulation environment with sensors to allow for dynamic patient movement. The various distance measurements were scaled and transformed into four quantitative risk outputs that can be used to describe the level of safety of the instrument during procedures. Verification tests were carried out to compare the occurrence of a high force collision with the detection of high risk from the procedure block risk outputs. These initial developments showcased the ability for the supervision methods to identify the presence of high risk for different instrument paths to assess the safety of dental robotic techniques. Future integrations with a three-state finite state machine could inform the robot of the corresponding accepted mode of human-robot interaction for real-time risk decision making.

The systematic approach to the safety of autonomous dental robot systems aims to standardise the use of automated risk management processes that can improve risk awareness of robotic systems. The risk measures were designed to be transparent and traceable, such that there is transferable understanding between dentists, patients and roboticists, which is critical for the development of robotic medical devices. Further, the combined quantitative approach provides vital resources for the developing robotic technologies and as objective evidence on procedure performance, which can be used to re-create digital dental procedures for post-operative analysis. The methods taken in this thesis begin the stages towards a wholistic understanding of patient safety with the inclusion of the observer and patient block supervision systems, as well as future developments for an automated risk management network which can include analysis of the causes of identified hazards to perform risk reductions and improve the efficiency of robotic dental procedures.

7.6 Future Directions

7.6.1 Optimisation of Dental Techniques

Robotic technologies can standardise repetitive actions to reduce variability and improve patient comfort. Before robots can perform cleaning dental procedures autonomously, the desirable technique motions, forces and instrument tip angles could be digitised to a level of accuracy that meets their clinical requirements [228, 229, 285, 367]. This is necessary before robots can fully integrate into dentistry. Patient-adaptable or patient specific algorithms could be developed from imitation or demonstration-based learning dental techniques trajectories [276, 340], and they may be designed to accommodate variations in dental arch shape, tooth positions, maximal oral opening, and patient cheek elasticity, while also having the option to include safety rewards. Robotic systems may also assess attachment loss during charting if they can accurately discern the location of the cement-enamel junction [278, 368]. However, future developments may need to consider the impact of the shape, wear, power supply and material on the performance of the dental instrument, such as for ultrasonic scaling tips [321, 369], and the changing anatomy of the operative sites during cleaning and restoration.

Following research should focus on automating the robotic control for dental instruments to effectively operate diagnostic devices and clean the teeth and dental pockets with low risk. Initial investigations to automate target localisation using virtual collision avoidance were carried out in Unity (Appendix F). Future work should involve integration with force feedback-control that can allow for simple localisation of the dental arch to produce sufficiently accurate low-risk and low force dental procedures. Further, analysis of the performance of emergency exit paths could make use of the spatial risk measurements to create field flow maps detailing the directions of decreasing risk gradients to avoid harm to oral tissues. These maps could be integrated with 3D occupancy maps used for risk-averse robotic navigation similar to motion path planners, such as A* algorithms that search possible paths

through space to identify the smallest cost (e.g. by time or distance) [183, 184, 370, 371]. The Unity simulation can be combined with the Robot Operating System (ROS) to operate various robots in simulation for their suitability to dental robotic procedures [372].

7.6.2 Simulation of the Dental Environment

Advanced immersive systems involving augmented reality (AR), as well as VR, have been developed as a tool for education and training in medicine and dentistry to promote greater understanding of complex biological systems. The MOOG Simodont provides training for dentists and dental students by tracking the instrument's position around a model with the inclusion of haptic feedback in an attempt to distinguish between different types of tissue structures [373-375]. However, given the complexity of natural anatomy, replicating the feeling of human body tissue is extremely challenging and systems to achieve this must be extremely advanced. The challenge to accurately represent the complexity of the dental environment makes it difficult to develop simulation models for robotic dentistry and then to assess their performance on dental models. As with mobile robots, sources of error will largely relate to the incomplete digital model of the environment, particularly when carrying out tests in simulation [130]. Without full head patient scans and tissue displacement measurements, oral soft tissues will always create ambiguity unless they can be accurately digitally modelled in real time for a patient [179, 180].

Early dental robot developments may choose to use lip or cheek retractors and mouth props with tongue guards to improve the safety of dental procedures using sharper instruments. Although addressing soft tissues was outside the scope of this thesis, the procedure block includes risks associated with the deformable soft tissues based on their expected relative position near the tracked hard tissue dental arches. Performing multi-point instrument risk tracking beyond the tip of the instrument could capture a more accurate representation of the risk of collision to the oral cavity, though the risks of sharp areas should be prioritised in risk

management. Moreover, the simulation developed for this thesis is a step towards a dynamic digital twin model that could incorporate improving soft tissue models for advanced collision analysis.

7.6.3 Artificial Intelligence for Autonomy

"Black box" deep learning methods perform well in structured environments where their tasks are well defined [338]. For example, an AI deep learning model that detected regions of dental plaque on teeth from targeted visual perception of intraoral images was more accurate than a trained dentist [336]. Although this is not suitable to risk-related decision-making methods for dental robot safety, individual supervision block measurements could incorporate simplified task-based AI to detect the location of the tongue and blood in the mouth from camera data, as well as the analysis of complex patient physiological data measured from a variety of sensors. This information can be used as inputs into the pre-defined supervision observer and patient blocks as interpreted data to assess whether the dental environment and patient are stable for the robotic operation. As numerous safety measurements of the supervision blocks overlap with other measured data, the presence of using AI for task-based data collection should not compromise the uncertainty and trustworthiness of the supervision system and, therefore, the dental robot.

A challenge for the development of autonomous dental robot systems is the hand-over in decision-making for medical applications. Whether built into a dental robot or as a standalone software, any system that performs diagnosis, prevention, monitoring, treatment or alleviation of diseases requires approval before successful commercialisation [376]. However, the degree of difficulty depends on the severity of the disease and the system's function [376]. This makes cleaning procedures for gingivitis and periodontitis, which only aim to improve the patient's oral health, more suited for higher levels of autonomy. Considerations will need to be taken into account for the use of higher levels of autonomy for more invasive techniques. These

operations are likely to remain supervised by a trained dental expert for operation. Unlike these systems, the supervision system has been designed to focus on risk features, rather than the management of dental diseases, minimising the complexity associated with automating medical decision making processes and lowers the barriers to receive approval. With safety mechanisms standardised for dental procedures, the compliant dental robotic systems can focus on receiving approval for operating at higher levels of autonomy.

7.6.4 Dental Robot System Testing

Future investigation into the dental procedure simulation must be carried out with improved instrument paths to assess the safety of robotic techniques and robustness of the developing supervision systems and the finite state machine for the mode of interaction. This could include improvements to the Unity simulation system to include estimated risk tracking along designed paths prior to applications with the robot. Identified high risk, and force for force feedback control systems, should trigger a form of emergency response for the robotic system. These risk levels simplify the risk decision-making process to ensure the robot responds to high risk before the causes of the risks are identified. The high-risk state could enforce that the robot pauses the procedure and assess the changing risk of the system. However, if an unacceptable risk is identified, the robot should begin to perform an emergency exit [74]. Future developments can be adjusted by applying weightings to tailor individual risk measures for different dental procedures, setup and patients before taking the maximum for its risk output. For instance, drilling into teeth during a restorative technique could scale the risk for depth into the tooth surface (ID1.3, $d_{1.3x}$).

The ability to fine tune parameters of the procedure block supervision system is beneficial as dental procedures can greatly vary, while the large number of risk measurements maintains high redundancy for safety. The use of Unity enables comparisons between different robotic designs and setups in testing with a variety of simulated environmental challenges and

complex patient head movements. This could be extended to include the impact the design setup on the perceived vibrations and noises from dental instruments. Integration with robotic systems could aid progress towards regulatory approval by standardising safety assessments for dental robots, thereby providing them with a tool to diagnose safety concerns [328]. The current setup could be used to assess and perform safety checks of Perceptive's dental robot that also uses the Meca500 robot arm to perform crown preparation on an awake patient [208, 217]. In addition, the patient posture change proposed in Chapter 3 could be considered to further improve patient safety during the automated procedures. However, this would require advanced visualisation of the oral cavity while the observer block supervision system is under development.

7.7 Conclusion

As robots are increasingly considered in dentistry, their adoption will largely be influenced by factors impacting the safety of a dental procedure, such as the procedure type, the design setup, the robot's risk awareness, and the patient's cooperation. This project encapsulated a broader understanding of designing for safety that included the development of safety measurements as precursors to the development of safety mechanisms or skills for robotic medical devices. These measurements aim to quantify risk in a way that is easily understood, manageable, and comparable. In addition to an innovative dental setup, this thesis promotes the development of automated risk management processes for autonomous robotic systems interacting with untrained patients in dynamic medical applications. This goes beyond current methods that rely on compliance to safety protocols that are built in accordance with tabulated hazard assessments. Even with potential advancements in nanodentistry with microrobots for dental treatments [333], the global demand for accessible dental care services will foresee the continued application of manual or future robotic techniques with dental instruments.

References

[1] OpenStax, C., "Anatomy & physiology," *Human Anatomy & Physiology,* 2014.

[2] Roberts, A. P. and Mullany, P., "Oral biofilms: a reservoir of transferable, bacterial, antimicrobial resistance," *Expert Review of Anti-infective Therapy,* vol. 8, no. 12, pp. 1441-1450, 2010.

[3] Auday, B. C., Buratovich, M. A., and Marrocco, G. F., *Salem Health: Magill's Medical Guide, Eighth Edition*. Ipswich, UNITED STATES: Salem Press, 2018.

[4] Angelino, K., Edlund, D. A., and Shah, P., "Near-Infrared Imaging for Detecting Caries and Structural Deformities in Teeth," *IEEE Journal of Translational Engineering in Health and Medicine,* vol. 5, pp. 1-7, 2017.

[5] NIH, "Oral Health in America: Advances and Challenges," National Institutes of Health, Online2021, vol. Section 2A, Oral Health Across the Lifespan: Children Available: https://www.nidcr.nih.gov/sites/default/files/2021-12/Oral-Health-in-America-Advances-and-Challenges.pdf#page=159, Accessed on: 22 October 2024.

[6] Pihlstrom, B. L., Michalowicz, B. S., and Johnson, N. W., "Periodontal diseases," *The Lancet,* vol. 366, no. 9499, pp. 1809-1820, 2005.

[7] Healthwise Staff. (2019). *Toothache and Gum Problems*. Available: https://www.uofmhealth.org/health-library/tooth#:~:text=Gingivitis%20is%20a%20gum%20disease,problems%20with%20the%20gum%20tissue.

[8] Hobbins, S., Chapple, I. L., Sapey, E., and Stockley, R. A., "Is periodontitis a comorbidity of COPD or can associations be explained by shared risk factors/behaviors?," (in eng), *International journal of chronic obstructive pulmonary disease,* vol. 12, pp. 1339-1349, 2017.

[9] Canakci, V. and Canakci, C. F., "Pain levels in patients during periodontal probing and mechanical non-surgical therapy," *Clinical Oral Investigations,* vol. 11, no. 4, pp. 377-383, 2007.

[10] Vollmer, A., Vollmer, M., Lang, G., Straub, A., Shavlokhova, V., Kübler, A., Gubik, S. *et al.*, "Associations between Periodontitis and COPD: An Artificial Intelligence-Based Analysis of NHANES III," *Journal of Clinical Medicine*, vol. 11, no. 23. doi: 10.3390/jcm11237210 Available: https://www.mdpi.com/2077-0383/11/23/7210

[11] Ortuéo, D., Martínez, C., and Caneo, C., "Association between number of remaining teeth and incident depression in a rural Chilean cohort," (in English), *BMC Oral Health,* Report vol. 23, p. NA, 2023.

[12] Muhammad, T. and Srivastava, S., "Tooth loss and associated self-rated health and psychological and subjective wellbeing among community-dwelling older adults: A cross-sectional study in India," (in English), *BMC Public Health,* vol. 22, pp. 1-11, 2022.

[13] Davis, D. M., Fiske, J., Scott, B., and Radford, D. R., "The emotional effects of tooth loss in a group of partially dentate people: a quantitative study," (in English), *Oral Health,* vol. 92, no. 11, pp. 11-20, 2002.

[14] James, S. L., Abate, D., Abate, K. H., Abay, S. M., Abbafati, C., Abbasi, N., Abbastabar, H. *et al.*, "Global, regional, and national incidence, prevalence, and years lived with disability for 354 diseases and injuries for 195 countries and territories, 1990-2017: a systematic analysis for the Global Burden of Disease Study 2017," *The Lancet,* vol. 392, no. 10159, pp. 1789-1858, 2018.

References

[15] Kassebaum, N. J., Bernabé, E., Dahiya, M., Bhandari, B., Murray, C. J. L., and Marcenes, W., "Global Burden of Severe Periodontitis in 1990-2010: A Systematic Review and Meta-regression," *Journal of Dental Research,* vol. 93, no. 11, pp. 1045-1053, 2014.

[16] Wagner, R. (2016). *WHY GUM DISEASE MAY INDICATE OTHER HEALTH COMPLICATIONS*. Available: https://www.thewagnercentre.com/2016/08/05/gum-disease-may-indicate-health-complications/

[17] DHSV, "Links between oral health and general health the case for action," Dental Health Services Victoria 2011, Available: https://www.dhsv.org.au/__data/assets/pdf_file/0013/2515/links-between-oral-health-and-general-health-the-case-for-action.pdf.

[18] Ide, M., Harris, M., Stevens, A., Sussams, R., Hopkins, V., Culliford, D., Fuller, J. *et al.*, "Periodontitis and Cognitive Decline in Alzheimer's Disease," (in English), *PLoS One,* vol. 11, no. 3, 2016.

[19] Yasny, J. S. and Herlich, A., "Perioperative Dental Evaluation," *Mount Sinai Journal of Medicine: A Journal of Translational and Personalized Medicine,* vol. 79, no. 1, pp. 34-45, 2012.

[20] Zoellner, H., "Dental Infection and Vascular Disease," *Seminars in thrombosis and hemostasis,* vol. 37, no. 3, pp. 181-192, 2011.

[21] Gurav, A. N., "Alzheimer's disease and periodontitis - An elusive link," *Revista da Associacao Medica Brasileira,* vol. 60, no. 2, pp. 173-180, 2014.

[22] Kotzé, M. J., "Prosthetic joint infection, dental treatment and antibiotic prophylaxis," (in English), *Orthopedic Reviews,* vol. 1, no. 1, 2009.

[23] Mirzashahi, B., Tonkaboni, A., Chehrassan, M., Doosti, R., and Kharazifard, M. J., "The role of poor oral health in surgical site infection following elective spinal surgery," *MUSCULOSKELETAL SURGERY,* vol. 103, no. 2, pp. 167-171, 2019.

[24] WHO. (2022, 12 March 2023). *Ageing and health*. Available: https://www.who.int/news-room/fact-sheets/detail/ageing-and-health

[25] Huber, M., "Health expenditure trends in OECD countries, 1970-1997," (in English), *Health Care Financing Review,* vol. 21, no. 2, pp. 99-117, 1999.

[26] WHO. (2022). *Global health expenditure database*. Available: https://apps.who.int/nha/database/Select/Indicators/en

[27] Peres, M. A., Macpherson, L. M. D., Weyant, R. J., Daly, B., Venturelli, R., Mathur, M. R., Listl, S. *et al.*, "Oral diseases: a global public health challenge," (in English), *The Lancet,* vol. 394, no. 10194, pp. 249-260, 2019.

[28] Righolt, A. J., Jevdjevic, M., Marcenes, W., and Listl, S., "Global-, Regional-, and Country-Level Economic Impacts of Dental Diseases in 2015," *Journal of Dental Research,* vol. 97, no. 5, pp. 501-507, 2018.

[29] Patel, J., Wallace, J., Doshi, M., Gadanya, M., Ben Yahya, I., Roseman, J., and Srisilapanan, P., "Oral health for healthy ageing," *The Lancet Healthy Longevity,* vol. 2, no. 8, pp. e521-e527, 2021.

[30] HPI, "National Dental Expenditures," Health Policy Institute, Online2022, Available: https://www.ada.org/-/media/project/ada-organization/ada/ada-org/files/resources/research/hpi/national_dental_expenditures_2022_infographic.pdf?rev=50ddc425582146878b26675f310406c0&hash=955F053A243B8EE8A27BE82149B54D11, Accessed on: 22 October 2024.

[31] OECD. Health expenditure indicators [Online]. Available: https://www.oecd-ilibrary.org/content/data/data-00349-en

[32] AIHW, "Oral health and dental care in Australia," Australian Institute of Health and Welfare, Canberra2020, Available: https://www.aihw.gov.au/reports/dental-oral-health/oral-health-and-dental-care-in-australia.

[33] Australian Institute of Health and Welfare, "Oral health and dental care in Australia," AIHW, Canberra2023, Available: https://www.aihw.gov.au/reports/dental-oral-health/oral-health-and-dental-care-in-australia.

[34] World Bank, W. D. I. Total Population of Australia [Online]. Available: https://databank.worldbank.org/reports.aspx?source=world-development-indicators#

[35] Yamalik, N. and Perea Pérez, B., "Patient safety and dentistry: what do we need to know? Fundamentals of patient safety, the safety culture and implementation of patient safety measures in dental practice," *International Dental Journal,* vol. 62, no. 4, pp. 189-196, 2012.

[36] De Stefano, R., "Psychological Factors in Dental Patient Care: Odontophobia," (in eng), *Medicina (Kaunas, Lithuania),* vol. 55, no. 10, p. 678, 2019.

[37] "New device set to combat fear of the dentist's drill," *Biotech Week,* p. 1411, 2011.

[38] Humphris, G., Crawford, J. R., Hill, K., Gilbert, A., and Freeman, R., "UK population norms for the modified dental anxiety scale with percentile calculator: adult dental health survey 2009 results," *BMC Oral Health,* vol. 13, no. 1, p. 29, 2013.

References

[39] Armfield, J., "The extent and nature of dental fear and phobia in Australia," *Australian Dental Journal,* vol. 55, no. 4, pp. 368-377, 2010.

[40] Duckett, S., Cowgill, M., and Swerissen, H. (2019). *Filling the gap | A universal dental scheme for Australia*. Available: https://grattan.edu.au/wp-content/uploads/2019/03/915-Filling-the-gap-A-universal-dental-scheme-for-Australia.pdf

[41] Uppoor, A. S., Lohi, H. S., and Nayak, D., "Periodontitis and Alzheimer's disease: oral systemic link still on the rise?," *Gerodontology,* vol. 30, no. 3, pp. 239-242, 2013.

[42] Abbayya, K., Puthanakar, N., Naduwinmani, S., and Chidambar, Y., "Association between periodontitis and Alzheimer's disease," (in English), *North American Journal of Medical Sciences,* Report vol. 7, p. 241, 2015.

[43] "Link between gum disease and cognitive decline in Alzheimer's," in *Mental Health Weekly Digest*, ed, 2016, p. 94.

[44] Jae-Young, L., Lim, K.-C., So-Yun, K., Paik, H.-R., Young-Jae, K., and Bo-Hyoung Jin, "Oral health status of the disabled compared with that of the non-disabled in Korea: A propensity score matching analysis," (in English), *PLoS One,* vol. 14, no. 1, 2019.

[45] Jorm, A., "The government will spend $48 million to safeguard mental health. Extending JobKeeper would safeguard it even more," in *The Conversation* ed. Online, 2020.

[46] Gamio, L., "The Workers Who Face the Greatest Coronavirus Risk," in *The New York Times*, ed. Online, 2020.

[47] "Don't Let COVID-19 Delay Your Dental Visit—Dentists Warn Patients About the Importance of Preventive Care," in *University Wire*, ed. Carlsbad, 2020.

[48] Kavitha, A., Bhavana, V., Aliveni, A., Swetha, K., Lakshmi, D. S., and Purnima, J., "Outlook of Indian Population towards Dental Treatments Post-COVID-19 Pandemic - An online survey," (in English), *Journal of Advanced Medical and Dental Sciences Research,* vol. 8, no. 7, pp. 44-48, 2020.

[49] Ogunbodede, E. O., Kida, I. A., Madjapa, H. S., Amedari, M., Ehizele, A., Mutave, R., Sodipo, B. *et al.*, "Oral Health Inequalities between Rural and Urban Populations of the African and Middle East Region," *Advances in Dental Research,* vol. 27, no. 1, pp. 18-25, 2015.

[50] Kandelman, D., Arpin, S., Baez, R. J., Baehni, P. C., and Petersen, P. E., "Oral health care systems in developing and developed countries," *Periodontology 2000,* vol. 60, no. 1, pp. 98-109, 2012.

[51] National Rural Health Alliance, "THE HEALTH OF PEOPLE LIVING IN REMOTE AUSTRALIA," 2016, Available: https://www.ruralhealth.org.au/sites/default/files/publications/nrha-remote-health-fs-election2016.pdf, Accessed on: 2 March 2023.

[52] (2014, December 4) Volunteer dentists praised. *Bite Magazine*. Available: https://www.bitemagazine.com.au/volunteer-dentists-praised/

[53] (2023). *Dentist average salary in Australia, 2023*. Available: https://au.talent.com/salary?job=dentist

[54] Wen, P.-C., Lee, C. B., Chang, Y.-H., Ku, L.-J. E., and Li, C.-Y., "Demographic and rural-urban variations in dental service utilization in Taiwan," *Rural and remote health,* vol. 17, no. 3, pp. 4161-4161, 2017.

[55] Somkotra, T. and Detsomboonrat, P., "Is there equity in oral healthcare utilization: experience after achieving Universal Coverage," *Community Dentistry and Oral Epidemiology,* vol. 37, no. 1, pp. 85-96, 2009.

[56] Meara, J. G., Leather, A. J. M., Hagander, L., Alkire, B. C., Alonso, N., Ameh, E. A., Bickler, S. W. *et al.*, "Global Surgery 2030: evidence and solutions for achieving health, welfare, and economic development," (in English), *The Lancet,* vol. 386, no. 9993, pp. 569-624, 2015.

[57] Dupont, P. E., Nelson, B. J., Goldfarb, M., Hannaford, B., Menciassi, A., O'Malley, M. K., Simaan, N. *et al.*, "A decade retrospective of medical robotics research from 2010 to 2020," *Science Robotics,* vol. 6, no. 60, p. eabi8017, 2021.

[58] Mohammad, S., "Robotic surgery," *Journal of Oral Biology and Craniofacial Research,* vol. 3, no. 1, p. 2, 2013.

[59] "Patients more likely to accept robotic dentistry for non-invasive procedures," in *NewsRx Health & Science*, ed: NewsRX LLC, 2018, p. 141.

[60] "Robotic surgery," *Dental Abstracts,* vol. 58, no. 6, pp. 311-313, 2013.

[61] Mavroforou, A., Michalodimitrakis, E., Hatzitheofilou, C., and Giannoukas, A., "Legal and ethical issues in robotic surgery," (in English), *International Angiology,* vol. 29, no. 1, pp. 75-9, 2010.

[62] Park, E. S., Shum, J. W., Bui, T. G., Bell, R. B., and Dierks, E. J., "Robotic Surgery," *Oral and Maxillofacial Surgery Clinics of North America,* vol. 25, no. 1, pp. 49-59, 2013.

[63] Borumandi, F., Heliotis, M., Kerawala, C., Bisase, B., and Cascarini, L., "Role of robotic surgery in oral and maxillofacial, and head and neck surgery," *British Journal of Oral and Maxillofacial Surgery,* vol. 50, no. 5, pp. 389-393, 2012.

[64] Barbash, G. and Glied, S., "New Technology and Health Care Costs -- The Case of Robot-Assisted Surgery," (in English), *The New England Journal of Medicine,* vol. 363, no. 8, pp. 701-4, 2010.

[65] Higgins, R. M., Frelich, M. J., Bosler, M. E., and Gould, J. C., "Cost analysis of robotic versus laparoscopic general surgery procedures," (in English), *Surgical Endoscopy,* vol. 31, no. 1, pp. 185-192, 2017.

[66] Matheson, E., Minto, R., Zampieri, E. G. G., Faccio, M., and Rosati, G., "Human–Robot Collaboration in Manufacturing Applications: A Review," *Robotics,* vol. 8, no. 4, p. 100, 2019.

[67] Villani, L., De Santis, A., Lippiello, V., and Siciliano, B., "Human-aware Interaction Control of Robot Manipulators Based on Force and Vision," London, 2009, pp. 209-225: Springer London.

[68] Shademan, A., Decker, R. S., Opfermann, J. D., Leonard, S., Krieger, A., and Kim, P. C. W., "Supervised autonomous robotic soft tissue surgery," *Science Translational Medicine,* vol. 8, no. 337, p. 337ra64, 2016.

[69] Corke, P., *Robotics, Vision and Control Fundamental Algorithms In MATLAB® Second, Completely Revised, Extended And Updated Edition*, 2nd ed. 2017. ed. (Springer Tracts in Advanced Robotics, 118). Cham: Springer International Publishing, 2017.

[70] Malm, T., "Safety design process for collaborative robots," VTT Technical Research Centre of Finland, Online2022, Available: https://publications.vtt.fi/julkaisut/muut/2022/VTT-R-00062-22.pdf, Accessed on: 3 March 2024.

[71] ISO. (2016). *TECHNICAL SPECIFICATION ISO/TS 15066:2016 (1st ed.)*. Available: https://www.diag.uniroma1.it/deluca/pHRI_elective/ISO_TS_15066_2016_en.pdf

[72] (2020). *A flexible and lightweight robotic arm*. Available: https://www.universal-robots.com/products/ur5-robot/

[73] Ars Automation. (2020). *A new flexible feeder for automatic parts feeding to an assembly workstation*. Available: https://www.youtube.com/watch?v=p14SRMQ0tOE

[74] Sharkawy, A.-N., Koustoumpardis, P. N., and Aspragathos, N., "Human–robot collisions detection for safe human–robot interaction using one multi-input–output neural network," *Soft Computing,* vol. 24, no. 9, pp. 6687-6719, 2020.

[75] Virk, G. S., "Collaborative robot safety requirements for manufacturing," in *Robot safety, Next-Generation Robotics & Automation, Birmingham, UK*, InnoTecUK, Ed., ed. Online: London Business Conferences Group, 2016.

[76] Guiochet, J., "Hazard analysis of human–robot interactions with HAZOP–UML," *Safety Science,* vol. 84, pp. 225-237, 2016.

[77] ISO. (2011). *ISO 10218-1:2011 (2nd ed.)*. Available: https://www.iso.org/standard/51330.html

[78] ISO. (2011). *ISO 10218-2:2011 (1st ed.)*. Available: https://www.iso.org/standard/41571.html

[79] ISO. (2016). *ISO/TS 15066:2016 (1st ed.)*. Available: https://www.iso.org/standard/62996.html

[80] Rosenstrauch, M. J. and Krüger, J., "Safe human-robot-collaboration-introduction and experiment using ISO/TS 15066," in *2017 3rd International Conference on Control, Automation and Robotics (ICCAR)*, 2017, pp. 740-744.

[81] Althoff, M., Giusti, A., Liu, S. B., and Pereira, A., "Effortless creation of safe robots from modules through self-programming and self-verification," *Science Robotics,* vol. 4, no. 31, p. eaaw1924, 2019.

[82] Nix, D. (2019). *Can Emergency Stop be used as an "on/off" control?* Available: https://machinerysafety101.com/2019/04/20/can-emergency-stop-be-used-as-an-on-off-control/

[83] Maurtua, I., Ibarguren, A., Kildal, J., Susperregi, L., and Sierra, B., "Human–robot collaboration in industrial applications:Safety, interaction and trust," *International Journal of Advanced Robotic Systems,* vol. 14, no. 4, p. 1729881417716010, 2017.

[84] Aljanakh, M., Shaikh, S., Siddiqui, A. A., Al-Mansour, M., and Hassan, S. S., "Prevalence of musculoskeletal disorders among dentists in the Hail Region of Saudi Arabia," (in eng), *Annals of Saudi medicine,* vol. 35, no. 6, pp. 456-461, 2015.

[85] Joshi, A., Soni, H., Hedaoo, A., Bande, C., Goel, M., and Mishra, A., "Prevalence of musculoskeletal disorders affecting general dental practitioners in nagpur and proposal of a new composite classification system," *Journal of Indian Association of Public Health Dentistry,* Original Article vol. 17, no. 3, pp. 241-246, 2019.

[86] (2014). *Disability Income Protection and Office Overhead Expense*. Available: https://www.insurance.ada.org/disability-insurance.aspx

[87] Bedi, H. S., Moon, N. J., Bhatia, V., Sidhu, G. K., and Khan, N., "Evaluation of Musculoskeletal Disorders in Dentists and Application of DMAIC Technique to Improve the Ergonomics at Dental Clinics and Meta-Analysis of Literature," *Journal of clinical and diagnostic research,* vol. 9, no. 6, pp. ZC01-ZC03, 2015.

[88] Leggat, P. and Smith, D., "Prevalence of percutaneous exposure incidents amongst dentists in Queensland," *Australian Dental Journal,* vol. 51, no. 2, pp. 158-161, 2006.

[89] ADA, Guidelines for Infection Prevention and Control, Davis, S., ed., 3rd ed. Online: Australian Dental Association 2024. [Online]. Available: https://ada.org.au/media/m42bj5e1/ada_guidelines_infection_control_guidelines.pdf.

[90] Goetze, E. (2020). *COVID-19 restrictions on dentists prompt warning to 'step up your oral hygiene'*. Available: https://www.abc.net.au/news/2020-03-31/coronavirus-can-i-go-to-the-dentist-saliva-blood-covid-19/12105738

[91] DBA. (2014). *Code of conduct*. Available: https://www.dentalboard.gov.au/Codes-Guidelines/Policies-Codes-Guidelines/Code-of-conduct.aspx

[92] ACSQHC, NSQHS Standards Guide for Dental Practices and Services, Online: Australian Commission on Safety and Quality in Health Care, 2015. [Online]. Available: https://www.safetyandquality.gov.au/sites/default/files/migrated/NSQHS-Standards-Guide-for-Dental-Practices-and-Services-November-2015.pdf.

[93] Thusu, S., Panesar, S., and Bedi, R., "Patient safety in dentistry – state of play as revealed by a national database of errors," *British Dental Journal,* vol. 213, no. 3, pp. E3-E3, 2012.

[94] (2016). *Dental Negligence*. Available: www.bannisterlaw.com.au/dental-negligence/

[95] Perea-Pérez, B., Labajo-González, E., Acosta-Gío, A. E., and Yamalik, N., "Eleven Basic Procedures/Practices for Dental Patient Safety," *Journal of patient safety,* vol. 16, no. 1, pp. 36-40, 2020.

[96] Bailey, E. and Dungarwalla, M., "Developing a Patient Safety Culture in Primary Dental Care," *Primary Dental Journal,* vol. 10, no. 1, pp. 89-95, 2021.

[97] Taicher, S., "Wrong tooth extraction: root cause analysis," *Quintessence Int,* vol. 41, pp. 869-72, 2010.

[98] Saraf, S. P., Saraf, P. A., Ratnakar, P., Hugar, S., Karan, S., and Tamgond, S., "Wrong tooth extraction--a cut throat in dental practice: an evidence based literature review," (in English), *Indian Journal of Dental Advancements,* Report vol. 7, p. 51+, 2015.

[99] Cullingham, P., Saksena, A., and Pemberton, M. N., "Patient safety: reducing the risk of wrong tooth extraction," *British Dental Journal,* vol. 222, no. 10, pp. 759-763, 2017.

[100] Athanassoglou, V., Patel, A., McGuire, B., Higgs, A., Dover, M. S., Brennan, P. A., Banerjee, A. *et al.*, "Systematic review of benefits or harms of routine anaesthetist-inserted throat packs in adults: practice recommendations for inserting and counting throat packs," *Anaesthesia,* vol. 73, no. 5, pp. 612-618, 2018.

[101] Smith, R. A. (2007). *Mark My Tooth*. Available: https://psnet.ahrq.gov/web-mm/mark-my-tooth?q=/webmm/case/156

[102] Afrow, J. (2018). *Joint Commission In Dental Settings*. Available: https://www.jointcommission.org/assets/1/6/The_Joint_Commission_Dental_Care_Presentation.pdf

[103] Care For Smiles Dental. (2018). *The FDI Dental Numbering System*. Available: https://www.careforsmiles.com.au/smile-gallery/fdi/

[104] Turcot, A., Hamel, D., and Tessier, M., "Hand-Arm Vibration Syndrome in Dentistry: A Questionnaire Survey among Dentists and Review of Literature," *Proceedings,* vol. 86, no. 1, p. 17, 2023.

[105] Cezar-Vaz, M. R., Daiani, M. X., Clarice Alves, B., Vaz, J. C., Letícia Silveira, C., Cynthia Fontella, S. A., Valdecir Zavarese da, C. *et al.*, "Musculoskeletal Pain in the Neck and Lower Back Regions among PHC Workers: Association between Workload, Mental Disorders, and Strategies to Manage Pain," (in English), *Healthcare,* vol. 11, no. 3, p. 365, 2023.

[106] Leggat, P. and Smith, D., "Musculoskeletal disorders self-reported by dentists in Queensland, Australia," *Australian Dental Journal,* vol. 51, no. 4, pp. 324-327, 2006.

[107] Myers, J., John, A., Kimball, S., and Fruits, T., "Prevalence of tinnitus and noise-induced hearing loss in dentists," (in English), *Noise & Health,* vol. 18, no. 85, 2016.

[108] Collin, V., Toon, M., O'Selmo, E., Reynolds, L., and Whitehead, P., "A survey of stress, burnout and well-being in UK dentists," (in English), *British Dental Journal,* vol. 226, no. 1, p. 40, 2019.

[109] Lo Sasso, A. T., Starkel, R. L., Warren, M. N., Guay, A. H., and Vujicic, M., "Practice settings and dentists' job satisfaction," *The Journal of the American Dental Association,* vol. 146, no. 8, pp. 600-609, 2015.

[110] Kiersz, A., Gillett, R., and Hoff, M., "47 jobs that will always be bad for your health, and how much they pay," in *Business Insider*, ed. Online: Insider Inc, 2020.

[111] NHS Improvement, "Provisional publication of Never Events reported as occurring between 1 April 2018 and 31 March 2019," National Health Service NHS England 2019, Available: https://www.england.nhs.uk/wp-content/uploads/2020/08/Provisional_publication_-__NE_1_April_2018_to_31_March_2019.pdf, Accessed on: 9 September 2020.

[112] Varenne, B., Petersen, P. E., and Ouattara, S., "Oral health status of children and adults in urban and rural areas of Burkina Faso, Africa," *International Dental Journal,* vol. 54, no. 2, pp. 83-89, 2004.

[113] Rello, J., Koulenti, D., Blot, S., Sierra, R., Diaz, E., De Waele, J. J., Macor, A. *et al.*, "Oral care practices in intensive care units: a survey of 59 European ICUs," (in English), *Intensive Care Medicine,* vol. 33, no. 6, pp. 1066-70, 2007.
[114] Jones, D. J., Munro, C. L., and Grap, M. J., "Natural history of dental plaque accumulation in mechanically ventilated adults: A descriptive correlational study," (in English), *Intensive & Critical Care Nursing,* vol. 27, no. 6, pp. 299-304, 2011.
[115] Sakaeda, G., Matsubara, T., Ishii, H., and Takanishi, A., "Development of automatic teeth cleaning robot driven by cam mechanism," in *2017 IEEE International Conference on Mechatronics and Automation (ICMA)*, 2017, pp. 536-540.
[116] Yuen, H. K., Wolf, B. J., Bandyopadhyay, D., Magruder, K. M., Selassie, A. W., and Salinas, C. F., "Factors that limit access to dental care for adults with spinal cord injury," *Special Care in Dentistry,* vol. 30, no. 4, pp. 151-156, 2010.
[117] Horner-Johnson, W. and Dobbertin, K., "Dental insurance and dental care among working-age adults: differences by type and complexity of disability," *Journal of Public Health Dentistry,* vol. 76, no. 4, pp. 330-339, 2016.
[118] da Rosa, S. V., Moysés, S. J., Theis, L. C., Soares, R. C., Moysés, S. T., Werneck, R. I., and Rocha, J. S., "Barriers in Access to Dental Services Hindering the Treatment of People with Disabilities: A Systematic Review," (in eng), *International journal of dentistry,* vol. 2020, pp. 9074618-9074618, 2020.
[119] Wilson, N. J., Lin, Z., Villarosa, A., Lewis, P., Philip, P., Sumar, B., and George, A., "Countering the poor oral health of people with intellectual and developmental disability: a scoping literature review," *BMC Public Health,* vol. 19, no. 1, p. 1530, 2019.
[120] (2022). *Dental Care*. Available: https://www.alz.org/help-support/caregiving/daily-care/dental-care
[121] D'Addazio, G., Santilli, M., Sinjari, B., Xhajanka, E., Rexhepi, I., Mangifesta, R., and Caputi, S., "Access to Dental Care-A Survey from Dentists, People with Disabilities and Caregivers," (in eng), *International journal of environmental research and public health,* vol. 18, no. 4, p. 1556, 2021.
[122] AIHW, S, C., JE, H., and A, E., "Oral health and dental care in Australia: key facts and figures 2015," AIHW, Canberra2016, Available: https://www.aihw.gov.au/getmedia/57922dca-62f3-4bf7-9ddc-6d8e550c7c58/19000.pdf.aspx?inline=true.
[123] Grap, M. J., Munro, C. L., Ashtiani, B., and Bryant, S., "Oral care interventions in critical care: frequency and documentation," (in English), *American Journal of Critical Care,* Article vol. 12, p. 113+, 2003.
[124] Haveman, C. W. and Redding, S. W., "Dental management and treatment of xerostomic patients [Patients with "dry mouth"]," (in English), *Oral Health,* vol. 89, no. 10, pp. 53-71, 1999.
[125] Kumar, S., Gupta, R., Arora, R., and Saxena, S., "Severe oropharyngeal trauma caused by toothbrush - case report and review of 13 cases," (in English), *British Dental Journal,* vol. 205, no. 8, pp. 443-7, 2008.
[126] Poirier, B., Jensen, E., and Sethi, S., "The evolution of the teledentistry landscape in Australia: A scoping review," *Australian Journal of Rural Health,* vol. 30, no. 4, pp. 434-441, 2022.
[127] Woodford, S. C., Robinson, D. L., Mehl, A., Peter, V. S. L., and Ackland, D. C., "Measurement of normal and pathological mandibular and temporomandibular joint kinematics: A systematic review," (in English), *Journal of Biomechanics,* vol. 111, 2020.
[128] Borenstein, J., Everett, H. R., Feng, L., and Wehe, D., "Mobile robot positioning: Sensors and techniques," *Journal of Robotic Systems,* vol. 14, no. 4, pp. 231-249, 1997.
[129] Kalaitzakis, M., Cain, B., Carroll, S., Ambrosi, A., Whitehead, C., and Vitzilaios, N., "Fiducial Markers for Pose Estimation," (in English), *Journal of Intelligent & Robotic Systems,* vol. 101, no. 4, 2021.
[130] Siegwart, R., Nourbakhsh, I. R., and Scaramuzza, D., *Introduction to Autonomous Mobile Robots, Second Edition*. Cambridge, UNITED STATES: MIT Press, 2011.
[131] Hata, N., "Surgical Navigation Technology," in *Intraoperative Imaging and Image-Guided Therapy*, Jolesz, F. A., Ed. New York, NY: Springer New York, 2014, pp. 249-257.
[132] Brief, J., Edinger, D., Hassfeld, S., and Eggers, G., "Accuracy of image-guided implantology," *Clinical Oral Implants Research,* vol. 16, no. 4, pp. 495-501, 2005.
[133] Gambarini, G., Galli, M., Stefanelli, L. V., Di Nardo, D., Morese, A., Seracchiani, M., De Angelis, F. *et al.*, "Endodontic Microsurgery Using Dynamic Navigation System: A Case Report," *Journal of Endodontics,* vol. 45, no. 11, pp. 1397-1402.e6, 2019.
[134] (2020). *MicroTracker* Available: https://www.claronav.com/microntracker/
[135] (2020). *NaviDent Targeting Perfection*. Available: https://www.claronav.com/navident/
[136] (2020). *X-Guide*. Available: https://www.nobelbiocare.com/en-int/x-guide
[137] (2011). *Precision for a perfect smile* Available: http://www.robodent.de/page61/page61.html
[138] (2011). *Precision for a perfect smile | Instruments*. Available: http://www.robodent.de/page61/page66/page66.html
[139] (2020). *NaviDent Targeting Perfection Surgical Videos*. Available: https://www.claronav.com/navident/surgical-videos/

[140] Rehman, U. and Cao, S., "Augmented-Reality-Based Indoor Navigation: A Comparative Analysis of Handheld Devices Versus Google Glass," *IEEE Transactions on Human-Machine Systems,* vol. 47, no. 1, pp. 140-151, 2017.
[141] Haider, A. and Hel-Or, H., "What Can We Learn from Depth Camera Sensor Noise?," *Sensors*, vol. 22, no. 14. doi: 10.3390/s22145448 Available: https://www.mdpi.com/1424-8220/22/14/5448#:~:text=Depth%20cameras%20use%20sensing%20technology,camera%20(see%20Figure%201).
[142] Ansari, R., "Robotically-Guided Dental Implant Placement: Extending Surgical Expertise," in *oralhealth*, ed. Online: Oral Health, 2020.
[143] Kopycka-Kedzierawski, D. T., Billings, R. J., and McConnochie, K. M., "Dental screening of preschool children using teledentistry: a feasibility study," *Pediatric dentistry,* vol. 29, no. 3, pp. 209-213, 2007.
[144] Yuzbasioglu, E., Kurt, H., Turunc, R., and Bilir, H., "Comparison of digital and conventional impression techniques: evaluation of patients' perception, treatment comfort, effectiveness and clinical outcomes," *BMC Oral Health,* vol. 14, no. 1, 2014.
[145] Logozzo, S., Franceschini, G., Kilpelae, A., Caponi, M., Governi, L., and Blois, L., "A Comparative Analysis Of Intraoral 3d Digital Scanners For Restorative Dentistry," 2008.
[146] Katarmal, B. (2023). *Dr. Bharat Katarmal Dental & Implant Clinic.* Available: https://www.drkatarmal.com/2014/11/how-intra-oral-scanner-works.html
[147] Mott, K., "Taking impressions to the next level," (in English), *Dental Products Report,* vol. 52, no. 11, pp. 12-13,15, 2018.
[148] Planmeca. *CAD/CAM SOLUTIONS.* Available: https://publications.planmeca.com/Brochures/CAD_CAM/CADCAM_bro_en_low.pdf
[149] Al-Hassiny, A. (2019). *Review of the Intraoral Scanners at IDS 2019*. Available: https://instituteofdigitaldentistry.com/ids-2019/review-of-the-intra-oral-scanners-at-ids-2019/
[150] (2020). *how does Invisalign treatment work?* Available: https://www.invisalign.com.au/how-invisalign-works
[151] Pagano, S., Moretti, M., Marsili, R., Ricci, A., Barraco, G., and Cianetti, S., "Evaluation of the Accuracy of Four Digital Methods by Linear and Volumetric Analysis of Dental Impressions," (in eng), *Materials (Basel, Switzerland),* vol. 12, no. 12, p. 1958, 2019.
[152] Lee, J.-S., Jeon, Y.-S., Strauss, F.-J., Jung, H.-I., and Gruber, R., "Digital scanning is more accurate than using a periodontal probe to measure the keratinized tissue width," *Scientific Reports,* vol. 10, no. 1, p. 3665, 2020.
[153] Kihara, H., Hatakeyama, W., Komine, F., Takafuji, K., Takahashi, T., Yokota, J., Oriso, K. *et al.*, "Accuracy and practicality of intraoral scanner in dentistry: A literature review," *Journal of Prosthodontic Research,* vol. 64, no. 2, pp. 109-113, 2020.
[154] Róth, I., Czigola, A., Fehér, D., Vitai, V., Joós-Kovács, G. L., Hermann, P., Borbély, J. *et al.*, "Digital intraoral scanner devices: a validation study based on common evaluation criteria," (in English), *BMC Oral Health,* Report vol. 22, p. NA, 2022.
[155] ISO. (2017). *IEC/TR 60601-4-1:2017 (1st ed.)*. Available: https://www.iso.org/obp/ui/en/#iso:std:iec:tr:60601:-4-1:ed-1:v1:en
[156] Chinzei, K., "Safety of Surgical Robots and IEC 80601-2-77: The First International Standard for Surgical Robots," *Acta Polytechnica Hungarica,* 2019.
[157] Vincent, J., "Please remain calm while the robot swabs your nose," ed. Online: The Verge, 2020.
[158] Crowe, S., "Danish startup develops throat swabbing robot for COVID-19 testing," in *The Robot Report*, ed. Online, 2020.
[159] Grüneberg, P., "Empowering Patients in Interactive Unity with Machines: Engineering the HAL (Hybrid Assistive Limb) Robotic Rehabilitation System," in *Humans and Devices in Medical Contexts: Case Studies from Japan*, Brucksch, S. and Sasaki, K., Eds. Singapore: Springer Singapore, 2021, pp. 255-280.
[160] Virk, G. S., "Robot standardisation: Personal care, medical and modularity," InnoTecUK, Ed., ed. Online: IEEE RAS Standards Strategy Meeting, Madrid, Spain, 2018.
[161] Changyue, Z., "Highly efficient auto throat swab robots introduced for COVID-19 tests," in *Global Times*, ed, 2022.
[162] EuroNews, "COVID-19 tests in northern China administered by robot," in *EuroNews*, ed. Online, 2021.
[163] huaxia, "Across China: Chinese city uses robots to collect throat swab samples for COVID-19 testing," ed. XINHUANET.com: Xinhua, 2021.
[164] Li, S.-Q., Guo, W.-L., Liu, H., Wang, T., Zhou, Y.-Y., Yu, T., Wang, C.-Y. *et al.*, "Clinical application of an intelligent oropharyngeal swab robot: implication for the COVID-19 pandemic," *European Respiratory Journal,* vol. 56, no. 2, p. 2001912, 2020.

[165] Lee, A., Baker, T. S., Bederson, J. B., and Rapoport, B. I., "Levels of autonomy in FDA-cleared surgical robots: a systematic review," (in English), *NPJ Digital Medicine,* vol. 7, no. 1, p. 103, 2024.
[166] BGIA, "Design of workplaces with collaborative robots," in "BG/BGIA risk assessment recommendations according to machinery directive," Institute for Occupational Safety and Health of the German Social Accident Insurance2011, Available: https://publikationen.dguv.de/widgets/pdf/download/article/4387, Accessed on: 21 March 2024.
[167] Leary, K., "A Chinese Robot Dentist Operated on a Human Patient for the First Time Ever," ed. Online: Futurism, 2017.
[168] (2019). *Robotic Technology*. Available: https://www.neocis.com/products-and-services/yomi-robot/
[169] Parmar, A., "Florida startup aims to make robot use in dental implants ubiquitous," in *MedCity News* ed. Online: Breaking Media, Inc, 2017.
[170] Al-Ghaili, H. (2017). *Robot dentist tested in China*. Available: https://www.youtube.com/watch?v=iEq8ekcJ7X8
[171] Dogramadzi, S., Giannaccini, M. E., Harper, C., Sobhani, M., Woodman, R., and Choung, J., "Environmental Hazard Analysis - a Variant of Preliminary Hazard Analysis for Autonomous Mobile Robots," (in English), *Journal of Intelligent & Robotic Systems,* vol. 76, no. 1, pp. 73-117, 2014.
[172] Sutton, R. T., Pincock, D., Baumgart, D. C., Sadowski, D. C., Fedorak, R. N., and Kroeker, K. I., "An overview of clinical decision support systems: benefits, risks, and strategies for success," (in English), *NPJ Digital Medicine,* vol. 3, no. 1, 2020.
[173] Andras, I., Mazzone, E., van Leeuwen, F. W. B., De Naeyer, G., van Oosterom, M. N., Beato, S., Buckle, T. *et al.*, "Artificial intelligence and robotics: a combination that is changing the operating room," (in English), *World journal of urology,* vol. 38, no. 10, pp. 2359-2366, 2020.
[174] Battaglia, E., Boehm, J., Zheng, Y., Jamieson, A. R., Gahan, J., and Majewicz Fey, A., "Rethinking Autonomous Surgery: Focusing on Enhancement over Autonomy," *European Urology Focus,* vol. 7, no. 4, pp. 696-705, 2021.
[175] Gómez Rivas, J., Toribio-Vázquez, C., Taratkin, M., Marenco, J. L., and Grossmann, R., "Autonomous robots: a new reality in healthcare? A project by European Association of Urology-Young Academic Urologist group," *Current opinion in urology,* vol. 31, no. 2, pp. 155-159, 2021.
[176] Inoue, S., Nakauchi, M., Umeki, Y., Suzuki, K., Serizawa, A., Akimoto, S., Watanabe, Y. *et al.*, "First clinical experiences of robotic gastrectomy for gastric cancer using the hinotori™ surgical robot system," (in English), *Surgical Endoscopy,* vol. 38, no. 3, pp. 1626-1636, 2024.
[177] Motoyama, D., Matsushita, Y., Watanabe, H., Tamura, K., Otsuka, A., Fujisawa, M., and Miyake, H., "Perioperative outcomes of robot-assisted partial nephrectomy using hinotori versus da Vinci surgical robot system: a propensity score-matched analysis," (in English), *Journal of Robotic Surgery,* vol. 17, no. 5, pp. 2435-2440, 2023.
[178] Fan, G., Ma, J., Wang, J., Wang, Y., Chen, Y., Wu, Y., Cai, S. *et al.*, "Comparison of the Hinotori surgical robot with the da Vinci robotic system in radical prostatectomy: a systematic review and meta-analysis," *Journal of Robotic Surgery,* vol. 19, no. 1, p. 82, 2025.
[179] Guo, Z., Zelin, W., Zhang, Q., Zhao, X., Chen, F., Jin-Hee, C., Zhang, Q. *et al.*, "A Survey on Uncertainty Reasoning and Quantification for Decision Making: Belief Theory Meets Deep Learning," ed. Ithaca: Cornell University Library, arXiv.org, 2022.
[180] Mcheick, H. and Mohammad, A. F., "The evident use of evidence theory in big data analytics using cloud computing," in *2014 IEEE 27th Canadian Conference on Electrical and Computer Engineering (CCECE)*, 2014, pp. 1-6.
[181] Pieper, L., Stiesch, M., Eich, L., Haddadin, S., and Grischke, J., "Interproximal tooth cleaning operated by a tactile robot. An in vitro analysis," *International journal of computerized dentistry,* vol. 0, 2023.
[182] Mönnink, C., Eich, L., Haddadin, S., Stiesch, M., and Grischke, J., "Dentronics: Tooth cleaning with a tactile, collaborative robot. An in vitro proof of concept," *International journal of computerized dentistry,* vol. 0, pp. 1-17, 2023.
[183] Gul, F., Rahiman, W., and Nazli Alhady, S. S., "A comprehensive study for robot navigation techniques," *Cogent Engineering,* vol. 6, no. 1, p. 1632046, 2019.
[184] Rubio, F., Valero, F., and Llopis-Albert, C., "A review of mobile robots: Concepts, methods, theoretical framework, and applications," *International Journal of Advanced Robotic Systems,* vol. 16, no. 2, p. 1729881419839596, 2019.
[185] Yang, G.-Z., Cambias, J., Cleary, K., Daimler, E., Drake, J., Dupont, P. E., Hata, N. *et al.*, "Medical robotics—Regulatory, ethical, and legal considerations for increasing levels of autonomy," *Science Robotics,* vol. 2, no. 4, p. eaam8638, 2017.
[186] Yan, A., "Chinese robot dentist is first to fit implants in patient's mouth without any human involvement," ed: South China Morning Post, 2017.

[187] Haidegger, T., "Autonomy for Surgical Robots: Concepts and Paradigms," *IEEE Transactions on Medical Robotics and Bionics,* vol. 1, no. 2, pp. 65-76, 2019.
[188] Sun, X., McKenzie, F. D., Bawab, S., Li, J., Yoon, Y., and Huang, J.-K., "Automated dental implantation using image-guided robotics: registration results," *International Journal of Computer Assisted Radiology and Surgery,* vol. 6, no. 5, pp. 627-634, 2011.
[189] Wu, J., Hui, W., Chen, S., Niu, J., Lin, Y., Luan, N., Zhang, S. *et al.*, "Error Analysis of Robot-Assisted Orthognathic Surgery," *The Journal of craniofacial surgery,* vol. 31, no. 8, pp. 2324-2328, 2020.
[190] Van den Bempt, M., Liebregts, J., Maal, T., Bergé, S., and Xi, T., "Toward a higher accuracy in orthognathic surgery by using intraoperative computer navigation, 3D surgical guides, and/or customized osteosynthesis plates: A systematic review," *Journal of Cranio-Maxillofacial Surgery,* vol. 46, no. 12, pp. 2108-2119, 2018.
[191] "Six Tips For Overcoming Fear Of The Dentist," ed: Fraser Dental, 2020.
[192] Beyond Dental. (2024). *Dental Hygiene Appointments & Treatment*. Available: https://beyond-dental.co.uk/general-dentistry/dental-hygiene/
[193] Ahire, M., Dani, N., and Muttha, R., "Dental health education through the brushing ROBOTUTOR: A new learning experience," (in eng), *Journal of Indian Society of Periodontology,* vol. 16, no. 3, pp. 417-420, 2012.
[194] Liu, J., "A novel motion generation strategy for robotic tooth brushing simulator," *Industrial robot,* vol. 40, no. 4, pp. 355-362, 2013.
[195] Lang, T., Staufer, S., Jennes, B., and Gaengler, P., "Clinical validation of robot simulation of toothbrushing - comparative plaque removal efficacy," (in English), *BMC Oral Health,* vol. 14, p. 82, 2014.
[196] Grischke, J., Johannsmeier, L., Eich, L., and Haddadin, S., "Dentronics: Review, First Concepts and Pilot Study of a New Application Domain for Collaborative Robots in Dental Assistance," in *2019 International Conference on Robotics and Automation (ICRA)*, 2019, pp. 6525-6532.
[197] Kan, T.-s., Cheng, K.-j., Liu, Y.-f., Wang, R., Zhu, W.-d., Zhu, F.-d., Jiang, X.-f. *et al.*, "Evaluation of a custom-designed human–robot collaboration control system for dental implant robot," *The International Journal of Medical Robotics and Computer Assisted Surgery,* vol. 18, no. 1, p. e2346, 2022.
[198] Kaber, D. B. and Endsley, M. R., "The effects of level of automation and adaptive automation on human performance, situation awareness and workload in a dynamic control task," *Theoretical Issues in Ergonomics Science,* vol. 5, no. 2, pp. 113-153, 2004.
[199] Nahavandi, S., "Trusted Autonomy Between Humans and Robots: Toward Human-on-the-Loop in Robotics and Autonomous Systems," *IEEE Systems, Man, and Cybernetics Magazine,* vol. 3, no. 1, pp. 10-17, 2017.
[200] Tso, K. S. and Backes, P. G., "A fail-safe tele-autonomous robotic system for nuclear facilities," *Robotics and Computer-Integrated Manufacturing,* vol. 10, no. 6, pp. 423-428, 1993.
[201] Brown, A. S., "Chapter 5 - Risk management," in *Clinical Engineering (Second Edition)*, Taktak, A., Ganney, P. S., Long, D., and Axell, R. G., Eds.: Academic Press, 2020, pp. 49-66.
[202] de Castro, A., "'Hierarchy of controls'," *The American Journal of Nursing,* vol. 103, no. 12, p. 104, 2003.
[203] ISO. (2010). *ISO 12100:2010 (1st ed.)*. Available: https://www.iso.org/standard/51528.html
[204] Nix, D. (2011). *Understanding the Hierarchy of Controls*. Available: https://machinerysafety101.com/2011/02/28/understanding-the-hierarchy-of-controls/
[205] Leitgeb, N., *Safety of Electromedical Devices: Law, Risk, Opportunities*, 1. Aufl. ed. Springer Verlag, Wien, 2010.
[206] WorkSafeBC. *Controlling risks*. Available: https://www.worksafebc.com/en/health-safety/create-manage/managing-risk/controlling-risks
[207] Wang, L., Wang, D., Zhang, Y., Ma, L., Sun, Y., and Lv, P., "An automatic robotic system for three-dimensional tooth crown preparation using a picosecond laser," *Lasers in Surgery and Medicine,* vol. 46, no. 7, pp. 573-581, 2014.
[208] Ackerman, E. (2024) A Robot Dentist Might Be a Good Idea, Actually Perceptive's autonomous robot offers more accurate, steadier, and faster dentistry. *IEEE Spectrum*. Available: https://spectrum.ieee.org/robot-dentist
[209] Paleri, V., Rixen-Osterbro, J., Oozeer, N., and Rajgor, A. (2021). *Trans-oral robotic surgery for head and neck cancer - NEW*. Available: https://www.entuk.org/patients/conditions/55/transoral_robotic_surgery_for_head_and_neck_cancer_new/
[210] Benito, D., Michel, M. C., Thakkar, P. G., Goodman, J. F., Sadeghi, N., and Joshi, A. S., "A cost effective custom dental guard for transoral robotic surgery," *Journal of robotic surgery,* vol. 14, no. 1, p. 91, 2020.
[211] Yee, S., "Transoral Robotic Surgery," *AORN Journal,* vol. 105, no. 1, pp. 73-84, 2017.

[212] Hussain, A., Malik, A., Halim, M. U., and Ali, A. M., "The use of robotics in surgery: a review," *International Journal of Clinical Practice,* vol. 68, no. 11, pp. 1376-1382, 2014.

[213] Datteri, E., "Predicting the Long-Term Effects of Human-Robot Interaction: A Reflection on Responsibility in Medical Robotics," (in English), *Science and Engineering Ethics,* vol. 19, no. 1, pp. 139-60, 2013.

[214] Wesler, A., "Dentist becomes 1st in LA to use Yomi robot for dental implants," in *Spectrum News 1*, ed. Online: Charter Communications, 2022.

[215] Neocis. (2020). *Neocis Announces New FDA 510(k) Clearance for Yomi® to Enhance CT Scanner Compatibility*. Available: https://www.globenewswire.com/news-release/2020/05/12/2032207/0/en/Neocis-Announces-New-FDA-510-k-Clearance-for-Yomi-to-Enhance-CT-Scanner-Compatibility.html

[216] Liu, C., Liu, Y., Xie, R., Li, Z., Bai, S., and Zhao, Y., "The evolution of robotics: research and application progress of dental implant robotic systems," *International Journal of Oral Science,* vol. 16, no. 1, p. 28, 2024.

[217] Mitchell, A., "Robot dentist performs world's first 'fully automated' procedure," in *New York Post*, ed. Online: Nationwide News Pty Ltd, 2024.

[218] Chia, S. H., Gross, N. D., and Richmon, J. D., "Surgeon Experience and Complications with Transoral Robotic Surgery (TORS)," *Otolaryngology–Head and Neck Surgery,* vol. 149, no. 6, pp. 885-892, 2013.

[219] Begum, S., "New Covid-19 swab test robot offers safe, more comfortable procedure for patients," in *The Straits Times*, ed. Online: SPH Media Limited, 2020.

[220] Deaker, E. M., Zoellner, H., Göktoğan, A. H., Martin, E., and Brooker, G., "The future of dental care: The manipulation of dental instruments and preparation towards automated tooth cleaning," presented at the 2023 45th Annual International Conference of the IEEE Engineering in Medicine & Biology Society (EMBC), Sydney, Australia, 2023. Available: https://ieeexplore.ieee.org/document/10340087

[221] Li, X., Liu, T., Hou, Q., Zeng, X., Xiong, Y., Yang, Y., Li, Z. *et al.*, "Comparison of Prone With Lithotomy Position in Removal of Posterior Myoma in Transvaginal Natural Orifice Endoscopic Surgery: A Prospective Cohort Study," *Journal of minimally invasive gynecology,* vol. 31, no. 9, pp. 795-802, 2024.

[222] Walter, T. and Ricard, J.-D., "Extended prone positioning for intubated ARDS: a review," *Critical Care,* vol. 27, no. 1, p. 264, 2023.

[223] Vishnuvardhan, G. D. and Bhakaney, P., "Favorable or Unfavorable? Awake-Prone Positioning's Effectiveness on COVID-19 Patients-A Research Study," *DPU's Journal of Ayurved, Homeopathy and Allied Health Sciences,* vol. 3, no. 1, pp. 9-11, 2024.

[224] Callihan, M. L. and Kaylor, S., "Proning Pains: Recognizing the Red Flags of Body Mechanics for Health Care Workers Involved in Prone Positioning Techniques: JEN," (in English), *Journal of Emergency Nursing,* vol. 47, no. 2, pp. 211-213, 2021.

[225] Mecademic. (2021). *Meca500 Six-Axis Industrial Robot Arm*. Available: https://www.mecademic.com/en/meca500-robot-arm

[226] Chang, E., Taek, K. H., and and Yoo, B., "Virtual Reality Sickness: A Review of Causes and Measurements," *International Journal of Human–Computer Interaction,* vol. 36, no. 17, pp. 1658-1682, 2020.

[227] Bhowmik, A. K., "Virtual and augmented reality: Human sensory-perceptual requirements and trends for immersive spatial computing experiences," *Journal of the Society for Information Display,* vol. 32, no. 8, pp. 605-646, 2024.

[228] Giménez, B., Özcan, M., Martínez-Rus, F., and Pradíes, G., "Accuracy of a Digital Impression System Based on Active Triangulation Technology With Blue Light for Implants: Effect of Clinically Relevant Parameters," *Implant dentistry,* vol. 24, no. 5, pp. 498-504, 2015.

[229] "Proceedings of the Workshop on Quantitative Evaluation of Periodontal Diseases by Physical Measurement Techniques," *Journal of Dental Research,* vol. 58, no. 2, pp. 547-553, 1979.

[230] Nabeel, Y., Sameera, R., and Rai, R., "DIGITAL IMPRESSIONS IN CURRENT DAY PROSTHODONTICS," *Guident,* vol. 10, no. 10, pp. 29-32, 2017.

[231] Mollbach, E. and Albert, M., *COHeReNT: A HRN-based Risk Assessment Method Tailored to Human-robot Collaboration*. 2020, pp. 4124-4131.

[232] Nichols, K. A. and Okamura, A. M., "A Framework for Multilateral Manipulation in Surgical Tasks," *IEEE Transactions on Automation Science and Engineering,* vol. 13, no. 1, pp. 68-77, 2016.

[233] Weinstein, P., Milgrom, P., Hoskuldsson, O., Golletz, D., Jeffcott, E., and Koday, M., "Situation-specific child control: A visit to the dentist," *Behaviour Research and Therapy,* vol. 34, no. 1, pp. 11-21, 1996.

[234] Giubilato, E., Cazzagon, V., Amorim, M. J. B., Blosi, M., Bouillard, J., Bouwmeester, H., Costa, A. L. *et al.*, "Risk Management Framework for Nano-Biomaterials Used in Medical Devices and Advanced Therapy Medicinal Products," (in English), *Materials,* vol. 13, no. 20, p. 4532, 2020.

[235] Mitchell, A. H., "Engineering Controls and Safer Medical Devices," in *Preventing Occupational Exposures to Infectious Disease in Health Care: A Practical Guide*, Mitchell, A. H., Ed. Cham: Springer International Publishing, 2020, pp. 101-115.
[236] Choucha, A., Travaglini, F., De Simone, M., Evin, M., Farah, K., and Fuentes, S., "The Da Vinci Robot, a promising yet underused minimally invasive tool for spine surgery: A scoping review of its current role and limits," *Neuro-chirurgie,* vol. 71, no. 3, pp. 101624-101624, 2025.
[237] Seo, J., Shim, S., Park, H., Baek, J., Cho, J. H., and Kim, N.-H., "Development of Robot-Assisted Untact Swab Sampling System for Upper Respiratory Disease," *Applied Sciences,* vol. 10, no. 21, p. 7707, 2020.
[238] (2025). *Improving ergonomics and efficiency at your CAD workplace*. Available: https://3dconnexion.com/au/spacemouse/?gad_source=1&gclid=Cj0KCQiAoJC-BhCSARIsAPhdfSgxIbzDRtyRbPvrc37oiqTZ_bLz5Sz86e3FW1ToJPkWPSBIdKdJh40aAk_bEALw_wcB
[239] (2025). *Inverse3*. Available: https://www.haply.co/
[240] Leadership and Worker Engagement Forum, "Leadership and worker involvement toolkit," HSE, Ed., ed. Online: Health and Safety Executive, 2012.
[241] Leitgeb, N., *Safety of Electromedical Devices: Law - Risks - Opportunities*, 1 ed. Vienna: Springer Wien, 2010.
[242] Hao, M. and Nie, Y., "Hazard identification, risk assessment and management of industrial system: Process safety in mining industry," *Safety Science,* vol. 154, p. 105863, 2022.
[243] Zhao, X. and Bai, X., "The Application of FMEA Method in the Risk Management of Medical Device during the Lifecycle," in *2010 2nd International Conference on E-business and Information System Security*, 2010, pp. 1-4.
[244] Salisbury, J. P., "Using Medical Device Standards for Design and Risk Management of Immersive Virtual Reality for At-Home Therapy and Remote Patient Monitoring," (in English), *JMIR Biomedical Engineering,* vol. 6, no. 2, 2021.
[245] Bruun, A. M., "FMEA vs Hazard Traceability Matrix in ISO 14971," ed. Online: LinkedIn, 2021.
[246] Agarwal, N., "ISO 14971: Harnessing Preliminary Hazard Analysis (PHA) To Develop Safer Medical Devices," in *Med Device Online*, ed. Online, 2020.
[247] Chung, H.-Y., Ting, T.-H., and Chang, K.-H., "A Novel Intuitionistic Fuzzy Set-Based Risk Priority Number Method for Solving Chemical Experiment Risk Evaluation," *Systems,* vol. 12, no. 5, p. 155, 2024.
[248] Tsai, Y. and Lin, C.-Y., "Investigation on Improving Strategies for Navigation Safety in the Offshore Wind Farm in Taiwan Strait," *Journal of Marine Science and Engineering,* vol. 9, p. 1448, 2021.
[249] Egerton, A. (2016). *10 Tips for Event Tree Analysis*. Available: https://egertonconsulting.com/10-tips-for-event-tree-analysis/
[250] Nano, G. and Derudi, M., *A Critical Analysis of Techniques for the Reconstruction of Workers Accidents*. 2013, pp. 415-420.
[251] Saw, J. L., Flauw, Y., Demeestere, M., Valerie, N., Blanc-Vannet, P., Hollifield, K., and Wilday, J., *The EU FireComp Project and Risk Assessment of Hydrogen Composite Storage Applications using Bow-tie Analysis*. 2016.
[252] Gullo, L. J. and Dixon, J., *Design for safety* (Quality and reliability engineering series). Hoboken, NJ, USA: John Wiley & Sons, Ltd, 2018.
[253] R.S NESS Group. (2021). *Risk Management in Medical Device*. Available: https://rs-ness.com/risk-management-in-medical-device-2/
[254] Mohamadfam, I., Soleimani, E., Ghasemi, F., and Zamanparvar, A., "Comparison of Management Oversight and Risk Tree and Tripod-Beta in Excavation Accident Analysis," *Jundishapur J Health Sci,* Research Article vol. 7, no. 1, p. e23554, 2015.
[255] Bentz, W., Qian, L., and Panagou, D., "Expanding human visual field: online learning of assistive camera views by an aerial co-robot," (in English), *Autonomous Robots,* vol. 46, no. 8, pp. 949-970, 2022.
[256] Harper, C. and Virk, G., "Towards the Development of International Safety Standards for Human Robot Interaction," *International Journal of Social Robotics,* vol. 2, no. 3, pp. 229-234, 2010.
[257] (2020). *Fault Tolerance*. Available: https://www.imperva.com/learn/availability/fault-tolerance/#:~:text=Fault%20tolerance%20refers%20to%20the,more%20of%20its%20components%20fail.
[258] Calvano, C. N. and John, P., "Systems engineering in an age of complexity," *Systems Engineering,* vol. 7, no. 1, pp. 25-34, 2004.
[259] WIRB-Copernicus Group (WCG). (2015). *ROBOTICALLY-ASSISTED SURGICAL DEVICES*. Available: https://www.fdanews.com/ext/resources/files/07-15/072015-robots-surgery.pdf?1436973876
[260] *Human-robot interaction : safety, standardization, and benchmarking*. Boca Raton, FL: CRC Press/Taylor & Francis Group, 2019.

[261] (2015). *What Is a De Novo Classification?* Available: https://www.thefdagroup.com/blog/2015/08/what-is-a-de-novo-classification/

[262] McLean, T. R. and Waxman, S., "Robotic surgery litigation," (in English), *Proceedings of the Institution of Mechanical Engineers,* vol. 224, no. C7, pp. 1539-1545, 2010.

[263] Mishra, A., Priyanka, M., Pradeep, K., and Reddy Pathakota, K., "Comparative Evaluation of Pain Scores during Periodontal Probing with or without Anesthetic Gels," *Anesthesiology Research and Practice,* vol. 2016, p. 5768482, 2016.

[264] Alkanan, S. A. M., Alhaweri, H. S., Khalifa, G. A., and Ata, S. M. S., "Dental pain perception and emotional changes: on the relationship between dental anxiety and olfaction," (in English), *BMC Oral Health,* vol. 23, pp. 1-11, 2023.

[265] Sikka, N., Robinson, H., Little, C., and Pourmand, A., "ED approach to electrical toothbrush associated hand injury, a unique case of non-oropharyngeal injury," *The American journal of emergency medicine,* vol. 35, no. 4, pp. 667.e3-667.e5, 2017.

[266] Endsley, M. R., "Toward a Theory of Situation Awareness in Dynamic Systems," *Human Factors,* vol. 37, no. 1, pp. 32-64, 1995.

[267] Machin, M., Dufossé, F., Blanquart, J.-P., Guiochet, J., Powell, D., and Waeselynck, H., "Specifying Safety Monitors for Autonomous Systems Using Model-Checking," in *Computer Safety, Reliability, and Security*, Cham, 2014, pp. 262-277: Springer International Publishing.

[268] Zheng, G., Gu, L., Li, X., and Zhang, J., "Computer-assisted Preoperative Planning and Surgical Navigation System in Dental Implantology," in *2007 6th International Special Topic Conference on Information Technology Applications in Biomedicine*, 2007, pp. 139-142.

[269] Maggio, E. (2020). *AI Medical Device Makers Still Protected By Preemption – But For How Long?* Available: https://www.expertinstitute.com/resources/insights/ai-medical-device-makers-still-protected-by-preemption-but-for-how-long/

[270] FDA. (2024). *Medical Device User Fee Amendments (MDUFA)*. Available: https://www.fda.gov/industry/fda-user-fee-programs/medical-device-user-fee-amendments-mdufa

[271] S, N., "Reinforcement Learning and Game Theory- An Intuitive Understanding," in *Medium*, ed. Online: Medium, 2019.

[272] Korb, W., Kornfeld, M., Birkfellner, W., Boesecke, R., Figl, M., Fuerst, M., Kettenbach, J. *et al.*, "Risk analysis and safety assessment in surgical robotics: A case study on a biopsy robot," *Minimally Invasive Therapy & Allied Technologies,* vol. 14, no. 1, pp. 23-31, 2005.

[273] Park, D., Hoshi, Y., Mahajan, H. P., Kim, H. K., Erickson, Z., Rogers, W. A., and Kemp, C. C., "Active robot-assisted feeding with a general-purpose mobile manipulator: Design, evaluation, and lessons learned," *Robotics and Autonomous Systems,* vol. 124, p. 103344, 2020.

[274] Yan, Y., Wang, H., Yu, H., Wang, F., Fang, J., Niu, J., and Guo, S., "Machine Learning-Based Surgical State Perception and Collaborative Control for a Vascular Interventional Robot," *IEEE Sensors Journal,* vol. 22, no. 7, pp. 7106-7118, 2022.

[275] Tam, C. (2020) Could AI Robots Perform Brain Surgery? This Taiwanese Company Thinks So. *Hive Life Magazine*. Available: https://hivelife.com/brain-navi/

[276] Yip, M. and Das, N., "Robot Autonomy for Surgery," 2017.

[277] "Robots can't really replace dentists," *Dental Abstracts,* vol. 63, no. 4, pp. 225-226, 2018.

[278] Gibbs, C. H., Hirschfeld, J. W., Lee, J. G., Low, S. B., Magnusson, I., Thousand, R. R., Yemeni, P. *et al.*, "Description and clinical evaluation of a new computerized periodontal probe-the Florida Probe," *Journal of Clinical Periodontology,* vol. 15, no. 2, pp. 137-144, 1988.

[279] Walmsley, A. D., Walsh, T. F., Lumley, P. J., Burke, F. J. T., Shortall, A. C. C., Hayes-Hall, R., and Pretty, I. A., "Chapter 5 - Management of inflammatory periodontal diseases," in *Restorative Dentistry (Second Edition)*, Walmsley, A. D., Walsh, T. F., Lumley, P. J., Burke, F. J. T., Shortall, A. C. C., Hayes-Hall, R., and Pretty, I. A., Eds. Edinburgh: Churchill Livingstone, 2007, pp. 31-46.

[280] Pérez-Portilla, T., Ortíz-Benitez, D., Lucas-Rincón, S., Canseco-Prado, G., Delgado Pérez, V., Scougall-Vilchis, R., Robles, L. *et al.*, *The Importance of Toothbrushing and Oral Hygiene in Maintaining Oral Health*. 2023.

[281] Perio-tools.com. *How to use the online periodontal chart*. Available: https://www.periodontalchart-online.com/uk/

[282] Arnett Dental. *Periodontal Disease and Gum Therapy*. Available: https://www.arnettdmd.com/periodontal-gum-therapy

[283] van Wijk, A. J. and Makkes, P. C., "Highly anxious dental patients report more pain during dental injections," *British Dental Journal,* vol. 205, no. 3, pp. E7-E7, 2008.

[284] Spiers, A. J., Baillie, S., Pipe, T. G., and Asimakopolous, G., "Negating the fulcrum effect in manual laparoscopic surgery: Investigating skill acquisition with a haptic simulator," *The International Journal of Medical Robotics and Computer Assisted Surgery,* vol. 13, no. 4, p. e1837, 2017.

[285] Thakur, M. and Kaur, R. (2016). *Periodontal probes*. Available: https://www.slideshare.net/malvika014/periodontal-probes-64860621

[286] Omar, H., Alhajrasi, M., Felemban, N., and Hassan, A., "Dental arch dimensions, form and tooth size ratio among a Saudi sample," *Saudi Medical Journal,* vol. 39, no. 1, p. 86, 2018.

[287] Chavoshzadeh Natanzi M, Azimi Zavaree M, Tora-bi M, Taghavi Damghani F, Hakimaneh M, Shayegh Sh, and Taghavi Damghani F, "Evaluation of the curve of spee, curve of wilson and monson's sphere in Iranian adults," *Journal of Craniomaxillofacial Research,* vol. 6, no. 3, 2020.

[288] Nelson, S. J., *Wheeler's Dental Anatomy, Physiology and Occlusion: Wheeler's Dental Anatomy, Physiology and Occlusion - E-Book*. Elsevier Health Sciences, 2019.

[289] Triviño, T., Siqueira, D. F., and Scanavini, M. A., "A new concept of mandibular dental arch forms with normal occlusion," *American Journal of Orthodontics and Dentofacial Orthopedics,* vol. 133, no. 1, pp. 10.e15-10.e22, 2008.

[290] Sachdeva, S., Tripathi, A., and Kapoor, P., "Dermatoglyphic Assessment in Subjects with Different Dental Arch Forms: An Appraisal," (in English), *Journal of Indian Prosthodontic Society,* vol. 14, no. 3, pp. 281-288, 2014.

[291] DentaGama, "Curve of Spee," Available: https://dentagama.com/news/curve-of-spee

[292] Douillet, N. (2021, 2/20/2022). *Line plane intersection (3D) v2.3*. Available: https://github.com/NicolasDouillet/line_plane_intersection/

[293] Dhanrajani, P. J. and Jonaidel, O., "Trismus: Aetiology, Differential Diagnosis and Treatment," *Dental Update,* vol. 29, no. 2, pp. 88-94, 2002.

[294] Li, X.-Y., Jia, C., and Zhang, Z.-C., "The normal range of maximum mouth opening and its correlation with height or weight in the young adult Chinese population," *Journal of Dental Sciences,* vol. 12, no. 1, pp. 56-59, 2017.

[295] Nagi, R., Sahu, S., Gahwai, D., and Jain, S., "Study on evaluation of normal range of maximum mouth opening among Indian adults using three finger index: A descriptive study," (in English), *Journal of Indian Academy of Oral Medicine and Radiology,* Report vol. 29, p. 186, 2017.

[296] Agrawal, J., Shenai, P., Chatra, L., and Kumar, P., "Evaluation of normal range of mouth opening using three finger index: South India perspective study," (in English), *Indian Journal of Dental Research,* Report vol. 26, p. 361, 2015.

[297] Agerberg, G., "Maximal mandibular movements in children," *Acta Odontologica Scandinavica,* vol. 32, no. 3, pp. 147-159, 1974.

[298] Patil, S. and Maheshwari, S., "Proposed new grading of oral submucous fibrosis based on cheek flexibility," *Journal of clinical and experimental dentistry,* vol. 6, no. 3, pp. e255-8, 2014.

[299] Sven. (2023). *inpolyhedron - are points inside a triangulated volume?* Available: https://au.mathworks.com/matlabcentral/fileexchange/37856-inpolyhedron-are-points-inside-a-triangulated-volume

[300] Himmelsbach, U. B., Wendt, T. M., Hangst, N., Gawron, P., and Stiglmeier, L., "Human–Machine Differentiation in Speed and Separation Monitoring for Improved Efficiency in Human–Robot Collaboration," *Sensors (Basel, Switzerland),* vol. 21, no. 21, p. 7144, 2021.

[301] Podgorelec, D., Uran, S., Nerat, A., Bratina, B., Pečnik, S., Dimec, M., Žaberl, F. *et al.*, "LiDAR-Based Maintenance of a Safe Distance between a Human and a Robot Arm," *Sensors,* vol. 23, no. 9, p. 4305, 2023.

[302] Moel, A., Denenberg, S., and Wartenberg, M., "Implementing Effective Speed and Separation Monitoring with Legacy Industrial Robots—State of the Art, Issues, and the Way Forward," in *The 21st Century Industrial Robot: When Tools Become Collaborators*, Aldinhas Ferreira, M. I. and Fletcher, S. R., Eds. Cham: Springer International Publishing, 2022, pp. 235-254.

[303] Duane, B., "Indemnity in Australia," (in English), *British Dental Journal,* vol. 202, no. 4, p. 177, 2007.

[304] D'Cruz, L., "Mind the gap," *British Dental Journal,* vol. 225, no. 10, pp. 930-932, 2018.

[305] Gupta, D., Thomas, S., Dagli, R., Solanki, J., Bhateja, G., and Mahajan, R., "Professional indemnity insurance used among graduated and post graduated dental surgeons in Mumbai city, India," (in English), *Journal of Health Research and Reviews,* Survey vol. 1, p. 44, 2014.

[306] Samaras, C. D., "Insurance for the new dentist: Doctor, protect thyself," in *Dental Economics*, ed. Online: Dental Economics, 2008.

[307] (2019). *Indemnity requirement*. Available: https://www.gdc-uk.org/registration/your-registration/indemnity

[308] Mecademic, "User Manual," in "Meca500 (R3)," Mecademic Robotics, Canada2021, Accessed on: 12 July 2022.

[309] Bonev, I. (2024). *What are Singularities in a Six-Axis Robot Arm?* Available: https://mecademic.com/insights/academic-tutorials/what-are-singularities-6-axis-robot-arm/

[310] Barnes, S. (2024). *The Cervical Spine*. Available: https://teachmeanatomy.info/neck/bones/cervical-spine/
[311] van Eijden, T. M., "Biomechanics of the Mandible," *Critical Reviews in Oral Biology & Medicine,* vol. 11, no. 1, pp. 123-136, 2000.
[312] Mecademic. (2021, 14 September 2021). *Mecademic ROS Package*. Available: https://github.com/Mecademic/ROS/tree/master
[313] ATI. (2025). *F/T Sensor: Nano17*. Available: https://www.ati-ia.com/products/ft/ft_models.aspx?id=Nano17
[314] ATI, "F/T Sensor Data Acquisition (DAQ) Systems," in "Manual," ATI Industrial Automation, Online2022, Available: https://www.ati-ia.com/app_content/documents/9620-05-DAQ.pdf, Accessed on: 20 January 2025.
[315] NI, "NI 6259 Specifications," in "PCI/PCIe/PXI/PXIe/USB-6259 Specifications | M Series Data Acquisition:," National Instruments Corporation, Online2023, Available: https://www.ni.com/docs/en-US/bundle/pci-pcie-pxi-pxie-usb-6259-specs/page/specs.html, Accessed on: 20 January 2025.
[316] VectorNav. (2023). *VN-100*. Available: https://www.vectornav.com/products/detail/vn-100
[317] VectorNav, "VN-100 User Manual," in "Inertial Navigation Modules," 2023, Accessed on: 20 September 2024.
[318] Lague, S. (2019). *Bézier Path Creator*. Available: https://assetstore.unity.com/packages/tools/utilities/b-zier-path-creator-136082
[319] Freed, H. K., Gapper, R. L., and Kalkwarf, K. L., "Evaluation of Periodontal Probing Forces," *Journal of Periodontology,* vol. 54, no. 8, pp. 488-492, 1983.
[320] Ruppert, M., Cadosch, J., Guindy, J., Case, D., and Zappa, U., "In Vivo Ultrasonic Debridement Force in Bicuspids: A Pilot Study," *Journal of Periodontology,* vol. 73, no. 4, pp. 418-422, 2002.
[321] Lea, S. C., Landini, G., and Walmsley, A. D., "Ultrasonic scaler tip performance under various load conditions," *Journal of Clinical Periodontology,* vol. 30, no. 10, pp. 876-881, 2003.
[322] Lea, S. C., Landini, G., and Walmsley, A. D., "The effect of wear on ultrasonic scaler tip displacement amplitude," *Journal of Clinical Periodontology,* vol. 33, no. 1, pp. 37-41, 2006.
[323] Flemmig, T. F., Petersilka, G. J., Mehl, A., Hickel, R., and Klaiber, B., "The effect of working parameters on root substance removal using a piezoelectric ultrasonic sealer in vitro," *Journal of Clinical Periodontology,* vol. 25, no. 2, pp. 158-163, 1998.
[324] Wiegand, A., Burkhard, J. P. M., Eggmann, F., and Attin, T., "Brushing force of manual and sonic toothbrushes affects dental hard tissue abrasion," *Clinical Oral Investigations,* vol. 17, no. 3, pp. 815-822, 2013.
[325] Zappa, U., Cadosch, J., Simona, C., Graf, H., and Case, D., "In Vivo Scaling and Root Planing Forces," *Journal of Periodontology,* vol. 62, no. 5, pp. 335-340, 1991.
[326] Wagner, J., Thomas, G., and Stanford, C., "Forces exerted by a conventional dental explorer during clinical examination," (in English), *Caries Research,* vol. 37, no. 5, pp. 365-8, 2003.
[327] Tavenard, R. (2017). *Soft-DTW weighted barycenters*. Available: https://tslearn.readthedocs.io/en/stable/auto_examples/clustering/plot_barycenter_interpolate.html
[328] Valori, M., Scibilia, A., Fassi, I., Saenz, J., Behrens, R., Herbster, S., Bidard, C. *et al.*, "Validating Safety in Human–Robot Collaboration: Standards and New Perspectives," (in English), *Robotics,* vol. 10, no. 2, p. 65, 2021.
[329] Alafaleq, M., "Robotics and cybersurgery in ophthalmology: a current perspective," *Journal of Robotic Surgery,* vol. 17, no. 4, pp. 1159-1170, 2023.
[330] Aghajanian, C. M. and Silva-Paulus, M. (2021) Luum invented a robot that can apply eyelash extensions on humans. *Business Insider*. Available: https://www.insider.com/luum-invented-robot-that-can-apply-eyelash-extensions-on-humans-2021-10
[331] Liang, J. and Kroemer, O., "Contact Localization for Robot Arms in Motion without Torque Sensing," ed. Ithaca: Cornell University Library, arXiv.org, 2021.
[332] Mecademic, "1. Basic theory and definitions," in "Programming Manual for the Meca500 Industrial Robot," Online2025, Available: https://resources.mecademic.com/en/doc/11.1/Meca500/MC-PM-MECA500/basic-theory-and-definitions.html, Accessed on: 15 July 2025.
[333] Pallardy, C. (2023) The Latest in Dental Robotics. Available: https://www.agd.org/constituent/news/2023/04/17/the-latest-in-dental-robotics
[334] Jayaweera, M., Amarasinghe, H., and Johnson, N. W., "Reshaping dental practice in the face of the COVID-19 pandemic: leapfrogging to Dentronics," (in English), *Oral Diseases,* 2021.
[335] AssetLand. (2021). *Modular Realistic Hospital vol.2*. Available: https://assetstore.unity.com/packages/3d/environments/urban/modular-realistic-hospital-vol-2-185567
[336] You, W., Hao, A., Li, S., Wang, Y., and Xia, B., "Deep learning-based dental plaque detection on primary teeth: a comparison with clinical assessments," *BMC Oral Health,* vol. 20, no. 1, p. 141, 2020.

[337] Park, D., Kim, H., and Kemp, C. C., "Multimodal anomaly detection for assistive robots," *Autonomous Robots,* vol. 43, no. 3, pp. 611-629, 2019.
[338] Ackerman, E., "Deep Learning Goes to Boot Camp: The U.S. Army wants to Team Humans and Robots on the Battlefield," *IEEE Spectrum,* vol. 58, no. 10, pp. 56-62, 2021.
[339] Grischke, J., Johannsmeier, L., Eich, L., Griga, L., and Haddadin, S., "Dentronics: Towards robotics and artificial intelligence in dentistry," *Dental Materials,* vol. 36, no. 6, pp. 765-778, 2020.
[340] Zhang, T., McCarthy, Z., Owen, J., Lee, D., Chen, X., Goldberg, K., and Abbeel, P., "Deep Imitation Learning for Complex Manipulation Tasks from Virtual Reality Teleoperation," ed. Ithaca: Cornell University Library, arXiv.org, 2018.
[341] Pavlović, A. (2023). *Everything you need to know about the FDA 510(k) submission*. Available: https://www.qualio.com/blog/fda-510k-submission
[342] Convergence Medical Robotics. (2024). *V01 Surgical Robot*. Available: https://www.convergenceortho.com/v01
[343] Convergence Medical Robotics. (2024). *Our Journey*. Available: https://www.convergenceortho.com/journey
[344] Norton, H., "The World's First Arthroscopic Robot - Chris Jeffery - Convergence Medical," in *The Crux of Medtech*, ed. Online: Cruxx, 2024.
[345] Stai, B., Heller, N., McSweeney, S., Rickman, J., Blake, P., Vasdev, R., Edgerton, Z. *et al.*, "Public Perceptions of Artificial Intelligence and Robotics in Medicine," *Journal of Endourology,* vol. 34, no. 10, pp. 1041-1048, 2020.
[346] Rayan, S., Skatawi, B., Ghaday, S., Abutaleb, M., Alshareef, M., Alamar, M., Abualkhair, L. *et al.*, "Predicting Artificial Intelligence Acceptance in Dental Treatments Among Patients in Saudi Arabia: A Perceived Risks and Benefits Perspective," (in English), *Oral,* vol. 5, no. 2, p. 28, 2025.
[347] Philips. (2024). *Philips Sonicare DiamondClean Smart*. Available: https://www.philips.com.au/c-p/HX9954_56/sonicare-diamondclean-smart-sonic-electric-toothbrush-with-app
[348] Liang, Y., Fan, H.-W., Fang, Z., Miao, L., Li, W., Zhang, X., Sun, W. *et al.*, "OralCam: Enabling Self-Examination and Awareness of Oral Health Using a Smartphone Camera," *Proceedings of the 2020 CHI Conference on Human Factors in Computing Systems,* 2020.
[349] McGrath, P. A., "Psychological aspects of pain perception," *Archives of Oral Biology,* vol. 39, pp. S55-S62, 1994.
[350] Ayer, W., Jr., *Psychology and Dentistry : Mental Health Aspects of Patient Care*. Florence, UNITED KINGDOM: Taylor & Francis Group, 2005.
[351] Daly, S., Newcombe, R. G., Claydon, N. C. A., Seong, J., Davies, M., and West, N. X., "A randomised controlled trial to determine patient experience of a magnetostrictive stack scaler as compared to a piezoelectric scaler, in supportive periodontal therapy," *Journal of Dentistry,* vol. 93, p. 103279, 2020.
[352] Najafpour, E., Asl-Aminabadi, N., Nuroloyuni, S., Jamali, Z., and Shirazi, S., "Can galvanic skin conductance be used as an objective indicator of children's anxiety in the dental setting?," *Journal of clinical and experimental dentistry,* vol. 9, no. 3, pp. e377-e383, 2017.
[353] Hamari, J., Koivisto, J., and Sarsa, H., "Does Gamification Work? -- A Literature Review of Empirical Studies on Gamification," in *2014 47th Hawaii International Conference on System Sciences*, 2014, pp. 3025-3034.
[354] Zheng, X. and He, X., "Relieving Children's Fear During Medical Process by Gamification Medical Navigation Application," Cham, 2020, pp. 260-266: Springer International Publishing.
[355] Wiederhold, M. D., Gao, K., and Wiederhold, B. K., "Clinical use of virtual reality distraction system to reduce anxiety and pain in dental procedures," (in eng), *Cyberpsychology, behavior and social networking,* vol. 17, no. 6, pp. 359-365, 2014.
[356] Tanja-Dijkstra, K., Pahl, S., White, M. P., Andrade, J., Qian, C., Bruce, M., May, J. *et al.*, "Improving dental experiences by using virtual reality distraction: a simulation study," (in eng), *PloS one,* vol. 9, no. 3, pp. e91276-e91276, 2014.
[357] Alshatrat, S. M., Alotaibi, R., Sirois, M., and Malkawi, Z., "The use of immersive virtual reality for pain control during periodontal scaling and root planing procedures in dental hygiene clinic," *International Journal of Dental Hygiene,* vol. 17, no. 1, pp. 71-76, 2019.
[358] Cunningham, A., McPolin, O., Fallis, R., Coyle, C., Best, P., and McKenna, G., "A systematic review of the use of virtual reality or dental smartphone applications as interventions for management of paediatric dental anxiety," *BMC Oral Health,* vol. 21, no. 1, p. 244, 2021.
[359] Abouzeid, H. L., Chaturvedi, S., Abdelaziz, K. M., Alzahrani, F. A., AlQarni, A. A. S., and Alqahtani, N. M., "Role of Robotics and Artificial Intelligence in Oral Health and Preventive Dentistry - Knowledge, Perception and Attitude of Dentists," *Oral health & preventive dentistry,* vol. 19, p. 353, 2021.

[360] Krishnaprakash, G., Jodalli, P., Shenoy, R. P., Mohammed, I. P., Junaid, and Amanna, S., "Dentists' Knowledge, Attitude, and Perception Regarding Robotics and Artificial Intelligence in Oral Health and Preventive Dentistry: A Cross-sectional Study," *Journal of clinical and diagnostic research,* vol. 17, no. 7, pp. 47-51, 2023.

[361] Alotaibi, S. F., Almutairi, G. M., Maryam Farhan, A.-A., Alotaibi, R. A., Nawal Ibrahim, F., Shoaa Abdullah Shaaf, A., Fahad Abdulla Mohammed, A. *et al.*, "The Role of Dental Assistants in Modern Dentistry: A Systematic Approach to Improving Dental Care," (in English), *Journal of International Crisis and Risk Communication Research,* vol. 7, no. S3, pp. 202-205, 2024.

[362] Gebhardt, J. S., Harth, V., Groneberg, D. A., and Mache, S., "Job Demands and Resources Perceived by Dentists in a Digital Dental Workplace and Perceived Effects on Job Satisfaction and Stress: A Qualitative Study," *Clinics and Practice*, vol. 15, no. 5. doi: 10.3390/clinpract15050092 Available: https://www.mdpi.com/2039-7283/15/5/92

[363] Smadi, L., Sharaireh, A., Al-Khateeb, O., Odat, S., and Yusuf, D., "Assessing Dental Students' Readiness for AI in Dentistry: A Comprehensive Analysis at Jordan University," (in English), *Journal of International Dental and Medical Research,* vol. 18, no. 1, pp. 374-383, 2025.

[364] De Backer, P., Simoens, J., Mestdagh, K., Hofman, J., Eckhoff, J. A., Jobczyk, M., Van Eetvelde, E. *et al.*, "Privacy-proof Live Surgery Streaming: Development and Validation of a Low-cost, Real-time Robotic Surgery Anonymization Algorithm," *Annals of surgery,* vol. 280, no. 1, pp. 13-20, 2024.

[365] Cooper, A. M., Ibrahim, A. A., Lyu, A. H., and Makary, A. M., "Underreporting of Robotic Surgery Complications," *Journal for Healthcare Quality,* vol. 37, no. 2, pp. 133-138, 2015.

[366] Guthrie, P., "Robotic surgical system under scrutiny," (in eng), *CMAJ : Canadian Medical Association journal = journal de l'Association medicale canadienne,* vol. 186, no. 1, pp. 22-22, 2014.

[367] Srikanth, K. V., Reddy, B. V. R., Darshan, B. M., Saraswathi, P. K., and Archana, A., "Periodontal Probes - A Review," (in English), *International Journal of Clinical Dental Science,* vol. 3, no. 2, 2012.

[368] Pihlstrom, B. L., "Measurement of Attachment Level in Clinical Trials: Probing Methods," *Journal of Periodontology,* vol. 63, no. 12S, pp. 1072-1077, 1992.

[369] Arabaci, T., Cicek, Y., Dilsiz, A., Erdogan, İ., Kose, O., and Kizildağ, A., "Influence of tip wear of piezoelectric ultrasonic scalers on root surface roughness at different working parameters. A profilometric and atomic force microscopy study," *International Journal of Dental Hygiene,* vol. 11, no. 1, pp. 69-74, 2013.

[370] Kozłowski, K. R., *Robot Motion and Control 2009* (Lecture Notes in Control and Information Sciences, 396). London: Springer London, 2009.

[371] Nambiappan, H. R., Arboleda, S. A., Lundberg, C. L., Kyrarini, M., Makedon, F., and Gans, N., "MINA: A Robotic Assistant for Hospital Fetching Tasks," (in English), *Technologies,* vol. 10, no. 2, p. 41, 2022.

[372] The Robot Report, "Unity demos how synthetic data can help robots learn," in *The Robot Report*, ed. Online, 2021.

[373] Huang, T.-K., Yang, C.-H., Hsieh, Y.-H., Wang, J.-C., and Hung, C.-C., "Augmented reality (AR) and virtual reality (VR) applied in dentistry," *The Kaohsiung journal of medical sciences,* vol. 34, no. 4, pp. 243-248, 2018.

[374] Zafar, S., Lai, Y., Sexton, C., and Siddiqi, A., "Virtual Reality as a novel educational tool in pre-clinical paediatric dentistry training: Students' perceptions," *International Journal of Paediatric Dentistry,* vol. 30, no. 6, pp. 791-797, 2020.

[375] Roy, E., Bakr, M. M., and George, R., "The need for virtual reality simulators in dental education: A review," *The Saudi Dental Journal,* vol. 29, no. 2, pp. 41-47, 2017.

[376] IMDRF, "Software as a Medical Device (SaMD): Application of Quality Management System," International Medical Device Regulators Forum, Online2015, Available: https://www.imdrf.org/sites/default/files/docs/imdrf/final/technical/imdrf-tech-151002-samd-qms.pdf, Accessed on: 29 October 2024.

[377] Gilman, S., Dirks, D., and Hunt, S., "Measurement of head movement during auditory localization," *The Journal of the Acoustical Society of America,* vol. 11, pp. 37-41, 1979.

[378] Ryan Jin Young, K., Benic, G. I., and Ji-Man, P., "Trueness of ten intraoral scanners in determining the positions of simulated implant scan bodies," (in English), *Scientific Reports (Nature Publisher Group),* vol. 11, no. 1, 2021.

[379] Perceptive. (2024). *Meet modern dentistry.* Available: https://www.perceptive.io/

[380] Mecademic, "User Manual," in "Meca500 (R3)," Mecademic Robotics, Canada2024, Accessed on: 12 July 2022.

[381] Deaker, E. M., Zoellner, H., Martin, F. E., Göktoğan A. H., and Brooker, G., 2025, "Simulated Risk Mapping for Safe Robotic Dental Techniques: Spatial Assessments of Instrument-Patient Interactions." In "Recent Advances in Digital Dentistry: Era of AI and Immersive Technologies (virtual, augmented and mixed reality)." Special Issue, *International Journal of Dentistry*, (submitted).

Appendix A: Analysis of a Change in Patient Posture

A.1 Introduction

For a robot to safely control a dental instrument around a conscious patient, it must be able to manage a dynamic operative environment. This is critical as an unrestrained patient has the ability to move the head in numerous directions creates uncertainty and increases the risk of instrument collision. A dental robot would need to account or respond appropriately to expected and unexpected patient movement to ensure a safe and efficient dental procedure can be performed. Movements of the human head are produced by a variety of complex joints in the neck and jaw. The head can rotate in three axes. Flexion and extension (nodding) and bending (tipping) movements are produced at the condyloid joint between the skull and the first vertebra (Figure A.1A,B) [310]. Pivot and plane neck joints between the first and second vertebrae determine the side-to-side rotation of the head (Figure A.1C) [310].

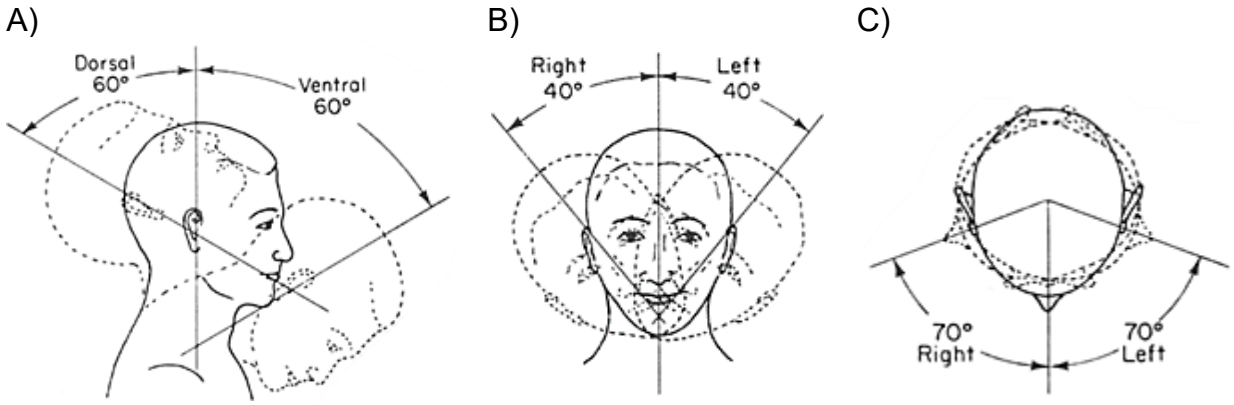

Figure A.1. Neck pivot joint movement produced by the cervical vertebrae with expected angles of rotation for each axis of rotation: A) Neck flexion (tipping) with a range of ±60°; B) Lateral bending with a range of ±40°; C) Neck rotation (side-to-side) with a range of ±70° [377].

The risk of collisions between the patient's oral features and the instrument as a result of patient head movement during dental procedures varies depending on the direction of movement, the speed and accuracy of the robot's reaction and the relative positions of the dental arches and soft tissues. Ideally, any movement of the patient would not result in an unplanned collision between the instrument and their oral cavity. This section evaluates the impact of changes to the direction of patient head rotation as a result of changes in patient posture for the maxillary arch. For the purposes of this investigation, the position of the headrest is estimated to dictate the relative position of the pivot point for side-to-side head rotation. Three postures were used for this analysis, including a supine-like posture, prone-like posture (suggested in Deaker *et al.* (2023)) and a seated posture (Figure A.2).

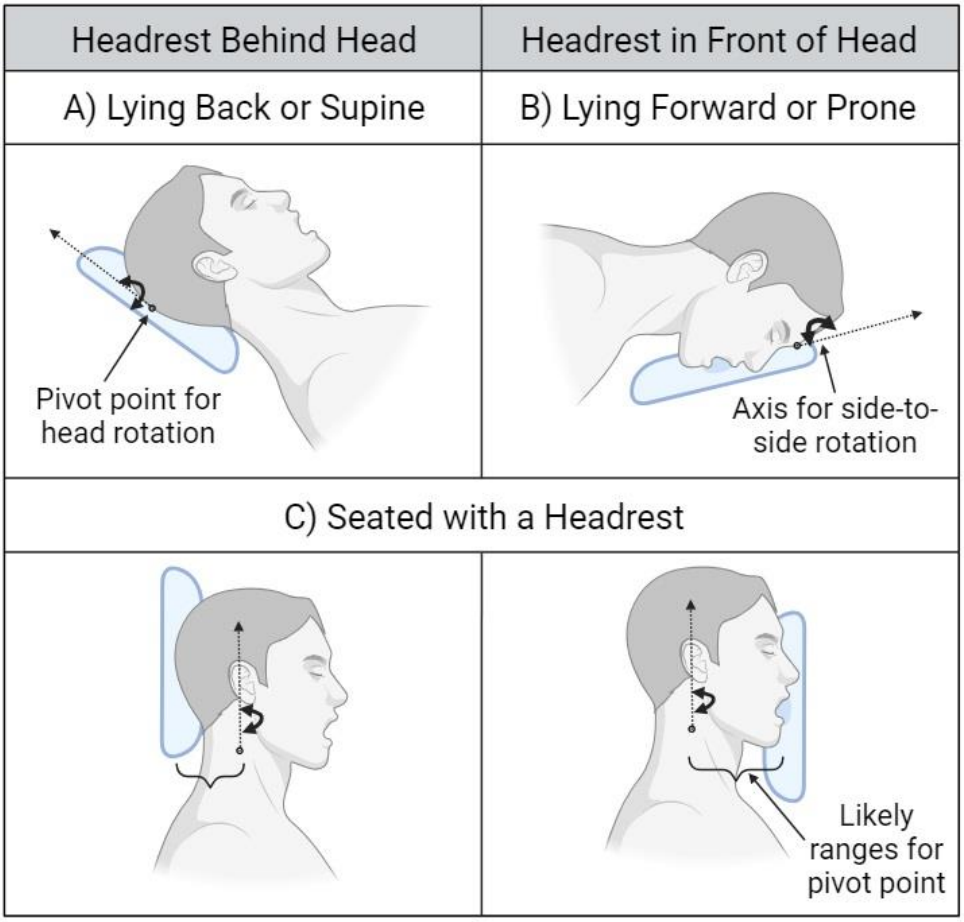

Figure A.2. Diagram of the three patient postures and their relative pivot points positions for side-to-side head rotations: A) A supine-like posture with a headrest behind the head; B) Prone-like posture with a headrest in front of the head; and C) Seated posture with a back or frontal headrest (created in BioRender.com).

The regions of the mouth with the highest chance of collision are identified as the locations of where the dental arch will next be positioned as a result of a rotation about the pivot point. Statis analysis is performed to assess the angle at which the instrument could contact the head model as a result of an angle of rotation. Low angles of rotations can indicate the most likely regions of contact. The time at which the instrument would contact the tissues would depend on the speed of the patients movement, dictating the amount of time which the robot has to respond to avoid an unplanned collision. Potential speed vector magnitudes and directions for points along the dental arches that can increase the relative speed of an instrument and the risk of a collision (Figure A.3). The buccal (cheek-side) regions are included for relative

outward rotations and lingual (tongue-side) region rotations are included for relative inward rotations.

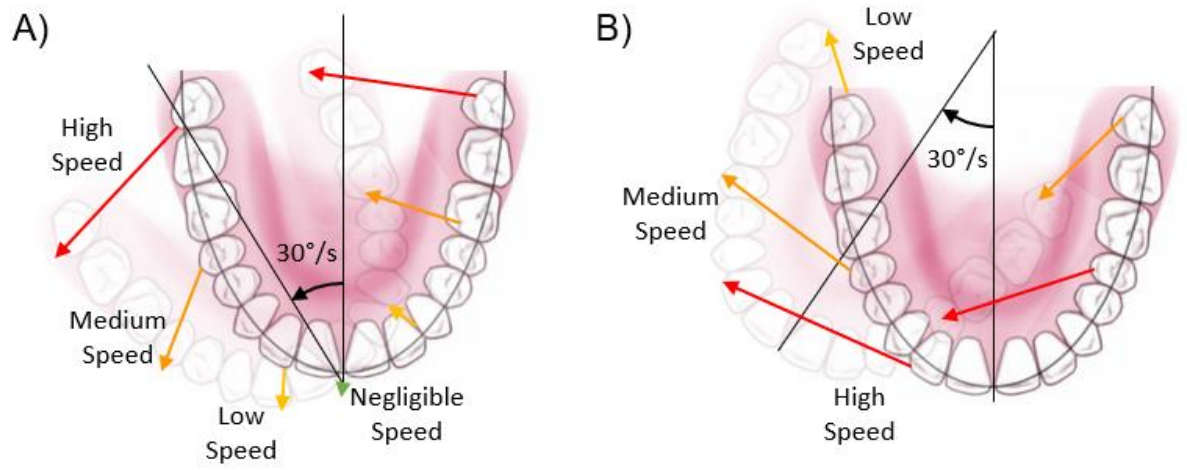

Figure A.3. The predicted relative motion of a side head rotation as a result of a change in pivot point: A) A pivot point at the front of the mouth for a prone posture; and B) A pivot point at the back of the mouth for a more supine posture. Expected amount of relative movement: negligible in green; low in yellow; medium in orange; and high in red.

A.2 Methods

A digital model of a silicone local anaesthetic (LA) head model available from OneDental (Castle Hill, NSW Australia). A scanned head model was converted to an STL file from DICOM images using Simpleware ScanIP (Figure A.4A). These were imported into MATLAB as 3D triangulation data which had an origin point positioned at the back of the mouth (Figure A.4B). A mesh of the head model was created using the *extendedObjectMesh()* function. As rotations of the model would occur around the origin, the *translate()* function was used to shift the position of the mesh forward around the origin by 50 mm for the forward shifted pivot point (prone posture) and back by -50 mm for the backward shifted pivot point (supine posture). A 50x50 point grid was overlayed across the $z = 10$ mm plane for the regions $-40 \text{ mm} \leq x \leq 40 \text{ mm}$ and $-80 \text{ mm} \leq y \leq 40 \text{ mm}$.

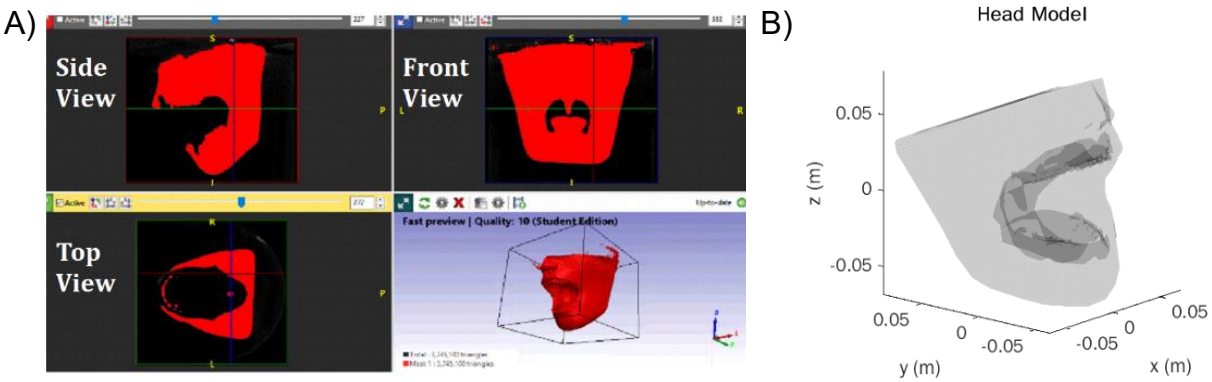

Figure A.4. The silicone LA head model: A) Orthogonal views of DICOM images in ScanIP; and B) the head model STL imported into MATLAB with the dental arches.

Iterative calculations were performed for each mesh head position with a varying head rotation angle of 0° to 30° with an interval of 1°. Each mesh was rotated using the *rotate()* function. The *inpolyhedron* function was used to test if each grid point was inside the mesh [299]. Points inside the mesh were assigned a risk value associated with the angle of rotation if not previously assigned at a lower angle of rotation, or otherwise were assigned as "Not a Number" (NaN). Low value assigned angles represent highest risk of collision for the instrument. The data was analysed using the *fitdist()* function for a Kernel distribution. The number of grid points assigned for each distribution was used to scale the output distributions against the total number of assigned grid points.

A.3 Results

The results observe regions of the mouth in a single z-plane that are most likely to introduce a collision with an instrument sitting in free space as a result of a patient head rotation. While a patient is in supine posture with a pivot point origin behind their head, a small change in angle of 1° introduces 67 grid points to a risk of collision without robot tracking (Figure A.5A). By comparison, the 37 grid points at 2° in prone posture and 27 grid points at 6° for the seated position (Figure A.5B,C). This is presented visually in Figure A.6. The seated patient posture appears to produce a twisting action (Figure A.6D), with the least loss in free space

grid points throughout the whole 30° rotation (Figure A.5D). The prone posture reduced the movement of the dental arch at the front of the mouth, but maintained a higher change in movement at the back of the mouth (Figure A.6C), albiet with less motion than the supine posture (Figure A.6B).

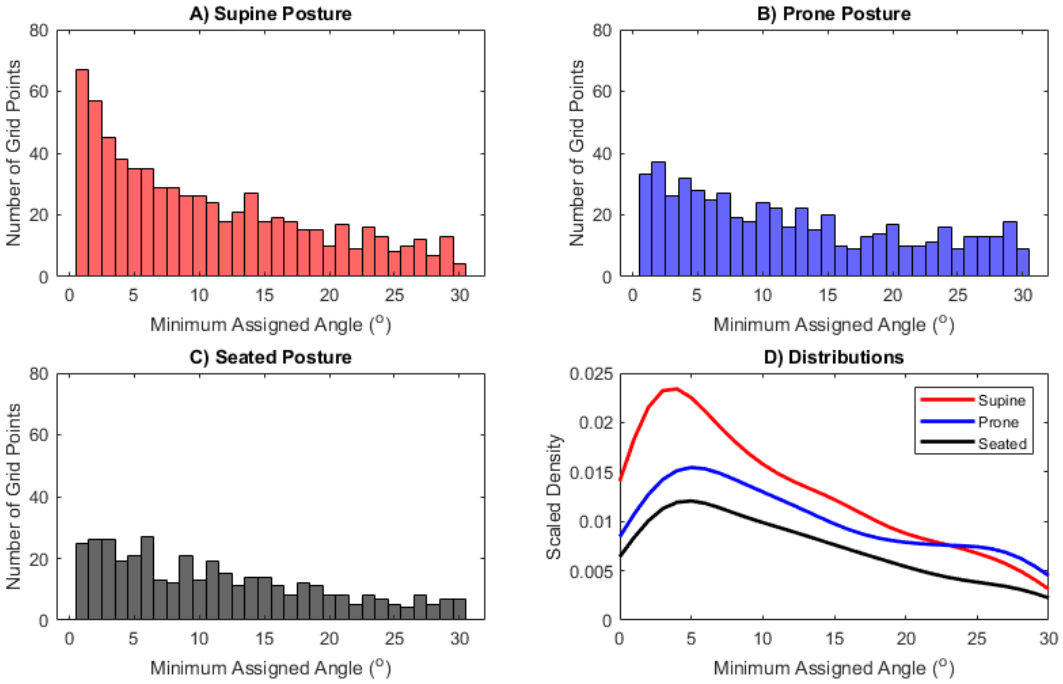

Figure A.5. Histograms for the A) supine posture, B) prone posture and C) seated posture representing the number of grid points that are changing from free space to space occupied by the rotating maxilla dental arch. The minimum assigned angle is the angle at which the free space grid point is the angle of motion that it is first occupied within the head model mesh. D) Scaled density outputs for probability distribution functions with Kernel distributions.

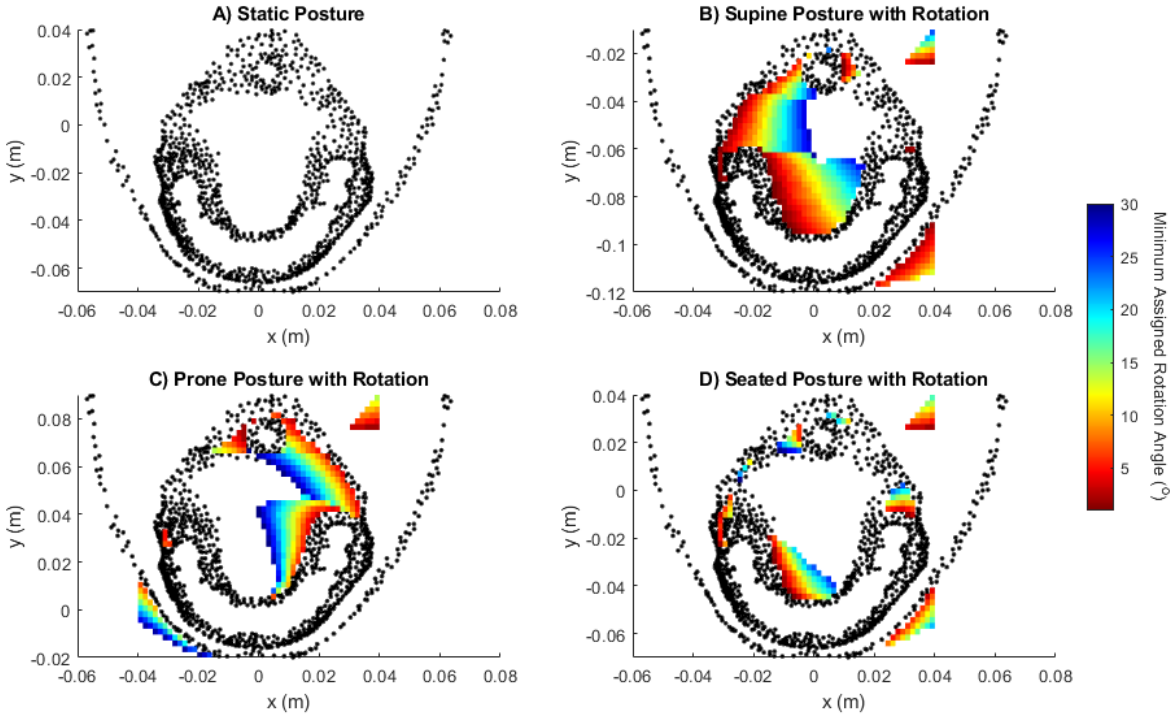

Figure A.6. A) The static condition with no head rotation presented by data points that round to 0.01 m in z by two decimal places. Likelihood estimates of collision to nearby tissues of the maxilla dental arch due to a rotation of the patient's head: B) in supine posture (pivot point shifted backward by -50 mm in y-axis); C) in prone posture (pivot point shifted forward by +50 mm in y-axis); and D) in seated posture. Dark red indicates low angle rotation (i.e. instrument locations most at risk of a collision as a result of a rotation). Dark blue indicates a high angle of rotation is needed to cause a collision.

A.4 Implications

The shift in pivot point for the various patient positions caused a change in the regions with the highest chance of instrument contact upon movement. For a dental robot setup, the preliminary results indicate that a seated posture is most optimal, shortly followed by the proposed prone posture. However, when observing specific regions of the mouth, it may be most ideal for dental robots to operate in front regions of the mouth in prone posture and back regions of the mouth in a seated posture. Along with higher risks of inhalation and ingestion of debris and liquids, the supine posture is predicted to produce the highest change in oral tissue positions under rotational patient head movement.

Alternating the posture of a patient between prone and a forward seated posture may be advantageous during longer procedures to prevent excessive pressure being applied for extended periods of time on the soft tissues of the body and of the face. However, it should be considered that the seated posture may be less naturally restraining to head movement, compared to a lying down posture. This is because the patients head remains resting on their multi-degree of freedom neck joint, rather than having the weight of their head passing on to a compressible foam headrest. In this case, other forms of head motion are likely to result for a seated posture, suggesting that the prone posture may best reduce the likelihood of unplanned collisions for robotic operations.

Future assessments will need to be carried out on the speed of a robot's response and the local speed of the oral tissue movement to perform an appropriate emergency response during unsafe patient movement. Emergency exit paths could be designed to account for the next likely location of oral tissues as a result of the expected direction of head movement to minimise the risk of collisions. Safer movement of the patient occurs when the local space around the instrument moves away from the instrument during patient movement, thereby producing a more transient contact. The risk of delays in robot motion tracking will depend on the surface area and flexibility of the dental instrument. This may be more likely to occur when the instrument is suspended in the oral cavity and lacking high accuracy position information received from force feedback, a major benefit of a dentist's "finger rest". Moreover, the presence of the tongue will influence whether the instrument is most at risk to perform movements suspended in free space around the maxillary or mandibular arch during operations.

Appendix B: Risk Management Network Framework Design

B.1 Summary

Similar to the risk supervision system, the design for the "Risk Management Framework" followed the structure for Endsley's Situation Awareness Model with hazard perception, comprehension and projection, followed by decision-making, actions performed and feedback (Chapter 4, Section 4.4, Figure 4.4A). The role of the risk management framework will be to define a method understand the perceived hazards identified from the supervision risk measures to estimate their cause and suggest a method of recovery. The following outlines the methods for hazard comprehension and predictive analysis for future dental robot systems. These are evaluated given that a risk value is quantified by the product of severity and the probability of harm (Chapter 4, Section 4.2, Figure 4.2).

B.2 Hazard Comprehension

To evaluate the likely causes of detected hazardous situations, an initial top-down approach was considered to link each hazardous situation to all possible causal factors. For this, each would be assigned a weighted probability in relation to the interpreted data measured, summing to a total of 1 (Figure B.1). Two challenges of this structure were identified as the need for a large array of causal factors for each specific potential hazard in the system and difficulty in providing a good estimate of their relevance. This is likely to result in errors for the causal analysis. Further, it would be challenging to predict the values for different hazardous situations when taking a bottom-up approach with assigned weighted probabilities for known operative scenarios.

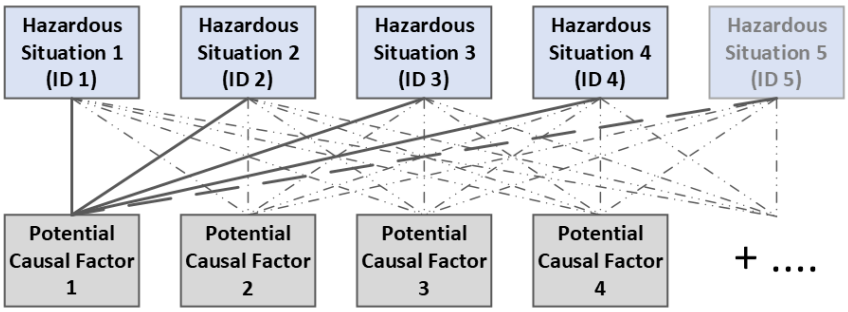

Figure B.1. Initial network (top-down) for determining the likely causal factors for detected the hazardous situations.

Similar to a neural network with hidden layers, a new intermediate layer was proposed to group different causal factors based on defined risk groups (Figure B.2). This additional layer provides a more intuitive and descriptive analysis of hazardous situations relating to the overall risks of a particular patient, procedure and setup. The risk factors were divided into twelve groups with multiple causal factors identified for each (Section 4.4.2, Table 4.8). These risk factors vary in degree of severity to harm, such as: a patient with an unexpected dental arch shape; the use of a sharper or more worn instrument; and the use of a less optimal patient posture. Their influence on the detected hazardous situations varies either between procedures or over the course of a procedure.

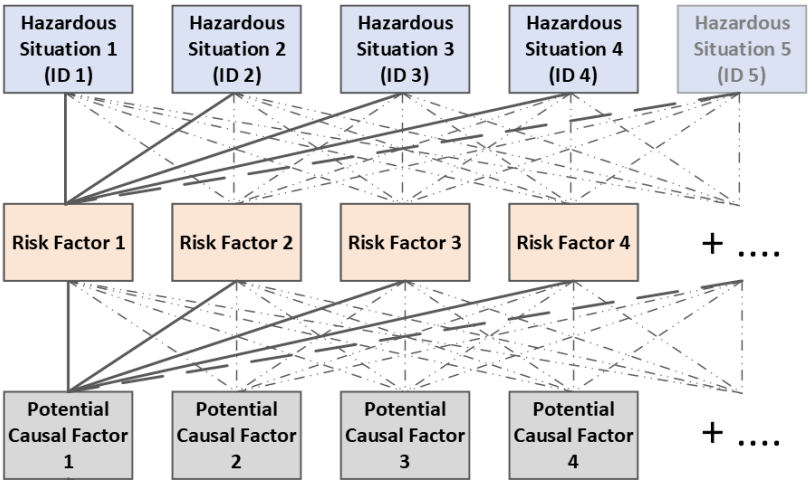

Figure B.2. Supervision block risk management network (RMN): Internal risk analysis network (top-down) for determining the likely causal factors for detected the hazardous situations.

The detected risk rating of an interpreted data measurement, R_{ID}, can be converted to the estimate the severity of a related risk factor, S_{RF}, in a particular instance, i, based on their predicted relevance to that hazard indication. The predicted relevance, $P_{ID|RF}$, is a fixed or time-varying, t, probability weighting that accounts for the known dynamic properties of dental procedures, such as an expected decrease in a given patient's compliance over long procedures. This would be summed across all interpreted data variables to evaluate the prevalence of an identified related risk factor (Equation B.1). The presence of different causal factors, $R_{i,CF}$, can then be calculated in terms of risk using the tracked severity of the related risk factors of defined probability weightings, $P_{CF|RF}$ (Equation B.2).

Equation B.1. $$S_{i,RF} = \sum_{ID}\left(\frac{R_{i,ID}}{P_{t_i,ID|RF}}\right)$$

Equation B.2. $$R_{i,CF} = \sum_{RF}\left(S_{i,RF}P_{t,CF|RF}\right)$$

B.3 Hazard Prediction & Projection

An added benefit of the descriptive risk factors is that they indicate likely hazardous scenarios for an operation prior to the procedure (Figure B.3). This uses an initial estimate for the predicted severity of risk factors ($S_{0,RF}$) based on the patient setup in the potential cause of

hazardous situations can be defined or estimated prior to a procedure. To perform predictive analysis, the risk rating can be estimated using an estimated severity rating for each related risk factor (Equation B.3). This would be useful to compare the impact of varying patient compliance, dental technique and operative setup, as well as other risk factors, on the likelihood of high patient risk. This could be performed prior to a procedure, such as when $i = 0$, for the expected impact of time-varying and fixed risk factors. In addition, changes in risk factor severity can be tracked over time for the procedure and compared to their initial values. This can be represented as a ratio, λ_{RF}, calculated at each instance, i (Equation B.4).

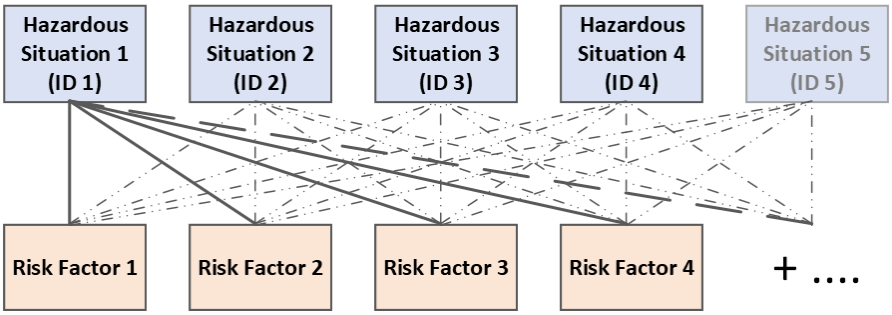

Figure B.3. Network diagram (bottom-up) to predict likely hazardous situations (expected interpreted data measurements) from defined risk factors for a given scenario.

Equation B.3. $$R_{t,ID} = \sum_{RF}\left(S_{i=0,RF} P_{t,ID|RF}\right)$$

Equation B.4. $$\lambda_{i,RF} = \frac{S_{i,RF}}{S_{0,RF}}$$

Beyond calculating the overall risk of a system for fast decision making, the probability of the sixteen identified forms of patient harm, P_{PH}, can be evaluated at each instance, i, using the interpreted data detected from the system (Figure B.4, Equation B.5). As identified in the risk analysis process of Section 4.3, only the probability of a risk can be altered for the potential of patient harm from a dental robot. This predictive calculation takes the estimated fixed severity, S_{PH}, for the defined type of patient harm (Table 4.3) to evaluate the effectiveness of the risk management network in detecting false positives and negatives for harm. These values

can be used to perform verification testing and carry out improvements for both the analysis of patient harm and the design of the risk management network. This can be useful in the development of accurate severity and probability weightings for the identified risk factors and causal factors.

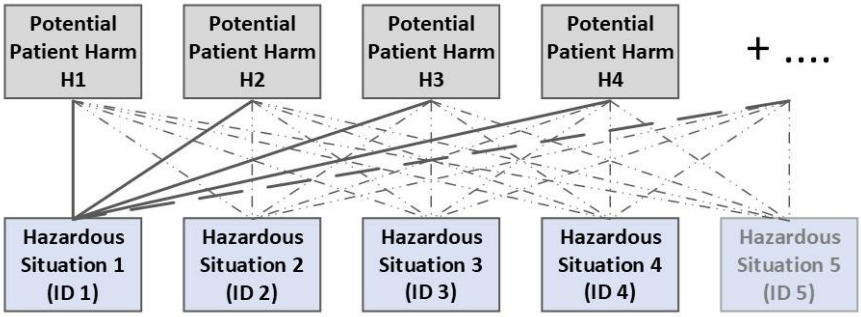

Figure B.4. Expanded network (bottom-up) to estimate the most likely forms of patient harm based on the detected hazardous situations.

Equation B.5. $$P_{i,PH} = \sum_{ID} \left(\frac{R_{i,ID}}{S_{i,PH}} \right)$$

B.4 Risk Recovery Actions and Success

Possible risk reduction methods are linked to specific causal factors for the risk management network (Figure B.5). For an identified high risk causal factor, R_{CF}, at an instance, i, actions taken to mitigate risks can be prioritised in terms of its ease and cost to implement, its effectiveness and the risk of the related detected hazard. Risk reduction methods may also be preferred for related risk factors that have shown to present a large difference from the initially predicted value, λ_{RF}, by computing scalars for the causal factors, λ_{CF}, with its relevant weightings at an instance, i (Equation B.6). The success of a risk management method can be evaluated by the ratio in risk of the causal factor from the current instance, i, to an instance before the method was implemented, i_{RM} - 1 (Equation B.7).

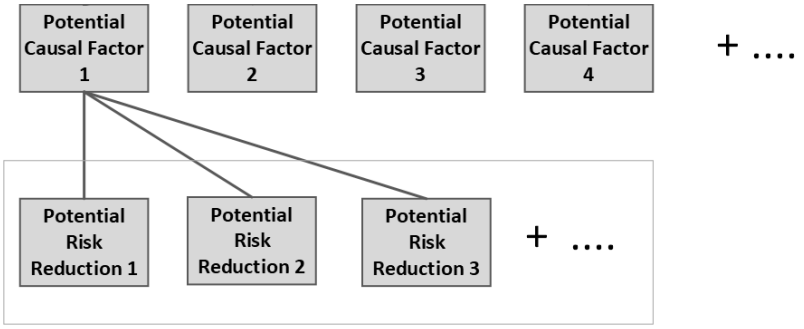

Figure B.5. Section of the supervision block risk management network (RMN) for showing possible risk reductions for recovery based on a likely causal factor influencing the risks of the hazardous situations (top-down).

Equation B.6. $$\lambda_{i,CF} = \sum_{RF}\left(\lambda_{i,RF} P_{t,CF|RF}\right)$$

Equation B.7. $$\lambda_{i,RM} = \frac{R_{i,CF}}{R_{i_{RM-1,CF}}}$$

Appendix C: Generating a "Patient" Scenario

C.1 Model Scanning

For the development of the procedure block of a supervisory system, instrument positions and paths around the oral cavity were selected based on likely target locations and orientations for an instrument using a silicone local anaesthetic (LA) head model available from OneDental (Castle Hill, NSW Australia). Following the suggested workflow for an autonomous dental robot system (Step 1 in Figure 3.8, Chapter 3), the head model was scanned using an intraoral scanner. Intraoral scans were carried out using the CEREC Primescan by Dentsply Sirona (Charlotte, NC United States) which has high accuracy (Figure C.1A) [378]. The models were imported into MATLAB as 3D triangulation data and were converted to point clouds (Figure C.1B). The intraoral scan data were used to create a planned surface detection application with a periodontal probe dental instrument from predetermined target locations and orientations.

A) 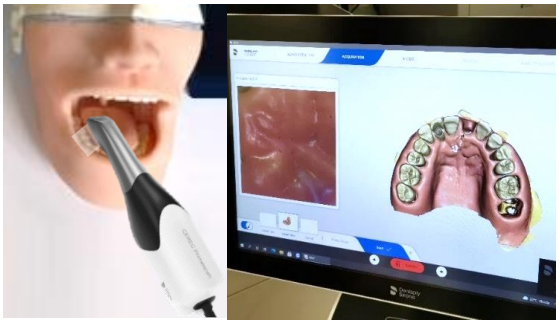

B) 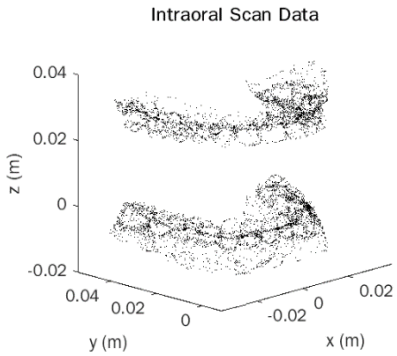

Figure C.1. A) Example images of real-time scanning of the dental arches with a CEREC Primescan and a computer image of a periodontal model scan. B) The head model dental arch intraoral scan data in MATLAB with the maxilla jaw shifted upwards for visualisation.

C.2 Digital Dental Arch Analysis

For dental arch analysis of intraoral scan data, the orientation of the imported arches was assessed to determine if it was the mandible or maxilla. This was assessed using a low-resolution MATLAB *surf* function. This was achieved by quickly comparing the average height of the dental arch to the surface's centre point, where the centre point is low for the mandibular arch and high for the maxillary arch. Knowing which arch was assessed, the tops of the teeth were found using half the distance to the maximum tooth height for a grid of nine regions for each arch in the shape of a hash symbol (#). The empty back region was used to confirm that the arch was oriented forwards.

A curve following the tops of the teeth of each arch was then created to represent the occlusal curved profiles (OCPs). An algorithm to find the tops of the dental arches and mean locations for the tops of the teeth was used for eight sections around the arches (Figure C.2A). An additional point (no. 5 at x=0) was included using data from the front middle-half section of the arches. To generate the 3D occlusal curves, splines were combined and smoothed, from points [4:1], [4:6] and [6:9] (Figure C.2A), to generate curves with 58 points along their lengths. Initial methods had used the equation for an ellipse with the width (w) and depth (d) to define the curved profiles in Deaker *et al.* (2023) [220] (Figure C.2B).

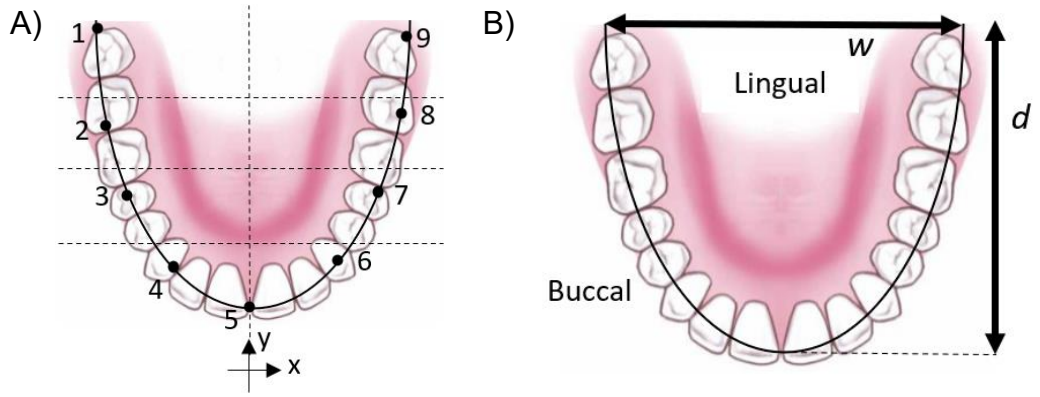

Figure C.2. Diagrams showing the top view of an occlusal curve profile along a dental arch. A) The arch split into 8 sections and the curve was made using the means of the highest data points for points [2:3] and [7:8]. The maximum y-value used for points 1 and 9. An additional point (no. 5 at x=0) was included using data from the midline of the arches. The peak's x and y locations for points 4 and 6 were used. B) Measurements of a dental arch including the width (w) and depth (d). The dental arch regions are identified as lingual (tongue side) and buccal (cheek side).

C.3 Target Selection

The target points from the intraoral scan data were chosen with the highest change in surface normal vectors in MATLAB as an indicator of areas prone to the buildup of debris, particularly along the gingival margin (gumline). These are useful target locations for a surface detection application as they are more specific to the patient. Each surface normal vector was calculated from the original triangulated model for points around the teeth, excluding regions of the oral mucosa by applying limits in the z-direction. The target points of interest were chosen using a moving region of interest with a width of 2 mm in the x, y, and z axes and data points with largest differences in the mean surface normal vector of that region were included as potential target points. This represented approximately 10% of the data points for the upper and lower dental arches. To reduce overlap, the total number of target points in each quadrant of the dental arch was reduced to 25 targets.

C.4 Target Frames of Reference

As a single point of data is insufficient to provide enough information for the instrument's required rotation, the target point frame's axes must be defined (Figure C.3A). To avoid regions that are very likely to result in soft tissue collision, the ideal safer path for a dental instrument will be referred to as the occlusal curved profile that forms along the occlusal plane on the tops of the teeth in each arch. This can act as a guide for instruments as they move towards the back of the mouth to reach targets (Figure C.3B). To achieve this, the tangents of the occlusal arch curves were used to estimate ideal instrument handle axis (x-axis) and the surface normal vector for the triangulated intraoral scan data was used to define the direction of the tip axis (z-axis) at a given target location.

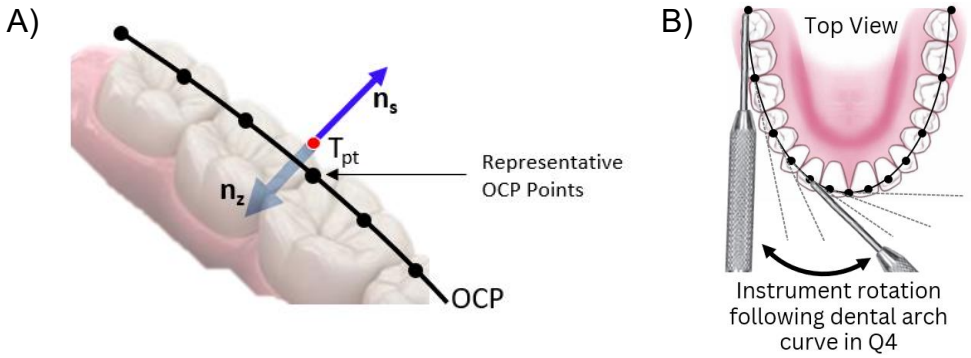

Figure C.3. A) Example target (T_{pt}) with its z-axis vector ($\mathbf{n_z}$) defined by the negative of the surface normal vector, $\mathbf{n_s}$ (directed into the model). B) Ideal instrument rotation with the curved shape of the mandibular jaw in the right-side quadrant (Quadrant 4, Q4). These orientations are flipped along the jaw midline for targets on the left sides of the mouth (e.g. for Quadrant 3).

The curved profile tangent vectors were calculated to point towards the back of the mouth, using either forward or backward difference methods, and were assigned to the nearby occlusal curve points (P_o). The closest occlusal curve point to each target was found using the *dsearchn* function before the offset was applied and its tangent ($\boldsymbol{t_o}$) then estimated the x-axis direction to find the direction of the y-axis from the right-hand rule cross product (Equation C.1, Figure C.4A). In cases where the curve tangent and surface normal vector were not perpendicular, the instrument handle needed to be rotated away from the estimated x-axis ($\boldsymbol{t_o}$)

to create the ideal tip angle to the surface. The x-axis vector ($\boldsymbol{n}_x$) was rotated to be orthogonal to the other frame axes by repeating the cross product (Equation C.2, Figure C.4B). This method was published in Deaker *et al.* (2023) [220]. Finally, as an extension, the estimated angulations of the upper tooth surfaces were calculated by averaging the normal vectors in a moving region of interest with a width of 2 mm in the x, y, and z axes for the occlusal curve data points.

Equation C.1. $$\vec{n}_z \times \vec{t}_o = \vec{n}_y$$

Equation C.2. $$\vec{n}_y \times \vec{n}_z = \vec{n}_x$$

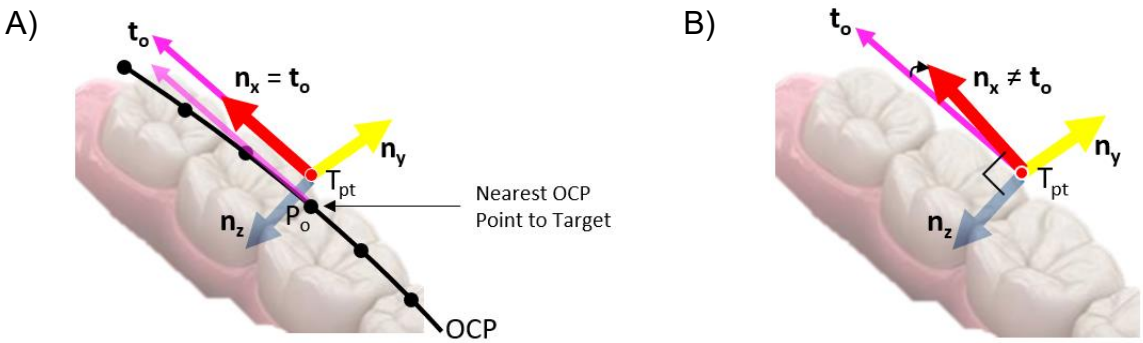

Figure C.4. Vector axes of the instrument tip from the offset for a sample target point. A) Use of the nearest occlusal curve point tangent to estimate the x-axis vector. B) Recalculation of the x-axis vector to create orthogonal axes vectors to define the tip's frame of reference (needed when n_z and t_o are not perpendicular), where the instrument would be angled away from the estimated curve profile tangent, t_o.

Target frame output vectors were input into rotation matrices, where three columns recorded x, y and z vectors, respectively. Plot transforms were placed around the oral cavity at their respective target locations, given by the quaternion output from *rotm2quat* function. The output Z-Y-X Euler angles were calculated using the *quat2eul* function. To observe changes in the Euler angles for the mandible, x-axis rotations less than zero for quadrant 3 and 4 targets were shifted by 2π such that the rotations would range from [0°,360°], simulating that the instrument was flipped to face towards the relevant dental arch (180° rotation of the handle). The averaged Euler angle was calculated from the magnitudes of reach axis rotation, with

deductions of 90° in the z-axis rotation for all targets and 180° in the x-axis rotation for mandible targets.

C.5 Instrument Frames of Reference

A PCPNT12 periodontal probe by Novatech (Chicago, IL United States) was chosen for the initial dental application simulations in MATLAB. This probe has a periodontal tip perpendicular to its handle, and this simplified analysis to determine the direction of the instrument's handle relative to that of the x-axis. For the surface detection application, the instrument's tip was chosen to be angled in line with the surface normal vector (Figure C.5A). The instrument axes were defined with the x-axis pointing along the direction of the handle and the z-axis pointing in the direction of the instrument tip (Figure C.5B). The tip offset (L_h) from the periodontal probe's handle (P_h) to its tip (P_{tip}) is 10 mm. Assuming the tip is at the target point, the position of the instrument handle reference frame can be calculated (Equation C.3).

Equation C.3. $$P_h = T_{pt} - L_h \mathbf{n}_z, \quad where\ T_{pt} = P_{tip}$$

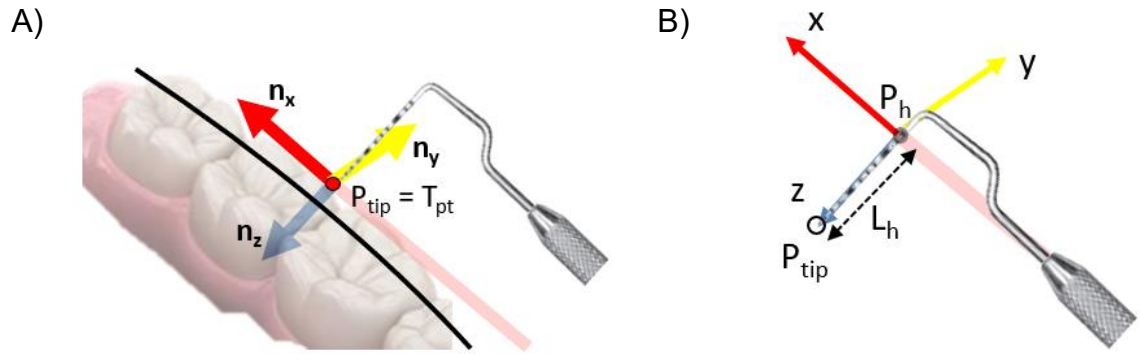

Figure C.5. A) Instrument at a target point with a frame of reference defined by the target frame axes vectors. B) Defined instrument frame of reference axes in line with the handle using an offset to the instrument handle (P_h) by a length (L_h) from the probe tip (P_{tip}).

C.6 Registration to the "Patient" Head Model

To create a realistic model of the positions of the dental arches and to develop methods to assess the risk of collision with oral tissues, while maintaining the ability to represent a dynamic mandible model, the head model (Appendix A, Figure A.4) was sectioned into oral features. The head model dental arch scans were initially sectioned for their relative position in Blender using Edit Mode to use for registration of the intraoral scan data. These were imported into MATLAB as 3D triangulation data (Appendix A, Figure A.4B). The sectioned dental arches were converted to point clouds in MATLAB and the corresponding intraoral scan data were down-sampled to manageable resolutions by skipping over 250 points of their point clouds to perform registration. This was carried out to avoid smoothing of the point cloud from resampling methods.

Two methods were trialled to align ("register") the intraoral point cloud data to the sectioned head model dental arches: Iterative Closest Point (ICP); and Coherent Point Drift (CPD). The arch occlusal curves were also aligned to the repositioned dental arches, along with the occlusal curve and scan surface normal vectors. The CPD method was used to rotate the intraoral scan points into the approximate position of the head model dental arches, while the ICP method was used to reposition the occlusal curves, and rotate calculated vectors and the surface normal vectors, as it provides a generic transformation matrix output.

Appendix D: Dental Instrument End Effectors

D.1 Iterative End Effector Design

With a compact robot arm, like the Meca500, the design of the end effector connection becomes increasingly important for robot control during dental applications. The design for the robot end effector took an iterative design process (Figure D.1). Initial designs attempted to reduce the number of tool changes with a multi-tool design (Figure D.1A). However, to achieve safe automated tool changes, the end effector needed the ability to lock the tool in place with high accuracy and to smoothly and safely rotate the tools when unlocked.

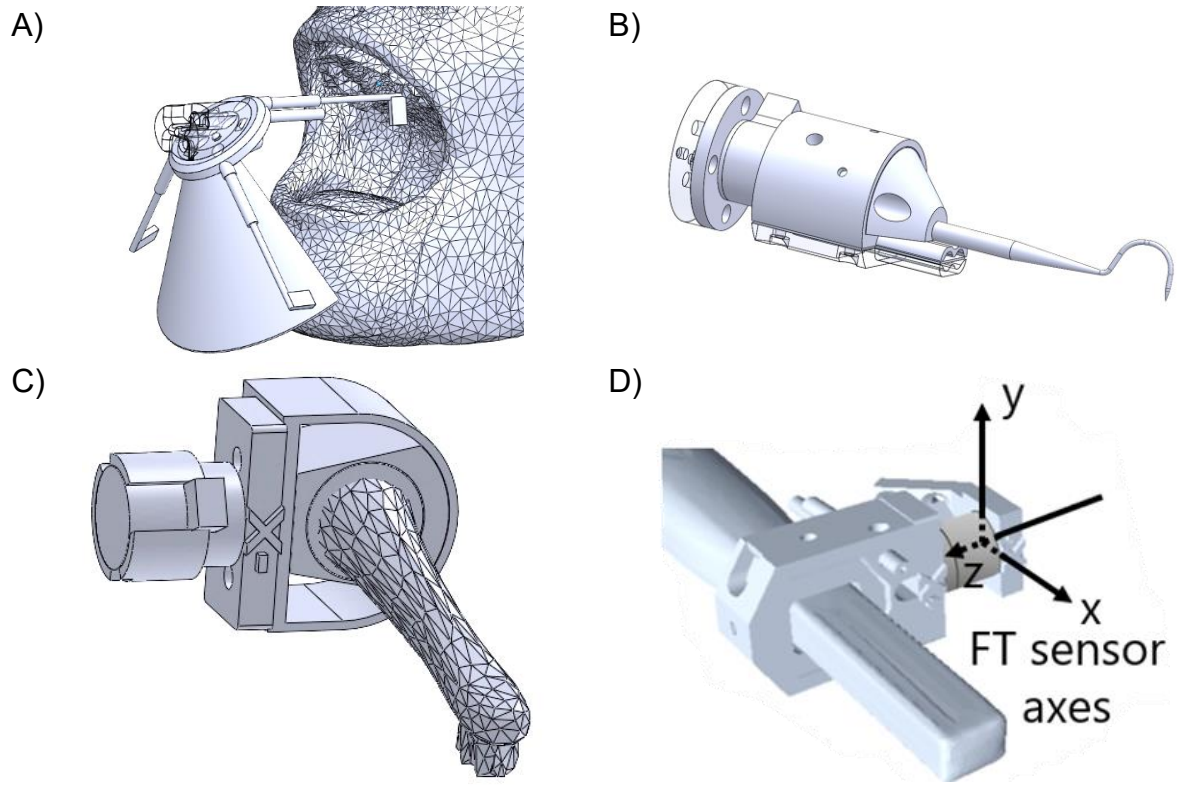

Figure D.1. Iterative end effector connection design depicted for a variety of different dental instruments: A) First multi-tool design; B) Second straight interchangeable tool connection design with the Nano17-e sensor; C) Third right-angled interchangeable tool connection design with the Nano17-e sensor; and D) Final interchangeable tool connection design at 45° to joint 6 that was used for experiments with the Nano17-e sensor, an endoscopic camera holder and two optional positions for air water spray supply. The Nano17-e sensor axes are displayed for the final design. The sonic toothbrush head and intraoral camera body shape were scanned with a 3D structured light desktop scanner, Einscan-S by Shining 3D (Hangzhou, China).

To simplify the end effector design, an interchangeable single dental instrument end effector was considered (Figure D.1B). This design attempted to include an endoscopic camera and air water spray below the instrument. This design aligned with the rotational axis of the 6th robot joint, meaning that the instrument could easily be rotated 180 degrees to operate on the opposite dental arch. However, this design was limited to instruments that had been modified for use with the robot. In the final designs, the instrument's handle was aligned in the x-axis of the Nano17-e sensor to avoid axis transformations for force measurements (Figure D.1C-D, Figure D.2). The chosen design for the dental robot test simulations had a 45° angle offset to joint 6, which combines some benefits of the straight end effector with the ability to use longer

instruments on the robot. This design is similar to Perceptive's dental robot end effector design [379].

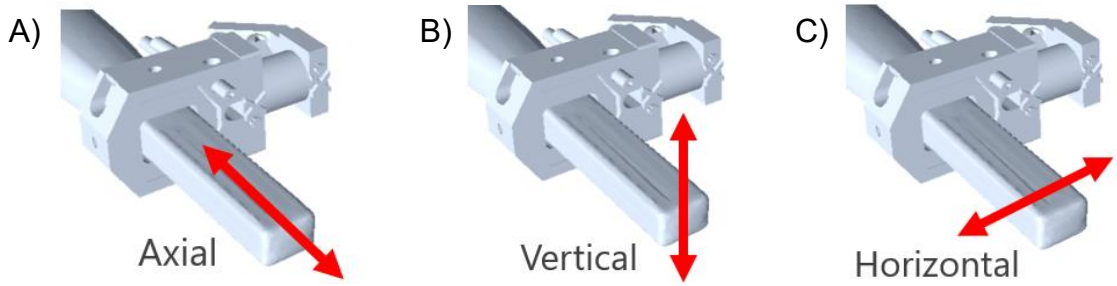

Figure D.2. Directions of forces that align with the Nano17-e force-torque sensor axes: A) X-axis for forces along the length of the instrument; B) Y-axis for forces in the vertical direction of the instrument; and C) Z-axis for horizontal lateral forces against the side of the instrument. This is displayed for the ProDENT intraoral camera dental instrument on the end effector.

D.2 Speed and Acceleration Limit Settings

The overall speed limits were calculated to allow the robot to quickly retract the length of the instrument out of the mouth in one second using the dimensions of the robot arm. The default joint velocity at 25% corresponds to: 37.5°/s for joints 1 and 2; 45°/s for joint 3; 75°/s for joints 4 and 5; and 125°/s for joint 6 [308]. Using the equation to calculate the sum of arc lengths for moving joints, the maximum velocity of the end effector (eef) is calculated at 1052.00 mm/s (Equation D.1). Using a scale factor of $\lambda_v = 10$, the maximum speed of 105.2 mm/s is achieved which is just larger than the ideal length of an instrument at 100 mm. This equates to a maximum robot angular velocity of 2.5%. As this was very slow, the velocity limit was multiplied by 6, the number of robot joints to 15%.

Equation D.1. $$\lambda_v v_{max} = \sum_{i=1}^{6} d_{max,i\rightarrow eef}\dot{\theta}_{i|25\%} = \frac{\pi}{180}(2 \times 265 \times 37.5 + (120 + 70 + 55) \times 45 + 100 \times 75 + (70 + 55) \times 75 + 100 \times 125) = 1052.0 \text{ mm/s}$$

The maximum acceleration of the robot joints was calculated using the maximum permissible forces that can be applied by collaborative robots. As mentioned in Chapter 1 (Section 1.5), the maximum quasi-static impact (squeezing) with a human face during any HRI

is 65 N, while a higher force of 130 N is allowed during contact with the skull and forehead [71, 74]. The default maximum acceleration torque at 100% of each joint are: 16.6 Nm for joints 1, 2 and 3; 2.5 Nm for joints 4 and 5; and 1.5 Nm for joint 6 [380]. A scale factor of $\lambda_a =$ 4 gives a maximum force of 64.54 N which is less than the 65 N maximum permissible force for contact with soft facial tissue (Equation D.2). Therefore, the maximum robot joint acceleration will be set to 25%.

Equation D.2. $$\lambda_a F_{max} = \sum_{i=1}^{6} d_{min,i\rightarrow eef}\tau_{i|100\%} = \frac{16.6}{0.12+0.07+0.055} + \frac{16.6}{0.265} + \frac{16.6}{0.12+0.07+0.055} + \frac{2.5}{0.1} + \frac{2.5}{0.07+0.055} + \frac{1.5}{0.1} = 258.15 \text{ N}$$

D.3 Robotic Technique Relative Velocity Limits

Calculations were carried out to define the velocities of dental techniques operated by dental robots using instruments with varying tip diameters around facial and oral features of a patient. Referring to the technical requirements, mentioned in Chapter 2 (Section 2.4), the biomechanical values for maximum permissible pressure and effective spring constant are 130 N/cm^2 and 150 N/mm for the hard dental arches (teeth and gingivae) and 110 N/cm^2 and 75 N/mm for soft oral tissues (oral mucosa), respectively [71, 75]. Using the energy equations of Chapter 2 (Section 2.2.4), the equations were rearranged (Equation D.3, Equation D.4) and used to calculate the permissible velocity, v, given the permissible pressure (P), contact surface area (A), effective mass (m) and effective spring constant (k) (Equation D.5).

Equation D.3. $$E_k = \frac{1}{2}mv^2 \quad \rightarrow \quad v = \sqrt{\frac{2E_k}{m}}$$

Equation D.4. $$E_p = \frac{1}{2}kx^2 \quad \rightarrow \quad E_p = \frac{1}{2}Fx = \frac{F^2}{2k}, \quad given\ F = kx$$

Equation D.5. $$E_k = E_p \quad \rightarrow \quad v = \frac{F}{\sqrt{mk}} = \frac{PA}{\sqrt{mk}}, \quad given\ F = PA$$

As the weights of individual robot links are not provided, the whole mass of the robot with the static base was used for the permissible velocity analysis. The effective mass was calculated by combining the masses of the robot (m_R) and a simulated human head (m_H) as properties acting in series (Equation D.6). The analysis was carried out assuming a lightweight Meca500 robot arm (4.5 kg) with a maximum rated payload of 500 g [225]. The head mass was assumed to be 4.54 kg, which is double that of the LA head model 2.27 kg and similar to the effective head mass for a total body mass of 75 kg from Chapter 2 (Table 2.3). The velocities near hard and soft tissues were calculated for dental instrument tip diameters ranging from 0.5 mm to 3.00 mm (Table D.1). Further, although a flexible dental instrument may increase the calculated safe speeds, the uncertainty of the instrument tip's position increases.

Equation D.6. $$m = \left(\frac{1}{m_R} + \frac{1}{m_H}\right)^{-1}, \quad where\ m_R = \frac{m_{Link\ 2-Link\ 6}}{2} + m_{EEF}$$

Table D.1. Permissible velocities (mm/s) for 500 g end effectors of varying tip diameters on a Meca500 robot arm that can result in collisions with hard and soft tissues of a head model (results for a head model mass of 4.54 kg).

Tissues Involved	**Velocity (mm/s)**					
Tip Diameter (mm)	*0.50*	*1.00*	*1.50*	*2.00*	*2.50*	*3.00*
Hard tissues (teeth and gingivae)	0.504	2.01	4.53	8.06	12.59	18.13
Soft tissues (oral mucosa)	0.603	2.41	5.42	9.64	15.07	21.70

D.4 Sensor Deflection Uncertainty Analysis

As well as the deflection of the dental instrument, the addition of a force-torque sensor on dental robot end effectors should be considered for its impacts on the position uncertainty of the instrument tip. This may limit the accuracy of robotic techniques, despite the robot being highly accurate, without feedback to confirm the position of the instrument using various tracking technologies during applications of force. The Nano17-e force-torque sensor was connected with a straight stainless steel dental explorer probe to assess its deflection under a

weight force. A laser pointer was attached to the probe to measure sensor deflections for the Nano17-e. A cup of water was suspended from a stiff stainless steel dental explorer probe in a vice (Figure D.3). The volumes of water used were added to a maximum force of 2 N to produce measurable laser pointer deflections at a 1.65 m distance.

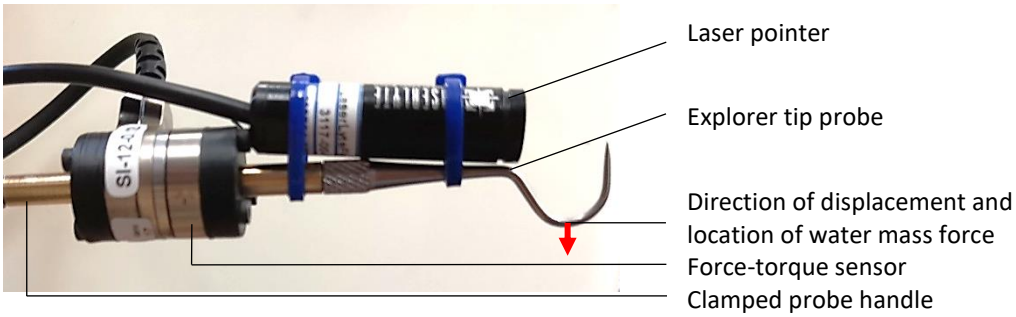

Figure D.3. Sensor angle deflection for increasing force on a dental instrument.

The measured sensor deflection in the x- and y-axes were approximately linear at a rate of 0.376°/N (Figure D.4A). The corresponding displacements for sensor angle deflections were computed for end effector connection with: a right-angled instrument (~30 mm offset, Figure D.1C,D); a shorter straight instrument (~65 mm offset, Figure D.1B); and a longer straight instrument (~100 mm offset, Figure D.1A). At approximately 2 N, the longer straight instrument had a maximum offset of 1.30 mm, compared to 0.39 mm for the right-angled instrument and 0.85 mm for the shorter straight instrument (Figure D.4B).

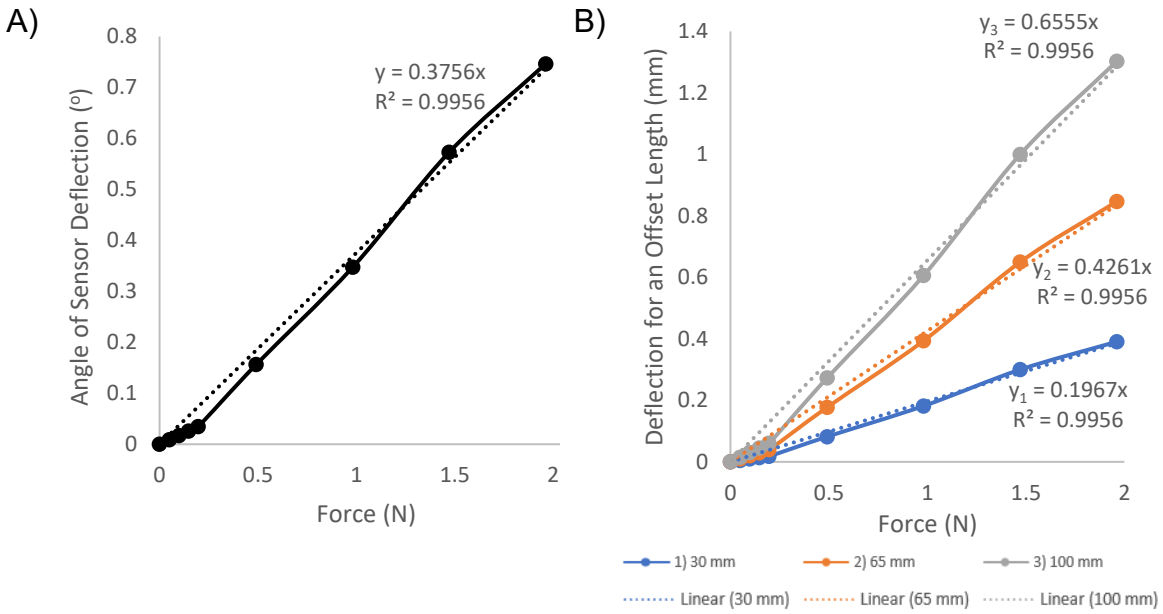

Figure D.4. A) Force-torque sensor angle deflection for increasing force on a dental instrument. B) Increase in position uncertainty of instrument tips from deflection of the force-torque sensor under force for a 30 mm offset right-angled end effector, a 65 mm long straight end effector and a 100 mm long straight end effector. The trendlines were approximated with a y-intercept of zero.

Appendix E: Unity Dental Simulation Experiments

E.1 Environment and Robot Setup

To confirm the setup is ready for performing dental simulation tests, the orientation sensor was tested for its ability to update the position of the head and jaw in Unity (Figure E.1). The robot was then connected and tested for its ability to follow the reference tip with movement of the head model (Figure E.2). This was then repeated for movement of the reference tip along the 3D paths (Figure E.3). For simulation testing with a periodontal probe, the position of the head model was localised to a higher degree of accuracy. This was carried out by localising four dental arch features with the thin periodontal probe. The head model was re-positioned to match the first point and then used the next three points to confirm its position in space relative to the dental instrument (Figure E.4). The risk measurements for the procedure block (ID1.1–1.4) are displayed in Unity with the periodontal instrument (Figure E.5). Screen

recordings were captured using OBS Studio of the Unity 3D scene, the camera view of the live setup and the Python server used to capture force-torque sensor data (Figure E.6).

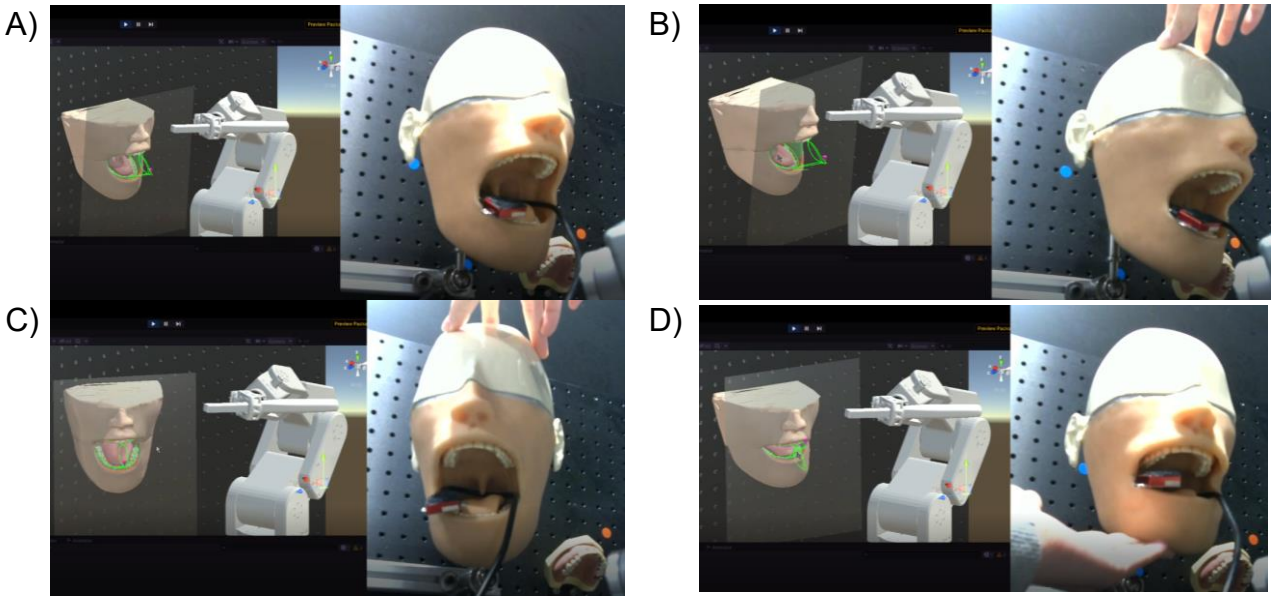

Figure E.1. Movement of the frontal plane and virtual head model in Unity with the physical model during orientation sensor testing: A) Forward head position; B) Slight left head rotation; C) Right head rotation; and D) Closing of the mouth by an elevation of the jaw.

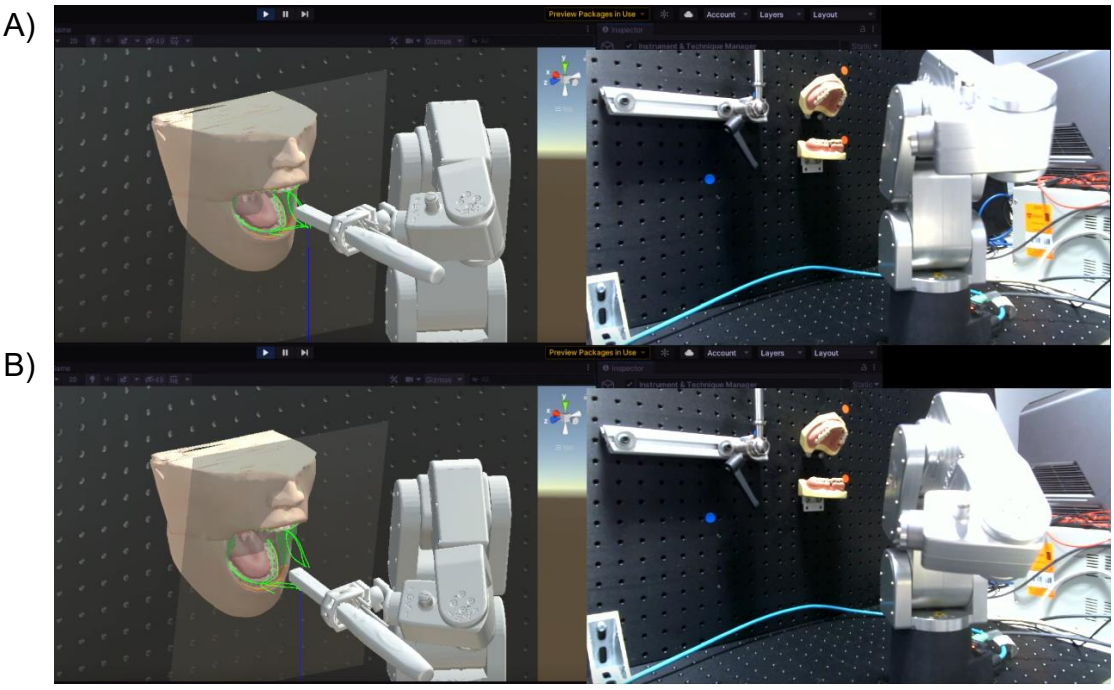

Figure E.2. The robot connected to Unity without the head model to follow the position and rotation of the reference tip: A) Instrument at the starting position outside the mouth; and B) Opening of the mouth by a simulated depression of the jaw. The location of the reference tip in space is indicated by the vertical blue line from the optical breadboard.

A)

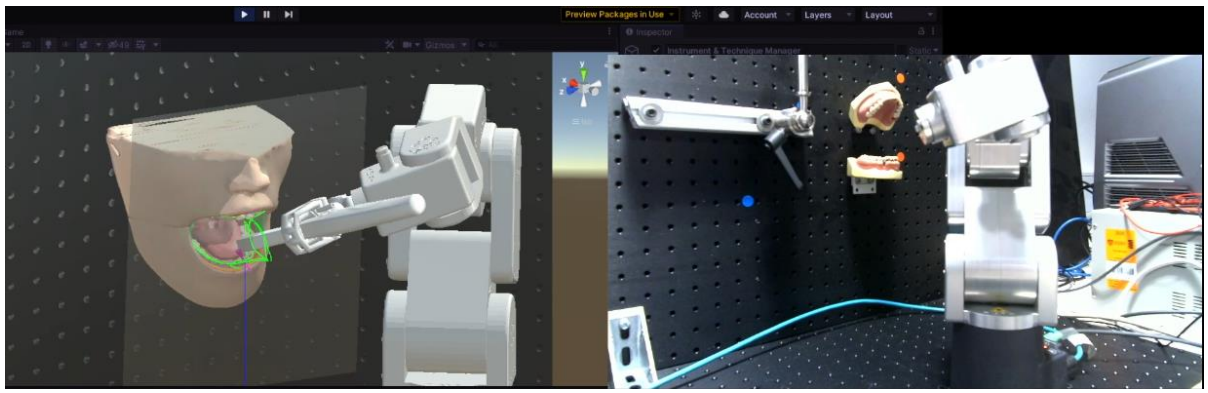

B)

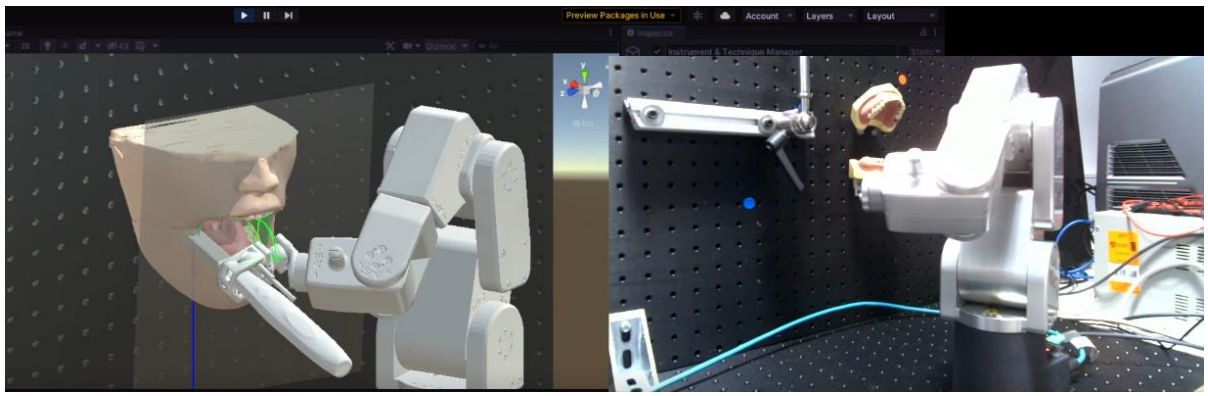

C)

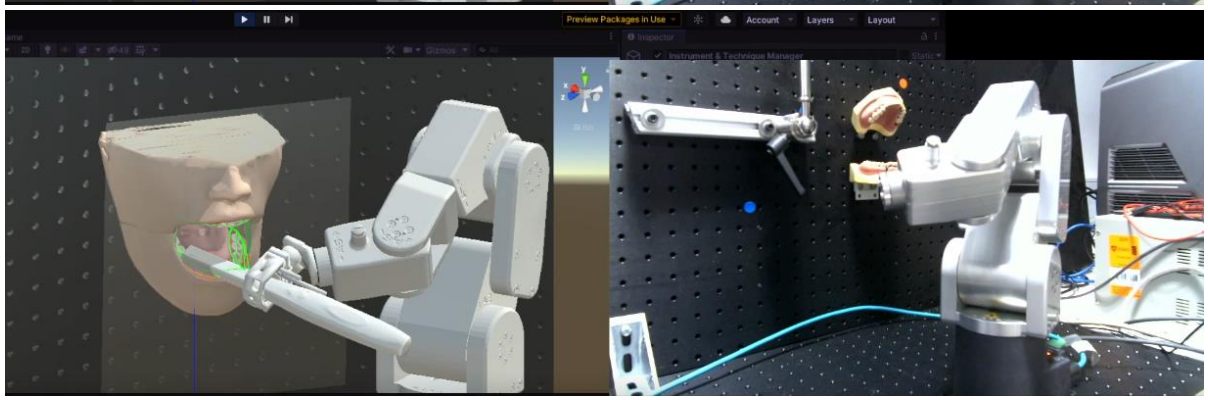

Figure E.3. The robot connected to Unity without the head model to follow the position and rotation of the reference tip along a selected path: A) Entering path at start of cycle (~15%); B) Near midpoint of a cycle (~50%) at the back of the mouth; and C) Right head rotation with the instrument part way into the mouth (~25% or ~75%). The location of the reference tip in space is indicated by the vertical blue line from the optical breadboard.

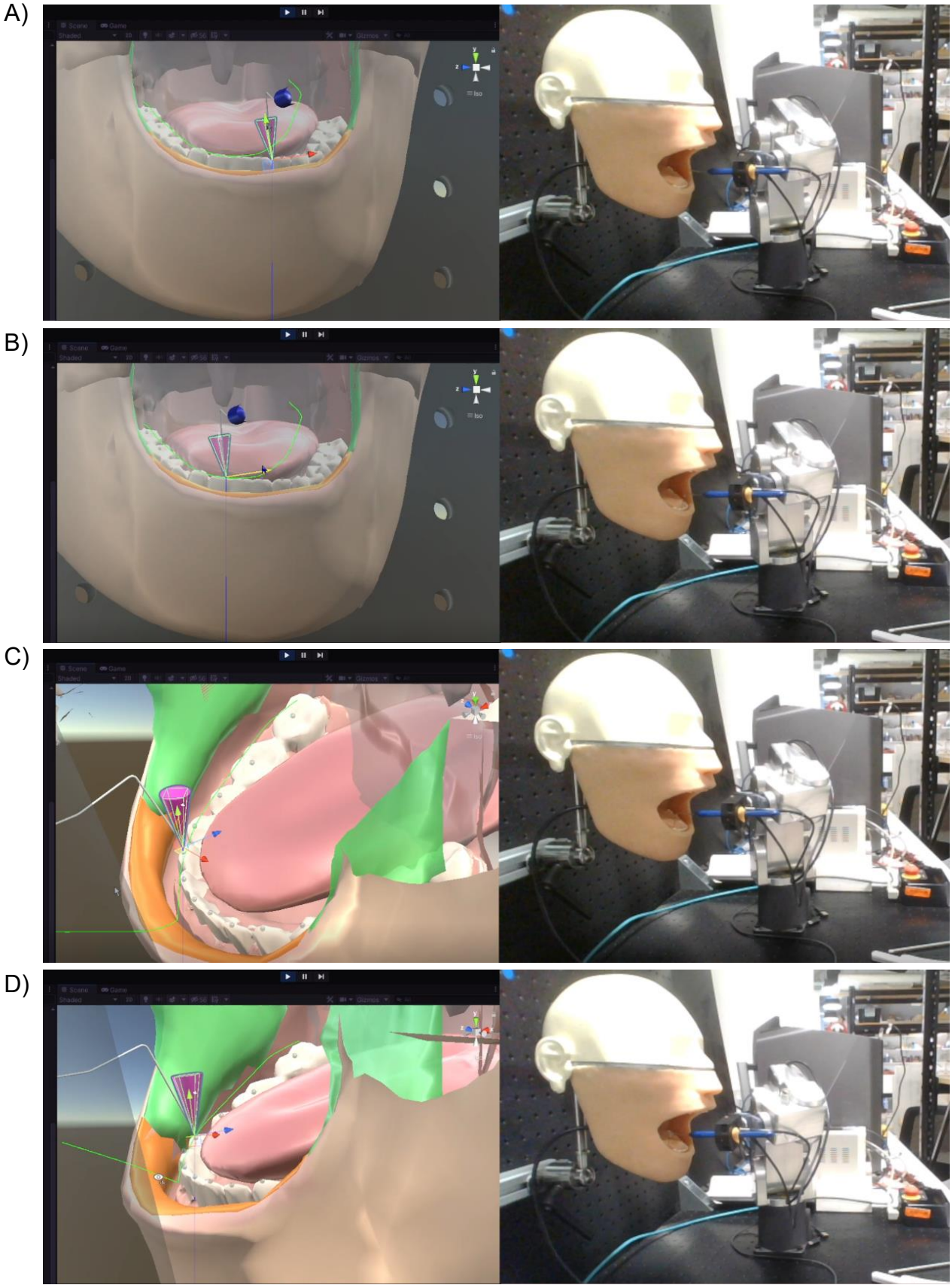

Figure E.4. Manual localisation of dental arch features for periodontal probing test case (T6): A) Point 1; B) Confirmation Point 2; C) Confirmation Point 3; D) Confirmation Point 4.

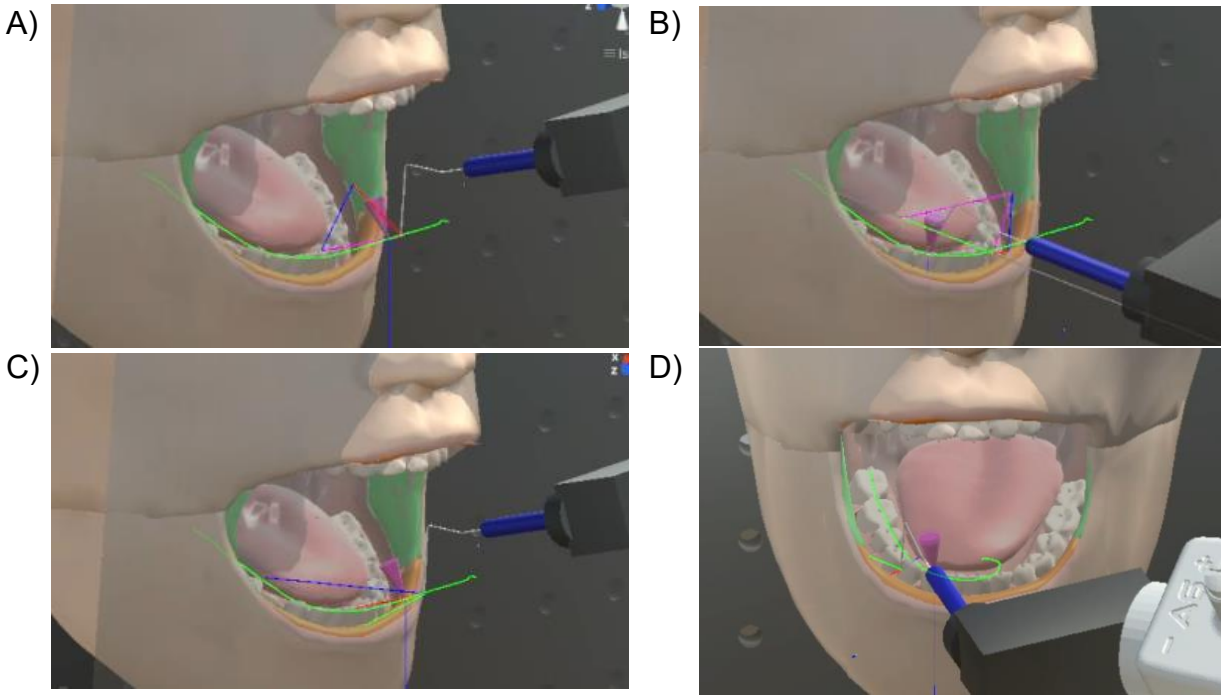

Figure E.5. Visual representations of the procedure block measurements in Unity: A) ID1.1 distances to the closest occlusal marker; B) ID1.2 distances from the centre of the frontal plane; C) ID1.3 distances from hard tissue surfaces (teeth, gingivae and throat surface); and D) ID1.4 distances from soft tissue surfaces (lips, cheeks and tongue).

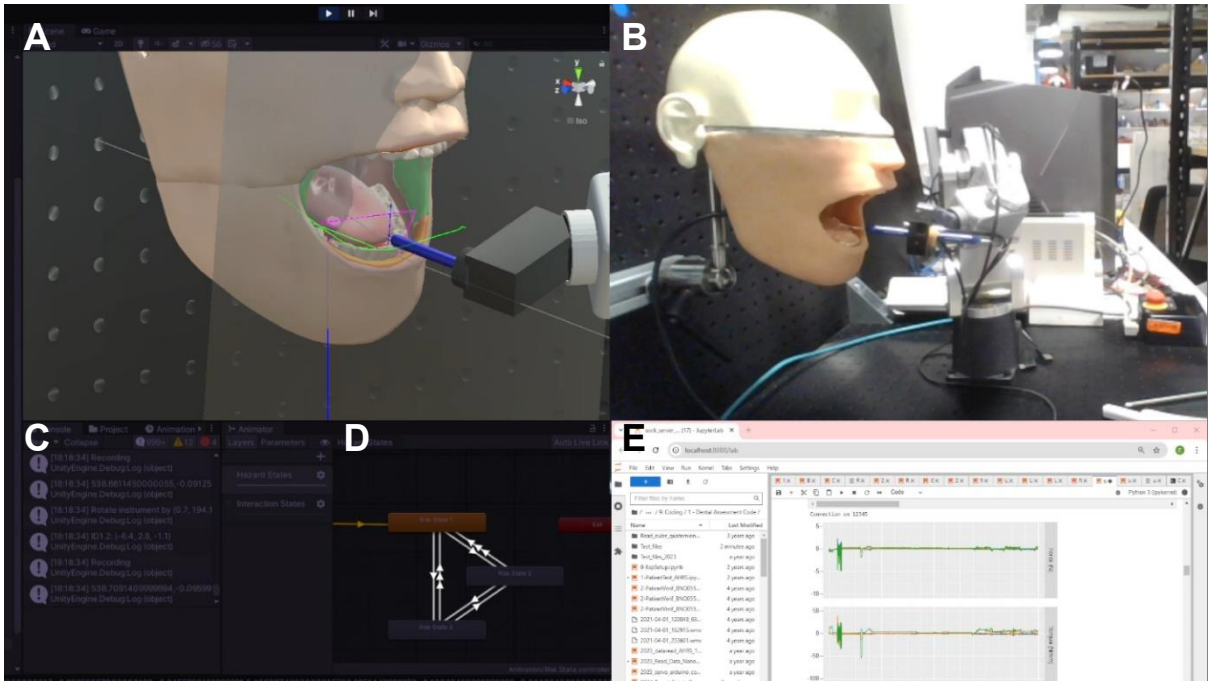

Figure E.6. Sample visual representation of the tracked risk measurements and forces during the periodontal probing test case (T6): A) Scene window of 3D environment; B) Dental setup with Meca500 holding a periodontal probe in Quadrant 4 of the head model; C) Logged risk data outputs displayed; D) Risk States shown in the Animator window; E) Python server displaying output force and torque measurements from the Nano17-e sensor.

E.2 Dental Simulation Test Cases

Following preliminary testing of the sensors and robot, the test cases T1 and T2 were performed involving passive model movement with the low and high risk paths with the ProDENT instrument (Figure E.7, Figure E.8). The conditions of high risk are presented for the expected location of the instrument (Figure E.8A) and the error in the risk measurement high risk detection (Figure E.8B). Active corrections of the ProDENT instrument's position with head and jaw movement along the low risk path is shown for test cases T3 and T4 (Figure E.9, Figure E.10). The sonic toothbrush test case (T5) is shown with its force data to highlight the impact of the vibrations on observing the force data without a low pass filter (Figure E.11). The periodontal probe test case (T6) followed localisation of the head model using the four dental arch features (Figure E.4, Figure E.12). It should be noted that the force data display is updated intermittently as shown in the lower right window of the image screen captures.

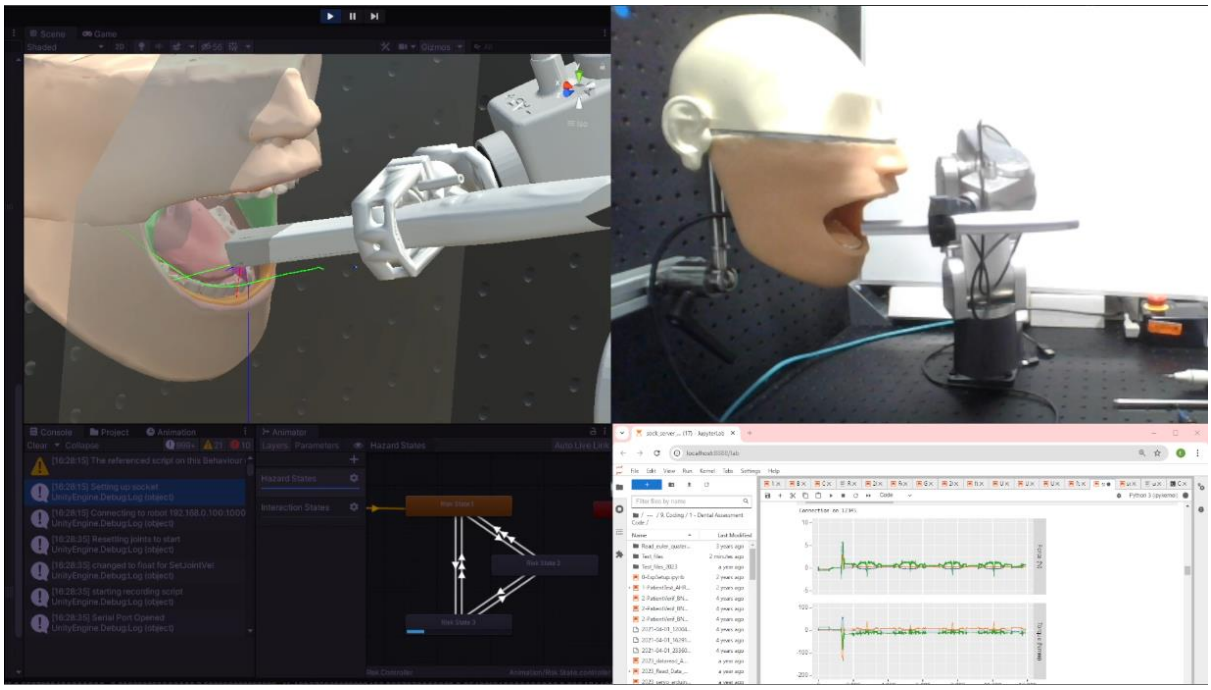

Figure E.7. ProDENT intraoral camera test case (T1) on the low-risk path with passive model movement. Risk State 3 is indicated as active for low-risk detection. ID1.4 distance measurements are visible in the Unity simulation window. The location of the reference tip in space is indicated by the vertical blue line from the optical breadboard.

A)

B)

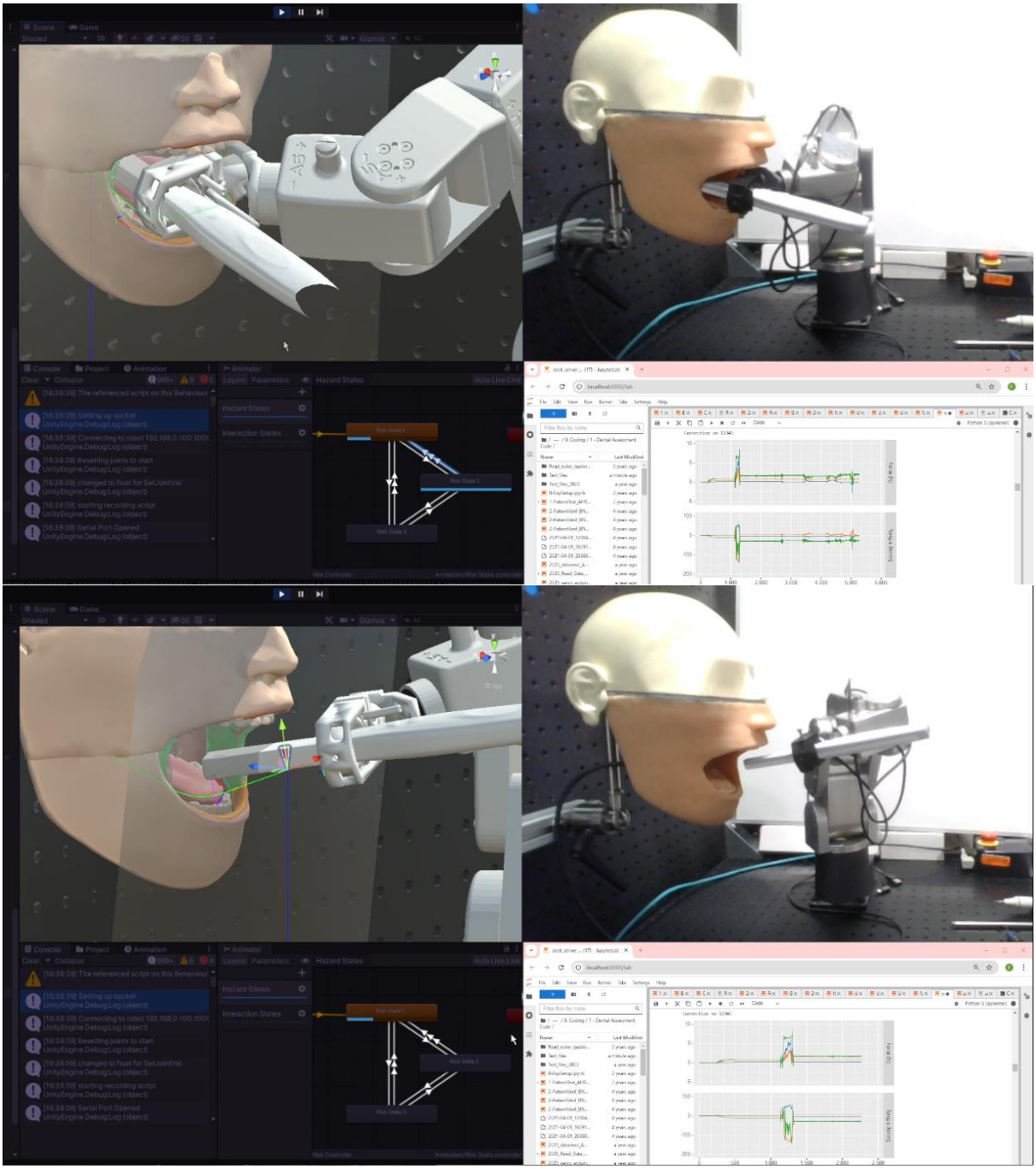

Figure E.8. ProDENT intraoral camera test case (T2) on the high-risk path with passive model movement. Transitions to Risk State 2 and then Risk State 1 are indicated as active for high-risk detection. A) Expected high-risk event for instrument at the back of the mouth. B) Error for high-risk event detection by the procedure block measurements. ID1.1 distance measurements are visible in the Unity simulation window. The location of the reference tip in space is indicated by the vertical blue line from the optical breadboard.

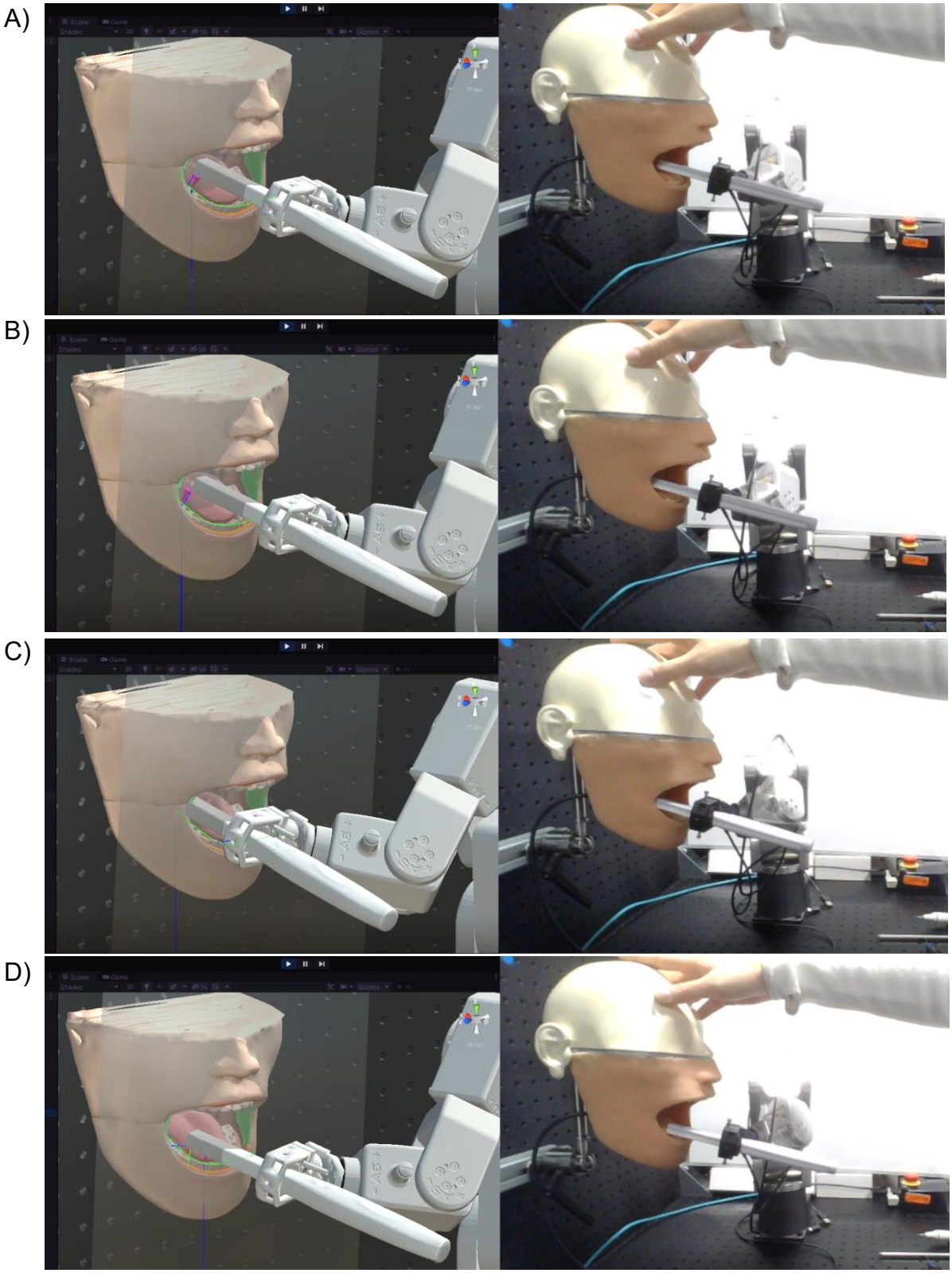

Figure E.9. ProDENT intraoral camera test case (T3) on the low-risk path with active head movement. A) Head turned to the right, pulling away from the instrument and B) the instrument correcting its position while moving along its path. C) Head turned back to the centre, pushing into the instrument and D) the instrument correcting its position on exit. The location of the reference tip in space is indicated by the vertical blue line from the optical breadboard.

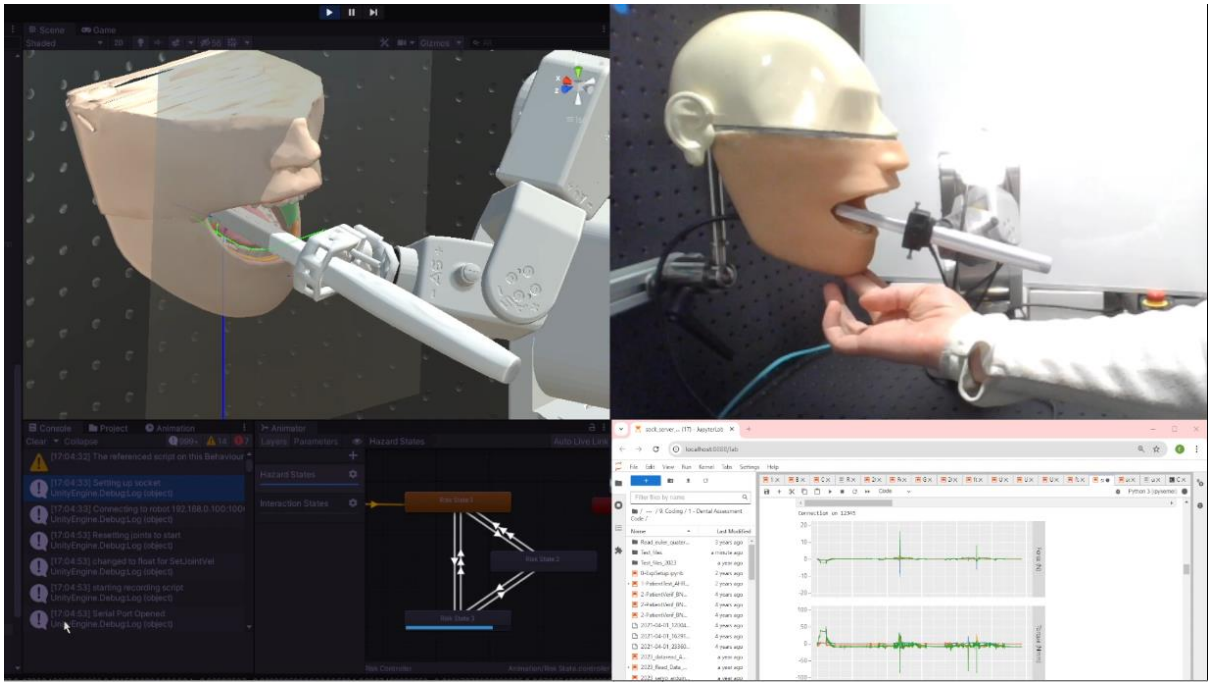

Figure E.10. ProDENT intraoral camera test case (T4) on the low-risk path with active jaw movement. The location of the reference tip in space is indicated by the vertical blue line from the optical breadboard.

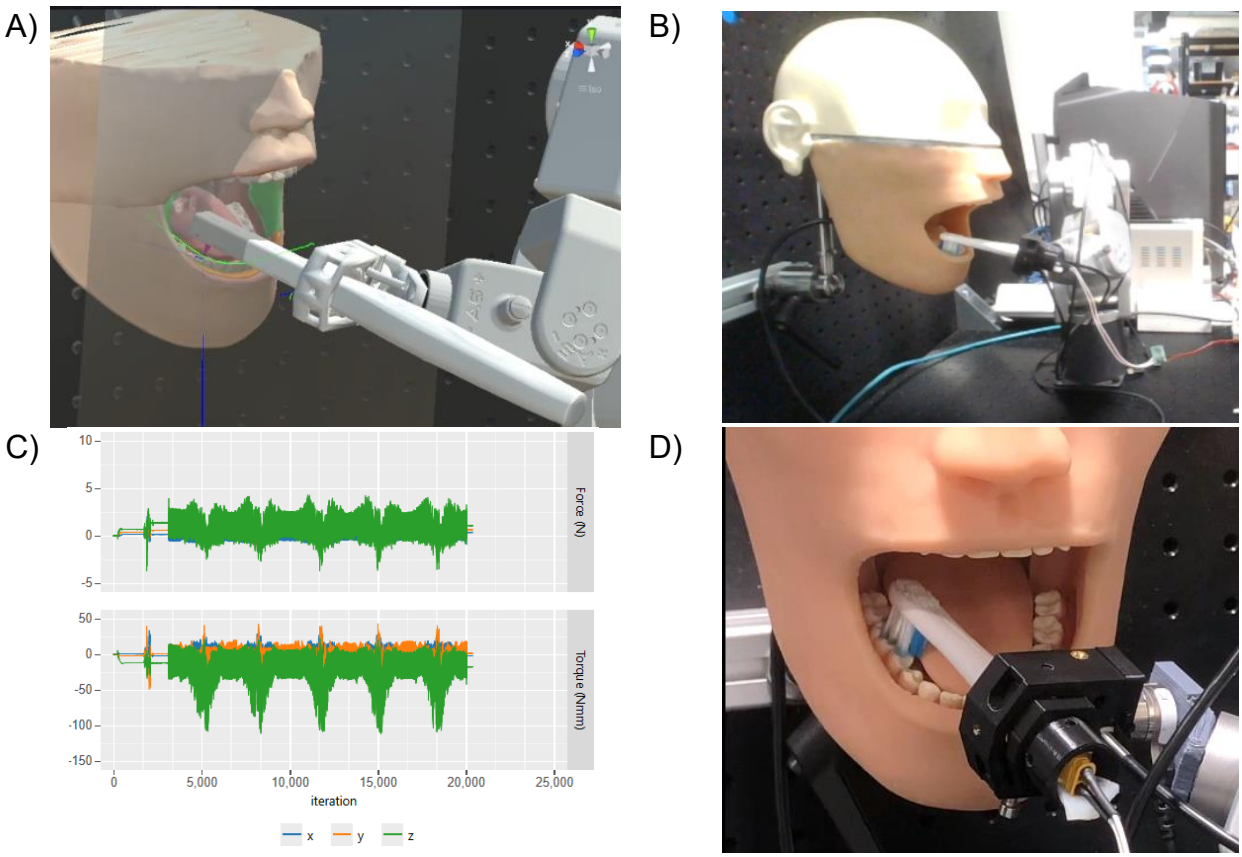

Figure E.11. Sonic toothbrush test case (T5) on the low-risk path with passive model movement. A) Unity simulation used for the instrument's position reference and B) the instrument shown simulating brushing teeth. C) Raw data from the force-torque sensor. D) Front view of the toothbrush in the mouth.

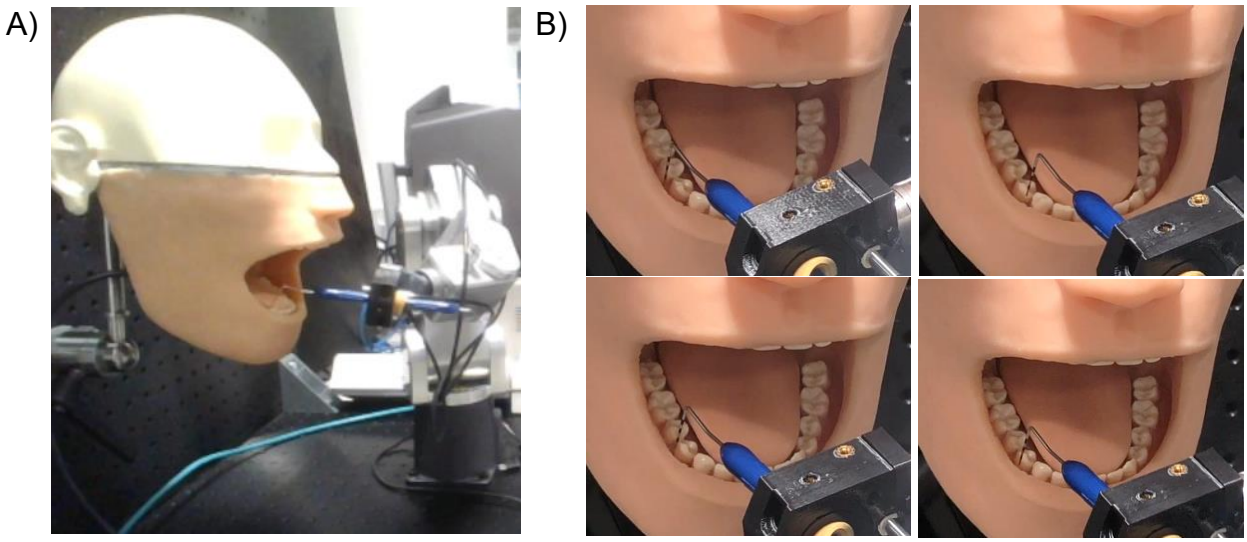

Figure E.12. Periodontal probing test case (T6) on the low-risk path with passive model movement. A) Side view of the periodontal probe in the model mouth. B) Front views of the periodontal probe at different positions of the path.

E.3 Active Test Case Raw Results

Raw data observations are presented for the two dynamic test cases over time with active manual input. For active head movement during the first two cycles of motion, the tracked head rotation starting point with an error of less than 5° and the forces in the x- and y-axes remained with less than 2 N ranges (Figure E.13). After the third repeat, the head model was poorly localised at an angle of rotation approaching 20° limiting progress on to the last two repeats (Figure E.13A). There was minimal change in jaw angulation with a small range of up to 1.4° of depression (Figure E.13B). The highest forces were experienced along the axial length of the instrument in the third motion cycle (Figure E.13C) and during each of the motion cycles for the horizontal forces (Figure E.13E).

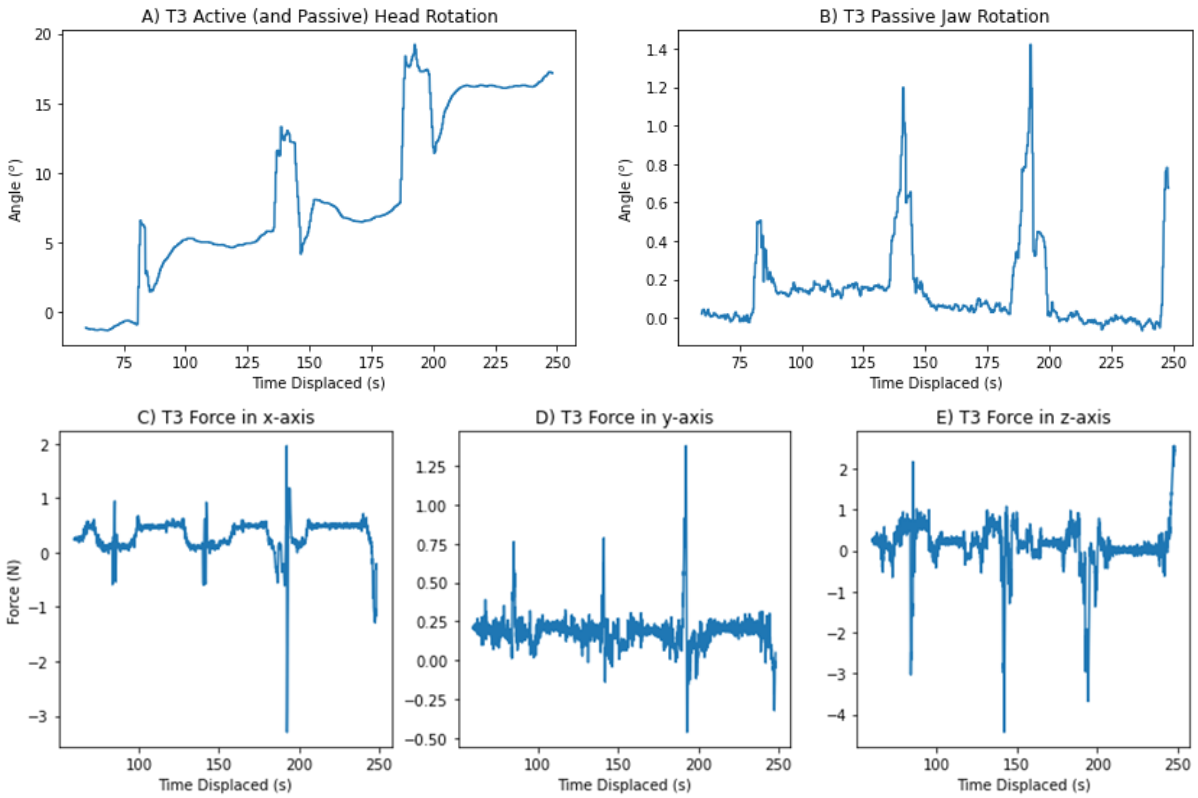

Figure E.13. Raw data for the tracked AHRS and force-torque sensor data for the ProDENT test case with active head rotation inputs (T3): A) Side-to-side head rotation, VN100 z-axis heading; B) Angle of passive jaw movement downwards depression (+), VN100 y-axis pitch; C) Instrument axial forces in Nano17-e x-axis; D) Instrument vertical forces in Nano17-e y-axis; and E) Instrument horizontal forces in Nano17-e z-axis.

During jaw elevations of the active jaw movement test case, there was occasionally an additional impact with the head model against the handle of the instrument or end effector holder (Figure E.14). Jaw elevations ranged from ~8–12° (Figure E.14B) with a varying impact depending on the depth of the instrument into the oral cavity and the direction of travel. The largest collisions occurred during repeats 1 and 3 (Figure E.14A) which experienced the highest total forces of ~19 N and ~31 N overall during the procedure, respectively. The forces were mostly acting in the axial and horizontal directions of the instrument, but a high force was also depicted in the third repeat for the y-direction. Following this, the program crashed during the fifth cycle.

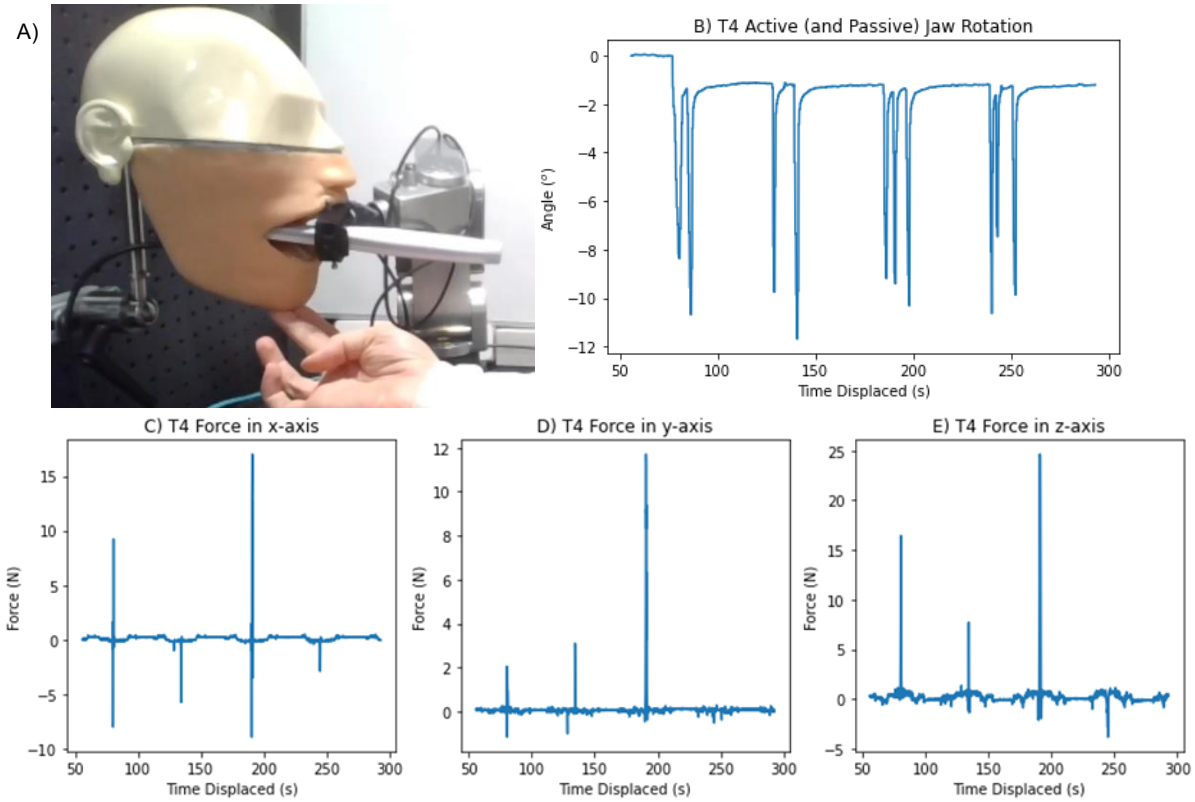

Figure E.14. A) Additional collision between the end effector instrument holder and the head model from motion cycle 1 and 3. Raw data for the tracked AHRS and force-torque sensor data for the ProDENT test case with active jaw rotation inputs (T4): B) Angle of jaw movement upwards elevation (-), VN100 y-axis pitch; C) Instrument axial forces in Nano17-e x-axis; D) Instrument vertical forces in Nano17-e y-axis; and E) Instrument horizontal forces in Nano17-e z-axis.

Appendix F: Autonomous Dental Explorations

F.1 Physical and Virtual Setup

A preliminary study for developing automated navigation methods for a dental robot was carried out using Unity's *Raycast* features for virtual model collision avoidance. A periodontal mandible model from OneDental (Castle Hill, NSW Australia, Figure F.1A) was scanned by structured light using a desktop Einscan-S by Shining 3D (Hangzhou, China). The scan data was converted from an STL to an object file and imported into Unity 3D (Figure F.1B). A mould of the dental arch was made out of silicone and the hard teeth were embedded within it (Figure F.1C). This was carried out to avoid potential damage to the dental model and its teeth in preliminary experiments, as well as a force-torque sensor that was positioned under the dental arch. A straight stainless steel dental instrument attached as the robot end effector and its dimensions were measured (Figure F.1C).

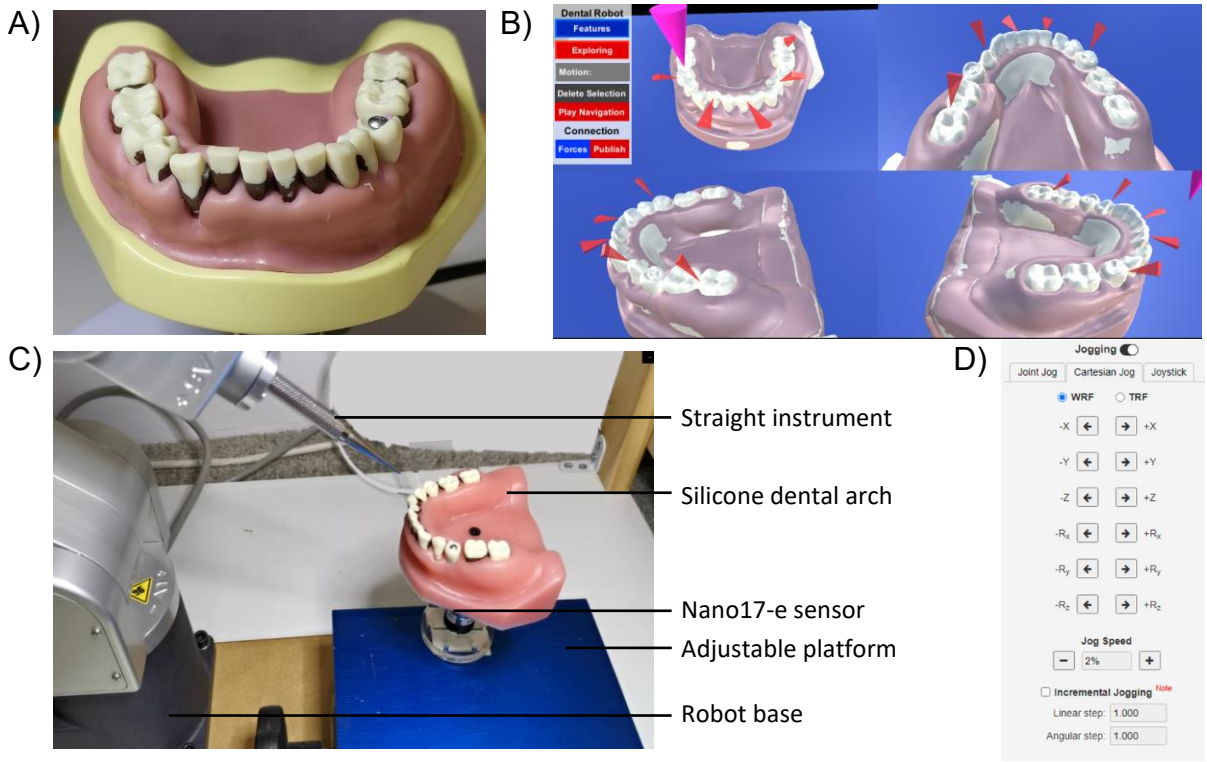

Figure F.1. A) OneDental periodontal dental arch model. B) Game Window 3D Unity environment interactive interface with multiple views of the intraoral scan dental arch and the five target locations created by a "click and place" spawn manager on the virtual model. C) Diagram of the robot setup with the Meca500, a force-torque Nano17-e sensor, a straight dental instrument and a silicone dental arch on a vertically adjustable platform. D) The Meca500 manual cartesian jogging panel on the Mecademic Web Interface.

The Unity interface was designed with a spawn manager and an interactive canvas with buttons to place a target location using a left mouse click on the dental arch to place a marker. While the game was running, five locations were selected, and their markers were placed on the tooth surface in the direction of the surface normal (Figure F.1B). Four cameras were positioned around the model to provide multiple perspectives of the dental arch model. The spawned marker objects representing the targets were copied to the main object Hierarchy window so that they could be accessed in Edit Mode.

The end effector tool reference frame position and orientation were sent to the robot through the Mecademic Web Interface using the *SetTRF* command configured as (-0.75 mm, -2.75 mm, 81 mm, 1.94º, -0.53º, 0º). This instrument orientation was maintained throughout the

dental application. The instrument tip on the robot end effector was moved to manually locate the target points using the Mecademic Web Interface jogging panel in cartesian space to the five locations set in Unity (Figure F.1D). Iterative Closest Point (ICP) was performed in MATLAB for the five target locations. The output transformation matrix was used to position the virtual model in Unity to match the relative position of the physical model.

To simulate the dental application, the position of each target was sequentially provided to a probe reference object such that the probe aimed to move directly towards the top of the marker placed at the target in 3D space around the Unity environment (5 mm away from target surface). The probe reference object was designed with five sensing arms that can perform surface detection of the virtual dental arch (Figure F.2). This was created to demonstrate autonomous collision avoidance of the dental arch for movement of the probe reference.

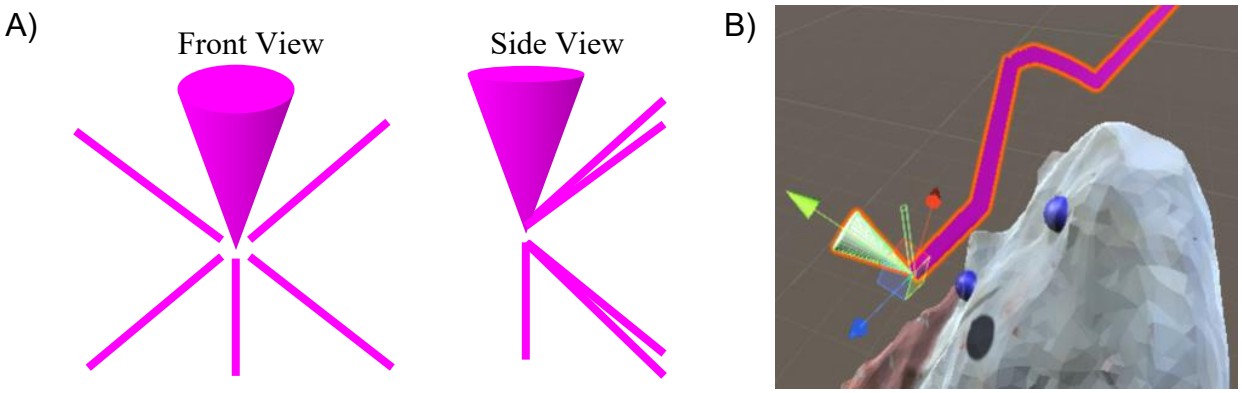

Figure F.2. A) Probe reference with five sensing "feelers" extending in the direction of movement; B) Collision avoidance of a dental arch model for the highlighted probe reference advancing towards a known target location.

The Unity simulation game controls included the ability to pause and play the reference probe's movement, stop at or skip the next target, and trigger an immediate exit to the starting position away from the model (Figure F.3A, Figure F.4A). Additional Unity functionality was included to apply a contact force on the dental model at the target sites. From 5 mm away from the model, the probe reference was designed to move towards the surface and apply a force equivalent to approximately 1 mm offset into the model. Force-torque sensor measurements

were captured from the Nano17-e sensor below the dental arch. After contact with the virtual surface model, the instrument returned to a distance of 5 mm from the target before continuing to the next target (Figure F.3B, Figure F.4B).

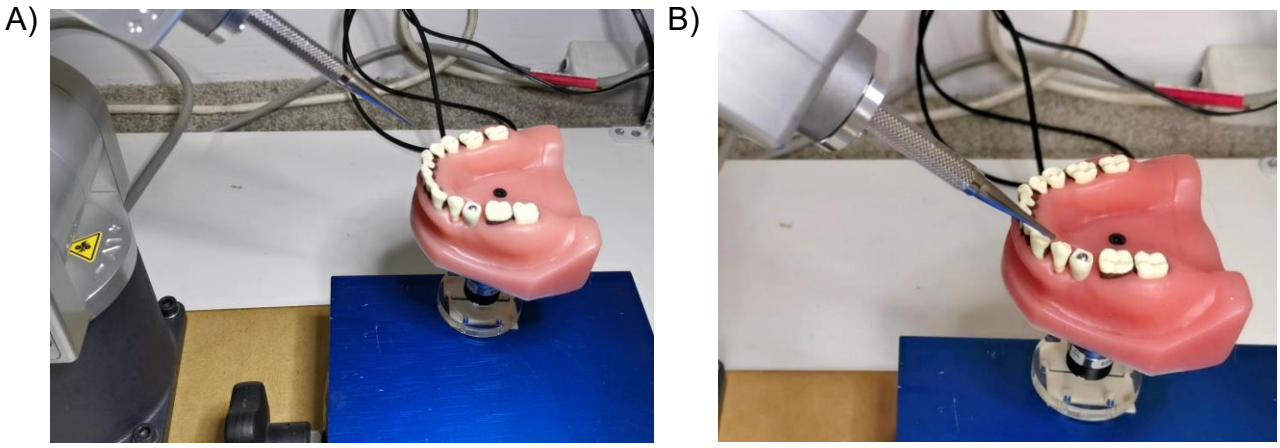

Figure F.3. The Meca500 robot end effector moving around a model dental arch in Unity: A) Initial pose (ready to follow probe reference); and B) Pose during motion.

F.2 Preliminary Results

From the instrument path around the dental model, five peaks were produced on the data measured by the force-torque sensor where the robot applied a force at a chosen target location (Figure F.5A-C). The low magnitude values would be attributed to the use of the silicone model. Disturbances to the force-torque sensor can be observed between the peak locations. This may have been produced by vibrations translated to the sensor through the platform from robotic movement. The variation in magnitude of these forces from 0.1 N to 0.7 N is expected to have been a result of model warping and poor tooth localisation for the deformable silicone model (Figure F.5C,D). The largest force measured occurred at the 5th target point which experienced the highest difference in position to the real model target samples following ICP transformation (Figure F.5D, Table F.1). Future developments should include the rotation of the instrument to optimal orientations relative to the target locations for this application with collision avoidance.

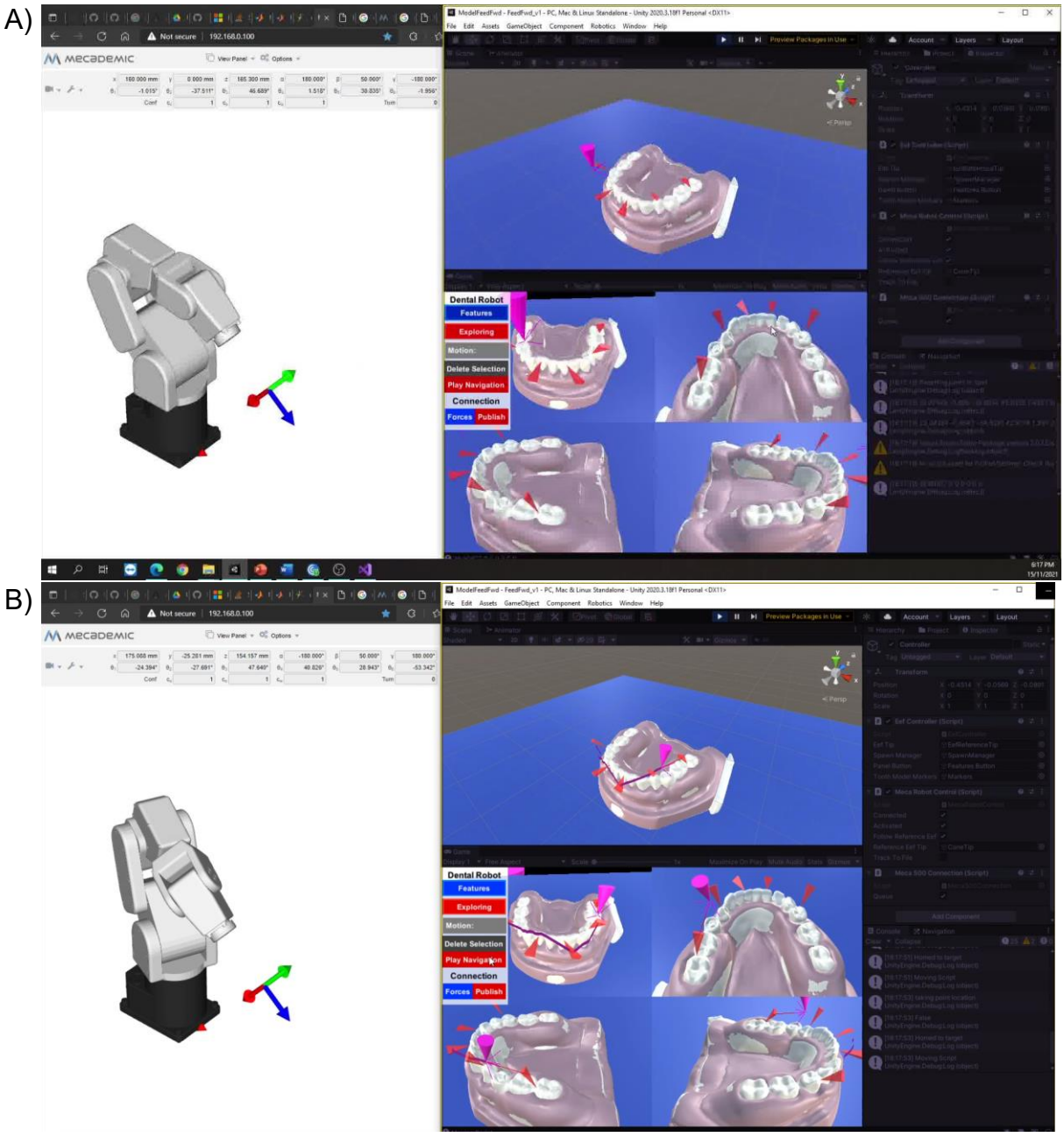

Figure F.4. Simulated Meca500 robot movement with the Mecademic Web Interface following the probe reference around the targets on the model dental arch in Unity: A) Initial pose (before following probe reference); and B) Pose during motion.

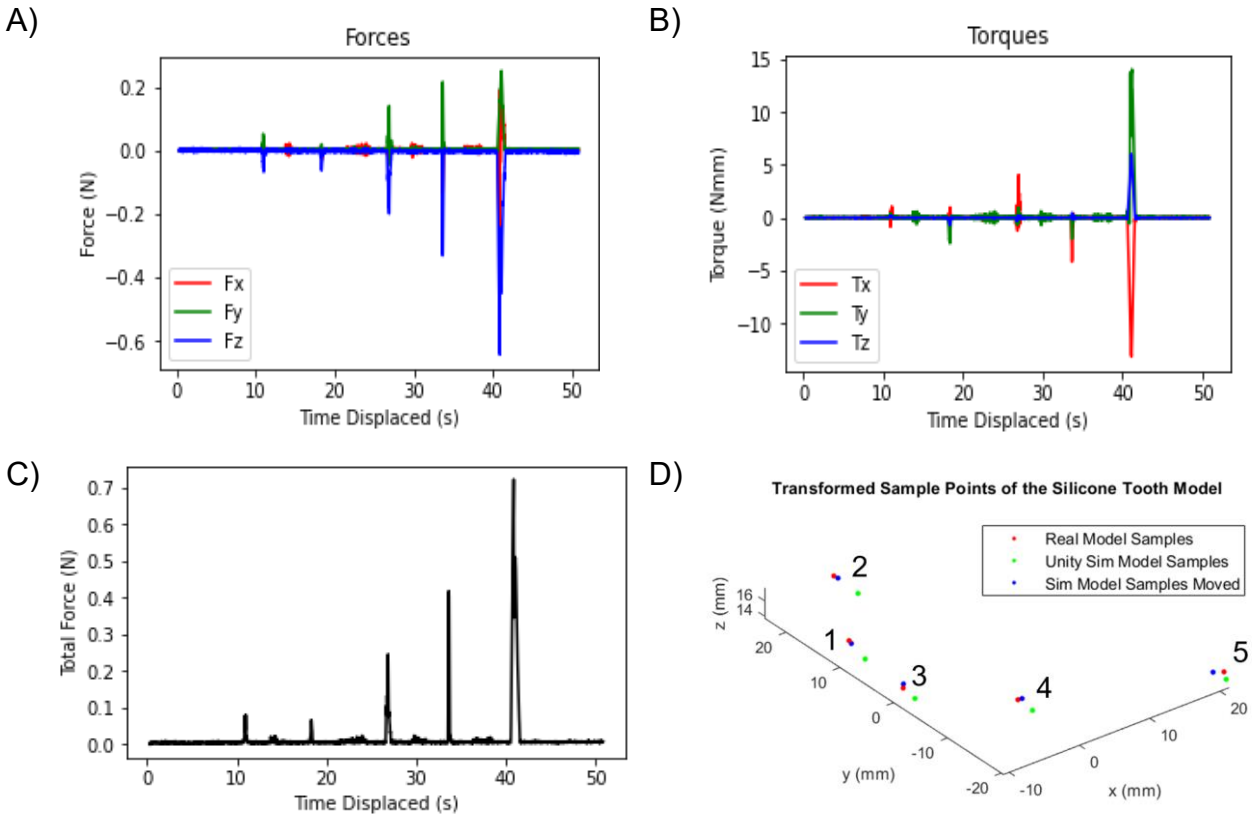

Figure F.5. Force-torque sensor measurements over time: A) Force components; B) Torque components; and C) Total force. D) The five target points from manual localisation compared to the initial position of the virtual targets and the transformed virtual model targets.

Table F.1. Virtual model transformation data from ICP registration with displacements and errors.

Model Axes	XYZ Euler (º)	Translation (mm)	Max Error (mm)	RMSE
x	-0.0278	-1.8124	0.9687	
y	-0.0399	1.3679	0.8763	0.8090
z	-0.0380	1.7011	0.3741	